Curtin
UNIVERSITY OF TECHNOLOGY

MARINE SEISMIC SURVEYS:

ANALYSIS AND PROPAGATION OF

AIR-GUN SIGNALS;

AND EFFECTS OF AIR-GUN EXPOSURE ON

HUMPBACK WHALES, SEA TURTLES,

FISHES AND SQUID

Prepared for

Australian Petroleum Production Exploration Association

By

Robert D. McCauley, Jane Fewtrell, Alec J. Duncan, Curt Jenner, Micheline-Nicole Jenner, John D. Penrose, Robert I.T. Prince, Anita Adhitya, Julie Murdoch, Kathryn McCabe

Centre for Marine Science and Technology,

AUGUST 2000

ABSTRACT

An experimental program was run by the Centre for Marine Science and Technology of Curtin University between March 1996 and October 1999 to study the environmental implications of offshore seismic survey noise. This work was initiated and sponsored by the Australian Petroleum Production Exploration Association. The program: characterised air-gun signal measurements; modelled air-gun array sources and horizontal air-gun signal propagation; developed an 'exposure model' to predict the scale of potential biological effects for a given seismic survey over its duration; made observations of humpback whales traversing a 3D seismic survey; carried out experiments of approaching humpback whales with a single operating air-gun; carried out trials with an air-gun approaching a cage containing sea turtles, fishes or squid; and modelled the response of fish hearing systems to air-gun signals. The generalised response of migrating humpback whales to a 3D seismic vessel was to take some avoidance manoeuvre at > 4 km then to allow the seismic vessel to pass no closer than 3 km. Humpback pods containing cows which were involved in resting behaviour in key habitat types, as opposed to migrating animals, were more sensitive and showed an avoidance response estimated at 7-12 km from a large seismic source. Male humpbacks were attracted to a single operating air-gun due to what was believed the similarity of an air-gun signal and a whale breaching event (leaping clear of the water and slamming back in). Based on the response of captive animals in cold water to an approaching single air-gun and scaling these results, indicated sea turtles displayed a general 'alarm' response at an estimated 2 km range from an operating seismic vessel and behaviour indicative of avoidance estimated at 1 km. Similar trials with captive fishes showed a common fish 'alarm' response of swimming faster, swimming to the bottom, tightening school structure, or all three, at an estimated 2-5 km from a seismic source. Modelling the fish ear predicted that at ranges < 2 km from a seismic source the ear would begin a rapid increase in displacement parameters. Captive fish exposed to short range air-gun signals were seen to have some damaged hearing structures, but showed no evidence of increased stress. Captive squid showed a strong startle responses to nearby air-gun start up and evidence that they would significantly alter their behaviour at an estimated 2-5 km from an approaching large seismic source.

keywords - seismic, noise effects, fish, whales, squid, sea turtles, underwater sound, air-guns

ACKNOWLEDGMENTS

CONTENTS

EXECUTIVE SUMMARY

In mid 1995 the Australian Petroleum Production Exploration Association initiated a research program to address the issue of environmental concerns created by marine seismic surveys used in petroleum exploration and production. This program was based at the Centre for Marine Science and Technology at Curtin University in Perth Western Australia, and ran from March 1996 to October 1999. The study:

- characterised the measurement of air-gun signals;
- modelled air-gun array configurations for source level with aspect and elevation;
- carried out horizontal propagation modelling of air-gun signals;
- described sets of field measurements of a 3D array and single air-gun;
- developed a model to predict exposure through time for a given seismic survey configuration, and by linking this to effect types predict regions impacted by the survey;
- monitored the movement and behaviour of humpback whales through an area in which a 3D seismic survey was running;
- under rigorous permit conditions carried out 16 trials where humpback whales were approached with a single operating air-gun to gauge responses;
- carried out two trials where captive green and loggerhead turtles were approached with a single operating air-gun;
- carried out trials of exposing various fishes to air-gun noise and measured behavioural, physiological and pathological effects;
- modelled the response of fish otoliths to applied air-gun signals;
- and carried out trials of exposing squid to air-gun approaches to gauge behavioural responses.

Extensive sets of measures were made of a single 20 cui air-gun used during trials and a 2678 cui, 3D, 16 gun array. These measurements highlighted the complexities of characterising air-gun signals and of defining the received level at a specified orientation to the array, water and receiver depth, range and set of local environmental parameters. It was found that an air-gun signals' total energy gave the most reliable and consistent measure of its level. Empirically derived corrections could then be applied to convert the energy measure to units used by other authors or for assessing biological effects. A myriad of factors dictated the horizontal propagation of an air-gun signal, so much so that each case needed to be considered separately.

A summary of the biological effects noted during the study, the air-gun level at which the effects were noted (in units of mean squared pressure) and the approximate horizontal range from a large seismic survey array to which this level extends, are listed on Table 1. It must be cautioned that these air-gun levels pertain to this set of observations. For the sea turtle results only two individuals were tested over two trials. There may be considerable variability in the level required to induce similar effects in species other than those tested or under different circumstances. This may be particularly true within the fishes for which large differences in inherent behavioural responses to applied stresses and in their hearing capabilities exist. It should also be noted that the results for trials with sea turtles, fishes and squid listed in Table 1 were carried out on caged animals. There are advantages and disadvantages to carrying out trials in cages. The rationale in this set of trials was that a detailed analysis of the types of effects under controlled conditions could be obtained and that an understanding of these effects could then guide follow up observations on wild or more free ranging species.

Animal group	Effects	Level (dB re 1 μPa mean squared pressure)	Approximate maximum range from measured array[1] (km)
humpback whales moving about seismic vessel	standoff[2] range for migrating humpbacks	157-164	1.8 - 4.6
humpback whales approached with air-gun in key habitat type	resting pods with cows begin avoidance	140	9 - 15
humpback whales approached with air gun in key habitat type	resting pods with cows standoff range	143	7.3 - 12
humpback whales approached with air-gun	maximum level of single air-gun tolerated by investigating probable male humpbacks, although this possibly due to visual clues	179	0.65 - 1.1
green & loggerhead turtle, cage trial	noticeable increase in swimming behaviour	166	1.5 - 2.6
green & loggerhead turtle, cage trial	turtle behaviour becomes increasingly erratic with avoidance probable	175	0.8 - 1.4
various fin-fishes, cage trials	common 'alarm' behaviour of forming 'huddle' on cage bottom centre, noticeable increase in alarm behaviours begins at lower level	156-161	2.1 - 5
fish ear model	rapid increase in hearing stimulus begins	> 171	1.1 - 1.8 km
fish *P. sexlineatus,* cage trials	persistent C- turn startle	182-195	0.2 - 0.8
various finfish, cage trials	no significant physiological stress increase	146-195	0.2 - 9.8
fish *Chrysophrys auratus* & others, cage trials	pathological damage to hearing systems	[3]????	[3]????
squid, cage trials	startle (ink sac fire) and avoidance to startup nearby	174	0.9 - 1.5
squid, cage trials	noticeable increase in alarm behaviours	156-161	2.1 - 5
squid	significant alteration in swimming speed patterns, possible use of sound shadow near water surface	166	1.5 - 2.6

Table 1: Summary of biological effects of nearby air-gun operations from this study. All units are given as dB re 1 μPa mean squared pressure. Superscripts are: 1 - Based on measurements from a 2678 cui array made in approximately 120 m water depth and calculated for 32 m depth receiver, with interpretation accounting for source beam pattern only. These ranges should be considered a **GUIDE** only and will differ from survey to survey depending on source, environment and receiver depth.; 2 - the 'standoff' range defines the closest distance at which these animals will approach an air-gun source or will allow the air-gun source to approach; 3 - Precise exposure history of trials known but ramped approach-departure meant levels required to produce damage not known.

The ranges quoted in Table 1 were derived by using the level for a given effect as measured in trials, and finding the range at which this level was reached as measured from a large 3D air-gun array. The ranges could be considered as "zones of effect". It must be noted that the ranges listed will vary depending on the circumstances of the particular seismic survey. The range to reach a specified level will be more or less for different sources or environments and cannot be quoted universally. In shallow water or for smaller

capacity arrays the ranges will likely be less, for larger arrays or more focussed 2D arrays the ranges may be greater.

To consider the scale of biological effects for a given seismic survey, as well as direct effects as listed in Table 1, scale and time factors need to be also factored into analysis. Thus the "zones of effect" (specific for each air-gun signal), the geographic layout of the seismic survey and the survey duration all need to be considered to give some idea of the full impact of a specified seismic survey. A small seismic survey may comprise only several thousand signals spread over several days in a comparatively large area, whereas an intense 3D program may involve several hundred thousand signals spread over weeks to months in a comparatively small area. To give a guide for interpreting this scale of effects for any given seismic program, an exposure model was produced. This output a contour plot of the number of air-gun signals exceeding some "effect threshold" for the survey region through time. This approach then produced a "probability" plot, with a prediction of the scale and persistence of effects in space and time.

A program to monitor the movements and behaviour of SW travelling humpback whales traversing the region of a 3D seismic program with E-W tracklines and which straddled the whales migratory route was carried out. Aerial surveys and observations from the seismic vessel showed no gross changes in the whales migratory pattern, although subtle changes may have occurred. Observations from the seismic vessel showed that fewer whales were seen within three km of the vessel when its air-gun arrays were operating as compared to when they were not operating, indicating localised avoidance. Conversely more whales were seen at greater than three km from the seismic vessel when its air-gun arrays were operating than when they were not operating, indicating either attraction to the vessel or some change in the sighting availability of whales. Possible use of the sound shadowing effect near the sea surface may have altered the sighting availability and the similarity between air-gun signals and whale breaching events may have attracted male humpbacks (see below).

Several humpback pods where followed as they approached the operating seismic vessel, either from a second vessel or as observed from the seismic vessel. The most common pod avoidance strategy was to alter course to pass behind the seismic vessel streamer tail-buoys (three km), although on one occasion a single believed male whale was seen to deliberately swim across the operating vessel's bow at 1.5 km.

Sixteen trials were carried out where pods of humpback whales were observed, approached with a single operating air-gun, and followed for an hour after cessation of air-gun approach. These trials were carried out in a large enclosed Bay (Exmouth Gulf) under strict permit guidelines. Observations of the behaviour and movement patterns of targeted pods were made. For various reasons five of the trials were inconclusive. Of the other eleven trials one involved a male only pod (single adult). This animal seemed completely oblivious to the intercepting air-gun, allowing it to approach to 100 m before changing course. The other ten trials were believed to involve pods with cows. In all these trials the results were consistent, avoidance manoeuvres to the approaching air-gun were made and some mean standoff range observed (a minimum range at which the animals would allow the air-gun to approach). The received air-gun level for the standoff range during these experimental air-gun approaches was considerably lower than that observed for the migrating humpbacks closing an operating seismic vessel. This was believed a function of the different behavioural states of the animals in each set of measurements. The humpbacks closing the operating seismic vessel were migrating, purposefully swimming SW. The approach trials were carried out in a large enclosed bay where the whales were resting, socialising or engaged in courting behaviours. This distinction in observed effects and behavioural states has important management implications.

Although avoidance of the intercepting air-gun was the consistent response of any pod containing a cow, in

nine of the 16 trials, 11 separate pods deliberately and systematically approached the operating air-gun. Nine of these pods were single adults only and all 11 pods involved mature animals. The approaching whales closed the air-gun vessel directly often at speeds up to 8 kn, usually circled or partly circled the vessel at 100-400 m then departed. Fortuitously the sounds produced by breaching humpbacks were measured during trials. Breaching events involve the 30-40 tonne animal leaping clear or partly clear of the water and slamming back in. The underwater sound produced by the breaching event was audibly very similar to an air-gun signal and although not identical, the two could be matched well in waveform character, energy levels and frequency content. It is believed the animals which systematically approached the operating air-gun during exposure trials were males either mistaking the air-gun signal for a breaching event and investigating, or simply considered it as a signal worth investigating.

To study the response of sea turtles, fin-fish and squid to air-gun noise, experimental trials were carried out on caged animals. The principal experimental site was in Jervoise Bay, Cockburn Sound, Western Australia using a 10 m long by six m wide by three m deep cage. Experiments were designed to mimic an operational seismic survey with multiple approach-departure scenarios, but on a much smaller geographical scale.

A green and loggerhead turtle were housed in the cage at a water temperature of 16° C, and approached with an operating air-gun over two trials, two days apart. The behaviour of turtles was assessed from underwater video recordings. As the air-gun level increased a corresponding increase in the turtles swimming behaviour was observed. At higher air-gun levels the turtles behaviour became increasingly erratic, possibly indicating that if they were not constrained they would have avoided the approaching source.

Nine sets of trials with fin-fish, two with squid and one with fin-fish and squid were carried out. Fish behavioural observations were made from two underwater videos placed in the cage during trials, physiological stress measurements were taken from cortisol levels in blood samples and the hearing structures of fish were examined using scanning electron microscopy. Additionally a simple model of the fish ear was used to examine the response of different sized fish otolith systems to a series of impinging air-gun shots.

These experimental results can be summarised as:
- for some fish a startle response (C-turn) to short range start up or high level air-gun signals;
- a greater startle response from some smaller fishes;
- evidence of alarm responses, with this becoming more noticeable with an increase of received air-gun level above approximately 156-161 dB re 1 µPa mean squared pressure;
- a lessening of severity of startle and alarm responses through time (habituation);
- an increased use of the lower portion of cage during air-gun operation periods;
- the tendency in some trials for faster swimming and formation of tight groups correlating with periods of high air-gun levels;
- a general behavioural response of fish to move to bottom, centre of cage in periods of high air-gun exposure (for levels approximately greater than 156-161 dB re 1 µPa mean squared pressure);
- no significant measured stress increases which could be directly attributed to air-gun exposure;
- evidence of damage to the hearing system of exposed fishes in the form of ablated or damaged hair-cells although an exposure regime required to produce this damage was not established and it is believed such damage would require exposure to high level air-gun signals at short range from the source.

The modelling results can be summarised as:

- above an air-gun level threshold of around 171 dB re 1 µPa mean squared pressure a rapid increase in absolute displacement parameters of the fish hearing system, suggesting that associated behavioural response and susceptibility to mechanical damage will increase accordingly;
- smaller otoliths tracked the input air-gun signal better than larger otoliths but showed lower absolute displacement parameters and returned to the rest position quicker, suggesting that smaller otolith systems may be at less mechanical risk from air-gun exposure than larger ones;
- the otolith system responded primarily to air-gun energy < 150 Hz, which encompassed the frequency of maximum energy of the input air-gun signals.

Squid showed strong alarm responses to a nearby air-gun starting up, with many firing their ink sacs and jetting directly away from the source. Firing of ink sacs was not evident if the air-gun was ramped up rather than started nearby. Squid exposed in approach-departure experiments showed evidence of an increase in alarm responses above approximately 156 dB re 1 µPa mean squared pressure. There was evidence that squid actively utilised the near surface sound shadow during trials, and initially increased their swimming speed as the air-gun approached but slowed near the point of closest air-gun approach.

INTRODUCTION

Offshore seismic surveys involve the use of high energy noise sources operated in the water column to probe below the seafloor. The impulsive signals produced are directed downwards through the seabed, to be reflected upwards again by density or velocity dis-continuities within the underlying rock strata. These returned signals are received, stored and processed by geophysicists to give profiles of the seafloor, commonly to depths of 10 km. The technique is essential for oil and gas exploration and development, is now commonly used to monitor the flow of hydrocarbons from producing fields and in modified forms is widely used in maritime engineering surveys.

The high source levels involved in seismic surveys has led to considerable concern over their environmental effects and possible effects on commercial fishing operations. In response to this concern the Australian Petroleum Production Association (APPEA) in conjunction with the Energy Research and Development Corporation (ERDC) funded a three year multi-disciplinary project based at Curtin University, to study the environmental implications of offshore seismic techniques in the Australian context. This project ran over March 1996 to October 1999, with the results presented in this document.

The issue of environmental effects of seismic surveys has a long history, although few species have been studied in any detail and all studies are of short term effects and immediate responses. Due to outcry from the public and environmental groups, a major part of the research effort has focused on marine mammals. Most of this work has been carried out in North America and is reviewed in Richardson et al (1995), although more recent work has been carried out in European waters (ie. Goold and Fish, 1998). A push to explore for petroleum reserves in the North Atlantic margin is likely to result in further marine mammal work in European waters and it is believed several marine mammal projects are underway or will commence soon in North America.

Fisherman have long advocated that marine seismic surveys alter fisheries catch rates. Several studies, particularly in North America and Norway have investigated these effects, which have for the most part concentrated on finfish. McCauley (1994) reviews effects on finfish and invertebrates from literature available to 1993. More recent work published includes an excellent study by Engås et al (1993 & 1996) on avoidance behaviour of fishes to an operating seismic vessel and an unpublished report by Wardle et al (in press) on observation of fish responding to a nearby air-gun.

That seismic surveys often create concern over potential effects is reflected in the diversity of requests received for information. During the course of this project the senior author has been contacted regarding information of potential seismic effects on a wide range species, including: a scallop fishery in the Irish Sea; squid fishery in the Falkland Islands; possible impacts on baitfishes and feeding seabirds off the W coast of South America; impacts on commercial fisheries off Nova Scotia, effects on migrating school sharks to the N of Tasmania; effects on abundance of blue wahoo off Victoria; effects on a drop line fishery in northern Australia; possible impacts on sea-turtles in Trinidad; and concerns over effects on marine mammals and sea turtles from various Australian and international regulatory agencies.

The project described in this document has set out to link the physical aspects involved in the transmission of air-gun signals through the sea to studies on the response of a range of marine species to nearby air-gun species. Thus it has been a multi-disciplinary approach. The project has:

- characterised the measurement of air-gun signals;

- modelled air-gun array configurations for source level with aspect and elevation;
- carried out horizontal propagation modelling of air-gun signals;
- described sets of field measurements of a 3D array and single air-gun;
- developed a model to predict exposure through time for a given survey configuration, and by linking this to effect types predict regions impacted by a given survey;
- monitored the movement and behaviour of humpback whales through an area in which a 3D seismic survey was running;
- under rigorous permit conditions carried out 16 trials where humpback whales were approached with a single operating air-gun to gauge responses;
- carried out two trials where captive green and loggerhead turtles were approached with a single operating air-gun;
- carried out trials of exposing various fishes to air-gun noise and measured behavioural, physiological and pathological effects;
- modelled the response of fish otoliths to applied air-gun signals;
- and carried out trials of exposing squid to air-gun approaches to gauge behavioural responses.

This report presents: aspects of the physics of air-gun transmission and signal characterisation; aspects of animal behaviour, physiology and pathology; and modelling work. The presentation and easy linking of these diverse topics would be difficult within the conventional scientific literature.

TECHNICAL DETAILS

1 - GENERAL METHODS

1.1   Experimental air-gun

A Bolt PAR 600B air-gun with 20 cui chamber was purchased for exposure trials. The air-gun could be deployed hanging vertically or towed in a towfish. A schematic diagram of its operational setup (in towed configuration) is shown in Figure 1. A timing control was set up which could trigger the air-gun in 5 s steps from 10 to 60 s. In practice only a 10 or 15 s fire rate were used.
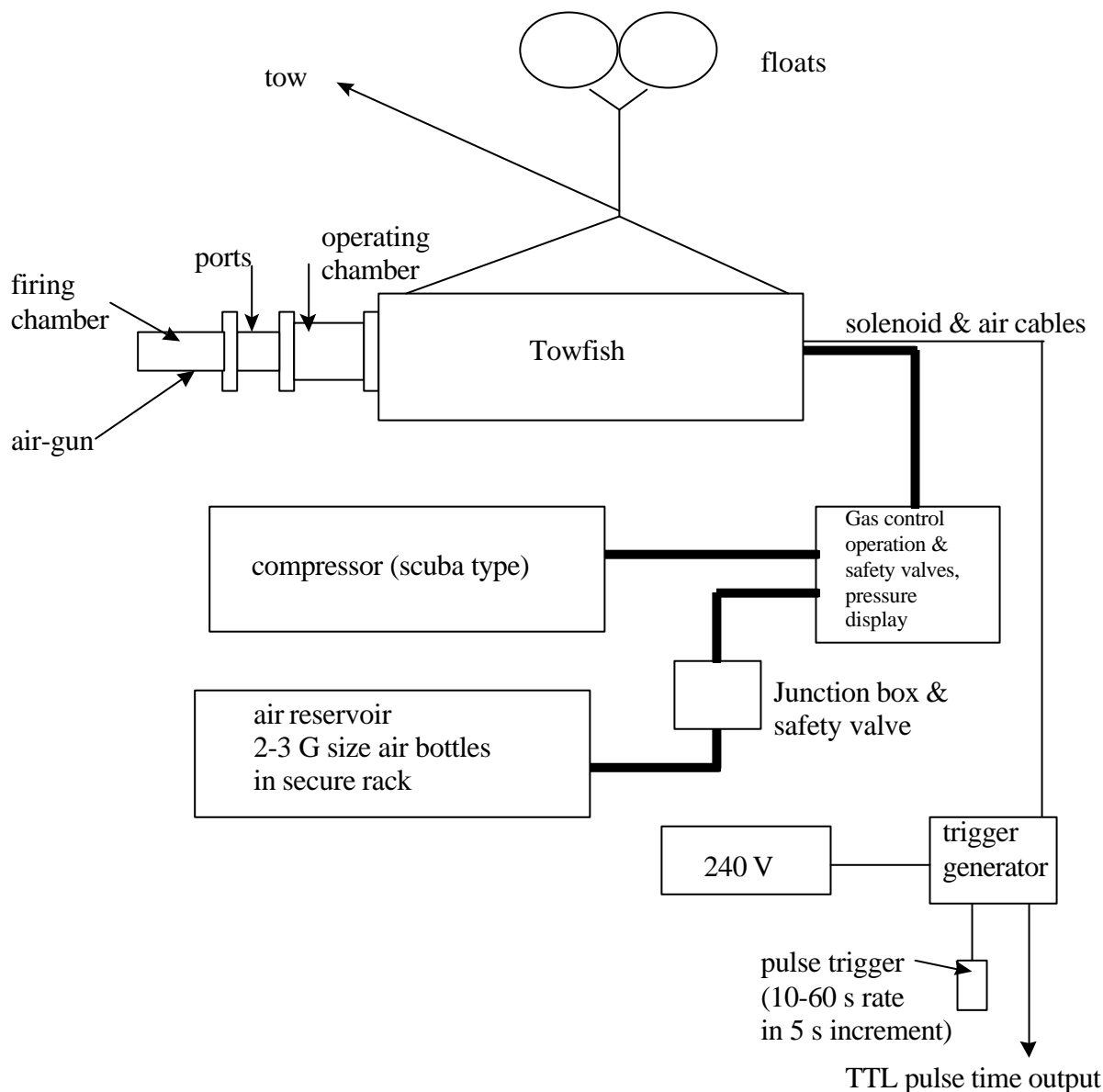
Figure 1 Deployment configuration of Bolt 600B air-gun used in exposure trials. The gun could be deployed hanging vertically from a davit (as used in Jervoise Bay trials), or as shown above, mounted in a towfish for towing (all Exmouth trials). The air-gun was used with a 20 cui firing chamber, operated as best as possible at 10-11 Mpa (1500-1600 psi) and deployed at 5 m depth (Jervoise Bay trials, 1996 Exmouth) or 3.5 m depth (1997 Exmouth trials).

Where sufficient gas was available an air-gun pressure of 10-11 MPa (1500-1600 psi) was maintained during all trials. The air-gun and bottle reservoir pressure were checked and recorded to log books at least

every ten minutes during trials. The air-gun was run off three G sized bottles of industrial nitrogen during all Jervoise Bay sea-turtle, fish or squid trials. With the three sized G bottles and the surface plumbing and air-gun with no leaks, around 320-350 shots could be fired before the gun pressure began to drop. After this gun pressure dropped slowly, until at around 500 shots the gun pressure had reached 7 MPa. The drop in gun pressure with shot number as determined from two trials is shown on Figure 2.

Bolt 600B pressures with shot numbers (3 x G sized nitrogen)
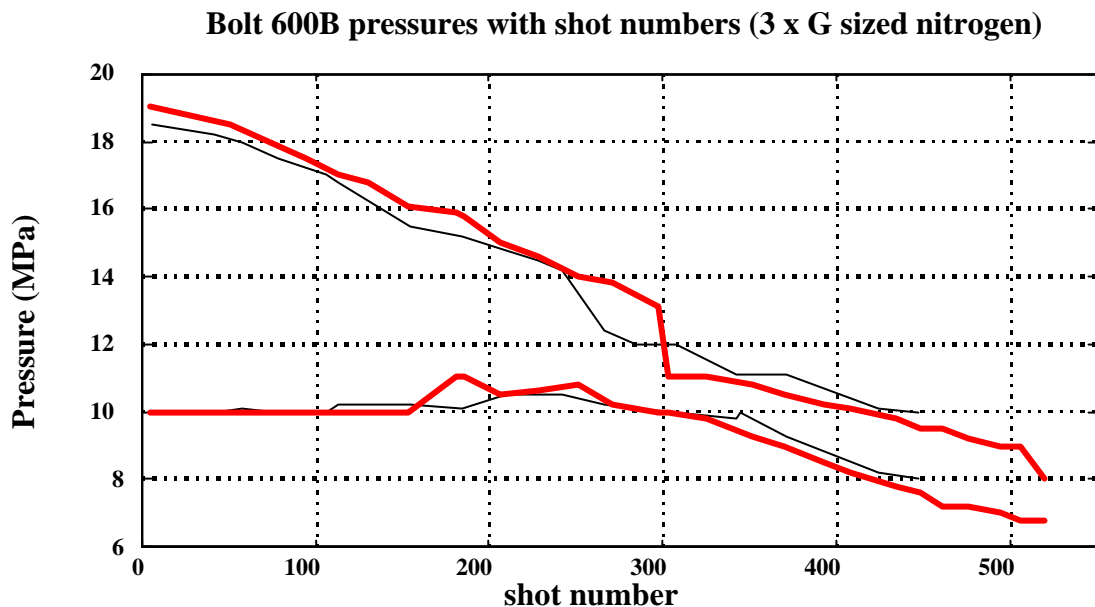
Figure 2 Drop in gun pressure with bottle pressure for Bolt 600 B air-gun, operating with 20 cui chamber, run off three G size industrial nitrogen bottles, and maintained preferentially at 10 MPa gun pressure. The upper curves are bottle pressure, lower curves gun pressure (maintained around 10 MPa until shot 320-350), and the different line thicknesses represent different trials.

During the two sets of trials carried out in Exmouth Gulf (1996 and 1997), the air-gun was operated off a Bauer 0.19 m^3/min (6.7 cu ft/min) compressor. Two G size 14 MPa rated air bottles were used as a reservoir. With this setup, the compressor pressure relief valved fully closed and at air-temperatures below 35° C, the air-gun could maintain a 10-15 s rate indefinitely. The pressure fell away as ambient air temperature increased.

The theory of operation and the acoustic characteristics of the Bolt air-gun are described in section 2.1.1

1.2   Recording Techniques

A range of recording equipment was used over the project duration. Hydrophones were deployed from drifting vessels, drifting housings, moored housings with mid-water hydrophones, moored housings with bottomed hydrophones, or in sea-turtle, fish or squid exposures, with hydrophones attached to or in the containment cage. All recordings were made to digital tape decks (Sony models D3 or D8) which recorded a time stamp to a separate tape track. Each recording set (start - stop, or for packages operating remotely on timers deploy - recovery), was given a recording number, with these numbers used throughout this report.

 Three housings were available during the project. Each of these was capable of being deployed in free run mode or with recording start time and duration controlled by timers.

Specifications of equipment used are given in Table 2. The combinations of gear used, and their designation used throughout this report, are given in Table 3. All recording equipment combinations gave a linear response from 20 Hz to 14 kHz, and were capable of calibration from 10 Hz to 14.5 kHz.

Type	Model; number of; and code	Specifications
hydrophone	Clevite CH17; (1 of)	sens. = -204.7; capacitance = 1.8 nF; cable length = 35 m
hydrophone	Massa TR 1025-C; (1 of)	sens. = -195; capacitance = 38 nF; cable length = 20 m
hydrophone	GEC Marconi SH 101X; (4 of)	sens = (080) -204, (081) -203.5, (082) -203.5, (083) -206; capacitance = 9.4 nF; cable length = all 45 m
hydrophone	Brüel & Kjær 8104; (1 of)	sens. = - 206.4; capacitance = 8.45 pF; cable length = 10 m
pre-amplifier	RANRL type; (4 of); codes UPMP, DPMP (comprising separate split channel amps) CPA6 & CPA7	low noise; input impedance = 1 MΩ; linear frequency response < 4 Hz - > 20 kHz; gain 20 or 40 dB
pre-amplifier	Purpose built; codes CPA1 to CPA5	input impedance = 470 kΩ; linear frequency response 23 Hz - 22 kHz; gain 0 or 20 dB
pre-amplifier	Purpose built; code APMP	input impedance = 10 MΩ; linear frequency response 5 Hz - 22 kHz; gain 20 or 40 dB
tape deck	Sony DAT D3 (1 of)	32 kHz sample rate; 4 hour tape; linear response 20 Hz - 14 kHz
tape deck	Sony DAT D8 (4 of)	32 kHz sample rate; 4 hour tape; linear response 20 Hz - 14 kHz

Table 2 Specifications of recording gear used. All tape decks were used in long play mode giving four hour tapes Sensitivity (sens.) is given as dB re 1 $V^2/\mu Pa^2$. RANRL was the Royal Australian Navy Research Laboratories. Serial numbers of the GEC hydrophones are given in brackets.

Designation	hydrophone	pre-amps	tape decks	timers
Portable 1	Clevite CH17	DPMP	D3 or D8	free run
Portable 2	GEC-Marconi (081)	DPMP	D3 or D8	free run
Housing 1	Massa TR 1025 C	UPMP	D8	free run or 3 min samples at any interval > 20 min
Housing 1A	GEC Marconi SH 101X (082), left GEC Marconi SH 101X (083), right	APMP or CPA series	D8	free run or 90 s samples at 15 min intervals
Housing 2	until Jan 1998 GEC Marconi SH 101X - (080) post Jan 1998 Brüel & Kjær 8104	APMP or CPA series	D8	free run or 90 s samples at 15 min intervals

Table 3 Designation and combination of recording gear used. Specifications of equipment listed are given in table 1.1. Serial numbers are given in brackets for the GEC-Marconi hydrophones. Housing 1 is capable of 120 m deployment, housings 1A & 2, 160 m deployments.

1.2.1 Calibrations

All hydrophones were supplied with factory calibrations sheets for sensitivity. The sensitivity of the Brüel & Kjær 8104 hydrophone was checked with a Brüel & Kjær type 4223 hydrophone calibrator, and found to be within 0.9 dB of the factory calibration specifications at the pre-set tones of 250 and 320 Hz used by the unit. The sensitivity of the other hydrophones were occasionally checked against the Brüel & Kjær hydrophone.

A pink and white noise generator was used to calibrate the gain used in each recording. Pink or white noise of known level was recorded through the pre-amplifier - tape deck combination at the appropriate gain switch settings, prior to or after each recording session, on the tape used during recording. This noise was then analysed (time averaged power spectra) for level during each analysis event, thus giving the system gain and frequency response appropriate for the gear used and the analysis configuration. All recordings were made and played into the analyser using battery powered equipment to avoid 50 Hz mains contamination. The white and pink noise generator output was periodically checked by inputting directly to a spectral analyser.

The total system response for each set of gear is determined by the hydrophone and pre-amplifier capacitance, the tape deck input impedance, and the tape deck and hydrophone frequency response. To check the full system response for each combination of gear used (appropriate hydrophone, pre-amplifier and tape deck), white or pink noise of known gain was recorded with the hydrophone in series. To do this the active leg of the noise signal was input to one side of the hydrophone circuit, and the other hydrophone leg connected to the active of the pre-amplifier input. The frequency response was then checked by analysing the recorded white or pink noise (time averaged power spectra). The resultant curves did not differ greatly from the curves obtained by simply inputting white or pink noise through the pre-amplifier only (no hydrophone in circuit), thus the field recorded noise was used for all calibrations.

1.3   Sea turtle / fish squid trials

Fourteen trials were carried out in which captive fish, squid or sea turtles were exposed to air-gun noise. Behavioural observations were made in all experiments and physiological measurements and pathological examinations carried out in selected fish and squid trials. Twelve of the experiments were carried out at Jervoise Bay, S of Perth and two in Exmouth Gulf. Jervoise Bay trials used a 10 x 6 x 3 m cage, Exmouth trials a 6 x 6 x 3 m cage. Cages were floating pens open at the top, although the Jervoise Bay cage was covered on top during acclimation periods for security reasons. Animals used for physiological measures and control animals were kept in smaller cages (0.5, 0.64, 1 m^3) during trials for ease of sampling or transportation (control fish were sampled then moved away from the site before trials began). All trials used the Bolt 600B air-gun.

Experiments were carried out under permits: Fisheries Department of Western Australia, Scientific Authority 29 (animal collection, 1996-1998); Department of Conservation and Land Management permits SF001918 (1996-1997) and SF002294 (1997-1998); Curtin University Animal Experimentation Ethics Committee permits - fish N-11/96 (1996-1997); fish - R27-98 (1997-1998) and sea turtles R29-98 & N41-97 (1997-1998).

1.3.1 Experimental protocol

A summary of the 14 experiments is given in Table 4. Twelve of these experiments were run inside the Jervoise Bay breakwater, in an industrial shipbuilding complex. Jervoise Bay lies at the N end of Cockburn Sound, S of Fremantle, Western Australia. The site layout is shown on Figure 3. Two trials were carried out in Exmouth Gulf.

All exposures involved the operation of the Bolt 600B air-gun with 20 cubic inch chamber, as described in section 1.1. The air-gun was deployed from a 6 x 2 m pontoon in Jervoise Bay and off a small vessel in Exmouth. The pontoon was kept at the Jervoise Bay cage site, firstly moored off each quarter, then later moved to a fixed four point mooring.

For comparison an example of an air-gun signal as received at Jervoise Bay at 115 m, and a comparative signal produced by a 2678 cui commercial air-gun array at 1.5 km is shown on Figure 4.

Trial	Date	Location	Species	Exposure type	Result type
1	17/02/97	JB	sbr	fix, exp=1:00:20	phy
2	04/03/97	JB	sbr, psx	fix, exp=1:00:45	beh, phy
3	09/04/97	JB	sbr, trv, psn, psx	fix, exp=1:00:38	beh, phy
4	29/05/97	JB	sbr, mul, her	fix, exp=1:00:31	beh, phy
5	04/07/97	JB	sbr, mul, squ, trv, cut	fix, 2 sep by 1:26:25, exp=0:59:50 & 1:01:30	beh, phy, pat
6	18/08/97	JB	gre, log	3 x a-d sep by 1:23:19 & 0:31:49, exp=0:34:17 & 0:29:35 & 0:24:30	beh
7	20/08/97	JB	gre, log	2 x a-d sep by 1:04:31, exp=0:30:00 & 0:30:18	beh
8	22/10/97	Exmouth	cod, psx, but, wra[1]	3 x a-d, exp=1:01:36	beh, pat
9	24/10/97	Exmouth	cod, wra[1], psx, but, sem, sfl	2 x a-d, exp=0:33:35	beh, phy, pat, pin
10	17/04/98	JB	squ	3 & 2 x a-d sep by 1:09:32, exp=0:48:41 & 0:22:04	beh
11	21/04/98	JB	squ	3 & 3 x a-d sep by 1:11:52, exp=0:46:48 & 0:39:13	beh, pat
12	15/06/98	JB	trv, dhu, bcd, wra[2]	2 & 2 x a-d sep by 1:24:14, exp=0:55:56 & 0:41:59	beh
13	19/09/98	JB	psn	2 x a-d sep by 1:12:13, exp=1:05:04 & 0:36:33	beh, phy, pat
14	16/11/98	JB	psn	4 x a-d sep by 0:16:11 & 1:11:20 & 0:03:50, exp=0:24:13 & 0:29:58 & 0:26:30 & 0:09:20	beh, pat

Species codes:

bcd = black-ass cod (*Epinephelus armatus*)

cod = black tipped cod (*Epinephelus fasciatus*), long finned rock cod (*E. quoyanus*), chinamen rock cod (*E. rivaltus*)

dhu = dhufish (*Glaucosoma hebraicum*)

her = herring (*Nematalosa vlaminghi*)

mul = mullet (*Mugil cephalus*)

psx = trumpeter (*Pelates sexlineatus)*

sem = spangled emperor (*Lethrinus laticaudis)*

squ = squid (*Sepioteuthis australis*)

wra[1] = wrasse (*Stethojulis strigiventer*)

but = western butterfish (*Pentpodus vitta*)

cut = cuttlefish

gre = green turtle (*Chelonia mydas*)

log = loggerhead turtle (*Caretta caretta*)

psn = pink snapper (*Chrysophrys auratus*)

sbr = silver bream (*Acanthopagrus butcheri*)

sfl = spanish flag or stripey sea perch (*Lutjanus carponotatus*)

trv = trevally (*Pseudocaranx dentex*)

wra[2] = wrasse

Results types:

beh = behavioural observations - two underwater cameras (B & W high resolution, colour)

phy = physiological measures - blood samples for cortisol and glucose levels, and blood smears for cell counts.

pat = pathological damage - fixation of macula surrounding otoliths for assessment of damage to hair cells (hearing damage)

pin = heart rate pinger

Table 4: Summary of experiments run at Jervoise Bay (JB). Fixed exposures (**fix**) involved a 10 dB signal range with the air-gun moved from 10-30 m off the sea-cage, **a-d** exposures involved air-gun approach-departures with normally a 35-45 dB signal range experienced at the sea cage, although a 70 dB range was used in trial 14. Note that several approach-departures may have occurred during each block of consecutive air-gun operations (times given). Approach-departures were achieved by towing the air-gun pontoon towards and away from the sea cage from normally 350-450 m start range (800 m in trial 14) to 5-15 m closest approach. In later experiments two exposure sets separated by around an hour were conducted. The exposure length for each continual set of air-gun shots is given. Representative fish from each experiment have been kept for morphological examination.
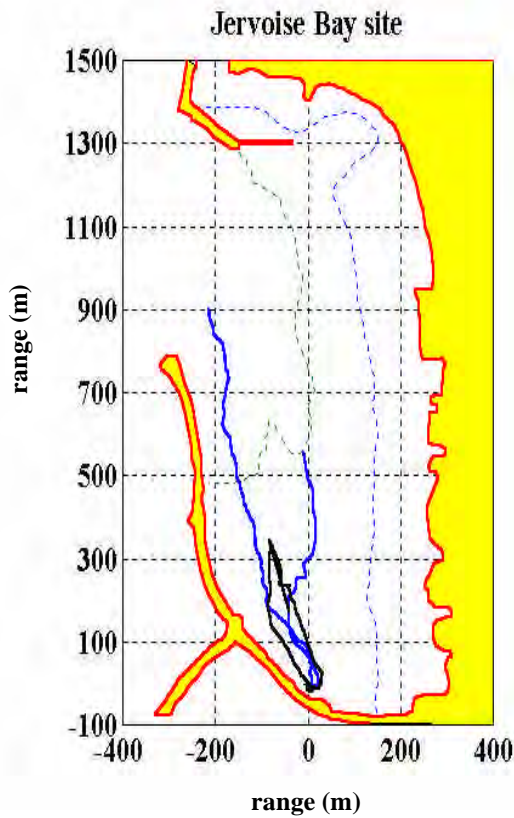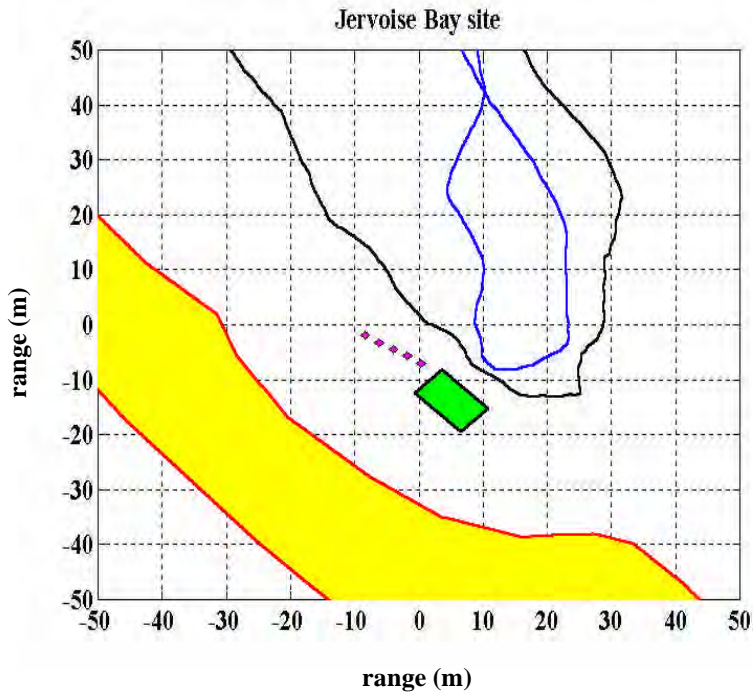
Figure 3: (**top**) Layout of large sea cage and smaller cages at Jervoise Bay site with two approach tracks of the air-gun pontoon shown. (**bottom**) Entire Jervoise Bay facility showing two tracks of the air-gun pontoon. The large sea cage is located at the S end of the breakwater.

The Jervoise Bay site is a uniform 9 m depth, with a fine muddy bottom. The cage was located 30 m off the breakwater wall, fixed by four chain-rope-chain moorings, one from each corner. In experiments 1-5, shown on Table 4, the air-gun was operated off the pontoon which was fixed on its moorings but ranged between 10-30 m off the sea cage. The air-gun pressure was dropped or raised accordingly, with the intention of changing the received mean squared pressure at the cage by as much as possible. It was found that using this technique only a 10 dB signal range could be achieved. During these experiments all cage monitoring equipment cabled back to the air-gun pontoon.

To enable a greater range of levels and a more realistic approach-depart scenario than could be achieved using the air-gun ranged from 10-30 m off the sea-cage, for trials 6, 7 and 10-14 the air-gun pontoon was towed towards and away from the sea cage using a 4.3 m dinghy lashed to the pontoon's port quarter. During trials 8 and 9 in Exmouth Gulf the air-gun was deployed from a vessel and this used to approach and depart the sea cage. Using a typical start range of 350-450 m and a closest approach of 5-15 m gave a signal range of 35-45 dB at the sea cage. In experiment 14 a start range of 800 m was used in one approach giving a 70 dB range of air-gun signals at the cage. A comparison of received signal energy for each technique is shown on Figure 5. For the approach-depart experimental regime the cage monitoring equipment was cabled back to a caravan on the breakwater, with the air-gun pontoon and monitoring site in radio contact.

Sound levels experienced by fish in the large sea cage were monitored using a GEC-Marconi SH101-X hydrophone situated in the cage centre or just outside the centre of the cage's long axis, with the hydrophone always at 3 m depth. Separate hydrophones at 50 cm and bottomed were deployed in trials 13 and 14 to monitor change in received signal with depth. Signals were recorded as per the methods section 1.2. The tape decks logged real time, thus allowing precise correlation of air-gun signal to behavioural observations.

Two sets of ambient sea-noise measurements were made in Jervoise Bay. These recorded 60 s samples at 15 minute intervals for three day periods. Jervoise Bay is a commercial ship building facility, thus there was some vessel traffic which may have cause elevated sea-noise levels within the Bay. These sets of sequential samples describe the 'typical' and maximum noise exposures experienced by fish held in the experimental facility during acclimation periods. The recorded levels for a 36 hour period showing typical vessel noise spikes are shown on Figure 6.

Sea cage:
The Jervoise Bay sea cage was originally constructed as 15 m long, six m wide by four m deep. Eight individually sealed 150 mm storm water pipes were used as flotation (the cage was thus floated at the surface). A flexible join was used on the long axis to cope with wave motion. Each corner of the cage was attached to a mooring (380 kg railway wheel or breakwater) using chain-rope-chain lines. Until November 1997 the cage was permanently lined with 40 mm mesh heavy ply trawl net. This was periodically cleaned by divers, with fouling being a major problem. After the first trial it was realised we needed a lighter mesh liner in the cage so as to more easily recover fish after experiments. A liner of 16 mm light net was made and this deployed in and lashed to the heavier net before and recovered with fish after each trial. Because of the lack of material available at the time the liner was made as 10 m long, which transpired to be a suitable length for coverage by the two underwater video systems. In November 1997 the cage was redesigned, and cut down to 10 m (long) x 6 m (wide) x 3 m (deep) and a light steel frame added to define the underwater section of the net. The heavy ply trawl net was not re-deployed. A new liner of 16 mm mesh was constructed which fitted neatly into the cage. This was deployed before each trial and recovered after, so reducing, but not eliminating, the fouling problem. In the late summer months fouling was

particularly heavy at the site, and a deployment of six weeks in early 1998 (trials 10 & 11) resulted in a weight of tube worms which almost sank the 4.3 m dinghy used to recover the net.
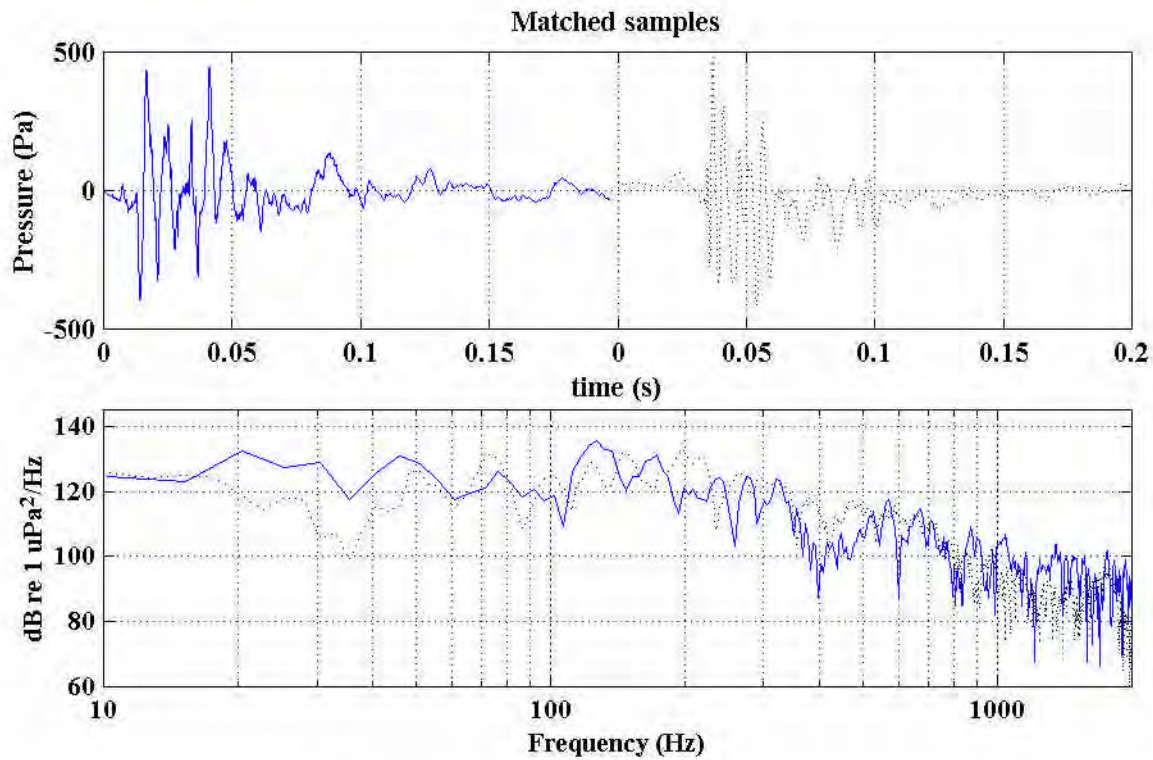
Figure 4 Comparative waveforms (top) and frequency spectra (bottom) of air-gun signal: as received 1.5 km from a 2678 cui air-gun array at 68° off the array bow from a hydrophone at 25 m depth (solid line); and as recorded at the Jervoise Bay sea cage with the Bolt 600 B air-gun at 115 m range (dotted lines). The signals were matched primarily on their total energy.
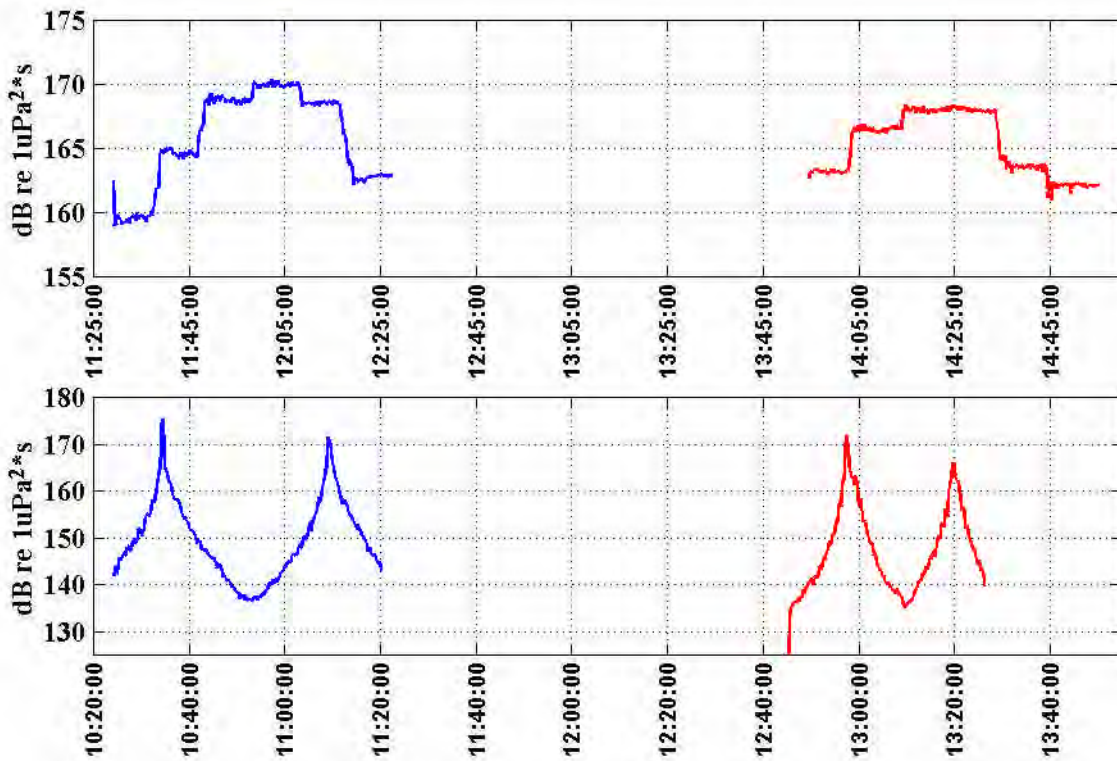
Figure 5 Air-gun exposure regimes for Jervoise Bay experiments. Top is the air-gun signal equivalent energy for experiment 5 (Table 4) with the air-gun pontoon range from 10-30 m off the sea cage, below is the equivalent energy for experiment 12 where the pontoon was towed from 350 m to 5 m from the sea cage.
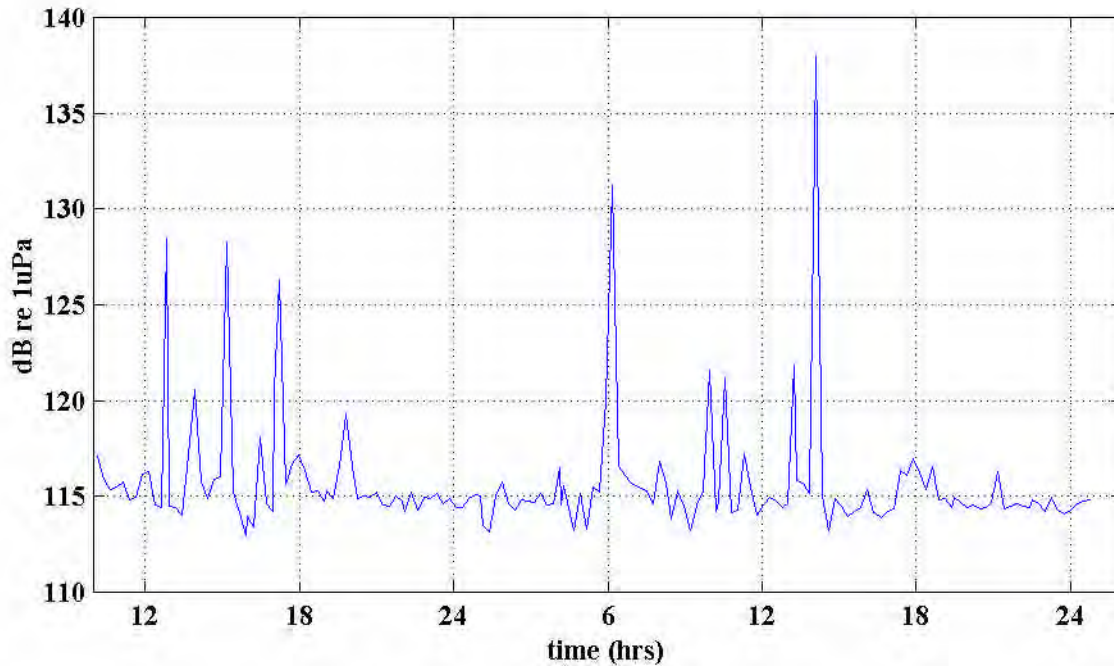
Figure 6 Background noise levels recorded in Jervoise Bay during acclimatization periods. Levels are given as broadband units (dB re 1 µPa). The spikes show the passage of nearby vessels (up to 60 m length, propeller and jet driven).

To reduce predation in the cage by shags and fisherman, a top of 40 mm trawl mesh was fitted to the cage and a sign warning of chemical contamination from fish in the cage attached. We lost fish to fisherman and routinely recovered fishing gear from the cage top, sides and mooring lines. The pontoon also made a good target for many of the stone-throwing inclined youth who frequented the breakwater, and became somewhat battered from direct hits with rocks over time.

The net used in the Exmouth Gulf trials (8 & 9 Table 4) was constructed in a similar fashion to the Jervoise Bay sea-cage. Its dimensions were 6 m x 6 m x 3 m depth (floated at the surface), and a 16 mm mesh liner was used. Owing to strong currents during these experiments (up to 1.5 knots) a steel frame for the underwater section of the net was constructed in Exmouth. The liner was attached to this. This deployment used a single point mooring off one corner of the cage. The net was moored in 10 m of water.

Capture and acclimation of animals

Animals were captured using: baited hooks; squid jigs; trawling; beach seining; gill nets; or purchased from commercial aquaculture farms. Most of the silver bream and pink snapper used in trials were bought from an aquaculture enterprise. These fish were used to define techniques. Animal transportation involved an aeration system using a SCUBA feed from compressed air bottles, large plastic bins or tubs and a water pumping system.

All experiments involved accumulating animals over time and acclimatizing them to the cage, the presence of divers in the cage and dinghy work around the cage. For Jervoise Bay trials this involved a two to four week period before trials. During the Exmouth trials the field work time schedule did not allow this and animals were in the cage for only a few days prior trials. All animals were fed pilchards or baitfish daily or every second day and the cage cleaned and checked by diver at least every four days. During the Jervoise Bay trials it was normal that animals learnt to correlate the dinghy arrival with being fed, so that they would come to the surface when the dinghy arrived. This learning behaviour was particularly strong in the squid.

1.3.2 Behavioural observations & analysis

Animals housed in the large sea cage were used in behavioural observations. A high resolution black and white video camera (Panasonic 1/3 CCD, WV-BP312 with 4.5 mm focal length lens) was placed in the SE cage corner and a colour, digital, video camera (Sony 1/3 CCD DC10P with 4 mm focal length lens) in the NE corner (Figure 3). These cameras had horizontal and vertical fields-of-view of 114° & 87° and 132° & 101° for the Panasonic and Sony cameras respectively.

Cameras were fixed into the cage corners by attachments to the net or a steel frame, by diver. Each camera had a spirit level for horizontal alignment. Different species tended to occupy different vertical sections of the cage, so the camera depth was adjusted to match the depth range of the most abundant species (as determined by observations during acclimatization periods). The cameras cabled back to pontoon or breakwater and were logged to tape on two Samsung VCR's. A single monitor which could be switched to either camera was used to view animals during trials. Once activated, the VCR displayed time bases were checked against a master watch to allow correlation of the air-gun operations with behaviour. For experiments made with the VCR's on the pontoon, sound was recorded to each VCR from a single microphone suspended on the pontoon. This allowed verbal notes and the air-gun signal (which could be clearly heard above water) to be logged to video tape. For experiments made with the cameras cabled back to the breakwater and the pontoon ranged from the sea cage, underwater sound was cabled to the VCR units from a Clevite CH17 hydrophone, through a 40 dB gain impedance matching amplifier. Thus the background noise and air-gun signal were logged to tape. The VCR units had an automatic gain control on the audio input, hence the air-gun signals were not recorded faithfully, but were present, so allowing correlation of behaviour with air-gun signal.

The experimental regime for behavioural observations involved an hours pre-exposure observation with the VCR's running, exposure observation and 45-60 minutes of post exposure observation. In later experiments a second air-gun exposure was carried out 50-100 minutes after the first exposure, and again a 45-60 minutes post exposure behavioural observation made. Thus from 3-5 hours of video for each camera (or 6-10 hours in total) were made for each trial with up to three hours of control periods (no air-gun operations).

A series of two character codes were used to describe behaviour from the video tapes. The full set of codes are listed in Appendix 1. To record behaviours from a video the codes were entered to computer whilst watching the video. For consistency a single observer scored all videos. Codes fell into the categories: general housekeeping (time calibrations, air-gun operations, animals in or out of view, etc); swimming patterns (horizontal, vertical, direction, rates, changes of direction, etc.), location within the field of view (top of field of view, middle, bottom, left hand side, right hand side), specific behaviours, and where applicable startle and alarm response codes. Codes were generally applied at the species level. For schools of fish or squid, codes were differentiated as applying to individuals or as a general behaviour of the school, for the turtle trials they were specific to each individual turtle. The data entry program recorded a time stamp for each carriage return. These times were subsequently adjusted to the master experiment time to correlate behaviour and air-gun noise exposure. The program was capable of being paused yet maintained its time base relative to the video.

The field of view of each camera did not overlap, thus camera results were considered as separate samples. The audio signal was present during all video scoring sessions. This was both an aid and bias in analysis. It was used to check on time correlations since the time of the first few and last air-gun shots per run was always recorded accurately by the air-gun operator, and could be used to precisely align the video scoring times with the master time base. This accounted for the reaction time of the video observer in

entering the data into computer. It also allowed precise definition of behaviours that correlated with air-gun signals. But the air-gun signal presence could be considered a bias, in that it meant video scoring was not done completely blind. Any bias was believed reduced by the automatic gain control on the VCR input. The high gain used on the input to the VCR (the preamplifier gain used was 40 dB for all trials) meant that except for very distant signals, the VCR normally clipped air-gun signals to a constant level. Thus although the presence of the air-gun signal was known to the scorer, information on its range from the sea cage based on the comparative level of signals was not available, so reducing observer bias. There were several behaviour codes which were un-equivocal. For example the depth location of fish could not be biased in scoring (if the fish were in the cage bottom they were in the cage bottom). In analysis several of these behaviours types were converted to times, so the number of behavioural scores became irrelevant.

1.3.3 Physiological techniques

Blood samples were taken from selected fish species (control and exposed) for monitoring of their stress response to nearby air-gun operations. These fish were housed in cages of volume 0.5 (two cages), 0.64 (two cages) or 1 m^3 (two cages), kept within 10 m of the large sea cage. In the 1 and 0.64 m^3 cages, fish were stocked at densities of up to ten fish per cage and at up to five fish per cage in the 0.5 m^3 cages. These were considered low stocking densities for the size of fish and cage. All animals were collected, acclimated and fed as for the fish in the large sea cage described above. Up to the point of a trial exposure, there was no difference in the treatment or stocking density between control and experimental fish. Cages were set up several days before trials began and on the day of the trial were not disturbed until samples (control or exposed fish) were required to be taken. The cages were located either hanging from the large sea cage flotation or parallel to the air-gun pontoons track, with the cage bottom at 3 m depth. This ensured that the hydrophones set up along the large sea-cage were indicative of levels received at each smaller cage.

The cages of exposed fish were not moved during a trial (other than being lifted to the surface for fish recovery) or during any sampling period after a trial. Samples were taken from control fish immediately before exposures began with the cages having not been moved to this point in time. During trials where control samples were to be taken at intervals after trials, cages containing un-sampled control fish were moved on the morning of the trial to an area sheltered from the air-gun noise during the trial, and returned to the large sea cage site immediately after air-gun exposures ceased. The cages were towed slowly from the bow of a dinghy. They were not sampled until several days after being moved (post trial). As there was some vessel traffic in Jervoise Bay (eg. Figure 6) it was considered prudent to keep all controls at the large sea cage site and not somewhere permanently sheltered from the air-gun track (and hence where the cages did not require moving). This ensured that control and exposed fish experienced the same conditions (water quality, sound exposures etc.) during the acclimation and post trial period. This decision was later justified by dolphins creating an anomalous spike in cortisol levels ten days after a trial.

To collect blood samples, fish were captured from the small cages using dip-nets, anaesthetised using MS222, and 5-10 ml of blood was collected from the ventral aorta using a syringe. Samples were immediately placed on ice, transported ashore, centrifuged to separate the cellular and plasma components, then held in a freezer. Exposed fish were first sampled at intervals ranging from a half hour after the first close air-gun passage, to a half hour after the first hour of air-gun exposure ceased. For several trials control and exposed fish were sampled at two day intervals for up to 14 days after a trial and in one trial fish were sampled every hour for five hours after the first passage of the air-gun.

In analysis five fish were used to define a sample point, with blood from each fish analysed separately and the results averaged for the sample. It was found that fish could be re-sampled at a minimum of 6-7 days.

Blood samples were analysed for the stress hormone cortisol, using radioimmunoassay kits (Cortictk-125, P2687 supplied by Sorin Biomedica) and scintillation counts. Glucose levels of the blood were also measured using kits supplied by Sigma Diagnostics (Glucose, procedure 510). As stated the results were averaged, such that five fish with the same treatment represented a sample.

1.3.4 Pathological techniques

Control and exposed fish were removed from a cage (large sea-cage or smaller cages) prior to and after air-gun noise exposure. These fish were sacrificed after anaesthesia (MS222, chilling down or both) and decapitated. The ears were then exposed and fixed in 4% gluteraldehyde solution buffered in seawater. After fixation the samples were washed in the buffer solution and the saccular macula (usually left and right macula) of each ear carefully removed. With practice the hair cell populated portion of the macula could be recognised with the unaided eye. All attempts were made to avoid placing forceps on this hair cell populated region. The maculae were dehydrated through a series of graded acetone solutions, critical point dried, mounted on a stub and sputter coated in gold. The samples were then observed through a scanning electron microscope (SEM, Philips XL 30). The sensory hair bundles present on the surface of the macula of the fish exposed to the air-gun noise and the macula of the non-exposed fish were compared for potential damage.

Only saccular macula were examined in this set of observations. Although it known that the other end organs of the fish inner ear may play some role in audition, it is considered that for non specialist fishes at least, the saccule is one of the more important end organs associated with hearing (Popper and Fay, 1993). All fishes examined in this project were non-hearing specialist fishes (with the distinction being that hearing specialist fishes have some direct coupling between a gas bubble and the inner ear system whereas non-specialist fishes do not, Popper and Fay, 1993). Prior to the trials it was not known if air-gun signals did cause any pathological effects to fish hearing systems, thus efforts were concentrated onto a single hearing end organ, the saccule macula.

Maculae from fish exposed and not exposed to air-gun noise were observed and any damage to the sensory hair bundles present on the maculae surface recorded. The left and right macula from each fish were examined at 80 X magnification. A split screen was then used to observe smaller sections at 470 X magnification. For a quantitative analysis of damage to pink snapper (*Chrysophrys auratus*) a grid of eighty nine sections per macula was used with the same section locations used for each macula. Each of these sections covered an area of 23,500 μm^2.

Similar methods to above were used for obtaining samples of the squid statocyst system. The organ responsible for detecting vibrations in the squid is called the statocyst. Squid were sampled before and after exposures and the squid statocyst was dissected to expose the inferior and superior macula neglecta and the macula princeps. These were then fixed as above and observed through the SEM.

1.4   Humpback trials - Geco Resolution work

Over the period 4th October to 8th November 1996 WMC Petroleum carried out the *Robert* seismic survey NE of Exmouth Cape, in permit WA-264-P. This comprised a 3D seismic program, followed by a smaller 2D component covering 98.2 km. The Geko-Prakla vessel, the *Geco Resolution* carried out the survey. The 3D tracklines ran E-W, within the area shown on Figure 7 (top). This 3D portion of the survey ran 50 km E-W at its N most trackline, 13 km to its S most trackline, and covered approximately 498 km^2. The *Geco Resolution* employed two 2678 cu in, 12 element air-gun arrays separated by 80 m, operated alternately at a mean eight s firing interval. Details of the air-gun array configuration are given in section 2.1.3. The vessel trailed four, three km long hydrophone streamers. The 3D component of the survey comprised 183,586 air-gun shots over 33.4 days. After the survey completion WMC Petroleum made available the differential GPS location with date and time stamp, for each 3D shot fired during the survey.

1.4.1 Aerial surveys

All aerial surveys employed a Partenavia twin engine high wing aircraft, chartered from Tropicair aviation of Carnarvon. The aircraft was heavily booked throughout the field period, thus aircraft availability to a large extent dictated the timing of flights. The aircraft operated from a dirt airstrip 10 km S of Exmouth. An aerial survey grid comprising 8 x 30 n mile (55.6 km) legs running on headings 330° (or 150°) at five n mile (9.3 km) intervals was established. The grid and transit leg are shown on Figure 7- top. The aerial survey region encompassed the seismic survey area, waters to the N of the seismic area, and the shallow waters inshore of the Island chain running NE of North West Cape. The heading of legs was chosen to minimise glare and to run at approximately right angles to the depth contours over the seismic survey area. The first leg began over Fly Island to the ENE of Exmouth. The aircraft was navigated by GPS co-ordinates, using visual cues on the shoreward end to guide the turns. The aircraft was flown at 1000 ft (305 m) and 120 knots (222 km/hr) at all times during flights. The aircraft had an endurance of slightly greater than four hours, consequently the aerial survey grid was laid out to give a total flight time of 3.5 hours.

The aerial survey area encompassed inshore (coastal side of island chain) and offshore (seaward side of island chain) waters. These offered different sighting conditions, the former comprising greenish waters and the latter deep blue water. These different water bodies gave different contrast for humpback whale sighting cues. Additionally it was found that wind and tidal regimes were often different between inshore and offshore, particularly with strong tidal rips sometimes present inshore but absent offshore.

A port and starboard observer in the rear seats were used on all flights. Information logged by observers included: port or starboard observer; on survey - 330/150° legs, or off survey - turns or transit; pod composition; pod orientation relative to aircraft; pod distance from aircraft trackline from calibrated markers on window or underwing stringlines; pod bearing relative to aircraft trackline; sighting conditions; and altitude (starboard observer). The aircraft track was logged to portable computer at 2 s intervals by a Garmin 89 aviation GPS unit. All observer notes were made aboard the aircraft verbally to separate tracks of a Sony TCD D8 digital tape deck, and transcribed at the end of each flight.

The sighting field of view was considered as within 100 - 3200 m of the aircraft trackline. The probability of sighting animals would be expected to vary within 3200 m of the aircraft's trackline. Since the study was comparative, in that it compared sets of flights before the seismic period with sets of flights during the seismic period, and that the techniques were constant, no sighting-bias corrections were made for distance off the trackline. The field of view was split into three sectors using underwing stringlines. The on-water range from the aircraft's trackline for the centre of each sector were 100-450 m, 450-1100 m, 1.1-3.1 km. Sightings beyond 3.1 km were noted but not used in analysis.

Exmouth region

Exmouth Gulf whale tracks
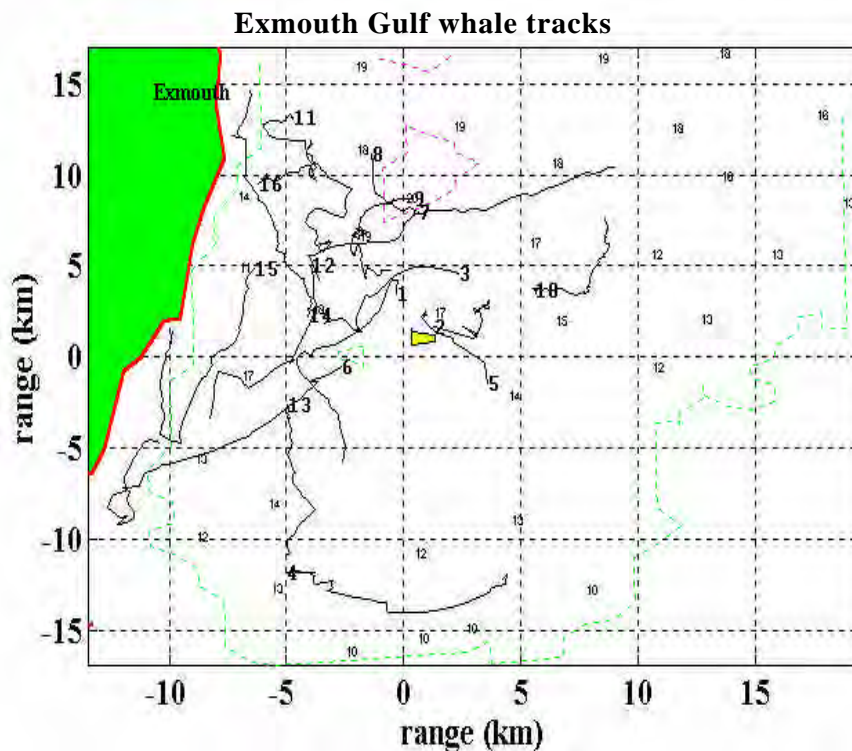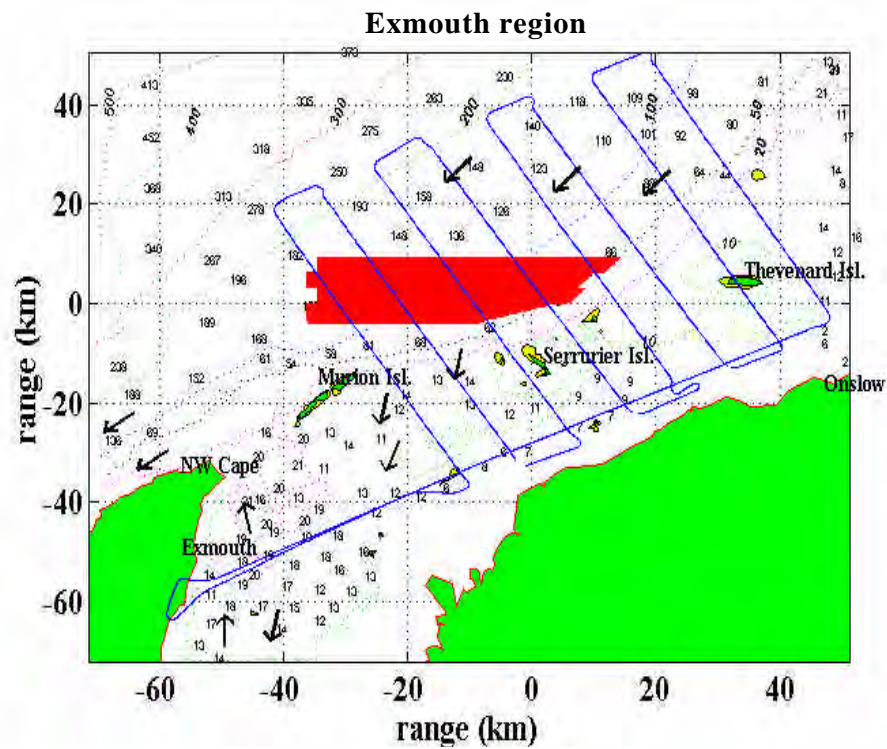
Figure 7 (**top**) Region of seismic survey off Exmouth showing seismic area (dark shaded), aerial survey full flight path and general movements of humpback whales through the region (arrows). Depths are in metres, scale is arbitrarily centred on 21° 30' S, 114° 40' E. (**bottom**) Region in Exmouth Gulf in which approach trials were carried out, showing the whale tracks for all trials (1-16). Scale centred on 22° 4' S, 114° 13' E.

1.4.2 *Blue Horizon* observations about the *Geco Resolution*

The 18.3 m long Exmouth based vessel, *Blue Horizon* was chartered for working about the *Geco Resolution* (eight days). Work carried out on the *Blue Horizon* included: deploying and retrieving drifting or bottom mounted acoustic recording equipment; taking ship board sea-noise measurements and salinity, temperature and depth profiles; and tracking the movements and behaviour of whales in the vicinity of the *Geco Resolution*.

The tracking of whales on interception courses with the *Geco Resolution* involved the *Blue Horizon* steaming around 10 km to the NW or NE of the *Geco Resolution* (depending on wether it was working a W or E trackline respectively) to locate whale pods. In the region of the seismic survey it was believed that most whales would be heading on approximately SW courses. Once located pods were followed with the *Blue Horizon* ideally maintaining a position from 200-500 m off the port or starboard quarter of the pods track. In practice this range varied from 50-3000 m as a result of whales approaching the vessel, stops for sea-noise recordings or because of rapid swimming by whales.

Observations of whale behaviour incorporated 30-40 minute segments during which all behaviours and movements of individual whales were logged. Behaviours, dive and blow times were called by the chief observer and recorded to notebooks. Whale bearings relative to the *Blue Horizon* were located by hand bearing compass or bearings relative to the *Blue Horizon* track and whale range determined from sextant angle below the horizon, or visually estimated. The *Blue Horizon* GPS position was logged to PC from a Garmin 45 unit or manually recorded with time from the ships Furuno unit.

1.4.3 Ship based observer

WMC Petroleum organised the logistics of placing an observer aboard the *Geco Resolution* for the duration of the *Robert* survey. The whale recording entailed observations of 40 minutes in the hour (a sighting block), with 9 blocks per day (0630-0710, 0830-0910, 0930-1010, 1030-1130, 1230-1310, 1330-1410, 1430-1510, 1530-1610, 1630-1710). Observations were made from either wing of the *Geco Resolution*'s bridge. The ships crew were requested to assist in distance measurement or calibration of equipment (a mate or the skipper was in the bridge at all times). Observations entailed noting: the sighting cue; pod composition; range and bearing from the ship; whale orientation with respect the ships heading; the whales track where possible; obvious whale behaviours; sighting conditions over the survey effort block; wind speed and direction; observers; the ships position at the start and end of blocks; the ships heading; wether the air-gun arrays were operating, started, or stopped over the block; information on other fauna sighted; photographic notes; and general notes.

The range to a whale pod was visually estimated in consultation with the crew or calculated by using 7 x 50 Fujinon binoculars with a range finding graticule. This consisted of a set of vertical graticule marks in one binocular eyepiece at fixed distances apart. On calibration each graticule unit was found to subtend 16.52' of arc. The top graticule mark was placed on the horizon and the number or fraction of graticule marks to the pod recorded. This measured the angle of the pod below the horizon. The range to the pod was determined from the angle of the pod below the horizon and the height of eye of the observer. The *Geco Resolution* bridge deck was 12 m above sea level, and the observer height of eye was taken to be 1.5 m. The ship board observer calibrated the eyepiece aboard the vessel by measuring the angle below the horizon in graticule units to objects whose range was determined by radar. These calibrations were then checked against the algorithm developed to give range from angle below the horizon and found to give a good match.

Bearings to pods were made using sighting compasses mounted on each wing of the bridge. These were

then referred to the ships true heading displayed on the GPS unit in the bridge to give the true bearing to pod. Where possible the position of pods with respect to the vessel was made every few minutes. In practice not all whale details could be recorded as many sightings were fleeting or once off, and whales often submerged before accurate position fixes could be made.

1.5 Humpback trials - exposure experiments

Humpback whales were approached with the operating Bolt 600B air-gun to ascertain any changes in movement patterns and behaviour. Seven trials were carried out in Exmouth Gulf in October 1996 and nine in October 1997.

Approach trials were carried out under Curtin University Animal Ethics permits N34-96 (1996) and R30/97 (1997), Western Australian Conservation and Land Management permits SF001918 (1996) and SF002294 (1997) and under the *Whale Protection Act (1980)* through the Australian Nature Conservation Agency, permits 96/00619 / P1996/047 (1996) / P1997/053 (1997). Details of the safeguards stipulated by the permits are given in Appendix 2.

Two vessels were used in trials, the 8.5 m length *Flying Fish* to deploy the air-gun and acoustic packages and the 12 m length *WhaleSong* as the observation vessel. The Bolt 600B air-gun with 20 cubic inch chamber was deployed towed vertically in a towfish 15 m astern the *Flying Fish* at 5 or 3.5 m depth (1996 and 1997 trials respectively). The air-gun was operated every 10 or 15 s (two and 14 trials respectively), at 10-11 MPa (1500-1600 psi) operating pressure.

The tracks of the *WhaleSong*, for each trial are shown on Figure 7 - bottom. Water depths in the study area ranged from 15-20 m over a sand/mud bottom.

A trial involved the *WhaleSong* locating a suitable pod, observing behaviour and movements for 30-70 minutes, then calling in the *Flying Fish* some 10-15 minutes before the end of the pre-exposure period. The *Flying Fish* would position itself approximately five km off the pod, on a heading which allowed the trial pod plenty of clear water for any avoidance response. The *Flying Fish* then deployed a moored housing with a four hour tape in the free run mode near its starting position. These used bottom mounted or mid water hydrophones. Recording equipment was as per Table 2 and Table 3. Within a designated time period (with actual start time not known by *WhaleSong* crew) the *Flying Fish* activated the air-gun and began approaching the pod at 2-3 knots. The mean approach speed during the 1996 trials was 1.18 ms^{-1} (2.4 knots) and during the 1997 trials 1.59 ms^{-1} (3.2 knots). As far as possible the *Flying Fish* maintained a constant heading towards the pod. The GPS position of the *Flying Fish* was logged to laptop computer every two s.

During exposures the *WhaleSong* observers continued behavioural observations and followed from a few hundred metres astern pods. During all *WhaleSong* observations details of several focal animals' identification cues, behaviour, respiratory rate and general pod interactions where made to notebooks according to a defined protocol, to eight mm video and to the audio track of the video. Whale photo-identification shots were made for reference to the Western Australian humpback whale identification catalogues. Positions of the target pod from *WhaleSong* were obtained using hand bearing compass to obtain bearings and by sextant angles below the horizon or visual estimates for range every three or five minutes (1997, 1996 trials respectively). The GPS position of the *WhaleSong* was logged to computer. All observations were made under motor, a 50 Hp four stroke outboard, ideally from 100-400 m astern the tracked pod, but occasionally closer when whales approached the vessel. Spot measures of background sea noise and air-gun levels were made from *WhaleSong*. After the air-gun exposure ceased 30-70 minutes of post exposure behavioural observations were made.

1.6 Analysis techniques

1.6.1 Signal analysis

Analysis of recordings was made by inputting signals to a Data Physics DP430 signal analyser card installed on a 166 MHz Pentium PC. The DP430 card was calibrated in March and September 1997 at the factory. The DP430 analyser enabled power spectra to be made directly from recordings, has a dedicated bank of 1/3 octave filters from 0.488 Hz to 20 kHz for 1/3 octave analysis, enabled signals to be digitised for later analysis, and has a programming capability for automating data collection and analysis.

A program was built which captured and saved input air-gun signals. This used a trigger function to capture the signal (using a delay to get the signal start), checked and rejected the signal if it did not pass a criteria (to reject shrimp or transient noise), then if accepted saved the digitised signal and capture time to files, reset the trigger setting and analysers input voltage range according to the captured signal, then reset the trigger and awaited the next capture. Thus the program could capture successive air-gun signals at a desired sample rate, had some shrimp and other unwanted transient rejection capability, and was capable of tracking the air-gun signal to maintain trigger level and the analyser's optimum dynamic range settings. The program was capable of capturing air-gun signals at a minimum two second interval. Sample intervals used in capture ranged through 48 to 784 µs in doubling increments with 4096 samples saved per capture.

Digitised air-gun signals (in volts) were then post processed either by being read back into the DP430 analyser (for 1/3 octave analysis), or in the Matlab signal analysis environment. Calibration factors were used to convert captured waveforms in volts to pressure units, or from converting DP430 analysed signals to waterborne sound units. Once processed (section 2.1.1) signals were checked for any transients which had slipped through the shrimp rejection process and these removed from further calculations.

Saved waveforms were analysed for frequency content in 1/3 octave bands over the centre frequencies 25 Hz - 5 kHz. A DP430 program recalled each air-gun pulse waveform, then in sequence, calculated its Fast Fourier Transform, auto power spectrum, then applied the 1/3 octave filters to give 24 1/3 octave levels in dB V^2. A calibration value (absolute value of the hydrophone sensitivity minus the gain in recording system from white or pink noise recorded in the field and as measured during analysis) was added to this, the 1/3 octave bandwidth correction applied and the 1/3 octave levels saved in units of dB re 1µPa^2/Hz. Thus the 1/3 octave levels for the entire sample block were measured. Valid 1/3 octaves for the differing sample rates are given in Table 5.

Sample rate (■■)	Valid 1/3 octave centre frequency range (Hz)
48	25 - 5000
96	25 - 4000
192	25 - 2000
384	25 - 1000
768	25 - 500

Table 5 Valid 1/3 octave centre frequencies for given sample rates, as output by DP430 program for analysing 1/3 octave content of air-gun signals.

Specifics measurements made of air-gun signals are described in section 2.1.1

1.6.2 Geographic processing

During all vessel trials, GPS date, time, latitude, longitude and status information were logged to laptop computer. Files were either raw data files as output by the particular GPS (NMEA output, usually a 2 s sample rate), or as saved by software for Garmin 38 or 45 GPS units. Differential GPS co-ordinates of air-gun shot points, with time and date stamps, were also supplied for several seismic surveys. All GPS latitude and longitude co-ordinates were transferred to a metric system. Co-ordinates were converted to the Universal Transverse Mercator reference (UTM), or to an x-y co-ordinate system with an arbitrary reference point, using equations given by Vincenty (1975) for great circle range and bearing between two latitude - longitude co-ordinates. Reference points were chosen central to each trial area.

For some vessel tracks transferred x-y co-ordinates were smoothed using a running linear fit for straight tracks (usually 5-10 points ahead and astern each point used in fit), or a running second order polynomial fit used for curved tracks.

For back calculating source location for a received air-gun shot for measurements from the 3D *Robert* seismic survey (section 1.4 for survey, 2.1 for field measurements) an iterative technique was used. At a first approximation the received time was used to estimate source-receiver range, this range was then converted to travel time, subtracted from the received time and the nearest shot-fire-time point located in the source position file. The range was recalculated and the process iterated until the shot time fell within 2 s of estimated travel time (based on travel time subtraction from received time) or 9 iterations were carried out (to allow for error in measurements of received time). Once the fired shot point was identified the vessels y position (latitude) and trackline heading were used to determine if the shot was from the port or starboard array (since the *Robert* survey tracklines ran E-W).

For calculating azimuth of receiver (hydrophone) from source (air-gun or array) a triangle was set up and the angle at the source location subtended by the vessels trackline and receiver location calculated. This used the source position, an arbitrary point ahead of the source's trackline, and the receiver position. The arbitrary point ahead was determined by extrapolating the vessels past track, or by using the position 10-100 smoothed or differential GPS points ahead. For calculating the azimuth of the 3D source array the appropriate port or starboard array had to be first determined and the trackline heading or position ahead chosen accordingly. All receiver-source azimuth's are given as angle from the array direction of tow, thus dead ahead was 0°, abeam 90° and astern 180°. Arrays were assumed to be symmetrical to direction of tow, thus port or starboard azimuth's were not discriminated.

1.7   Units & conventions

SI units are used throughout this report. In some instance imperial units are also given. All times stated are WST (equals UTC plus eight hours). All compass headings have been abbreviated. Unless otherwise stated errors about the means are 95% confidence limits of the mean.

All acoustic measurements are presented with full units. Band limits for the DP430 1/3 octave analyser are given in Appendix 3. Statistics of decibel values were calculated using values converted to intensities the statistics applied (including 95% errors), then these values converted back to decibel values (decibel statistics).

2 - RESULTS

2.1 Air-gun signals, arrays, propagation and exposure (R.D. McCauley, A.J. Duncan, J.D. Penrose)

2.1.1 Signal production and character

Air-gun signals are produced by the sudden release of compressed gas (usually air) into the water through a series of ports. The sudden out-rush of air results in a rapidly expanding bubble. The outflow across the ports and the rapid bubble expansion produces the primary noise pulse, a short signal with a wide frequency band of energy. The bubble formed, which if not broken up by some means, oscillates as it rises to the surface, producing a low frequency signal (< 50 Hz) of decaying amplitude. The bubble pulse frequency is dependant on the released gas volume, pressure and the air-gun depth.

Only a general description of air-gun operation is given. For more detailed references on the theory and operation of seismic noise sources see Barger and Hamblen (1980), Johnson (1994), Parkes et al (1984), Parkes and Hatton, (1986), Verbeek and McGee (1995) or Duncan (1998).

A generalised air-gun showing a common mode of operation is shown in Figure 8. When charged the operating chamber is filled with high pressure gas via a feed line, and the firing chamber is filled with compressed gas via a small orifice (shuttle orifice, SO) through the shuttle centre. In the charged state the air passage (AP), is shut off by the solenoid valve (SV). The shuttle is forced hard up against the operating and firing chamber seals by the air pressure in the operating chamber. The difference in the shuttle piston areas between the ends of the shuttle in each of the operating and firing chambers, results in a small net force in the firing chamber direction which maintains the seals.
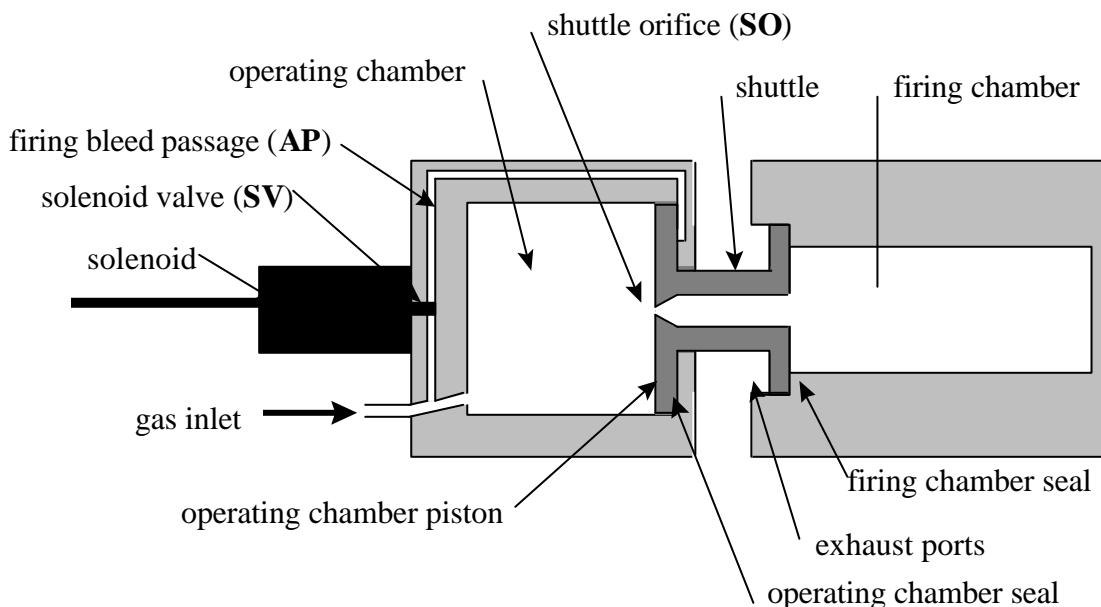
Figure 8 Generalised air-gun layout in charged state, with shuttle forced back and making seals.

When the air-gun is fired the solenoid valve (SV) is opened by a suitable electrical signal. This admits high pressure gas to the back face of the shuttle piston in the operating chamber. This equalises the pressure on either side of the operating chamber shuttle piston allowing the pressure on the firing chamber shuttle piston to rapidly force the shuttle into the operating chamber. This allows the firing chamber gas to escape violently through the exhaust ports.

After the air has been exhausted from the firing chamber the solenoid valve closes, the high pressure air enters the operating chamber and forces the shuttle piston towards the firing chamber, sealing the operating and firing chambers, and leaves the air-gun charged for the next shot. Typically an air-gun can cycle through charge-discharge in less than one second.

Three air-gun signals are shown on Figure 9, each displaying a number of features. A shot from the Bolt 600B air-gun at short range with no bubble suppression is shown on the top and middle plots plot. The primary pulse is evident as the sharp front of the signal (0.1 s on plot). This is followed by reflected signals (for the middle plot the gun-surface reflection was at @ 1.4 ms and gun-bottom reflection @ 5.6 ms after primary pulse) which interfere with the primary signal. The gun-bottom reflection is shown by the arrow for the middle plot. Once the reflected signals die off the bubble pulse becomes clearer. The bubble pulse frequency for the middle plot was 22.3 Hz.
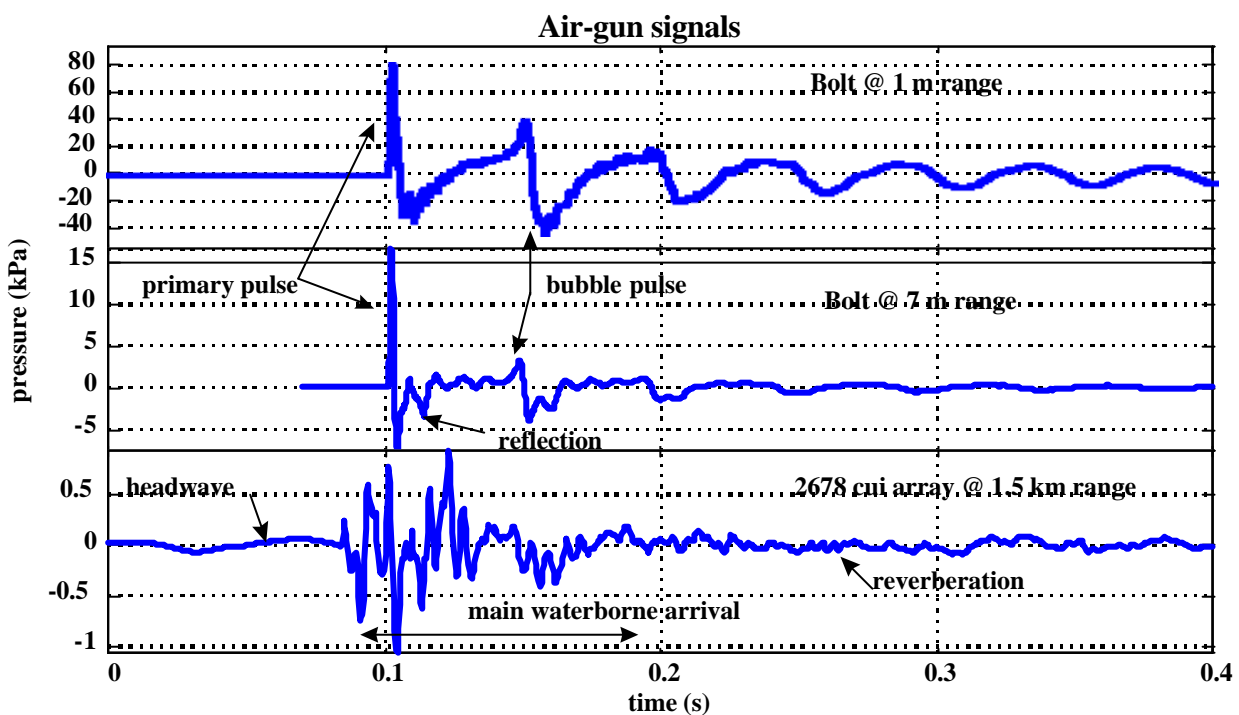
Figure 9 Representative air-gun signals (same time scale). (**top**) Signal from Bolt 600B air-gun as received by hydrophone mounted close to air-gun at 5 m depth in 400 m water depth with gun pressure 10 MPa. (**middle**) Signal from Bolt 600B air-gun at 4 m depth in 10 m water depth with receiver at 2 m, gun pressure 10 MPa. (Bottom) Signal recorded from a 2678 cui array at 1.5 km, where the array was at 7 m depth, hydrophone 40 m depth and an assumed operating pressure of 15 MPa.

The bottom plot shows a signal received at 1.5 km from a 12 element 2678 cui array (44 L, 3D configuration) by a hydrophone at 40 m depth in 110 m of water. In this signal a single primary pulse is not evident, rather the signal has become smeared in time due to the superposition of several signals (from the same shot) which have arrived at different times due to differing travel path lengths. The effect is to lengthen the signal. This plot also shows a portion of a low frequency signal arriving before the primary waterborne signal (indicated as the headwave on Figure 9). This is actually low frequency energy which has travelled through the bottom (travelling faster than the waterborne sound since the sediment sound speed is usually much greater than the waterborne sound speed), and then been re-radiated into the water and picked up by the hydrophone. It is sediment borne signals such as these which the geophysicists are interested in. The re-radiated sediment borne signals feature prominently in many received air-gun signals and in certain instances may be of much higher energy than the waterborne pulse. Although the waterborne pulse is

usually of most interest in studies of biological effects the headwave may have a number of biological ramifications. Headwaves are discussed further below, in section 2.1.4.

The three signals shown in Figure 9 highlight some of the problems inherent in describing air-gun signals. What does one actually measure? Where does the signal start and end? What are the biologically relevant features of the signal? What is the measure most relevant to horizontal sound propagation?

Important factors could be the peak pressure, signal energy, duration and ramp time. The air-gun signal's frequency content also needs to be considered. This will determine overlap with the hearing capability of exposed animals. Since sound propagation will preferentially favour and attenuate different frequencies, signals recorded at long range will have a different frequency composition than those received at short range from the same source.

The technique developed to retrieve and analyse air-gun signals comprised the following steps:
1. capturing the air-gun signals at an appropriate sampling rate (always 4096 samples);
2. saving this block;
3. converting the voltage waveform to pressure units using the recording and analysis calibration values
4. processing the captured sample block for 1/3 octave levels
5. analysing the signal waveform for a suite of parameters described below
6. saving all results

Several possible measures exit and are reported in the literature for describing impulsive air-gun signals. These include:
1. peak values - positive or negative peak values, mean peak value, or peak-peak;
2. measures which use the signal energy per unit area (intensity) then divide by the signal length to give mean intensity, or mean squared pressure;
3. or a measure of the signals energy.

Several of these measures cannot be validly compared. Each has biological significance and physical shortcomings. Measurements of signal peak values (+ve, -ve, peak-peak, etc) are relevant to animal hearing systems as they may determine the maximum displacements which occur in the mechanical transduction process of sound reception. But since hearing in most vertebrates requires temporal summation of nerve firings, peak levels may not reflect maximum perceived sound levels. Also the ducting of sound in shallow water results in a listener at range receiving the superposition of many multipath signals, each out of phase with respect the others. These multipath signals interfere with each other, making predicting peak levels at range extremely difficult as it requires a thorough description of all reflecting and refracting boundaries in the local environment. For this reason peak levels cannot be easily predicted with sound propagation models whereas a measure of energy content can.

Measurements which take into account the signal length will be more indicative of the signal level perceived by an animal since they begin to account for temporal summation of the nervous response. But for measures which incorporate the signal total length, the time boundaries used to define the signal start and end need to be accurately and unambiguously defined. The same signal may give different levels depending on the total signal length used in analysis. Variable levels of background noise, propagation phenomena such as headwaves (sound waves transmitted along the seabed-water interface), or different analytical device protocols, can change the signal start and end points and so bias the resulting measure.

For a given call the signal energy (E) is defined as the integral of power (P) over the duration of the signal

(T_o = time of signal start, T_e = time of signal end), or as:

$$E = \int_{T_0}^{T_e} \mathrm{P}dt$$

This can be expressed as energy per unit area as:

$$\frac{E}{A} = \int_{T_0}^{T_e} I dt$$

where A = unit area; I = intensity. Since for a plane wave $I = \dfrac{p_{s+n}^2}{rc}$, where p_{s+n}^2 = measured signal

squared pressure, which contains the signal plus background noise; r = density; and c = sound speed, then

Equation 1 $$\frac{E}{A} = \int_{T_o}^{T_e} \frac{p_{s+n}^2(t)}{rc} dt$$

The value $\dfrac{E}{A}$ is commonly termed "energy flux" although correctly it should be considered as the "energy per unit area". Since almost all underwater acoustic measurements use pressure sensitive transducers which convert sound pressure to voltage then it is common practice to present measurements in terms of pressure only. Since for a given medium the term rc (specific acoustic impedance) in Equation 1 is relatively constant then we can derive a measure directly proportional to 'energy per unit area' by dropping the specific acoustic impedance term of Equation 1, to give 'equivalent energy per unit area' (E_a) as

Equation 2 $$E_a = \int_{T_o}^{T_e} p_{s+n}^2(t) dt$$

Assuming the signal start and end points are the same, then mean intensity or mean squared pressure values are equal and derived from Equation 2 as:

Equation 3 $$rms = \frac{1}{T} \int_{T_0}^{T_e} p_{s+n}^2(t) dt$$

where
T is the signal length ($T_e - T_o$).

The pressure values measured by a hydrophone contain the summation of the signal and the background noise. If we assume that the background noise is statistically stationary and ergodic such that:

$$\int_{T_o}^{T_e} p_n^2(t) dt = \int_{T_n}^{T_n+(T_e-T_o)} p_n^2(t) dt$$

where p_n = noise pressure, then we get:

Equation 4 $$E_s(t) = \int_0^T p_{s+n}^2(t) dt - \int_{T_n}^{T_n+T} p_n^2(t) dt$$

where $E_s(t)$ = the 'equivalent signal energy per unit area' and is a measure directly proportional to the signals energy content without the background noise contribution. For brevity this value is referred to as 'equivalent energy' only throughout the rest of this document although it must be stressed that it is not a direct measure of energy.

A standardised method was used to derive various measures of received air-gun levels based on the above equations. This used the digitised signal captured at an appropriate sampling rate which included all or >95% of the air-gun signal energy. This was converted from a voltage waveform to a pressure waveform (Pa) using the recording and analysis calibration values. Peak to peak pressures (p_{pp}) were then read off this pressure waveform as:

Equation 5 $\qquad p_{pp} = \max\big(p(t)\big) + |\min\big(p(t)\big)|$

This was then converted to dB using the reference pressure (p_r) of 1 µPa (10^{-6} Pa), as

Equation 6 $\qquad dB = 10\log_{10}\left(\dfrac{p_{pp}^{2}}{p_r^{2}}\right)$

The signal pressure waveform was given as discrete samples at some sampling increment (T_s) which was equal to 1/(sample rate in Hz). This was used to estimate the equivalent energy function $E_s(t)$ (Equation 4) by:

Equation 7 $\qquad E_s(t) = T_s \sum_i^n \left(p_{(s+n)_i}^{2} - \overline{p_n^{2}}\right)$

where $p_{(s+n)_i}^{2}$ is the i th element of the pressure waveform, $E_s(t)$ is calculated in a cumulative fashion to give a vector of cumulative "equivalent energy", n was the last sample point in the pressure waveform and $\overline{p_n^{2}}$ the mean squared noise pressure level. This calculation included background noise preceding the signal, the air-gun signal, and background noise following the signal. For calculations the background noise level squared ($\overline{p_n^{2}}$) was obtained by either taking the mean squared pressure value for defined points within the captured sample with no air-gun signal, or by measuring mean squared pressure values between air-gun signals. A typical analysis for an air-gun signal showing the call waveform, the cumulative vector $E_s(t)$ and the call frequency spectra is shown on Figure 10. It can be seen that prior to the air-gun signal the cumulative squared pressure curve (above background levels) is zero or near zero. As the air-gun signal passes the cumulative energy increases in relation to the waveform, then once the signal has passed the cumulative squared pressure curve flattens out with no further increase. The maximum value of the curve was then proportional to the total energy in the signal (although was not itself a direct measure of energy). From this cumulative equivalent energy curve, Malme et al (1986) suggested the points at which the curve reached 5% and 95% of the total cumulative equivalent energy could be used to define the call start and end times ($T_o = T_{5\%}$ and $T_e = T_{95\%}$ respectively). This method has been further elaborated by Charles Greene (Greeneridge Sciences California, personal communication) as suitable for standardising the start and end times of impulsive air-gun signals. Thus the 5% and 95% points along the cumulative equivalent energy curve were used in calculations to standardise the air-gun signal start and end times.

The measures listed in Table 6 were thus calculated. Peak levels were calculated as discussed above (Equation 5 for peak-peak levels) and given in units of dB re 1µPa (technically the units should be dB re 1µPa², but the conventional notation is to drop the squared notation and present as units of dB re 1µPa). The call equivalent energy level was calculated as the mean value of the cumulative energy curve ($E_s(t)$) over the last 50-100 points of the curve, and presented with units of dB re 1µPa².s. The signal length (T) was defined by the 5% and 95% points of the curve $E_s(t)$. The mean squared pressure value was defined according to Equation 3 where the pressure squared integration was digitally implemented using a Matlab

function and the call length was as defined above. The background noise level used to determine the curve $E_s(t)$ was presented as dB re 1μPa according to Equation 6, replacing p_{pp} with p_n.

#	Measure	units
1	peak maximum pressure level	dB re 1μPa
2	peak minimum pressure level	dB re 1 μPa
3	peak-peak pressure level	dB re 1μPa
4	equivalent energy level	dB re 1 μPa^2.s
5	signal length	s
6	mean squared pressure level, intensity[1]	dB re 1μPa
7	noise level used in analysis	dB re 1μPa
8	90% energy passed	dB re 1μPa^2.s
9	maximum rate of change of equivalent energy	dB re 1μPa^2
10	time within defined signal start-end to 9	s
11	time within defined signal start -end to maximum +ve pressure	s
12	time within defined signal start -end to minimum -ve pressure	s

Table 6 Parameters calculated for use in source level analysis. Superscript: 1 - Provided the sample length is the same these are equal.

The 90% equivalent energy value was obtained from the curve $E_s(t)$ and was mathematically given as:

$$E_{90}(T) = \int_{T_{5\%}}^{T_{95\%}} p_{s+n}^2 dt - \int_{T_n}^{T_n+(T_{95\%}-T_{5\%})} p_n^2\ dt$$

The maximum rate of change of the equivalent energy curve was calculated as the maximum value of the differential of curve $E_s(t)$. The time from $T_{5\%}$ at which this maximum rate of change occurred, and of the times of the maximum positive and negative pressures were also calculated.

All the above details were saved for each air-gun signal analysed.

Provided the call signal was greater than 10 dB above the background noise level then the calculated equivalent energy level was equal to the mean squared pressure level minus $10\log_{10}(T)$.

There were several pitfalls in analysis and factors which confounded several of the measures given in Table 6. The major complicating factors were:
1. extraneous noise, such as fish or whale calling overlapping lower signal-to-noise ratio air-gun signals;
2. the headwave signal dominating the recorded signal;
3. the headwave signal artificially raising the background noise calculated during analysis.

There was nothing which could be done to remove overlap with fish or whale calls. Where these were of sufficient magnitude to interfere with the values calculated in Table 6, the signals were rejected.
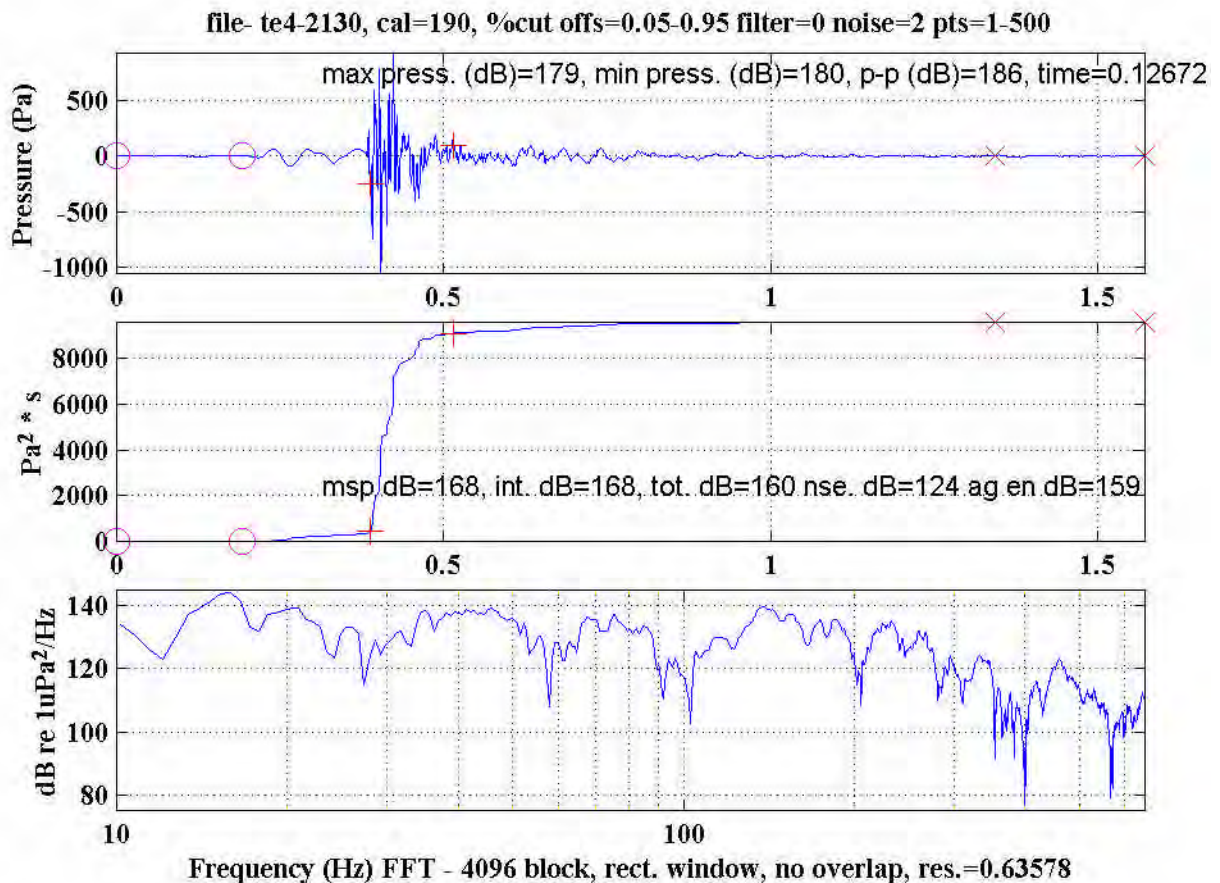
Figure 10: Output of air-gun analysis program for lower air-gun shot displayed on Figure 9. (**top**) Waveform of 2678 cui, 16 gun, array as measured at 1.5 km from hydrophone at 40 m depth. (**middle**) Cumulative squared pressure curve, (**bottom**) power spectra of entire waveform. Abbreviations are: p-p = peak-peak; msp=mean square pressure; int.=intensity (= mean square pressure); tot dB = equivalent energy; nse = noise level; ag en = 90% energy (see text for derivations). Circles denote the portion of the waveform curve from which the mean squared background noise pressure was determined, + signs denote 5% and 95% cumulative squared pressure points (signal start and end respectively) and the x signs denote the portion of the curve used to give the 'equivalent energy'.

The primary instance where headwave signals dominated (ie. more energy in the headwave than waterborne signal) was for recordings made using the single air-gun (no bubble suppression) with bottom coupled hydrophones. In these instances and for signals beyond a certain range, the capture program triggered on the headwave or noise rather than the waterborne signal. This either caused the transient removal algorithm to reject the signal, resulted in the possible capture of a portion of the headwave with no waterborne signal, or resulted in capture of noise. Consequently during analysis of these signals the rejection algorithm was tailored to the situation, the capture process manually interrupted as required and the captured blocks checked for aberrant signals.

The waterborne signals (as measured by suspended hydrophones) contained considerably less low frequency headwave energy than matched samples from bottom-coupled hydrophones (section 2.1.4). Thus for captured air-gun shots where the waterborne energy was required to be determined from measurements made with bottom coupled hydrophones, the signals were high-pass filtered at 20-30 Hz with a 5th order Butterworth filter. This removed the problem of raised background noise levels (3) above.

Problems encountered with the differing measurements listed in Table 6 were:

1. All measures were dependant on sample rate with the peak values most dependant;
2. Signal length was dependant on the presence and relative level of headwave signals compared to the waterborne signal or on the background noise for low signal to noise ratio (SNR) signals
3. Mean squared pressure was dependant on signal length and so on the presence of headwaves or the signal to noise ratio.

Because of the problems inherent in using the peak signals or the mean squared pressure, and that sound propagation models calculate transmission loss in energy terms, then the equivalent energy delivered by the air-gun shot has been used to describe air-gun signals throughout this document. Comparisons of the different measurements and conversion factors are given below.

2.1.2 Measured signals

Sample rate

The effect of differing sample rates on signal measures was investigated. The difference in received signal energy (equivalent energy, Table 6) from the 2678 cui array off Exmouth over 2.1 - 7 km range at two sampling increments (96 μs and 384 μs or 10.417 and 2.604 kHz), and the received signal from the Bolt air-gun in Exmouth Gulf over 170-6800 m range at 96 μs, 192 μs and 768 μs sample increments, are shown on Figure 11. It can be seen for the Bolt air-gun that increased sampling interval lowered the measured signal level. This was not as apparent for the 2678 cui air-gun array at the sampling increments displayed but did become apparent at a 768 μs sampling increment. Thus the differing sources had optimal sample rates, which were up to 192 μs (> 5.208 kHz) for the single Bolt air-gun and to 384 μs (> 2.604 kHz) for the air-gun array.

The different sample rates required to accurately describe the two sources reflect the sources' frequency content combined with the propagation characteristics of the region in which they were measured. The Bolt air gun signals were measured in 10-20 m water depth whereas the air-gun array signals were measured in 30-120 m water. The differences in frequency content with transmission are discussed below.

Sample rate comparisons - total energy
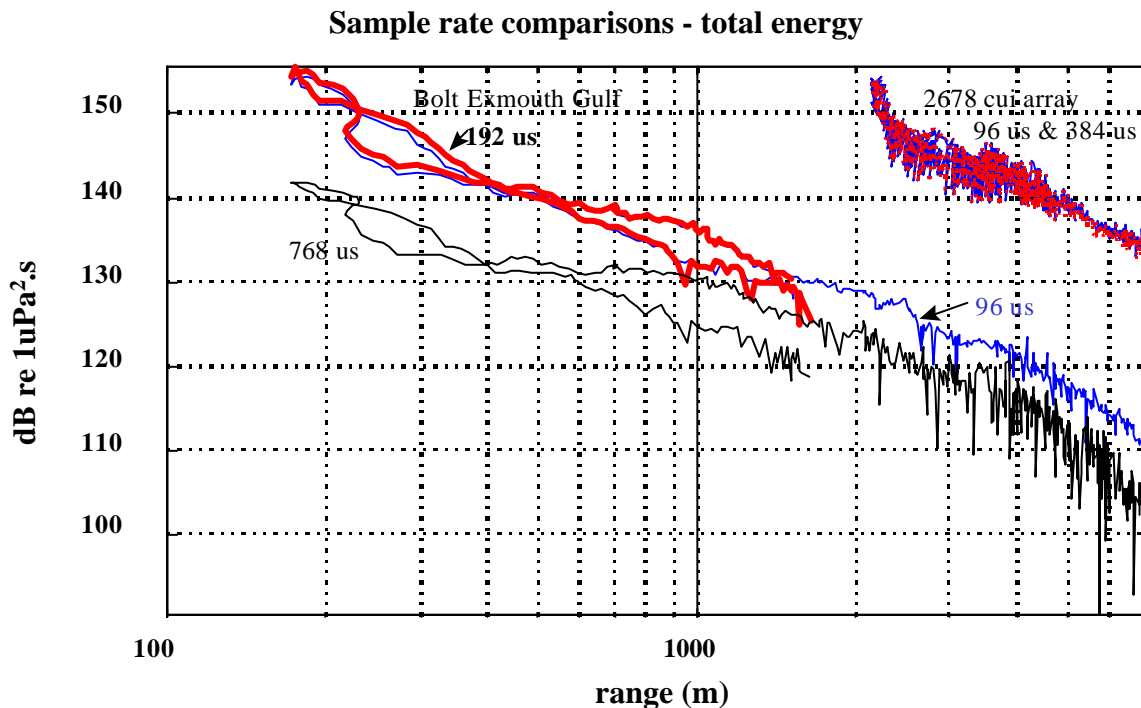
Figure 11 Received air-gun equivalent energy for 2678 cui air-gun array and Bolt air-gun with differing sample rates.

Comparisons of different descriptive measures

Comparisons of the measured signal peak-peak, mean-squared-pressure, and equivalent energy for the Bolt air-gun in Exmouth Gulf with the difference measures ([*peak-peak* minus *equivalent energy*] and [*mean-squared-pressure* minus *equivalent energy*]) are shown on Figure 12. The peak-peak and equivalent energy measures track each other for this run, but the mean-squared-pressure can be seen to fluctuate compared to the equivalent energy measurement. This measurement was made with the un-filtered signal from a bottom coupled hydrophone and illustrates the problems in the stability of the mean-squared pressure measurement (top plot, middle curve) due to the headwave signal distorting the calculated signal length. For this run all sample points were valid. The jumps in the calculated mean squared pressure level were all due to differences in the calculated signal lengths using the 5% and 95% criteria as given by the curve $E_s(t)$ derived from Equation 7. The 'bumps' (examples over 500-600 m or > 4000 m) in the mean squared pressure curve correlated with a low calculated signal length (in the range 20-60 ms) and the lower trending mean squared pressure points (for example over 600-1200 m) all correlated with a higher calculated signal length (in the range 140-240 ms). These signal length differences could then give 4-11 dB differences in the mean squared pressure calculations (ie. from Equation 3). These differences in calculated signal length were all due to variability in the headwave level received at the hydrophone. This headwave variation was in turn believed due to interference patterns generated in the subsea duct through which the headwaves travelled. A series of shallow subsea layering would result in multiple headwaves propagating, one at each density discontinuity boundary (ie. water-seabed, subsea layer 1 - subsea layer 2). These multiple headwave signals would interfere with each other (constructively or destructively), resulting in modal interference patterns in the headwave signal, which show up as an increase and decrease in their received level from the bottomed hydrophone at range from the source. This biased the calculated signal lengths which in turn resulted in the fluctuations in the mean squared pressure level observed.
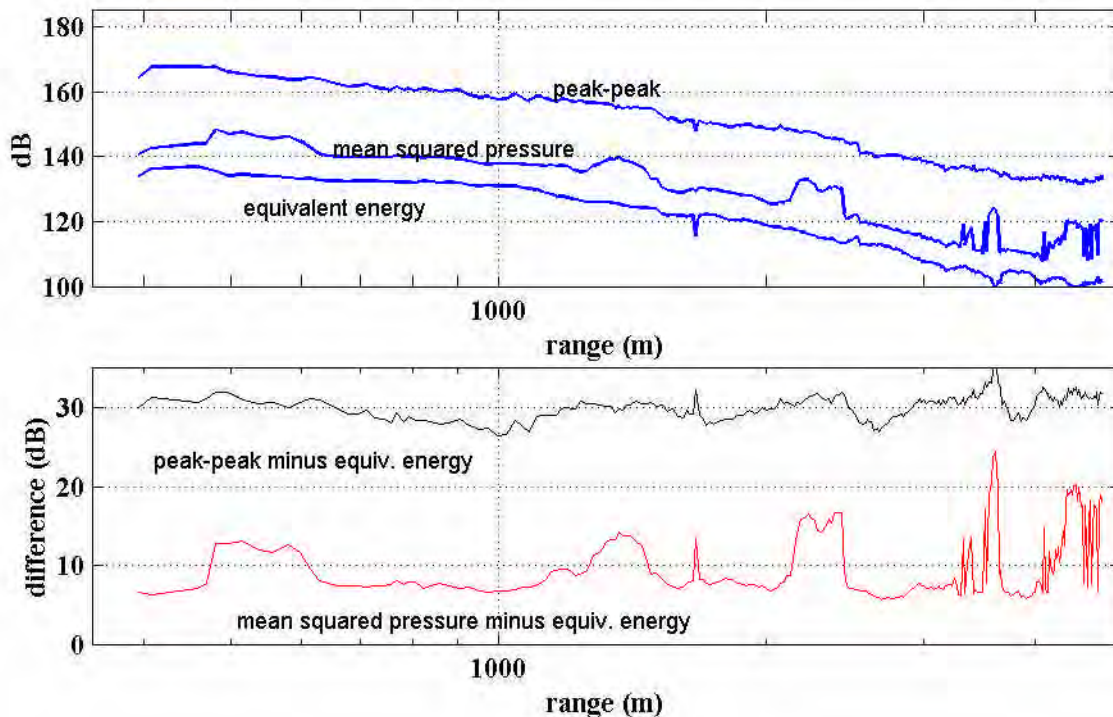
Figure 12 (**Top**) Received signal peak-peak, mean squared pressure and equivalent energy for the Bolt air-gun in Exmouth Gulf over 395-4765 m range (log scale). Note that units vary according to Table 6. (**Bottom**) Difference measures of signals *peak-peak* minus *equivalent energy* and *mean-square-pressure* minus *equivalent energy*, as an indication of how each measure tracks signal energy.

To give an indication of the variability of the mean squared pressure level calculated with range, the correlation coefficients of curves fitted to each of the peak-peak pressure, equivalent energy and mean squared pressure, with range, were calculated. Curves of the form:

Equation 8 $$RL = n \log_{10}(R) + aR + k$$

were fitted to each measure of the air-gun signal, where n, a and k were fitted constants, RL was the received level and R the range. The fitted constants and the calculate correlation coefficients (r^2) for each parameter are given in Table 7. It can be seen that the peak-peak and equivalent energy measure gave the best fits to the data, while the mean squared pressure gave the worst fit (lowest r^2 value) due to the influence of headwaves biasing the calculated signal length.

measure	n	a	k	r^2
peak-peak	-23.7988	-0.0032	232.6286	0.9798
equivalent energy	-19.5101	-0.0046	191.8185	0.9767
mean squared pressure	-30.5114	-0.0013	230.0460	0.8433

Table 7: Fitted constants as per Equation 8, for the peak-peak, equivalent energy and mean squared pressure levels with range as shown in Figure 12 (top, run 2183) and the correlation coefficient for each curve (r^2).

Given that the potential for pathological damage to the hearing systems of marine animals may be proportional to the peak pressures encountered, relationships between the air-gun shot equivalent energy with peak-peak pressure were calculated, and are shown on Table 8. The conversions given are empirical measures and are not a technically valid comparison since the units systems are different. But, since many workers describing biological effects have used some form of peak pressure measures to describe the air-gun signals in their experiments, then the values given are useful for comparing measurements systems. The peak to peak values appear to be tightly coupled to the equivalent energy measurement, at approximately 28 dB greater than equivalent energy for the 3D array and 30 dB greater than equivalent energy for the Bolt air-gun in Exmouth Gulf.

Record #	source	range (m)	min & max dB	mean dB	95% confid. dB	median dB	n
2090	2678 cui array	1520 - 22100	23.8 - 34.9	29.2	29.2 - 29.3	28.9	1109
2156	2678 cui array	2130 - 7100	23.9 - 31.3	27.3	27.2 - 27.4	27.0	566
2183	Bolt Exmouth	395 - 4765	26.5 - 35.9	30.5	30.2 - 30.7	30.4	248
2185	Bolt Exmouth	170 - 6820	24.1 - 33.7	30.0	29.9 - 30.2	29.5	438

Table 8: Relationship between air-gun signals equivalent energy and **peak-peak** measurements. Given are the source, (Bolt = Bolt 600B single air-gun, 20 cui chamber, 10 MPa operating pressure), range over which measurements were made and statistics of the decibel values of *peak-peak* minus *equivalent energy* for all measurements.

Similarly many workers have used mean squared pressure levels to describe air-gun signal levels in biological studies. Thus Table 9 gives a conversion of equivalent energy levels to mean squared pressure levels from the sources measured in this study. These comparisons are technically valid since equivalent energy can be derived from mean squared pressure levels. Thus the values given in Table 9 may be used to calculate approximate values of mean squared pressure from equivalent energy measurements given in this report.

Record #	source	range (km)	min & max dB	mean dB	95% confid. dB	median dB	n
2090	2678 cui array	1.5 - 22.1	8.5 - 20.8	12.7	12.6 - 12.8	12.6	1109
2156	2678 cui array	2.13 - 7.1	4.2 - 14.3	11.3	11.2 - 11.4	11.3	566
all *Geco Resolution*	2678 cui array	1.5 - 43.7	6.0 - 28.1	12.7	12.6 - 12.8	12.3	5352
2183	Bolt Exmouth	0.395-4.76	5.8 - 24.4	12.8	11.8 - 13.6	7.8	248
2185	Bolt Exmouth	0.170 - 6.820	5.7 - 22.5	14.6	14.2 - 14.9	13.2	438
all *Ex*	Bolt Exmouth	0.15 - 7	0 - 30.6	14.4	14.0 - 14.8	9.8	2051
all Bolt	Bolt	0.010-0.8	0 - 26.8	11.4	11.4 - 11.5	11.3	7713

Table 9: Relationship between air-gun signals equivalent energy and **mean squared pressure** measurements. Given are the source, range over which measurements were made and statistics of the decibel values of mean squared pressure minus *equivalent energy* for specified measurements.

The mean squared pressure measurements were a mean of 12.7 dB above the equivalent energy measures for *the Geco Resolution* 3D array and 11.4 or 14.4 dB above the equivalent energy for the Bolt air-gun in Jervoise Bay or Exmouth Gulf, respectively.

Air-gun measures with range

Measurements were made of the port and starboard 2678 cui air-gun array (see Figure 20 for source geometry) of the *Geco Resolution* operating NE of Exmouth Cape (see Figure 7 for location). Source-receiver bottom profiles varied between 5-120 m water depth at the receiver and 25-200 m water depth at the source. The source array depth was always constant at 7 m, while receiver depths ranged from 5 -55 m . Port and starboard arrays were separated by 80 m, with one array each side of the tow axis.

Measurements of the single Bolt air-gun in Exmouth Gulf at ranges from 170 m to 6.5 km in water depths of 15-20 m were also made during the 1996 and 1997 humpback whale trials. Receiver depths were varied between moored mid-water hydrophones and bottom mounted hydrophones. Some measurements of the Bolt air-gun as recorded in the Jervoise Bay fish and squid trials are also presented. In these trials the air-gun was always at 5 m depth, receivers at bottom, 3 or 0.5 m and water depth from 8-10 m.

All measurements of received air-gun shot equivalent energy and the source receiver geographical configuration are shown in Figure 13 for the *Geco Resolution* arrays. The measurements of the Bolt air-gun during Exmouth Gulf trials are shown in Figure 14 along with the location of recording sites in the Gulf. Measurements of the Bolt air-gun in Jervoise Bay are given with appropriate sea turtle, fish or squid trial results.

A curve was fitted to all measured values of the *Geco Resolution* array (5352 air-gun array shots), to give the received equivalent energy level as:

Equation 9: $$RL = -34 \cdot 3536 \times \log_{10}(R) + 2 \cdot .7784 \times 10^{-5} + 263 \cdot 2064$$

where:
RL = received equivalent energy (dB re 1 μPa^2.s)
R = range (m)

The mean receiver depth for the data used to generate this curve was 32 m.
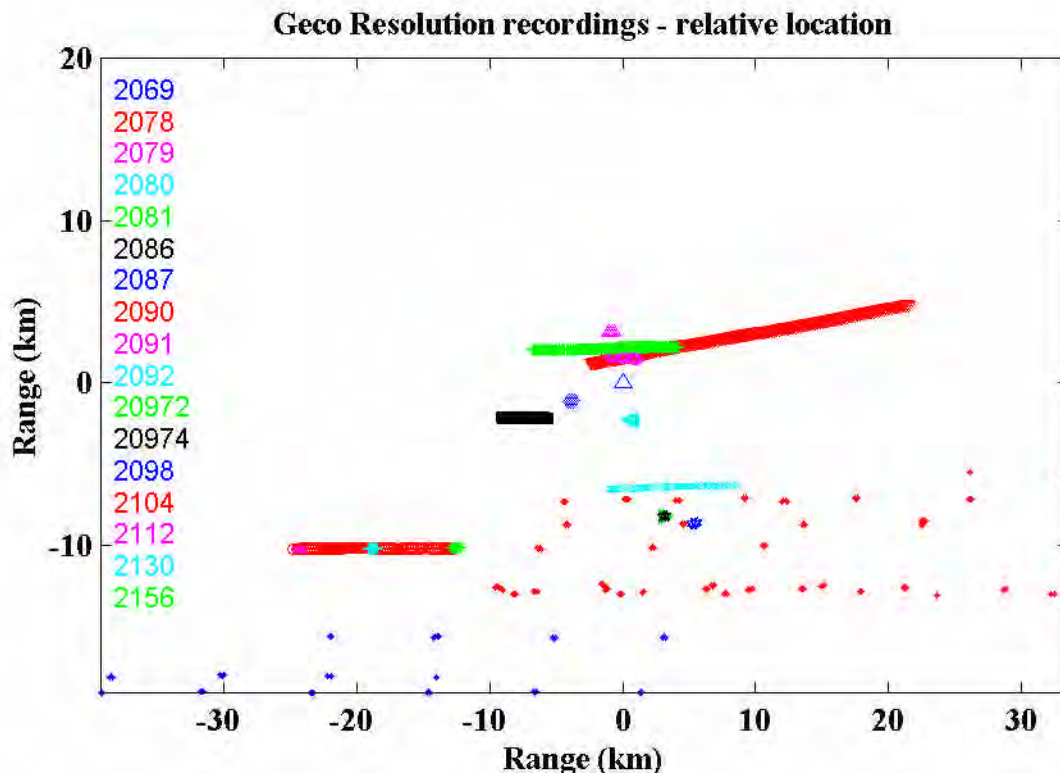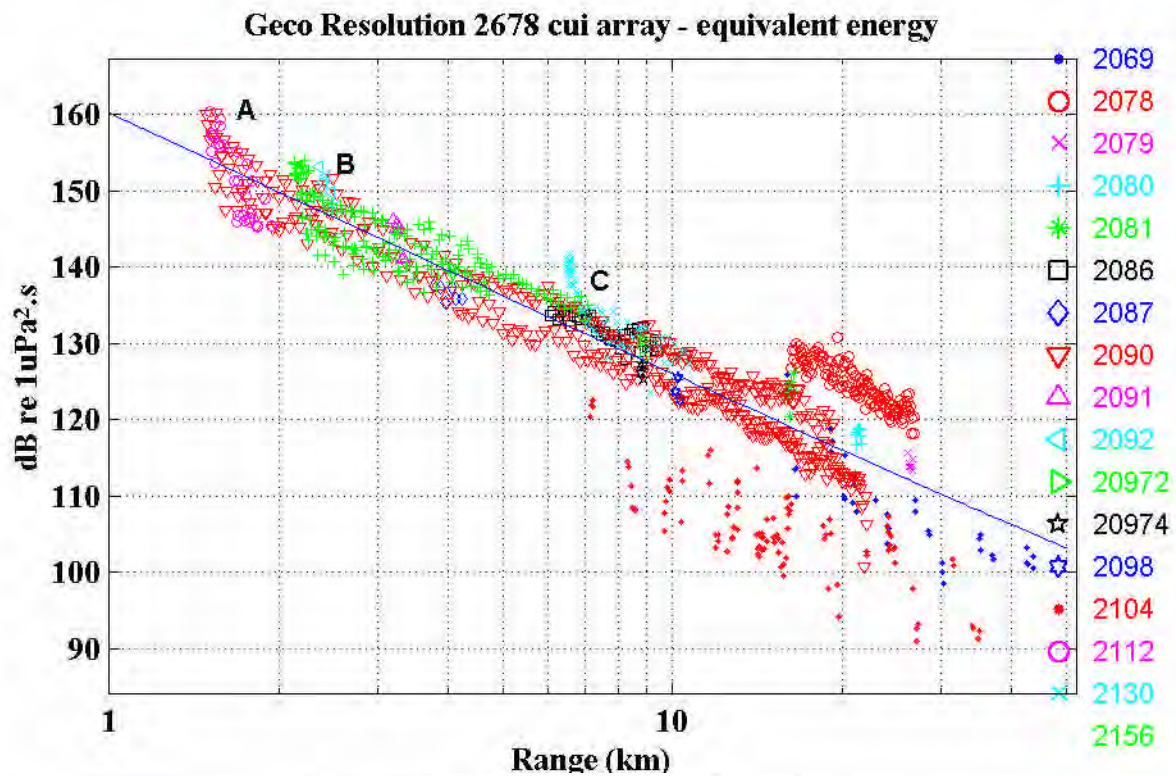
Figure 13: (**top**) Measurements of the 2678 cui array equivalent energy as measured from the 'Robert' seismic survey (every 5th sample shown). The line of best fit (equation 1) is shown. Three Recordings made as the receiver passed the array beam are shown as A, B, &C. (**bottom**) Relative location of air-gun array and receivers, normalised such that the array is located at the plot (0,0) location shown by the triangle. Colours and symbols are the same in each plot.
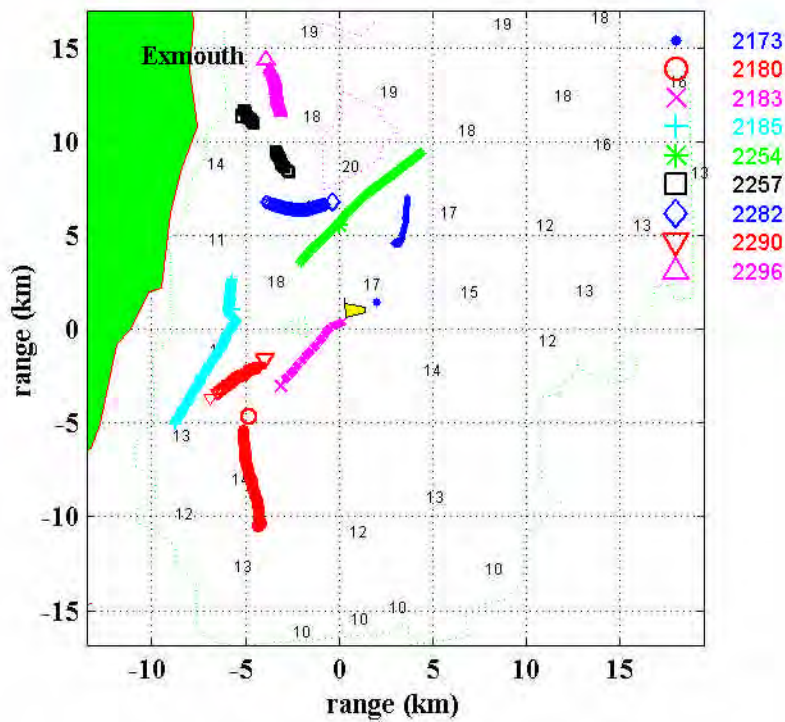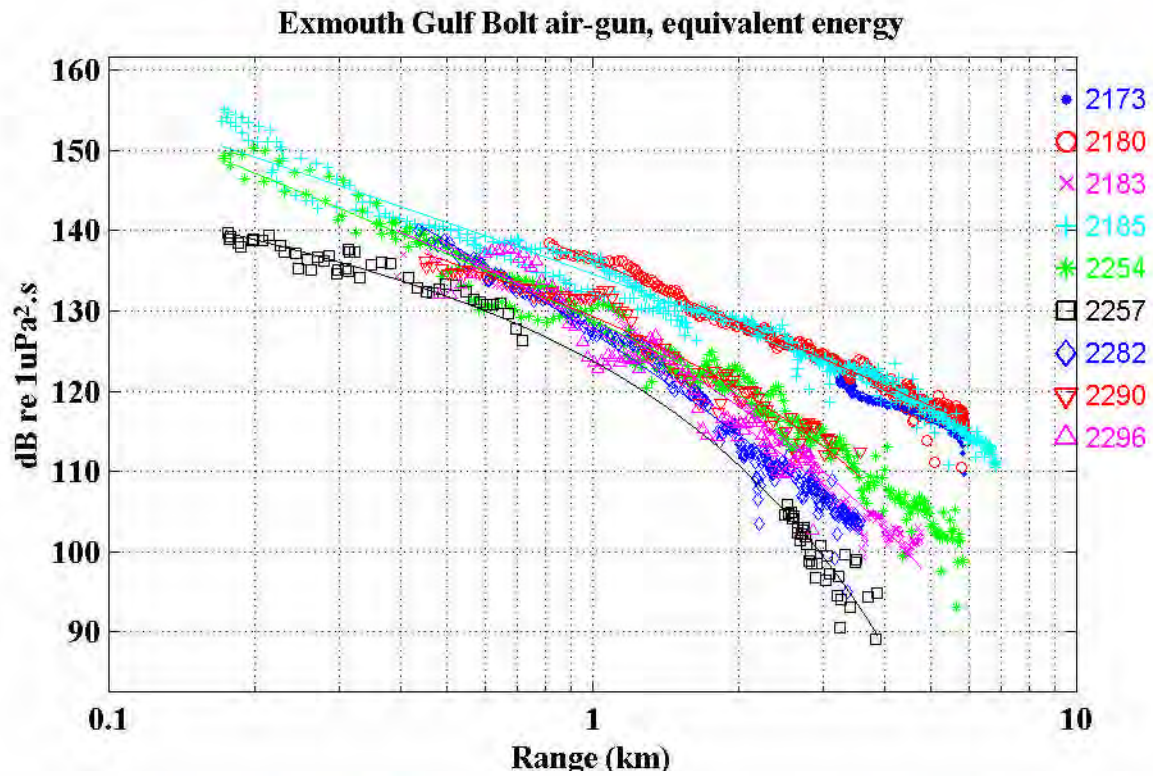
Figure 14: (**top**) All measurements of Bolt 600B air-gun proportional energy as recorded from within Exmouth Gulf during humpback whale trials. (**bottom**) Corresponding air-gun tracks and receiver locations (colours and symbols are the same between plots).

It can be seen from Figure 13 that there was considerable fluctuation in the received level of the 3D arrays with range, particularly at ranges > 7 km (> 35 dB difference). For this array these measured differences were due to:

1. port versus starboard array differences;
2. differences in the receiver depth;
3. the horizontal beam pattern of the array;
4. bathymetry travel path differences;
5. differing sound propagation characteristics along the different travel paths.

The Bolt air-gun shots recorded in Exmouth Gulf were made during humpback whale exposure trials (section 2.2.4), with the intention of matching a given range for noted whale response to some measure of the air-gun signal level. It can be seen from Figure 14 that at ranges > 1 km there were potentially large differences in the received air-gun level for different measurement sets. This compounded interpretation of the signal level received by the whale during trials, thus requiring investigation of why there should be such discrepancies in the measured signals. Factors 2 and 5 above were pertinent to the single air-gun measurement set, plus an extra consideration, that of source depth, was introduced into the interpretation of received signals.

The effect of factors 1-4 on the 3D array measurements, and where pertinent on the single air-gun measurements, are discussed below. This is followed by some discussion of the Exmouth Gulf results, which then introduces factor 5 above, the importance of local sediment types in sound propagation, and also discusses the effect of source depth. Using modelling techniques the directionality patterns inherent in multi element arrays are investigated at greater length in section 2.1.3, while similarly the effect of source depth and sediment types for the Exmouth data set are elucidated in section 2.1.4.

Port versus starboard 3D arrays
Although the port and starboard arrays were nominally identical the signals produced by consecutive array shots were audibly and quantitatively different. In practice each array has built in redundancy and is allowed to operate up to some defined point, or before the next scheduled service, with malfunctioning individual air-guns. Port and starboard backup arrays were towed, so that if an operational array signal character and level were deemed to be inadequate (each array's performance was continually monitored during operation) these backup arrays would be bought into service and the malfunctioning unit recovered. The observed differences between port and starboard arrays were presumably because of one or all of: slightly different compositions of functioning sections of the air-gun arrays; slight misalignment of the array configuration; or slightly different directionality patterns between port and starboard arrays and the receiver.

There appeared to be no consistent or net difference in received level between port and starboard arrays. To calculate this samples were matched and the total shot energy of the starboard shot which followed a port shot and fell within 10 s of it (or the next shot), was subtracted from the similar measure of the preceding port shot. Of 1287 such matched signals measured over 1.5 - 27 km horizontal range, the starboard signal equivalent energy ranged from 7.4 dB below to 9.2 dB above the preceding port shot, although the mean difference of 0.6 dB was negligible.

Differences in receiver depth
There were consistent differences in received levels for the same shot as recorded at two vertically spaced hydrophones. For the same shot shallower hydrophones always recorded mean lower signals than deeper hydrophones. For the long range *Geco Resolution* measurements the difference was a complex function of

range and appeared to oscillate about a mean value. The difference values between *deep-water* minus *shallow-water* equivalent energy for sets of matched shots (same shot vertically separated hydrophones) taken from the *Geco Resolution* (port-starboard arrays not differentiated), the Bolt air-gun in Exmouth Gulf, and the Bolt air-gun in Jervoise Bay (10 m water depth), are given in Table 10.

From Table 10 it can be seen that the mean differences may be substantial, and increase as the shallower hydrophone is bought closer to the surface. This is as would be expected from the Lloyds mirror effect, as described in Urick (1983).

#	Source	horizontal range (km)	shallow - deep hyd. depths (m)	deep - shallow diff dB range	mean diff (dB)	95% dB range	n
2090	3D array	1.5 - 19.2	25, 40	1.9 - 7.2	4.6	4.5 - 4.6	832
2112	3D array	1.6 - 1.8	5, 40	3.1 - 9.2	6.7	5.6 - 7.6	21
2112	3D array	1.5 - 1.6	20, 50	1.4 - 4.9	3.2	2.6 - 3.7	19
2112	3D array	1.7 - 1.9	25, 55	1.4 - 4.8	3.5	3.0 - 4.0	22
2156	3D array	2.1 - 4.7	15, 50	0.6 - 5.9	3.5	3.4 - 3.6	389
2185	Bolt Exmouth	0.5 - 6.8	3, 10	-3.1 - 8.2	3.77	3.6 - 3.9	324
2420 & 2424	Bolt Jervoise Bay	0.003 - 0.7	0.3, 9.5	-11.7 - 23.5	14.3	13.8 - 14.8	328
2429 & 2430	Bolt Jervoise Bay	0.002 - 1.2	3, 9.5	-25.2 - 10.9	2.34	2.0 - 2.6	482

Table 10: Difference statistics (decibel) for *deep-hydrophone* minus *shallow-hydrophone(s)* equivalent energy for matched shots. Given are the recording set number, source, horizontal range over which matched shots were recorded, depth of hydrophones, minimum and maximum values of *deep equivalent energy* minus *shallow equivalent energy,* mean difference, 95% confidence limits of difference, and number of shots.

Azimuth dependence for arrays

By combining many air-guns into arrays the source becomes directional in the horizontal plane. This topic is discussed further below (section 2.1.3 where the specific geometry of the 3D 2678 cui array is given). Examples of the resultant shift in received signal level can be seen in several sets from the 2678 cui 3D array shown on Figure 13. As the receiver came abeam the array a rapid increase in the received signal was measured. The received level can be seen to dramatically increase over short ranges during several recording sets (A, B and C on Figure 13). On each of these sets the hydrophone was set ahead of the *Geco Resolution* and the ship steamed past, thus passing the hydrophone abeam at some point.

An analysis of this increase in received signal as the receiver came abeam the array was carried out from measured signals of runs 2130 (18 m hydrophone) and 2156 (15 and 50 m hydrophones). In each set the ranges were moderate to large (2.1 - 4.7 km and 6.5 - 10.7 km respectively), thus the received level aspect dependence was expected to dominate over range effects for angles about the beam. The range dependence was removed for each set by fitting a curve of the form in Equation 8 to the measures taken with aspects in the range 0-60° and > 120° and subtracting the fitted values at each range from the measured values. A consistent trend was found, displayed on Figure 15, in which the received signal was up to 10 dB higher than predicted by a range dependant model only, with the peak level experienced slightly aft of the beam, over 95-100°. The levels measured forward of the beam also appeared to be greater than those measured aft the beam, which may explain the higher levels measured from set 2078, displayed on Figure 13.

Run - 2130 shots-1-232 (range 6.5-7.4 km)
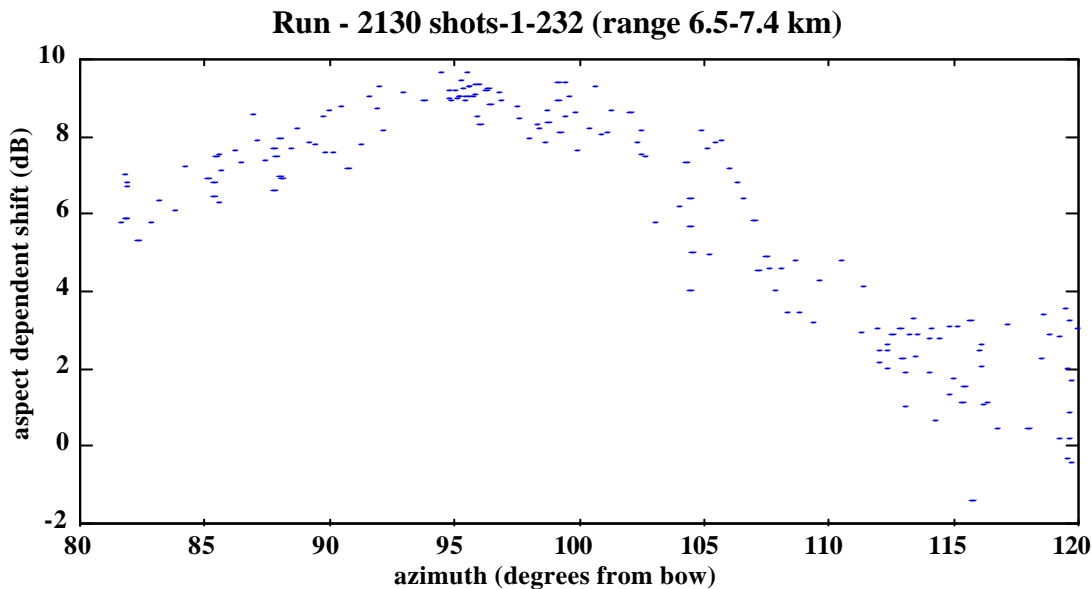
Figure 15: Dependence on aspect for received shot level as 3D array came about beam for recording set 2130, made at a range of 6.5-10.7 km (6.5-7.4 km measures shown).

Bathymetry travel path differences

Much of the difference in comparing measurement sets of received signal level at selected ranges could be explained by the differing propagation conditions along each shot's travel path. This is believed to be particularly emphasised in the 2678 cui 3D array shots as shown by recording set 2104 on Figure 13. These measurements were taken from a bottom mounted package set in 32 m of water operating on a timer over a three day period. At a given range the received air-gun levels varied by > 10 dB within the recording set, and by up to 30 dB between this data set and others (ie. set 2078 or 2090). The received level differences were believed due to the different propagation paths involved. Propagation to the receiver in set 2104 involved up slope travel paths. The water depth at the source ranged from 70-160 m while the receiver was in 32 m water. In contrast the travel paths in recording set 2078 and 2090 which displayed much higher received levels at longer range were over a relatively constant depth. These travel paths were from 50-70 m depth (source) to 70-90 m depth (receiver) for set 2078, and 90-130 m (source) to 95-100 m (receiver) for set 2090.

Propagation of signals up-slope involves increasing numbers of bottom-surface bounce paths as the water shallows. Energy is lost at each bounce, thus this type of propagation is known to be poorer than that along constant depth profiles (Urick, 1983). The combination of up slope propagation and the azimuth patterns of the array then give rise to the apparently anomalous received signals of set 2104 shown on Figure 13.

A similar large loss in signal strength for up-slope propagation conditions was observed for a set recorded in 10 m water with the 2678 cui 3D array operating nearby. In this set, despite a closest approach of 28 km (source in 132 m) the air-gun was not audible. The up-slope propagation path is shown on Figure 16.

41
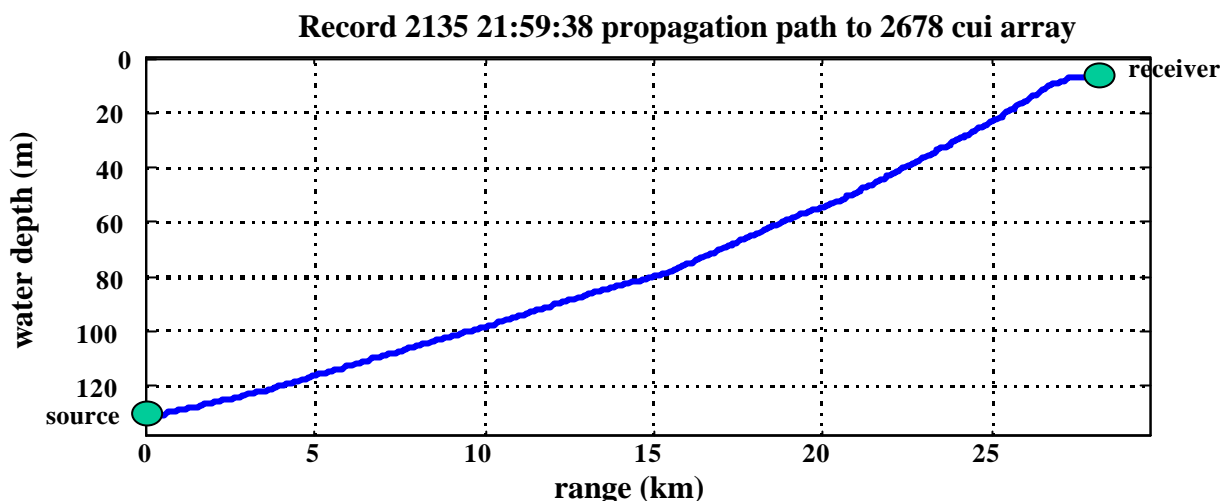
Figure 16: Upslope propagation path resulting in signal not audible at receiver.

Exmouth Gulf data set - dependence on sediment types and source depth

The Exmouth Gulf measured data (Figure 14) showed two general trends. The recording sets 2173, 2180 and 2185 gave the higher levels at a given range (type 1 curves), whilst all other recording sets (type 2 curves) showed comparatively greater losses at any given range with this loss increasing as the range increased.

The pertinent physical details for each set of recording data shown on Figure 14 are listed in Table 11. Also given on Table 11 are values for curves fitted according to the form of Equation 8. During the 1996 trials (recording numbers < 2200, trials 1-7) the currents in Exmouth Gulf were low so moored hydrophones could be set in mid water without excessive flow noise. During the 1997 trials (recording numbers > 2200, trials 8-16) tidal streams were strong thus all hydrophones had to be set on the bottom to avoid saturation at low frequencies with high levels of flow and cable strum noise. There were significant differences in the headwave signals recorded between bottom coupled and midwater hydrophones. For various reasons recordings were not able to be made during all trials.

# - run	air-gun depth (m)	water depth (m)	hyd. depth (m)	range (m)	fitted curve
2173 - 2	5	19	19	3220-5833	-7.72 log(ra) - 0.0018 ra + 153.83
2180 - 4	5	16	10	810-5870	-25.47 log(ra) - 0.0001 ra + 212.86
2183 - 5	5	17	17	395-4760	-20.62 log(ra) - 0.0045 ra + 195.29
2185 - 6	5	19	10	170-6820	-19.83 log(ra) - 0.0009 ra + 195.00
2254 - 8	3.5	20	20	170-5810	-23.77 log(ra) - 0.0021 ra + 202.33
2257 - 9	3.5	17	17	180-3870	-10.39 log(ra) - 0.0098 ra + 164.76
2282 -14	3.5	21	21	440-3570	-33.52 log(ra) - 0.0026 ra + 230.43
2290 - 15	3.5	16	16	450-3562	-15.43 log(ra) - 0.0044 ra + 180.07
2296 - 16	3.5	17	17	480-3000	-31.23 log(ra) - 0.0023 ra + 223.82

Table 11: Physical details for each of the air-gun sets shown on Figure 14. Given are: the recording and trial numbers; air-gun depth; mean water depth over run; recording hydrophone depth; range over which the measurements were made; and fitted curve parameters.

During the 1997 field work fish trials were carried out concurrently with the humpback trials. The fish cage was placed in shallow water (7-10 m), thus the air-gun depth was altered from the 1996 depth of 5 m, to 3.5 m, to allow the air-gun ample clearance off the bottom. For simplicity this depth was maintained

throughout all Exmouth 1997 trials.

Discounting recording set 2173 which was taken at long range only, the fitted curves (Table 11) show log-loss coefficients from -10 to -33, a linear loss with range term from 0.1 to 9.8 dB/km, and source levels from 153 to 230 dB re 1 μPa^2.s. The single Bolt air-gun has a source level of 196 dB re 1 μPa^2.s (based on near field hydrophone measurements) indicating that these fitted curves must have been strongly influenced by sound propagation conditions and the configuration of source and receiver during the trials. The source was measured at short range (< 15 m) immediately before and after the 1996 Exmouth trials and during the 1997 trials, with the pulse shape always as expected, discounting any possibility of the air-gun malfunctioning.

Several factors may have influenced the Exmouth received air-gun level curves. These include:
1. hydrophone depth in water column (possible vertical sound intensity profiles)
2. water depth
3. local differences in sediment types;
4. source depth (5 m 1996, 3.5 m 1997);
5. and the sound velocity profile through the water column.

The sound velocity profiles were measured in 1997 (the computer software controlling the CTD profiler failed during the 1996 trials). These indicated a uniform sound speed below 5 m water depth, with sound speed falling within 1531-1532 ms^{-1}. Surface heating created an 'afternoon effect', with surface temperatures up to 1.5^{o} higher than deeper waters in late afternoon (ie. 23.5^{o} at depth to 24.5-25° at the surface). Thus the surface sound speed differed slightly from the deeper waters in the late afternoon, but the difference was mostly less than 1 ms^{-1} and thus was not considered to be a significant factor in sound propagation.

Because of its importance in interpreting the humpback whale trial observations, the propagation of air-gun signals in Exmouth Gulf was modelled to elucidate which of factors 1-4 above were significant. This modelling exercise is described in Section 2.1.4.

The modelling results indicated that sediment type and source depth were the most critical factors in predicting the received air-gun level in Exmouth Gulf. Water depths were not largely different between measurement sets (Table 11). The higher set of measured curves (type 1) were all measured during the 1996 trials with mid-water and bottomed receivers with the source depth at 5 m, indicating that the source depth was critical. But one of the lower curves (type 2), recording set 2183, was also measured during 1996 with the source at 5 m depth thus indicating that local sediment types were also critical. The differing frequency content of the type 1 & 2 curves (presented below) also matched the modelling results. These suggested that the type 1 curves resulted from a shallow reflective layer (limestone pavement), whereas the type 2 curves were measured over regions without this layer. The location of the type 1 measurement sets compared with the type 2 sets indicated that the sediment types were patchily distributed throughout the Gulf (Figure 14).

Frequency content with range
Propagation effects preferentially favour and attenuate selected frequencies. Examples of this effect can be seen in Figure 17 for the approaching and departing 3D array in deep water (> 100 m) and Figure 18 for the departing Bolt air-gun in shallow water (< 20 m), using 1/3 octave values with centre frequencies from 25 - 1000 Hz. For the 3D array slight differences between the port and starboard 3D array frequency content can be seen at short range (Figure 17), with this influencing the frequency content of long range

signals.

The single Bolt air-gun shows large differences in the frequency content with range for different runs, as shown in Figure 18. Each of these runs was made with the air-gun departing from the receiver. The differences between the two sets of curves (level with range) measured in Exmouth Gulf (type 1 and type 2) can be seen by comparing the frequency content of run 2185 (made in 1996 with source at 5 m depth) against runs 2183 and 2254 (made in 1996 source at 5 m depth, 1997 source at 3.5 m depth, respectively). The type 1 curve has considerably more energy propagating in the 63 Hz and 160-630 Hz 1/3 octaves than the type 2 curves.

As stated above this difference is believed due to the presence (type 1) or absence (type 2) of a reflecting layer near the seabed water interface. The frequency content for the curves shown has been limited to the departing measurement legs over 200 m to 5 km range. The full frequency content of run 2185 actually shows the type 2 frequency content pattern on a portion of the approaching leg and the type 1 content on all of the departing leg, indicating the patchily distributed nature of the sediment types.
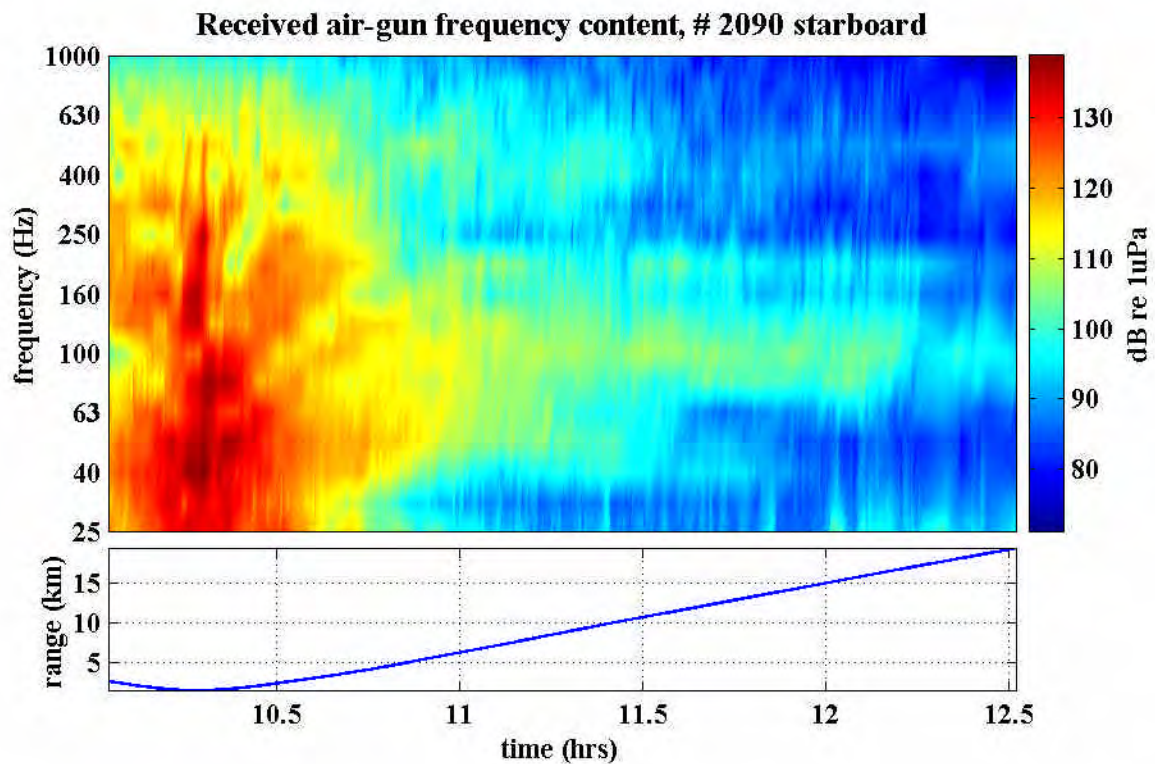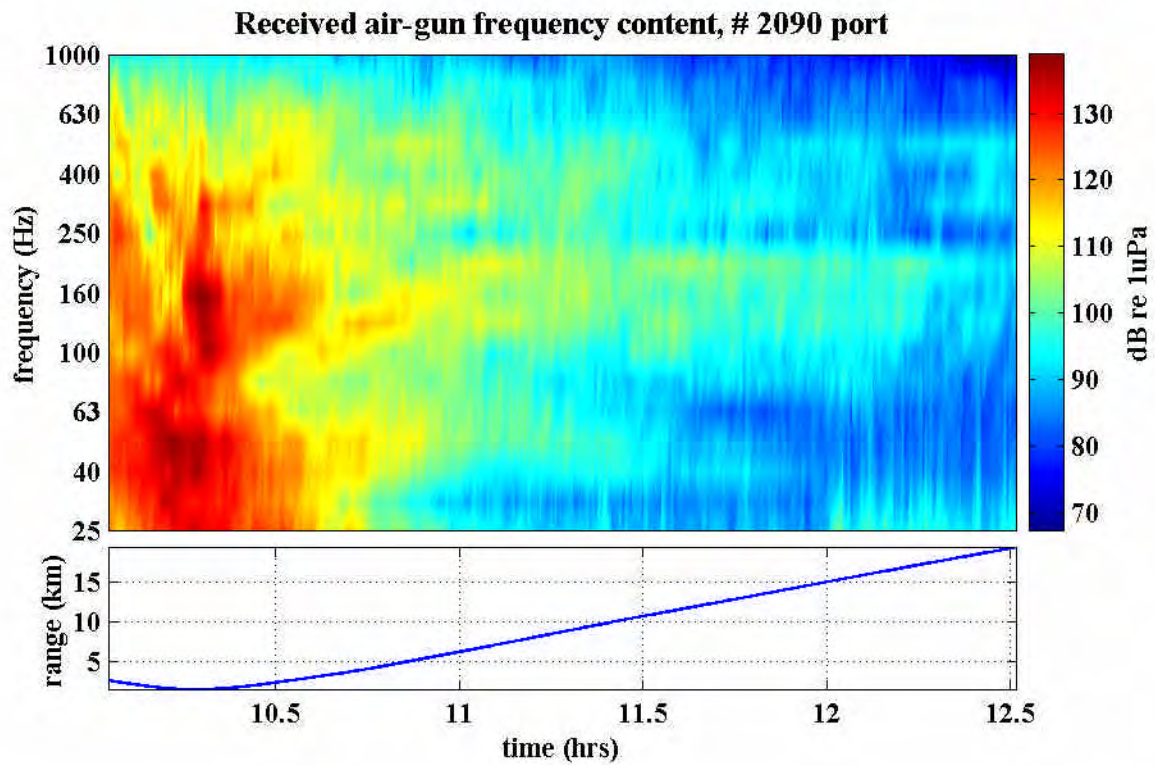
Figure 17: Frequency content of Geco Resolution port (**top**) and starboard (**bottom**) array, with time and range (red =highest levels, blue lowest, same colour scale used both plots). Slight differences in the frequency content of each array are evident
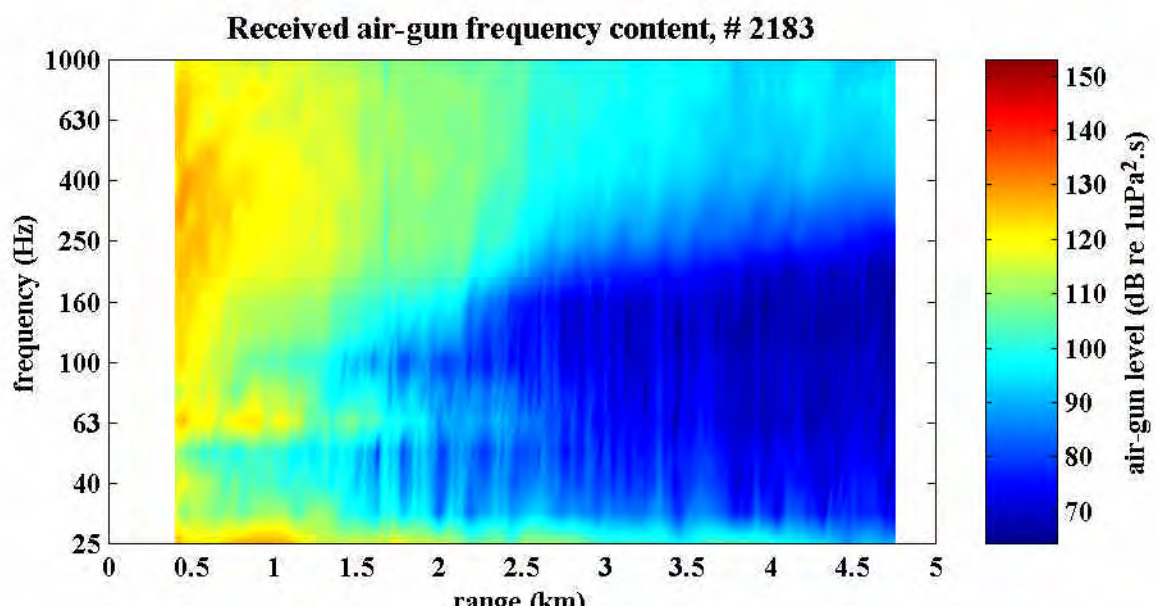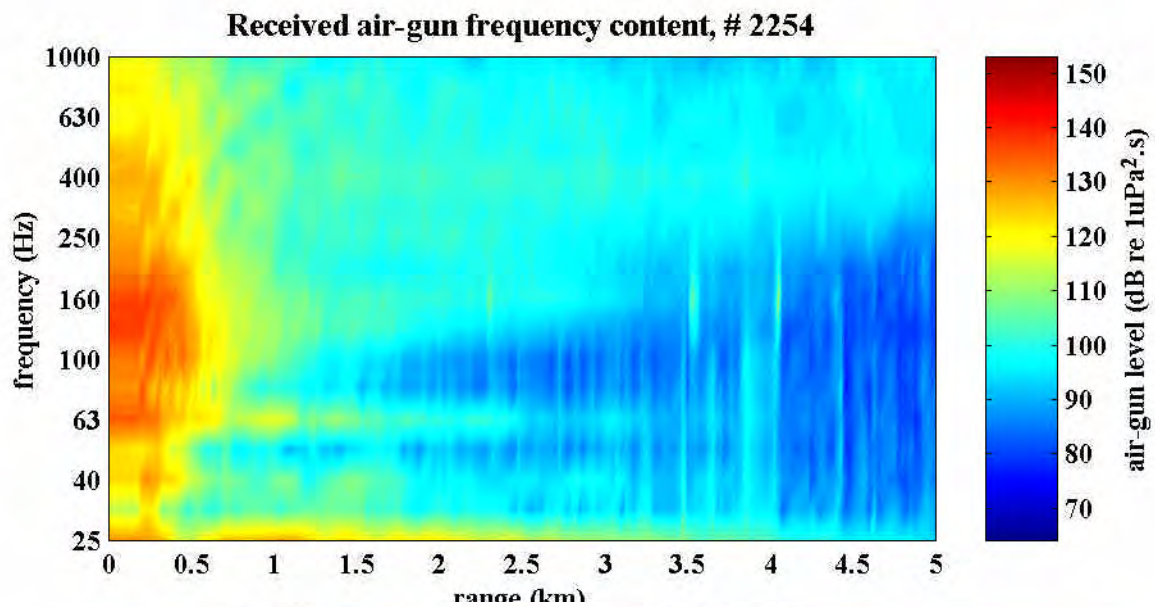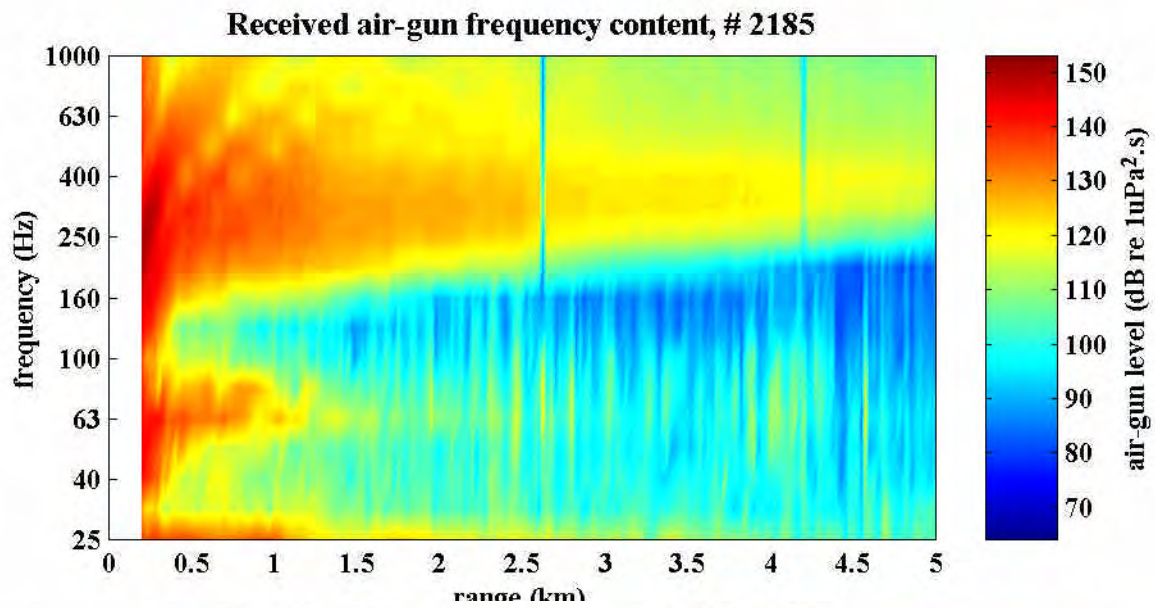
Figure 18: Frequency content with range, of single Bolt air-gun in Exmouth Gulf showing different sound propagation regimes (type 1 top, 2 middle and bottom).

2.1.3 Array modelling, 2D vs 3D

Commercial seismic sources are comprised of many elements grouped together in an array. This is done to increase the energy output of the signal, to 'shape' the signal according to the type of survey, to suppress bubble pulses and to enable redundancy in the source by providing spare elements. The three examples of sources in this report are the single Bolt 600B air-gun, which was effectively omni-directional at all frequencies, a 2D and a 3D source. The array configurations were as used in seismic surveys.

Two dimensional seismic sources consist of a single source towed behind the vessel and a single hydrophone streamer towed astern of the array. These sources are designed to focus the sound downwards and in line with the single streamer. An example source configuration for a 40 gun, 20 element array is shown on Figure 19. The forward and aft element of each gun row (in tow direction) were clusters of three air-guns. It can be seen that the long axis of the array is perpendicular to the tow direction. This is done to minimise the lateral beam width. In 2D surveys only a single 'slice' of bottom is profiled, this being along the tow direction.

Three dimensional seismic survey configurations use multiple streamers towed at set distances apart (nominally 100 m), so as to use seismic reflections at angles to the direction of tow as well as in the tow direction. An example 3D configuration is shown in Figure 20 for a 16 gun 12 element array. The forward element of each row was a cluster of three air-guns. For this array the design attempts to maximise the energy downward as for the 2D configuration, but since lateral transmission paths are required, is a compromise as to how much energy is delivered astern compared to abeam the array. As the name suggests, 3D surveys give a three dimensional sub-bottom profile.

To enable estimates of exposure through time for a given seismic survey (see section 2.1.5), a model was developed to predict air-gun array output at a number of frequencies for any orientation about a specified source array and configuration of air-guns.

The convention used in this document for directionality patterns is that an elevation angle of 0° corresponds to sound travelling vertically downwards, while an elevation of 90° is horizontal. Azimuth angles correspond to the horizontal angle from the tow direction of the array, that is forward end-fire is azimuth 0°, abeam is 90° and abaft end-fire is 180°.

The air-gun array model developed used a modified version of an air-gun bubble model given by Johnson (1994), to generate a signature for each air-gun in the array. The signatures of the individual air-guns were then summed with delays appropriate for the geometry of the array and the azimuth and elevation angles to a far field receiver. The energy spectral density of the resulting time series could then be computed.

The modifications to Johnson's model were as follows:
1. The damping was increased by a factor of five in order to give a decay rate for the bubble oscillation consistent with measured air-gun signals.
2. The output signal from Johnson's model was low pass filtered using a first order filter with a 3 dB cut-off at 300 Hz in order to compensate for the unrealistic zero primary pulse rise-time predicted by the model. Filter parameters were chosen to give a high frequency roll-off consistent with measured air-gun signals.
3. The amplitude of all air-gun signals were multiplied by a constant in order that the total signal energy of the array, (ie. $\int p^2 dt$), for an elevation of 90°, an azimuth of 0°, and no surface ghost matched the

arrays quoted specifications, at this azimuth and elevation.
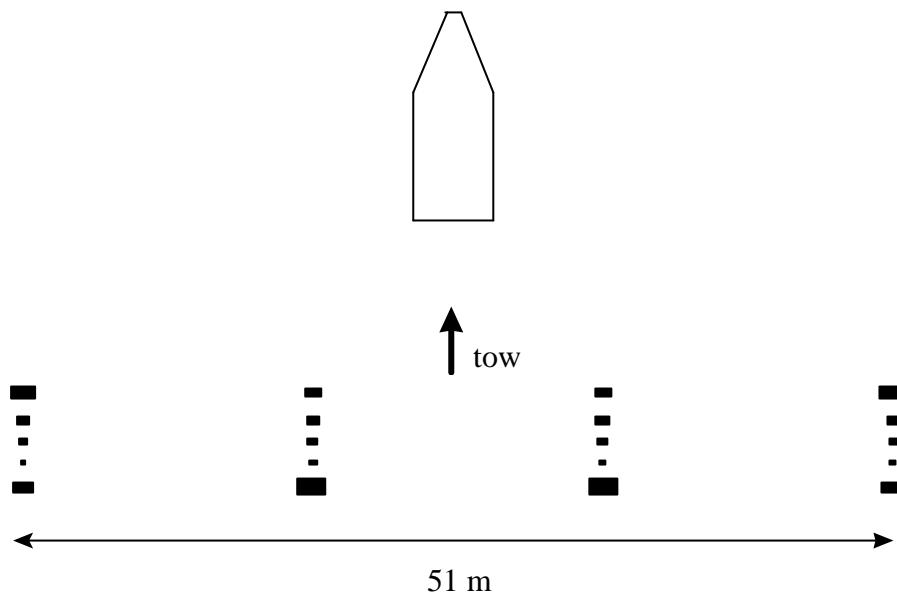
Figure 19: Example of two dimensional array configuration (2D). The size of array elements displayed are scaled to be show comparative, combined-element gun-volumes.
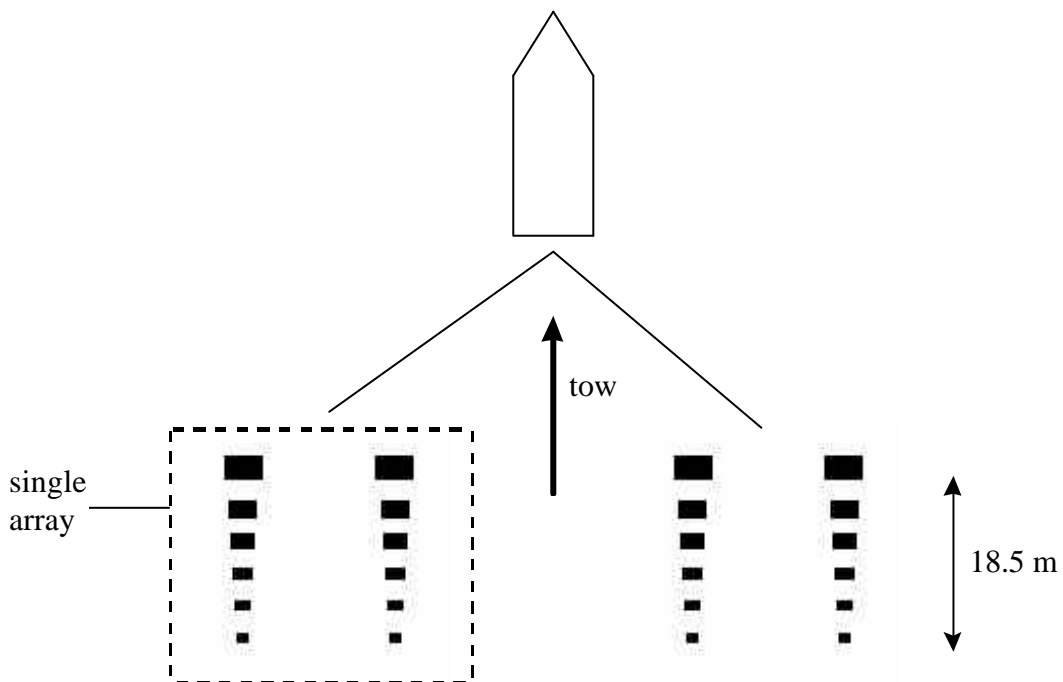

Figure 20: Example of three dimensional array configuration (3D). The size of array elements displayed are scaled to be show comparative, combined-element gun-volumes

Where several air-guns were mounted very close together they were modelled as a single air-gun with a volume equal to the combined volume of the cluster. No other account was taken of the interactions between air-guns.

This method has a number of limitations but produces results of adequate accuracy for use in predicting signal levels for biological effects studies. A comparison of the source waveform and spectral content for the 2D array calculated by the model and as specified by the Geophysical contractor, for an azimuth of 0° and an elevation of 90° with no surface ghost, is shown on Figure 21. Each signal has been low-pass filtered with a cut-off at 218 Hz, with a higher order filter used for the signal provided by the Geophysical contractor. The agreement between the supplied and calculated signals is good, although the simplified model shows high frequency ripples in the waveform that are not present in the sample signal. There is excellent agreement between the spectral content of the two signals although again there is more structure in the spectrum of the signal produced by the simple model. This is primarily due to the presence of high frequency harmonics of the bubble pulse in the simple model's output waveform.

Comparsion of calculated and supplied 2D array source
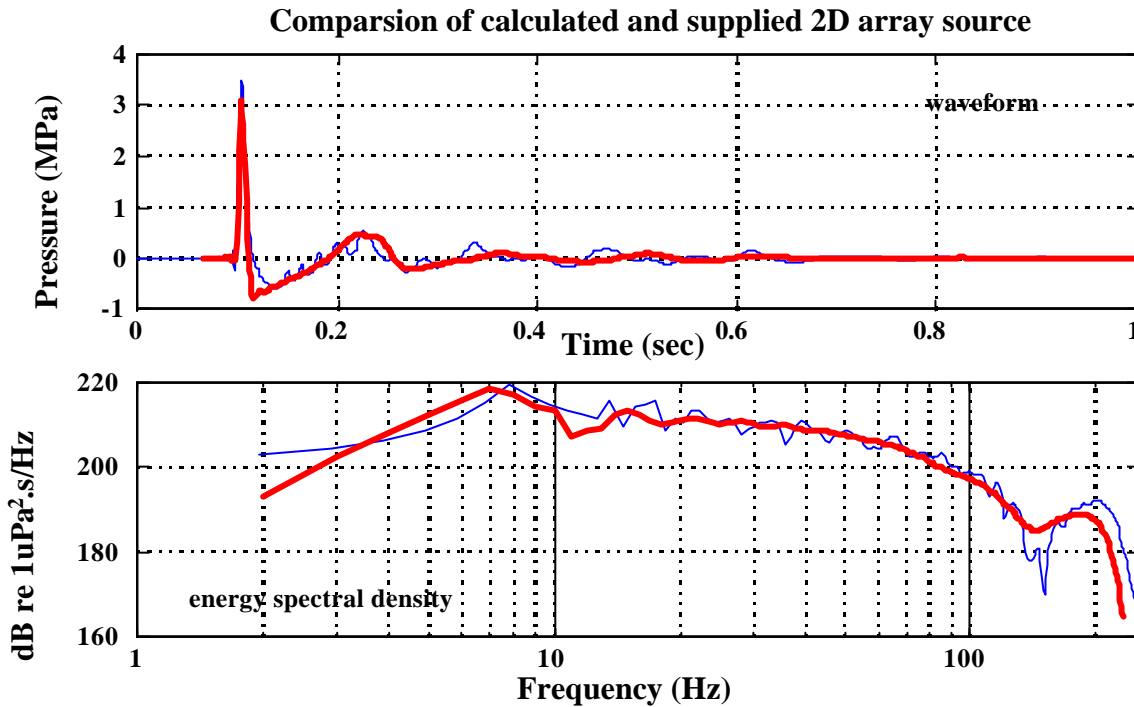
Figure 21: Comparison of source characteristics for calculated (thin line) and supplied (thick line), waveforms (**top**) and spectral content (**bottom**) for the 2D array shown on Figure 19.

The model output the array's source level at any specified orientation. Figure 22 shows a comparison of the horizontal beam patterns for the 2D and 3D arrays using 90° elevation (or in the horizontal plane). Each array focuses high frequency energy off its beam (perpendicular to tow direction), with this accentuated in the 2D array. The abeam focusing off the 3D array agrees with measurements made (Figure 13).The 2D array also focuses low frequency energy in the fore and aft directions. Most energy is required in the aft direction, or to align with the single streamer towed astern the array. In contrast low frequency energy (< 50 Hz) in the 3D array was uniform about the array, which is as required since lateral deep transmission paths are needed for the off axis streamers. There is some slight focusing of energy between 50-100 Hz in the fore and aft directions in the 3D array.

To compare the source levels of each array with aspect the broadband energy of the model output at horizontal elevation (90°) was calculated over the frequency range 15-950 Hz. The lower frequency cut-off was used since in practice little of this energy will propagate horizontally in shallow water. The resultant source level with azimuth is shown on Figure 23. It can be seen that there are higher source levels abeam for both arrays, higher levels again for end fire in the 2D array, and higher levels ahead of the beam than abaft it, for the 3D array. Given the frequency dependant nature of horizontal sound propagation in shallow

water it would be expected that these effects would be accentuated in measurements of each array at range (since the broadband source levels were strongly influenced by the low frequency energy which will not propagate well).
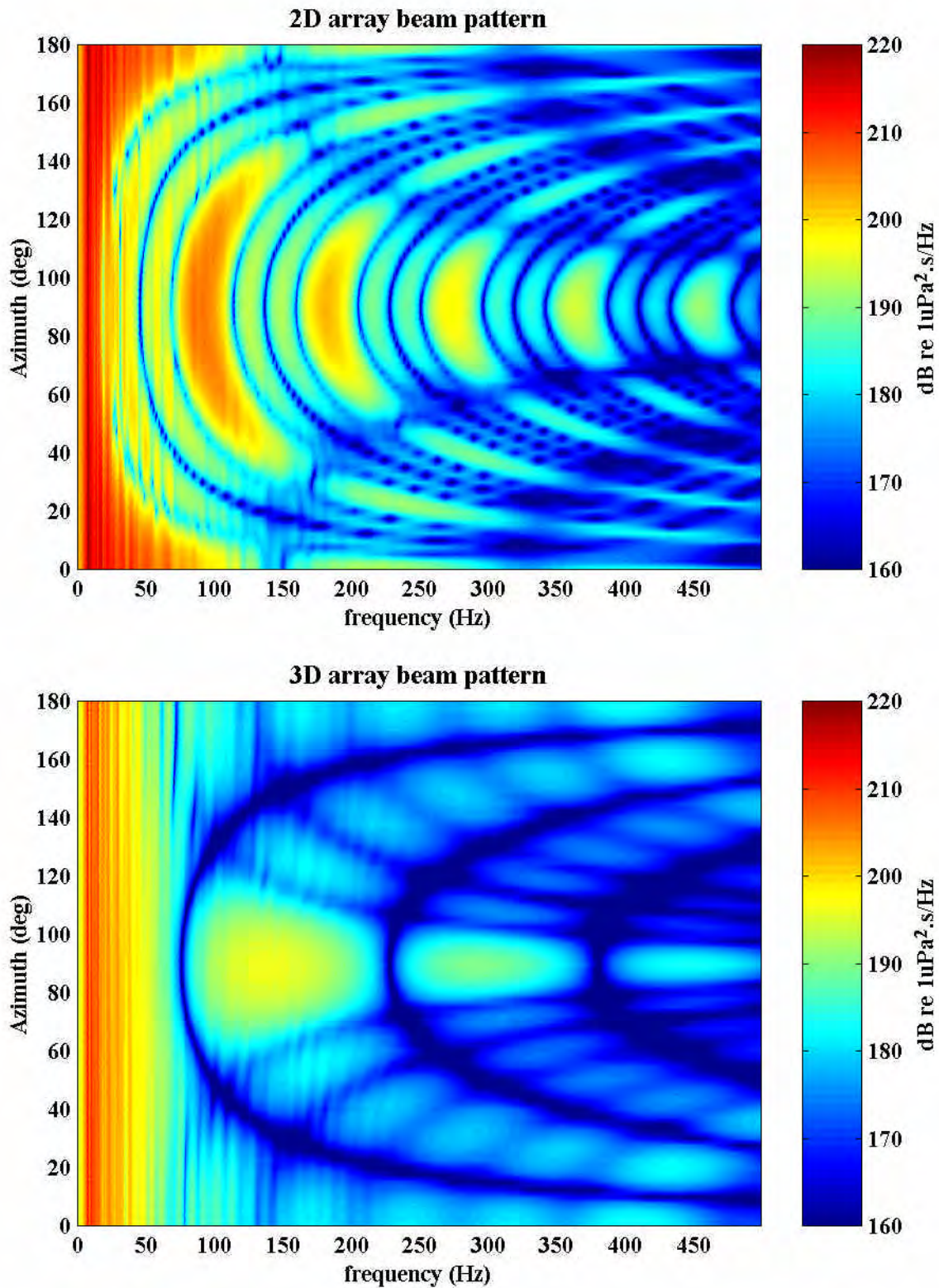
Figure 22: Modelled frequency content of 2D (**top**) and 3D (**bottom**) array's. The model used a 90º elevation (or in the horizontal plane) a 2.5º azimuth step size and no surface ghost in the calculation.

Broadband modelled source level for 2D and 3D array
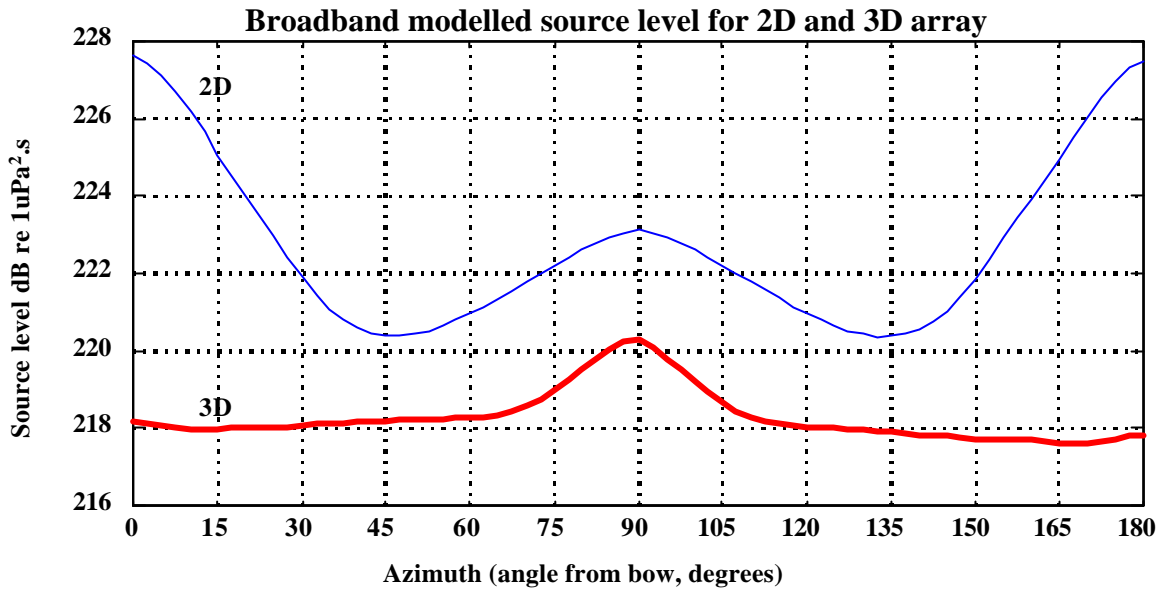
Figure 23: Modelled broadband source level of 2D and 3D arrays with azimuth (over frequency range 15 - 950 Hz).

For the exposure modelling described below the source spectra computed by the array model were integrated over frequency to produce equivalent acoustic source levels in octave bands as a function of azimuth. These source levels were then input into a model for predicting exposures through time.

2.1.4 Air-gun signal horizontal propagation

A number of numerical models are available for the calculation of horizontal acoustic propagation. They can be broadly categorised as ray tracing models, normal mode models and parabolic equation models.

As the name suggests, ray tracing models predict acoustic propagation by calculating the refraction and reflection along individual ray paths. These models are appropriate for frequencies sufficiently high that the ocean can be considered to be many wavelengths deep.

Normal mode models break the acoustic wave vector into horizontal and vertical components. They require the vertical component to satisfy appropriate boundary conditions at the water surface and seabed. This is equivalent to treating the ocean as an acoustic waveguide. They work efficiently for low frequencies where the water depth is a relatively small number of wavelengths deep but can only handle slow variations of depth and other acoustic properties with range.

Parabolic equation (PE) models make certain assumptions that allow the acoustic wave equation to be reduced to a parabolic equation form, which can be efficiently solved numerically. The chief assumption is that the sound energy propagates almost horizontally, with various numerical stratagems being used to relax this as much as possible up to the point where waves propagating more than 50° from the horizontal can be accommodated by some codes. Parabolic equation models are usually slower than normal mode codes but are applicable over a wide range of frequencies and have the significant advantage of being easily able to cope with range dependent water depth and seabed properties (ie. changing bathymetry profiles).

The details of acoustic propagation calculations are considerable, and have been much studied given their military importance. Useful starting references can be found in Jensen et al (1994) or Medwin and Clay (1998). For this study two propagation modelling examples are given, one using a PE code model, the

other using a normal mode model.

Timor Sea modelling example

In the first example propagation of the 2D array shown on Figure 19 as deployed in waters of northern Australia was used. The results of the model output were then used in exposure modelling, to hindcast the possible impact of the seismic survey on nearby fishing operations. The seismic survey region and the tracklines of the survey are shown on Figure 24.

Because of the wide range of seabed topography and steep bottom slopes in the survey area a parabolic equation model was selected as being the most appropriate for this project. The particular model used was the Range dependent Acoustic Model (RAM) written by Michael D Collins of the Naval Research Laboratory, Washington DC, the background to which is described in Collins (1992) and Collins (1993). A single run of RAM takes up to 30 minutes on a top end PC and computes the acoustic transmission loss as a function of distance between source and receiver for a fixed source, a constant receiver depth, and a single frequency. The transmission loss (TL) is defined as:

Equation 10:
$$TL = 10 \log_{10}\left(\frac{I_r}{I_s}\right)$$

where I_r is the acoustic intensity at the receiver and I_s is the source acoustic intensity referred to a distance of 1 metre from the source.

Ideally RAM would be run for a range of frequencies at every possible combination of source and receiver location. For the exposure modelling described below, given the large number of shot points in this particular survey (454,053), and the requirement to calculate received levels at a large number of receiver locations, an approximation technique based on a limited number of RAM runs was used.

The approach taken was to break the survey area up into regions of broadly similar topography and bottom types, and to run RAM for a number of propagation directions in each region to account for the different bathymetry profiles. These regions are described in Table 12. The propagation directions were taken along compass headings at 45° increments from 0° - 360°, except that runs were omitted where the dependence of the bathymetry with range was similar in different directions. For each path RAM was run for frequencies at octave intervals from 3.9 Hz to 500 Hz and for receiver depths of 15 m and 45 m. For each frequency the parameters n and a in the following equation:

Equation 11:
$$TL = n \times \log_{10}(r) + a \times r$$

where r is the range between source and receiver, were then fitted to the *TL* vs. range results produced by RAM by a least squares fitting routine. In the exposure model the fitted parameter values for the closest propagation direction were used in Equation 11 for all transmission loss calculations within the corresponding region. Where a propagation path crossed multiple regions a constant was calculated from the fitted parameters of each sequential region traversed, which when added to equation (2) using the fitted parameters from the last region traversed, ensured continuity at the boundaries of each region.
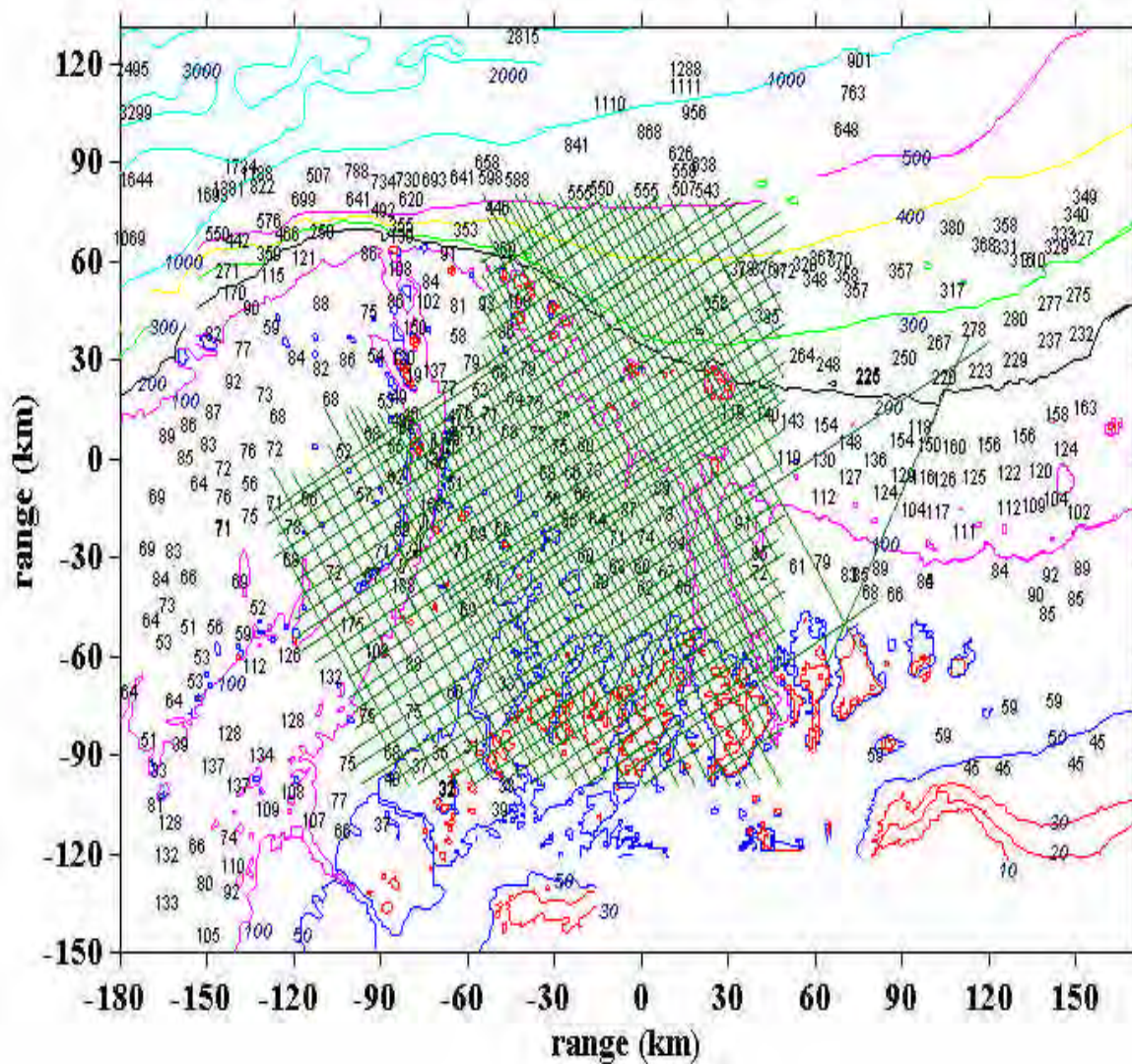
Figure 24: Region of seismic survey used for exposure modelling showing complex bottom topography and tracklines (spot depths shown in metres).

Designation	Depth range (m)	Description
A	14 - 100	Drowned estuary formation. Shallow shoals in 50 - 100m deep water.
B	60 - 110	Gently sloping, featureless.
C	7 - 200	Shelf-edge shoals in water depths > 100m
D	100 - 240	Narrow depression, long axis runs roughly N-S.
E	200 - 3000	Steep continental slope, sloping to NW.
F	200 - 2000	Steep continental slope, sloping to NE.
G	130 - 1000	Gentle continental slope, sloping to N

Table 12: Provinces used to model air-gun noise.

The properties of the seabed have an important influence on acoustic propagation at low frequencies as they determine the lower boundary conditions of the waveguide. The most important properties are compressional sound speed and density with shear sound speed and compressional absorption playing a secondary, but sometimes important role. For the region of this seismic survey, information available on subsea characteristics resulted in the compressional sound speed, shear-sound-speed and density profiles

which ranged from 1800 ms^{-1}, 600 ms^{-1}, 2050 kgm^{-3} at the sediment surface to 2400 ms^{-1}, 700 ms^{-1} and 2300 kgm^{-3} at 350 m depth below the seabed, respectively. A constant shear absorption of 0.0548 dB per wavelength was assumed. These values were the only estimates available for the entire survey area. Note that RAM does not take shear wave speed in the sediment into account. Another version of the program, RAMC, does have this capability but it is reported to have difficulty dealing with rapidly changing bathymetry as occurs in the survey area. The shear speed were comparatively low and unlikely to have a significant influence on propagation so it was decided to use RAM, rather than RAMC.

An estimate of the sound speed profile in the water column was obtained from the Australian Oceanographic Data Centre data set for the Indian Ocean. The sound speed profile was calculated from this data set using the formula of Medwin (1975). It gave a surface sound speed of 1544 ms^{-1} which dropped steadily to 1486 ms^{-1} at 600 m depth, then remained constant with increasing depth.

Some examples of the transmission loss curves calculated by RAM are given in Figure 25 together with plots of the fitted curves using fitted segments in the form of Equation 11 for each region crossed. The propagation path starts at the N extremity of the survey area and finishes at its S extremity and covers water depths ranging from 30 m to 500 m.

The procedure worked well when the water depth was either always greater than or always less than the cut-off depth in a given region. The cut-off depth refers to a phenomena in shallow water where for frequencies below a particular frequency, horizontally propagating sound energy is strongly attenuated. This is a wave-guide effect where sound of a given frequency cannot propagate if the water is too shallow. Depending on the seabed properties, the cut off depth corresponds to a water depth of between one quarter and one half of the acoustic wavelength (or the sound speed divided by the frequency).

There was poorer agreement between the RAM output and the fitted curves in regions where the water depth started off being greater than the cut-off depth but became less than the cut-off depth at some point along the propagation path (ie Figure 25 c). To avoid this problem in the exposure model the minimum depth along each propagation path was determined and in the exposure model the transmission loss was set to a very high value if this minimum depth was less than the cut-off depth for the frequency under consideration.

Figure 25: Comparison of RAM output and transmission loss calculated by joining fitted segments for low frequencies. (a), (b), (c) and (d) show transmission loss versus range at the specified frequencies for the bathymetry shown in (e) and a receiver depth of 15 m. Blue curve is output of RAM, red curve is result of joining fitted curve segments. Difference (fitted minus RAM) is also plotted below for each frequency.

55
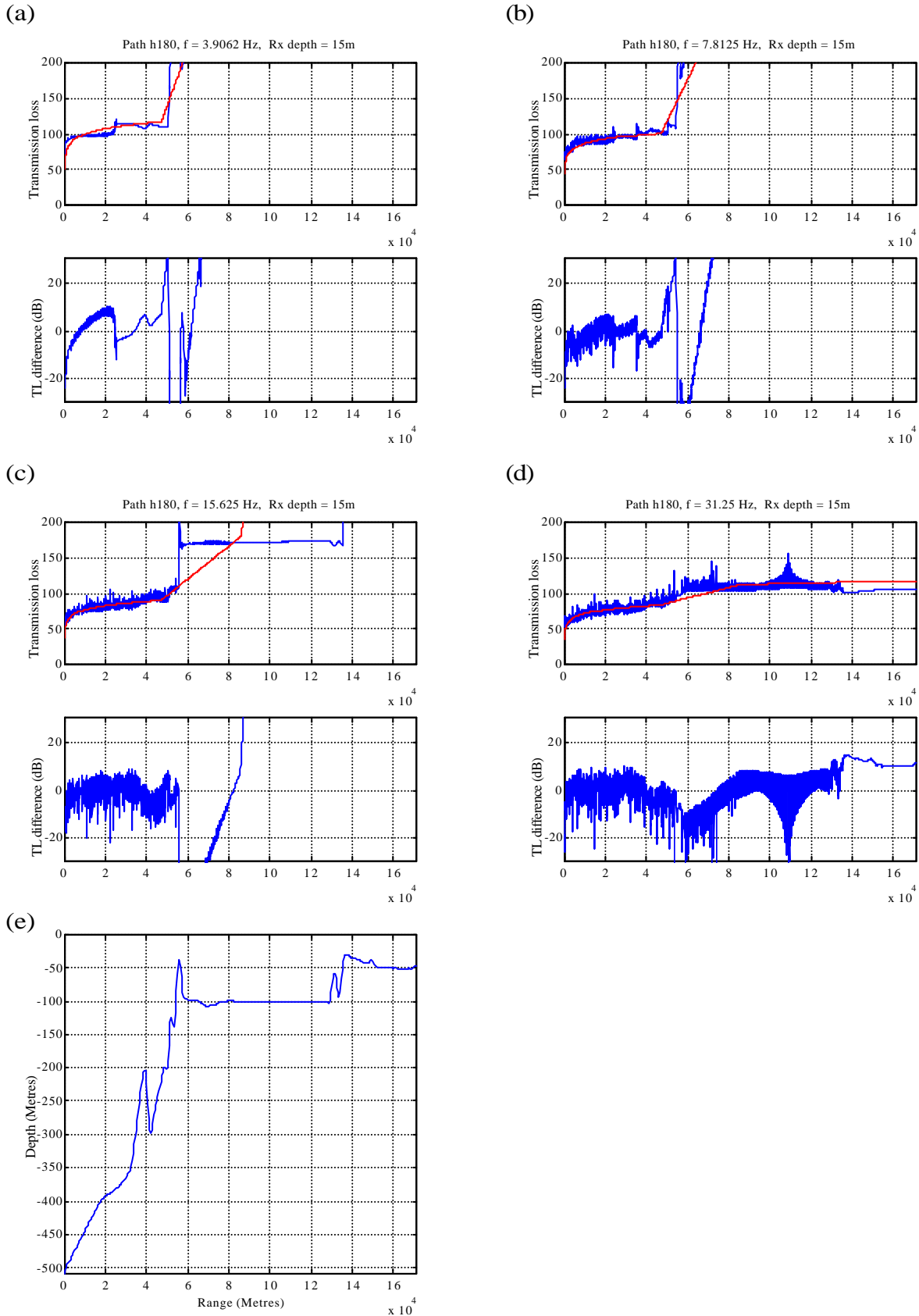
Exmouth Gulf modelling

The second example investigated using propagation modelling was that of air-gun shots from the Exmouth gulf humpback whale trials (Figure 14, section 2.2.4). The measured shots with range showed two general sets of curves, with discrepancies in level at ranges > 1 km. Modelling was carried out to determine which factors could have caused the discrepancies.

The available literature regarding bottom parameters was scarce. Hamilton (1997) presents a summary of available information for the general Exmouth region. This indicated that sediments of sand, sands and gravels, coral debris and sand and shell may have been present in the Gulf. Muds were also deemed to be present, from mud recovered with anchor gear during trials. Significantly, limestone pavements are also known to predominate within the region (Hamilton, 1997). No detailed information for Exmouth Gulf was available. Thus the sound speed and sediment depth for deeper layers were inferred from refraction measures of the headwaves produced by the Bolt 600B air-gun recorded during Exmouth humpback whale trials, using the method described by Hall (1996). While this method describes the sound speed and thickness of deeper sedimentary layers it does not describe very shallow or thin sediment layers (or the suspected shallow limestone pavement). Thus three sediment types were set up (A-C), involving mixtures of mud, the limestone pavement, sand and bedrock. One sediment profile type was run at two water depths (sediment type A, run for 18 and 10 m water depth respectively). As described in section 2.1.2 the sound speed profile in the water column was reasonably constant at 1531 ms^{-1}. Values for sound speeds and attenuation coefficients for each sediment type were as determined by refraction measures (deep sand and basement sound speeds) or from tables in Jensen et al (1994) for other measures. The normal mode propagation code KRAKEN (Porter, 1994) was used for modelling. It was found that for the configurations used KRAKEN could not deal with shear effects in the sediments, so all shear speeds and shear attenuation coefficients were set to zero. The four profiles used in modelling are given in Table 13.

Each profile type was run at 21 frequencies using 1/3 octave centre frequencies from 10 - 1000 Hz (Appendix 3) for source depths of 2.5, 3.5, 5 and 6.5 m. The KRAKEN model output the modal information for each profile configuration at each frequency. This was then transformed into a transmission loss array for the specified frequency with 1 m depth steps (ie. 1 - 18 m for types A, B and C) and 25 m range increments from 25 - 5000 m.

To convert the loss with frequency arrays (water depth x horizontal range for specified 1/3 octave centre frequency) to received air-gun level with range required:

- characterising the single air-gun for source levels at the 1/3 octave centre frequencies by summing the source air-gun spectra intensities over each 1/3 octave frequency band limits;
- for each 1/3 octave centre frequency setting up a source level array of similar dimensions to the transmission loss array and subtracting the modelled transmission loss to give received level at that frequency;
- at each frequency adding the calculated air-gun intensity to an appropriate background noise intensity to bring the signal to background levels;
- and summing the received intensities at each spatial point for each frequency and converting the single array back to dB values.

The source level of the Bolt-air-gun was obtained from near field hydrophone measurements made with the air-gun deployed at 4 m depth in 400 m of water off Perth (Duncan, 1999). The waveform and spectral content of the measured signal is shown on Figure 26.

Type number	medium	depth range (m)	compressional sound speed (ms^{-1})	density (g/cm^3)	compressional absorption (dB/λ)
A	water	0-18	1531	1	0
	limestone pavement	18-19	1650	1.6	0.8
	sand	19-248	1778	1.8	0.2
	basement	> 248	2985	2.5	0.1
B	water	0-18	1531	1	0
	mud	18-24	1530	1.6	0.8
	sand	24-248	1778	1.8	0.2
	basement	> 248	2985	2.5	0.1
C	water	0-18	1531	1	0
	mud	18-28	1530	1.6	0.8
	limestone pavement	28-29	1650	1.6	0.8
	sand	29-248	1778	1.8	0.2
	basement	>248	2985	2.5	0.1
D	water	0-10	1531	1	0
	limestone pavement	10-11	1650	1.6	0.8
	sand	11-248	1778	1.8	0.2
	basement	> 248	2985	2.5	0.1

Table 13: Details of profiles used in Exmouth Gulf KRAKEN sound propagation modelling.
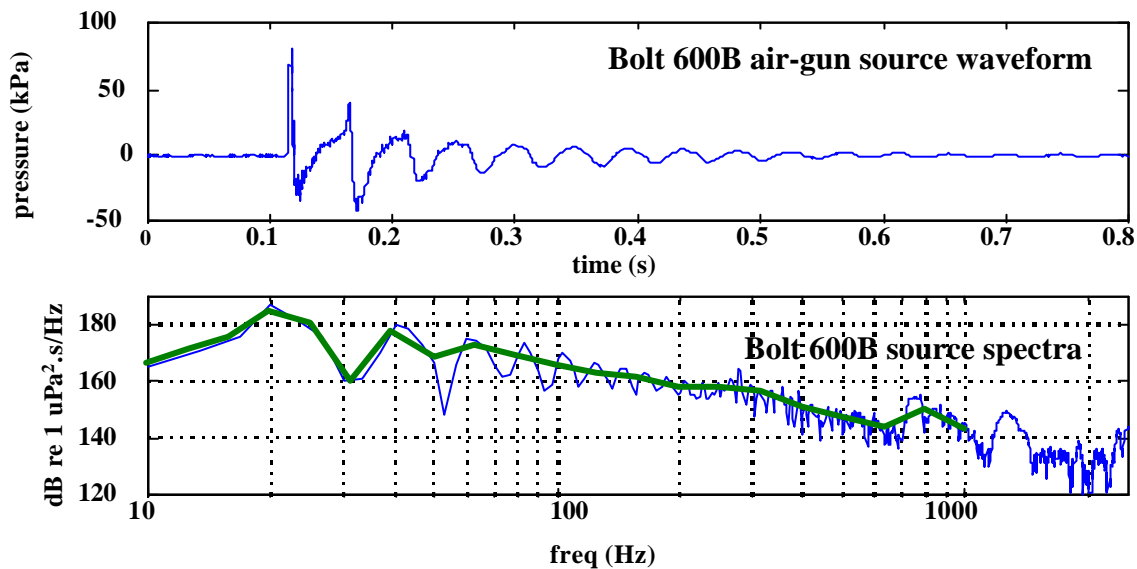
Figure 26: Waveform (**top**) and spectral content (**bottom**) of single Bolt air-gun as measured at 0.874 m (air-gun at 4 m depth, water depth 400 m) and converted to source levels (ie. level at 1 m range). The thin spectral line is as given by a 3.3 Hz resolution FFT, the thickened line is the 1/3 octave curve, as determined by summing intensities over 1/3 octave band limits from 10-1000 Hz centre frequency.

The background noise was obtained from measurements made in northern Australia for a sea state of 1 (or very calm conditions).

The model output showed consistent vertical sound intensity profiles with depth for all configuration types. These gave a sound shadowing effect near the surface, an increase in received level with increasing depth

on moving down to 6-10 m, then a reasonably constant level below this depth. The difference between surface and bottom levels became more marked with increasing range. The sound field as returned by the type A configuration for 18 m water depth, 25-5000 m range, with the source at 3.5 m depth is shown on Figure 27.

The model output was then used to compare the effect of varying: source depth; water depth and sediment type. Increasing the source depth was found to consistently increase the received signal at any specified range and depth. This was a function of the modal structure inherent in shallow water, such that the optimal position for placement of the source was at the apex of the primary mode at each frequency. This would be expected to occur towards midwater. The model output showing the received air-gun signal at 10 m depth for source depths of 2.5, 3.5, 5, and 6.5 m is shown on Figure 28 for the type C KRAKEN profile, overlaying the measured values.

For this example and a receiver depth of 10 m, increasing the source depth from 2.5 to 3.5 m or from 3.5 to 5.0 m increased the received signal by a mean of 3 dB, while increasing source depth from 5.0 to 6.5 m, increased the mean signal by 2 dB. Thus increasing the source depth from 2.5 to 6 m would result in an 8 dB signal increase. These results were consistent for all KRAKEN runs, indicating that source depth was crucial in determining the received air-gun level with range.

The effect of water depth was compared using profile A with 18 m water depth versus profile D with the same sediment structure as profile A but only 10 m water depth. Decreasing the water depth resulted in the signal dropping away more quickly at ranges > 1 km. This is shown in Figure 29 using a receiver depth one m above the bottom and a 3.5 m source depth.

Seabed properties are critical for determining sound propagation in shallow water. This can be seen on Figure 30 which compares KRAKEN model output for the three differing seabed compositions (type A. B and C, Table 13, source at 3.5 m, receiver at 10 m) against the measured data sets. The type A sediment, with no mud, predicted the general trend for the top set of measured curves and showed a similar small scale structure but over estimated the levels. The types B and C sediments with mud included, better predicted the lower set of curves but showed to much modal structure.

The frequency content of received air-gun signals calculated by KRAKEN for the sediment types A, B and C (Table 13) for the source at 3.5 m and the receiver at 17 m are shown on Figure 31. These revealed that the shallow limestone pavement in sediment type A produced the greater energy content at higher frequencies, as seen in the measured frequency content of the type 1 curves, shown on Figure 18. In comparison the frequency content output for sediment types with deep mud layers and no or deep limestone pavement (8 m or mud type B, 10 m of mud type C), showed very little of the high frequency energy returned in the signal at range. These curves agree with the two types of curves from the measured data, as shown on Figure 18. Thus it is probable that the type 1 measured curves were produced by reflected energy from a shallow limestone pavement, whereas the type 2 curves were made over mud or deep sand bottoms where substantially more high frequency energy was lost into the bottom.
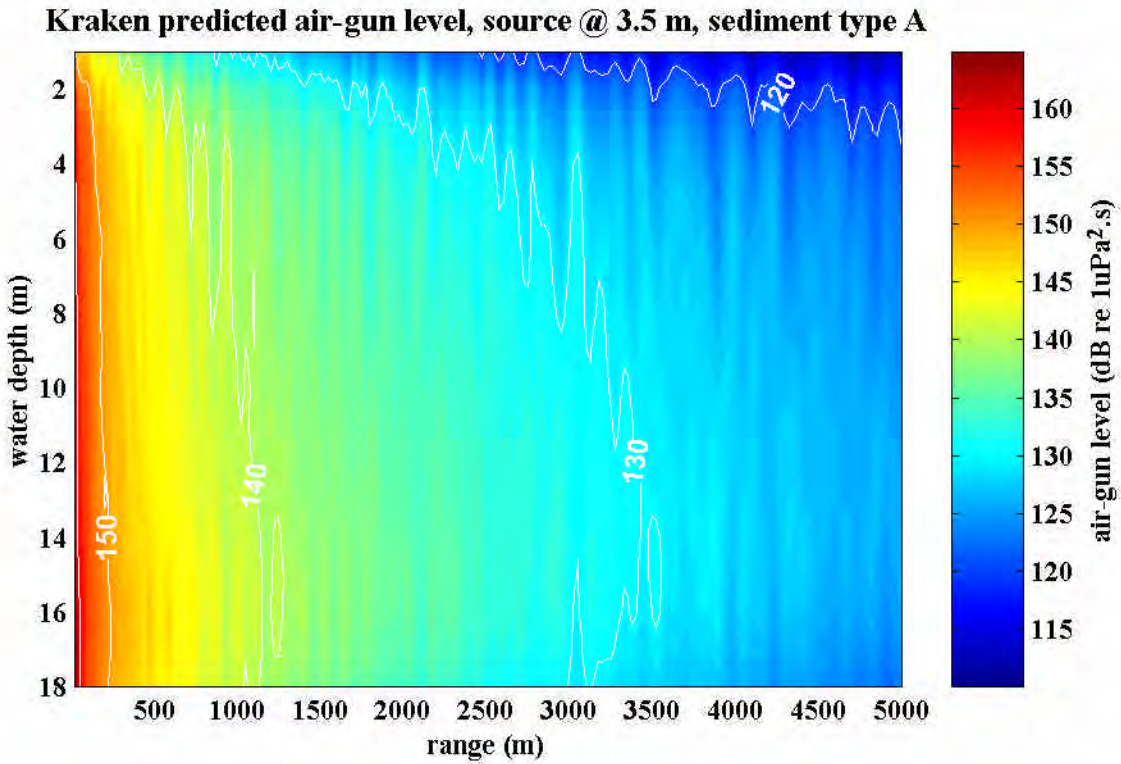
Figure 27: Sound intensity profile with depth and range for propagation of the single Bolt air-gun using the Exmouth Gulf type A, KRAKEN model configuration.
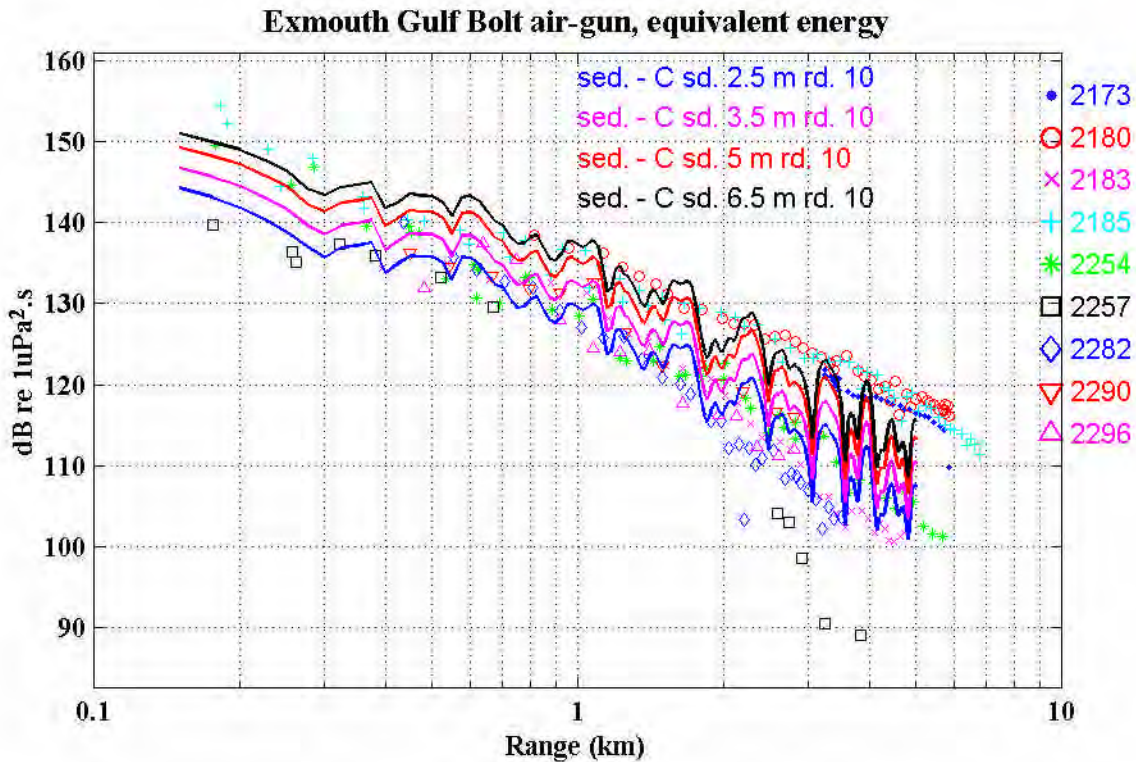
Figure 28: Calculated air-gun received level (equivalent energy) at 10 m depth in the water column for sources at 2.5, 3.5. 5 and 6 m depth using the type C Kraken profile, overlying the measured levels (down-sampled).
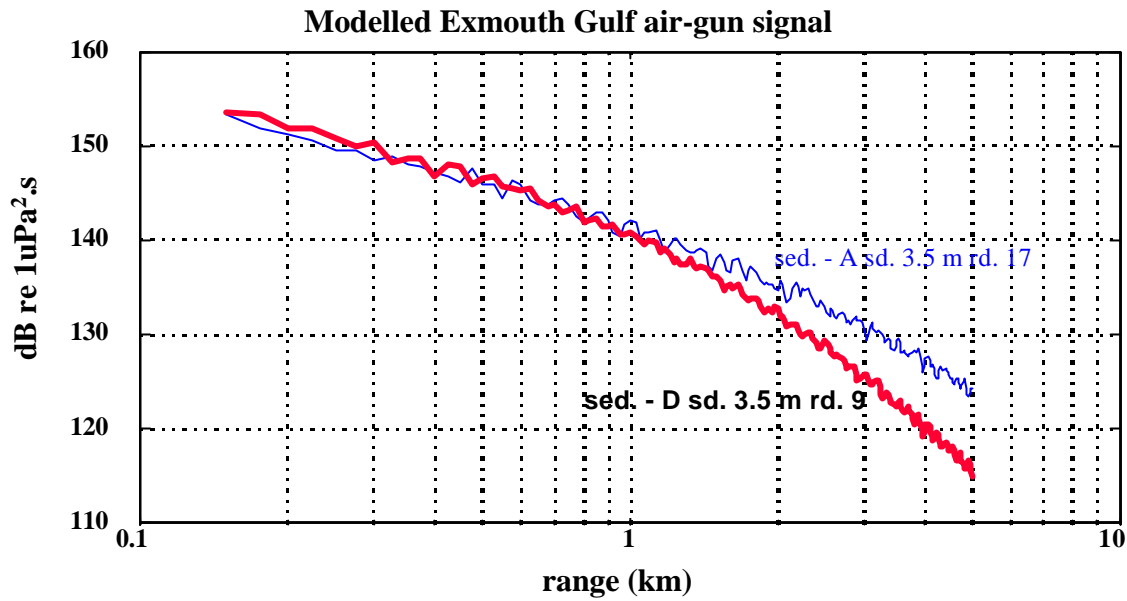
Figure 29: Effect of decreasing the water depth from 18 m (type A configuration) to 10 m (type D configuration) on the KRAKEN air-gun level output using the same sediment and water column parameters. Each plot was calculated using a 3.5 m deep source, but used a receiver one metre above the bottom.

It is believed that by judicious juggling of the mud, limestone pavement and underlying sand parameters, good fits to the measured data could be obtained.

The modelling of the air-gun propagation in Exmouth thus revealed that the source depth and sediment type were the primary parameters important in predicting air-gun levels for receivers deeper than mid water. Above mid-water the vertical sound intensity profile became increasingly important.
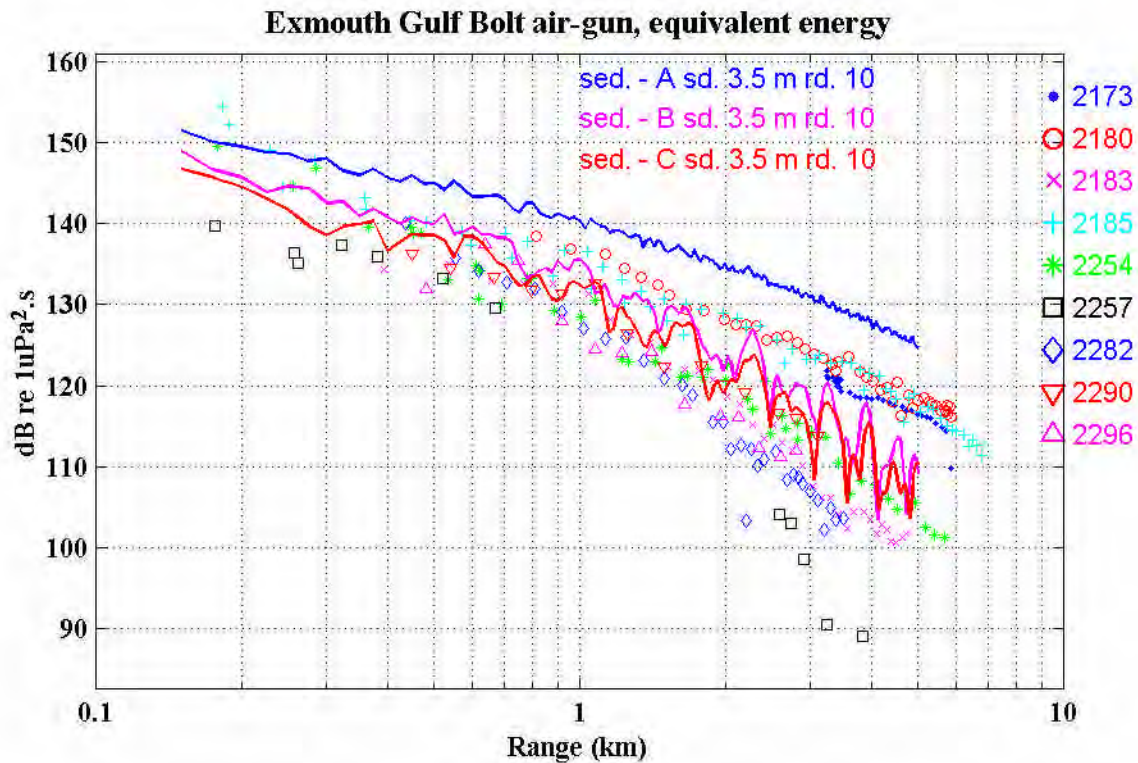
Figure 30: Modelled KRAKEN output (thick solid lines) for three sediment types, compared with measured data sets (down-sampled).
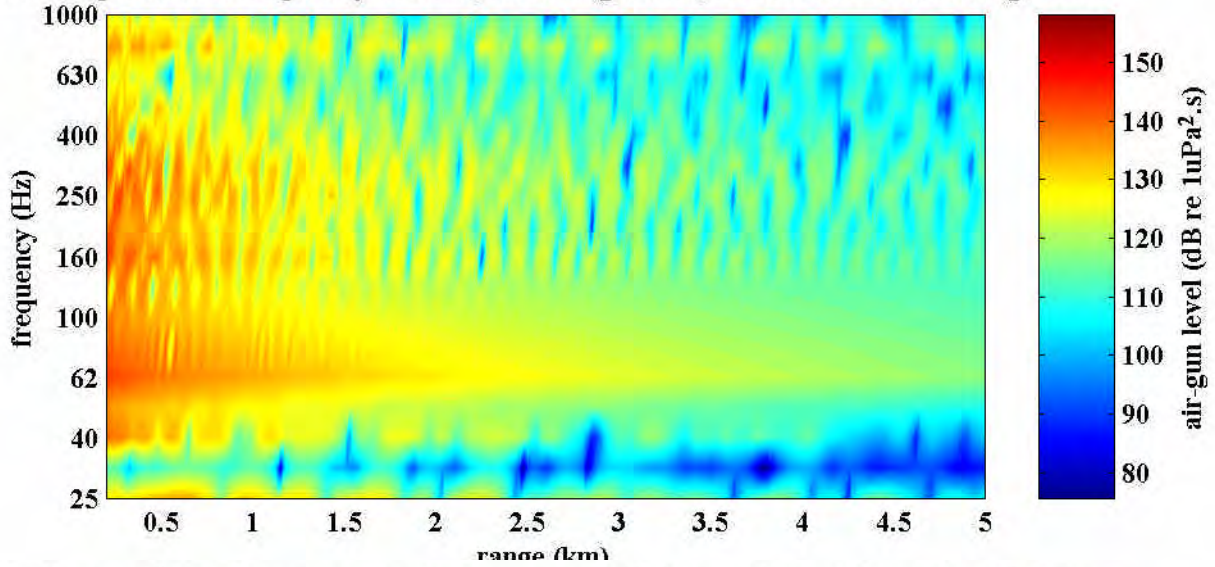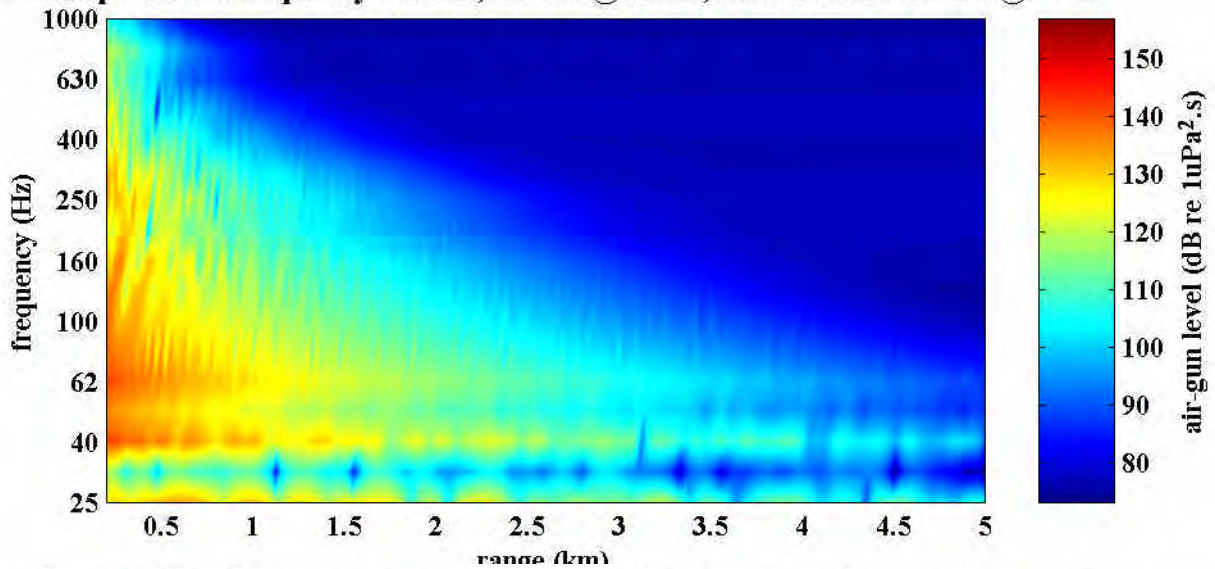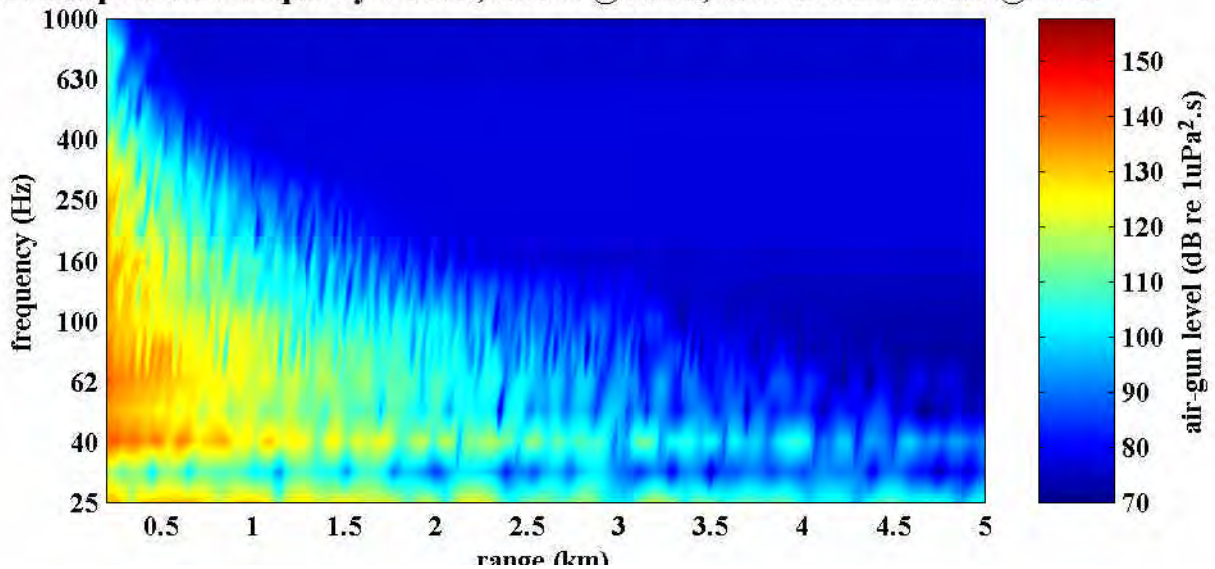
Figure 31: Frequency content of received air-gun signals with range as output by KRAKEN for the three sediment types, source at 3.5 m and receiver at 17 m depth. Frequencies were calculated in 1/3 octave steps.

2.1.5 Exposure modelling

Although the measurement and modelling of single air-gun or array shots provides valuable information on sound levels experienced by animals at specific times, depths and ranges, it tells little of exposures through time for a constantly moving seismic source. Since seismic surveys may be run over periods of many weeks over many hundred km^2, measures of the signal received over time will be crucial in determining the scale and persistence of any effects. Describing the air-gun exposure in time invokes two problems: 1) the magnitude of the task of calculating received levels for each air-gun shot over the region of a given seismic survey at a suitable spatial resolution for the duration of the survey; and 2) determining an appropriate way to present this information.

The results of the effects studies (sections 2.2 - 2.5) and from the literature (see Engås et al, 1996; Pearson et al, 1992; Skalski et al, 1992; McCauley, 1994; Richardson et al, 1995, and later in this document) suggest that above threshold air-gun signal levels behavioural changes occur in many species and that with increasing level these behavioural changes become increasingly significant. Assuming that one can predict that above a specified threshold the behaviour of a given species will be altered in some fashion, suggests presenting seismic survey exposure as the proportion of a region which experiences levels above a specified threshold, over the survey duration. This approach would be most useful for resident animal populations since they would be expected to normally reside in the region over the full survey length. The technique would be less applicable for migratory animals since they may simply pass around and through any potential disturbance.

Such an exercise was carried out using data from a seismic survey in northern Australia which took place over a 121 day period. This was done to present a framework for predicting the scale of potential biological effects for any given seismic survey. To do this a model was developed which used the output of source characterisation (section 2.1.3) and sound propagation modelling (section 2.1.4) combined with the navigation data for the survey, to produce contour maps of regions receiving exposure above set thresholds, through time.

The program split up a given seismic survey's geographic layout (time and shot point location) into a number of files consisting of sequential periods of air-gun operations, then calculated and saved for each of these periods a grid of points (in space) being the sum of shots which had exceeded a specified threshold level. These grids were then summed for all files (ie. the entire seismic survey) and presented as contour maps of the region, showing densities of shots exceeding the thresholds. These contour maps could be considered as indicators or predictors of the probability that within the higher value contours greater biological effects would have persisted through time. Although expressed here simply as number of shots above the specified threshold, the model output could be presented as some other unit through time, since the output files were saved for periods of consecutive shooting with start and finish times all known. Assuming one could predict the air-gun shot thresholds required for different effects (say possible disruption to fishery operations) then one could predict or hind-cast (as carried out in this example) the scale in time and place of possible effects.

The approach used in the exposure model for a given source and seismic trackline configuration was then to:
1. Split the seismic survey trackline data (date, time, latitude, longitude) files into periods of sequential shooting. This was done for a previously carried out survey for hind-casting effects, but could be just as easily done for planned surveys to predict possible effects;
2. Characterise the acoustic source, or air-gun array, for source levels over eight octave frequency bands

with azimuth (as per section 2.1.3);

3. Calculate acoustic propagation in the seismic survey region at the eight octave centre frequencies for representative bottom types and travel path topographies to give transmission losses with range (section 2.1.4);

4. Fit curves to the appropriate propagation model outputs and build up tables of cut off frequencies;

5. For selected shots across the survey area use the fitted propagation curves, source level with azimuth tables and cut-off information to calculate received air-gun levels for each frequency on a grid of sufficient spatial resolution. For each point in the spatial grid over the eight octave centre frequencies, this involved determining the array source level for the appropriate orientation, subtracting the appropriate transmission loss, then summing the received intensity at each frequency to give total received intensity at the point.

6. For each shot and all points in the grid, determine those above the specified threshold levels, (0/1) and save this data for each input file (trackline).

7. Present grid of all points (all tracklines) above thresholds as contour plots.

The general model flow is shown in Figure 32. The model used a series of decreasing sized grids, starting with a grid which encompassed the maximum and minimum extent of the survey area ± 50 km (grid G1). A 500 m resolution was used for all runs of the model. The first program loop (Figure 32) ran at the input file level, and built a second grid based on the co-ordinates of grid G1, but which encompassed only the respective file track-line extent ± 50 km (G2). All values of this grid (G2) were set to zero. The third loop incremented every nth shot within the trackline (every 5th shot used in the example given). For each specified shot point within this loop a grid (G3) centred on the nearest (x, y) coordinate of grid G1 to the shot point, was set up so that the vertical and horizontal ranges from the central point were 50 km minus twice the grid resolution (500 m for the given example). This array was 197 x 197 points. This grid was reduced in size by log scaling the vertical and horizontal ranges from the central point (since sound propagation loss is generally of a logarithmic form), resulting in grid G4 of dimensions 37 x 37 points centred about the nearest G1 point to the appropriate shot point. The values of this grid (G4) were set to zero.

The array source level (octave levels for appropriate azimuth and using 90° elevation) and transmission loss at the eight octave frequencies (for a receiver depth of 15 m) were calculated for each point of grid G4. Octave centre frequencies used were 3.9063, 7.8125, 15.625, 31.25, 62.5, 125, 250 and 500 Hz. The bathymetry profile along each G4 propagation path was checked at each frequency to determine if the cut-off depth limit had been exceeded (any point along bathymetry profile shallower than cut-off depth) and if so the transmission loss was set to 200 dB. The received G4 levels for each frequency were calculated (source level minus transmission loss as a dB value) and the intensities at each frequency then summed to give the received G4 level in broad-band units of dB re $1\mu Pa^{2}$.s. The values of received level for grid G4 were then grided back to grid G3 dimensions. Points within grid G3 and above the specified threshold were scored as one and these ones or zeros summed into grid G2. This was repeated for all specified shot points in the input file, and grid G2 saved for each input file.

The output values of grid G2 were then summed into grid G1 to give the number of shots which had exceeded the specified threshold. The final grid G1 was then adjusted for the shot increment used, and plotted as contour plot of shots above the thresholds.

The model was set up as per above and run using the 2D array characterisation described in section 2.1.3, the propagation modelling as described in section 2.1.4, for the seismic survey shown on Figure 24. The model output for shots above a equivalent energy threshold of 155 dB re 1 μPa^{2}.s is shown on Figure 33.

The greatest concentration of air-gun shots occurs in the plot centre shown by the > 40,000 shot contour. Within this contour level the greatest 'disruption' could potentially occur for the longest time period.

The model enabled us to produce contour plots for any given shot. An examples is shown for a shot at the S end of the survey region in shallow water, on Figure 34. The marked directionality pattern of the array is evident in this plot. This is due to the increase in radiated energy at end-fire and abeam the array, as shown on Figure 22, and would be expected given the array dimensions (Figure 19). The effects of shallow water (below cut-off frequency) can be seen in the SE portion of the contours.

Preparatory:

Set up directories, grid resolution, tracklines & shot increment for run

Load trackline summary data

Establish grid of easting & northing vectors to encompass max & min survey extent ± 50 km at specified resolution (500 m used, grid G1, 350.4 km E-W x 281 km N-S)

Size sub-array of grid G1 so that vertical & horiz. range from centre = 50 km - 2 x resolution (Grid G3)

size sub-array of G3 based on logarithmic scaling of range from centre point, (Grid G4)

Load grids of propagation region & bathymetry, source level lookup table, transmission loss coefficient lookup table, cut off depths with frequency

TRACKLINE LOOP

Build grid G2 as sub-array of G1 which encompasses max & min trackline extent ± 50 km

Locate G2 in G1

Get nav data for specific trackline

Set up which shots to use

SHOT LOOP

locate shot point nearest x & y coordinate in G2 grid

dimension G3, centring on nearest shot point coordinates, build G4 full array from this

get range, azimuth to array track, compass heading from shot point to each point in G4

get source level using azimuth (8 freq.) for each G4 point

get propagation regions traversed and bathymetry profile from shot point to G4 points

FREQUENCY LOOP (8 of)

get transmission loss

check cut off depth & set transmission loss to 200 dB if exceeded

next frequency

calculate received level each G4 point (source level - transmission loss) at each frequency

sum intensities to give received level at each G4 point

grid G4 array back to G3 dimensions

find received G3 levels above threshold

sum G3 above threshold into G2 array

next shot

Save G2 array, dimensions G1, location G2 in G1

next trackline

Process and plot output

Figure 32: Exposure model flow diagram
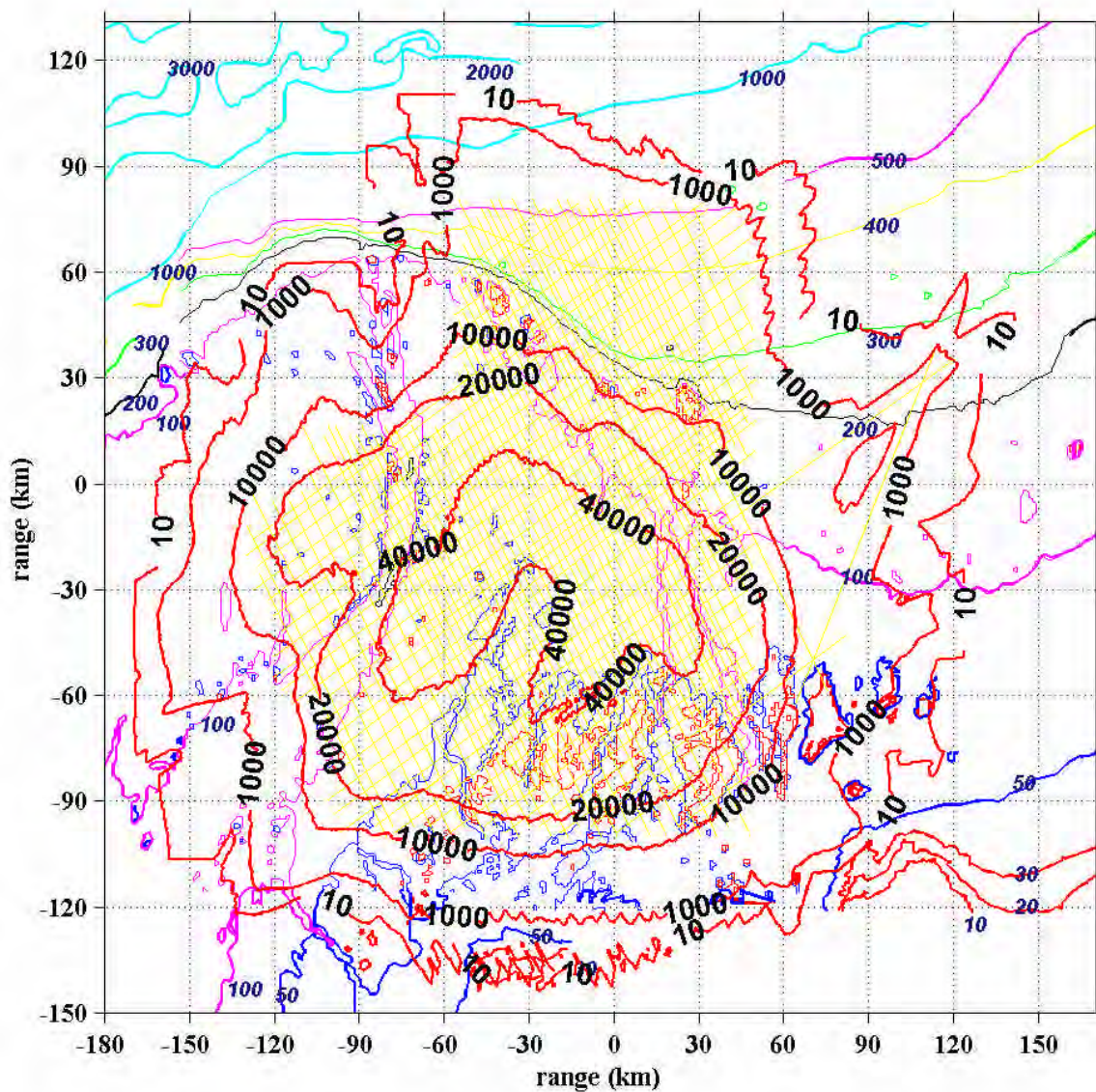
Figure 33 Contour plot of number of shots over survey duration exceeding 155 dB re 1 uPa^2.s, as output by exposure model. This survey ran over 121 days. The data could be presented alternatively with time included, perhaps as shots exceeding the threshold per day.

Figure 34 (**top**) Survey region showing file 1 trackline, grid G2 encompassing file extent +/- 50 km and grid G3 of 49 x 49 km for which received shot levels were calculated. (**bottom**) Contours of received shot level (dB ra 1 uPa^2.s) for grid G3. The water depth never exceeded 60 m. There were many points which required adjustment to the transmission loss as the minimum depth along the travel path (air-gun array to received point) was less than the cut-off frequency depth. Strong directionality patterns related to end-fire and abeam directionality of the array are evident. The tow direction was to the NE.

2.1.6 Headwaves

When sound from the water column hits the seabed some of the energy is reflected back into the water column and some is transmitted into the seabed. This situation is shown in Figure 35 which assumes that the seabed can be adequately modelled as a fluid, thus ignoring the presence of shear waves. The transmitted wave changes direction due to refraction by an amount that depends on the sound speeds in the two media and the direction of the incident sound.
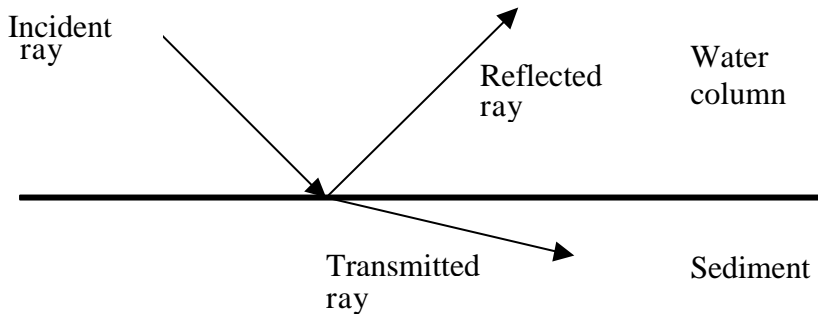
Figure 35: Geometry of reflection and refraction at the seabed.

The sound speed in the sediment is usually higher than in the water and in this case the transmitted ray is refracted towards the interface. At a particular angle of incidence, called the critical angle, the transmitted ray becomes horizontal and energy travels along the interface between the two media. This interface wave, or headwave, travels along the interface at a speed corresponding to the sound speed in the sediment and causes sound to be re-radiated back into the water column at the critical angle, resulting in the propagation path shown in Figure 36 (for clarity the reflected signals are not shown). This path is referred to as the bottom refracted path.
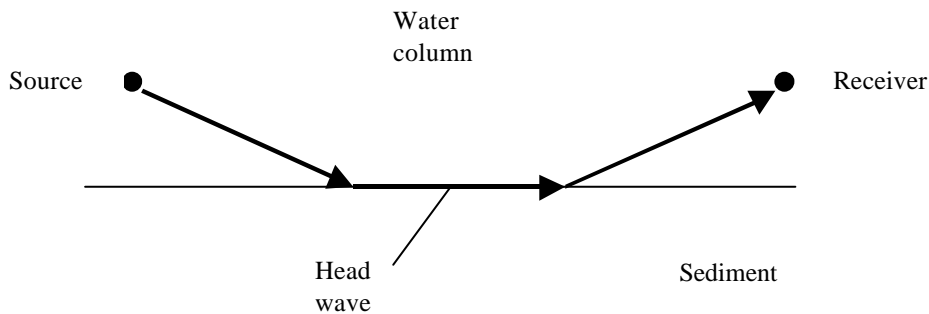
Figure 36: Bottom refracted path

Although the bottom refracted propagation path is longer than the direct path between the source and receiver, the headwave travels faster than the direct path signal so for sufficiently large source-receiver separations the bottom refracted signal arrives first. Although this explanation has referred to the interface between the water column and the sediment, headwaves and their corresponding refracted paths can exist wherever there is an interface between any two layers where the sound speed in the lower layer is higher than that in the upper layer. This is the basis of seismic refraction techniques used by geophysicists to map rock and sediment strata (which differs from the reflection techniques used in most conventional seismic surveys).

Some examples of recorded air-gun shots showing bottom refracted signals are given in Figure 37. These signals were recorded in shallow water (approximately 20 m deep) in Exmouth Gulf using the Bolt 600 B air-gun as the source and with a receiver hydrophone resting on the seabed. In each case the distinct high frequency burst commencing at 0.8 sec is the signal that has travelled by the direct through water path. At longer ranges the waterborne signal is preceded by a low frequency bottom refracted signal which is produced by the air-gun bubble pulse. As the distance between the air-gun and hydrophone increased, so did the time difference between the start of the bottom refracted signal and the start of the waterborne signal.
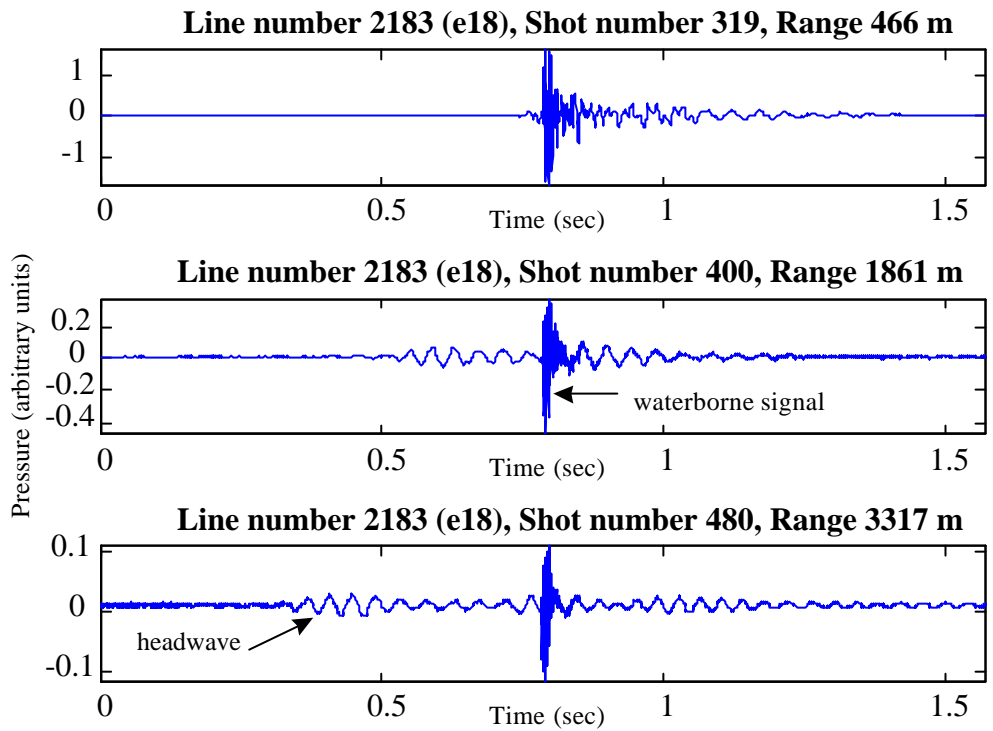
Figure 37: Air-gun signals from Exmouth Gulf recording set 2183 made with the Bolt 600B air gun during whale trials, showing the low frequency bottom refracted signals, or headwaves.

Animals which can sense sediment borne sound waves or which may couple their hearing systems to the sediment may be influenced by headwaves. The biological implications of the headwaves produced by air-gun arrays have not been addressed in this study.

2.2 Humpback whale response to nearby air-gun exposure (R.D. McCauley, M-N. Jenner, C. Jenner, K.A. McCabe J. Murdoch)

To investigate the response of great whales to seismic surveys a series of controlled approaches towards humpback whales (*Megaptera novaeangliae*) with an operating air-gun were carried out. The results of these trials are discussed in section 2.2.3. As the first set of trials was being planned funding was received to carry out observations of the movement of S travelling humpback whales about a proposed 3D seismic survey (*Robert* survey), which was to be carried out off Exmouth Cape, near where the approach trials were planned (see Figure 7 - top). The 3D survey ran from 4th October to 8th November 1996.

It was expected that the *Robert* seismic survey tracklines would cross the migration route of S bound humpback whales during or close to the southward migration peak. Although the exact migration route or its timing was not known before the survey, it was believed that humpback whales cleared the Monte Bello Islands (183 km NE of North West Cape) to the N and swam roughly SW or followed a depth contour, to close the coast to the E of North West Cape (arrows Figure 7 - top). Late September to mid October was expected to be the peak for cow-calf pods, which normally trail the main migratory body by 2-3 weeks (Chittleborough, 1953). Consequently a program to monitor the response of humpback whales transiting the seismic area was carried out.

This work comprised aerial surveys before and during the *Robert* survey to discern any possible gross changes in humpback migration patterns or habitat usage; observations from the seismic vessel the *Geco Resolution* of whale numbers and movements seen from the vessel; observations of whales on interception courses with the *Geco Resolution* from a small vessel; and acoustic measurements of the air-gun array and humpback vocalisations from 1.5-64 km from the *Geco Resolution*. Aerial surveys were not planned for after the seismic survey completion as it was expected the majority of animals would have passed through the region by the survey completion date. The field program was put together at short notice (three days for the first aerial surveys).

Details of the methods used are given in section 1.2 (acoustic equipment), 1.4 (*Geco Resolution* work), 1.5 (humpback exposure trials), and 1.6 (analysis).

All humpback whale work was carried out during the whales S migration period. Work by C & M-N Jenner since 1996 has confirmed that the migratory peak for whales transiting the Exmouth area is around early September, being seasonally variable. This is as described by Chittleborough (1953) for humpback whales during the height of the whaling period. The *Geco Resolution* work was carried out through September (one set of aerial surveys and ship based observations) and October (ship based observations, small vessel work about *Geco Resolution* and second set of aerial observations). The approach trials were carried out through October of 1996 and 1997. Thus the second set of *Geco Resolution* aerial surveys, the small vessel work about the *Geco Resolution* and the approach trials were carried out during the tail end of the migratory period.

It is important to realise that although the two sets of studies (observations about a working seismic vessel and experimental exposures), were carried out in close proximity, the 'normal' behavioural state of the respective humpback whales in the two studies was different. For the *Geco Resolution* work the humpbacks were migrating, that is swimming steadily SW, often accompanied by small and vulnerable calves. For the Exmouth Gulf work the humpbacks were resting, socialising or engaged in courting behaviours. This distinction is important in interpreting the results.

2.2.1 Whale movements from aerial surveys and *Geco Resolution* observer

The general migratory pattern of humpback whales through the study region is shown by the arrows on Figure 7 - top. Before the work began it was believed humpbacks travelling S would clear the Monte Bello Islands and travel SW in relatively deep water (30-120 m depth) to close the coast in the vicinity of North West Cape. It was not known if there was a preferred 'corridor' in the deep water nor where and what proportion of whales entered the shallow water defined by the chain of islands to the NE of NW Cape, so as to enter Exmouth Gulf.

The aerial surveys were carried out primarily to ascertain any preferred migration corridor used by humpbacks transiting the seismic region, to find where they crossed into Exmouth Gulf and to attempt to determine if these patterns altered due to the *Robert* seismic survey operations. Given the migratory pattern, with an expected bell shaped distribution curve of the number of animals passing any given point along the coast through time, and the resources available it was not considered practical to compare aerial survey abundances in the seismic region between pre, during and post survey sets of flights.

Details of the aerial survey methods are given in section 1.4.1. Briefly each survey involved eight 30 n mile (55.6 km) on-survey legs, on headings 330° or 150°, with observations also made off survey during turns and transit (Figure 7-top). These legs covered the seismic region, inshore waters and waters to seaward and to the N of the seismic region. The reliable sighting field of view was considered as 100-3200 m off the aircraft's trackline. This gave a total search area per survey of 2,756 km^2. Two sets of four flights were flown, the first set immediately before seismic operations began and the second set midway through the seismic survey program. Details of the aerial survey sightings are given in Table 14 (on-survey legs corrected for resights within a survey). The on-survey legs were further split between the inshore or green waters (inside the 20 m depth contour) and the blue water seaward of the 20 m contour, with surveyed areas of 1084 km^2 and 1672 km^2, respectively.

Date	#	total	on survey	off survey	green - on	Blue - on
Pre seismic						
21 Sep 1996	1	17/1/4-13	13/1/1-10-3.628	4/0/3-3	7/0/1-4-3.690	6/1/0-6-0.3.588
22 Sep 1996	2	aborted[1]				
27 Sep 1996	3	19/1/5-17	13/0/1-11-3.991	6/1/4-6	7/0/0-5-4.612	6/0/1-6-3.588
28 Sep 1996	4	12/1/2-12	5/1/1-6-2.177	7/0/1-6	4/1/1-5-4.612	1/0/0-1-0.598
total		**48/3/11-42**	**31/2/3-27-3.266**	**17/1/8-15**	**18/1/2-14-4.305**	**13/1/1-13-2.592**
During seismic						
19 Oct 1996	5	5/0/0-5	2/0/0-2-0.726	3/0/0-3	2/0/0-2-1.845	0/0/0-0-0
20 Oct 1996	6	11/0/0-7	5/0/0-3-1.088	6/0/0-4	0/0/0-0-0	5/0/0-3-1.794
22 Oct 1996	7	8/0/1-6	7/0/1-5-1.814	1/0/0-1	1/0/1-1-0.926	6/0/0-4-2.392
25 Oct 1996	8	4/1/2-5	2/0/0-2-0.726	2/1/2-3	0/0/0-0-0	2/0/0-2-1.196
total		**28/1/3-23**	**16/0/1-12-1.088**	**12/1/2-11**	**3/0/1-3-0.692**	**13/0/0-9-1.346**

Table 14: Sighting details of all aerial surveys for the grid as shown on Figure 7 - top. The on-survey legs (headings 330° or 150° Figure 7-top) have been split for blue water which encompassed the seismic survey region (seaward of the 20 m contour), and the green water inside of the 20 m contour. Values are given as: adults / juveniles / calves - pods - pods/1000 km^2 (for on-survey legs). Superscripts: [1] - flight aborted due to wind.

The set of aerial surveys carried out during the seismic period (surveys 5-8, Table 14) were all during periods when the air-guns were operating. The air-gun operation history over the 19-25th October is shown on Figure 38. The weather over the 24th October precluded seismic operations, aerial surveys and

any successful boat-based whale observations. Given that the air-gun arrays were operating before and during all these aerial surveys it has been considered valid to lump sightings data for this set of samples to compare with the lumped sighting data from the pre-seismic aerial survey observations and to treat each of the samples taken during seismic operations as being potentially influenced by the seismic program.
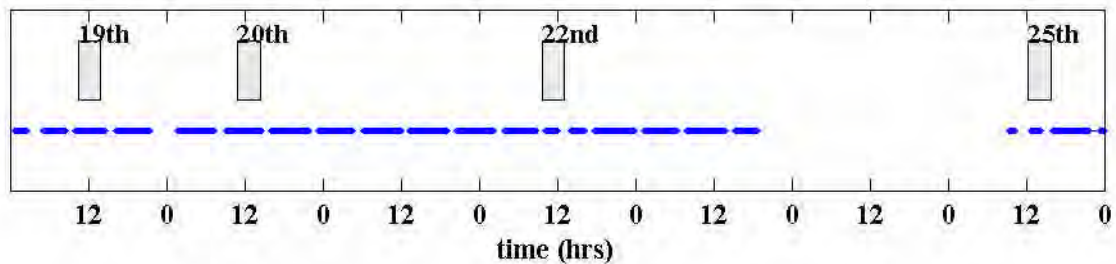
Figure 38: Presence of operating air-gun arrays over the period 19th-25th October (dark lines), with the timing of each aerial surveys shown by the respective grey boxes. The break in operations over the 24th was due to bad weather (with high seas inducing self noise in the streamers being the limitation to seismic operations).

The on-survey whale densities (pods/1000 km^2) shown on Table 14 revealed that there were considerable differences between the total pod densities observed between the two sets of aerial surveys. The difference in densities suggested that the migration peak occurred towards the end of September as expected, and that the second set of aerial surveys took place during the tail of the migration period.

The observer based aboard the *Geco Resolution* made 270, 40 minute observations (each referred to as a block) over 4th October - 5th November in winds < 15 knots (see methods 1.4.2 for details). During these observations she sighted 51 whale pods.

The sighting effort from the aerial surveys (on-transect-pods/km^2/flight) and the *Geco Resolution* observer (pods/observation-block/day) are plotted on Figure 39. The y-axis units differ for each set of densities, thus the data were normalised between zero and their respective maximum values so as to give an indication of any trends through time consistent between data sets. Although there was considerable scatter amongst the *Geco Resolution* observations (which would be expected given the pulsed nature of migrations), a general trend for a reduction of whales passing through the seismic region with time was evident. This general trend was interpreted as indicating that the seismic survey occurred during the tail of the migration, hence the different pod densities observed between pre and during seismic surveys were unlikely to have been attributable to the seismic survey presence.

The humpback whale sighting data derived from small vessel surveys within Exmouth Gulf over 1996-1998 and carried out by C & M-N Jenner is shown on Figure 40. Again this supports the notion that the second set of aerial survey flights were flown during the tail of the migratory peak.

The aerial surveys revealed differences in the proportion of whales seen along the blue and green water sections of the on-survey legs, between sets of flights. Approximately equal pod numbers were seen in the green water portion of the transects as compared to the blue water portion during the pre-seismic aerial surveys. During the second set of aerial surveys, with the seismic survey in progress, three times as many pods were seen in the blue water portion as opposed to the green water portion of on-survey legs (Table 14). These differences in the relative ratio of whales utilising the blue and green water portions of the aerial survey region raised the question of had the '*Robert*' seismic survey influenced the number of whales entering Exmouth Gulf. The sightings data of the Jenners (Figure 40) showed a drop in the 1996 sighting

rate within Exmouth Gulf as compared to 1997 and 1998, over the end of October, potentially reinforcing this notion.
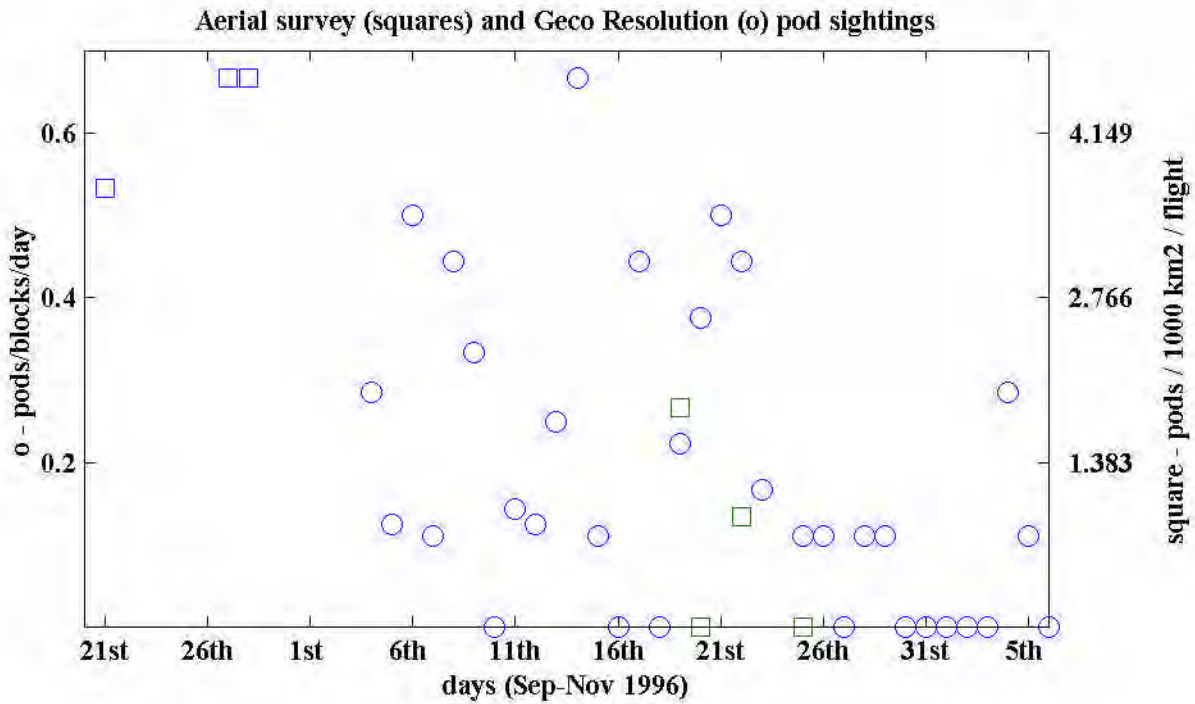
Figure 39: Sighting rates for *Geco Resolution* observer (circles, left hand scale, pods/observation-block/day) and aerial surveys (squares, right hand scale, pods-on-survey/1000 km2/flight) over the period 21st September 1996 to 5th November 1996, shown on the same plot. The 3D *Robert* seismic survey ran from the 4th October to 5th November.
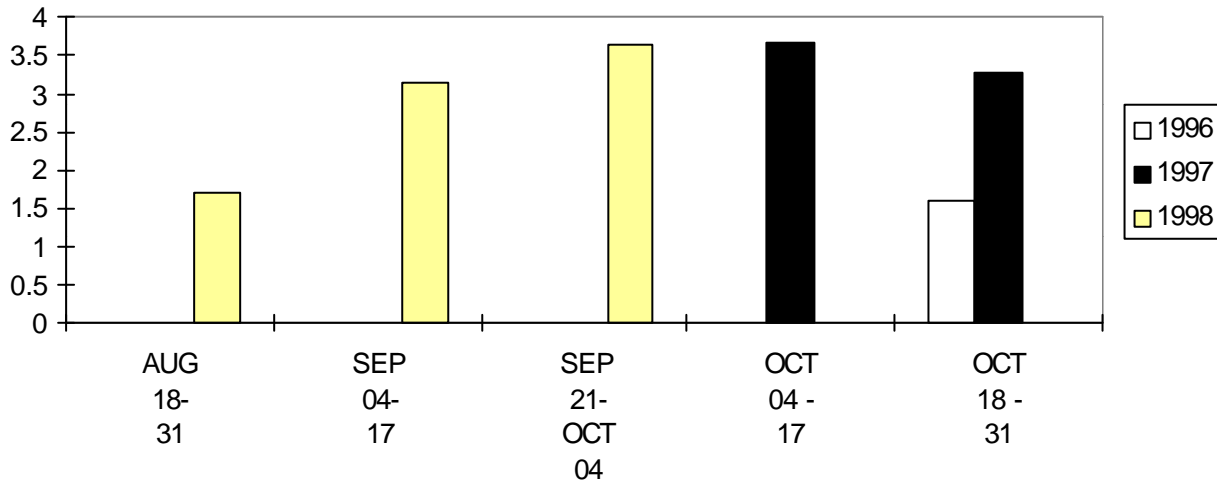
Figure 40: Humpback whale sighting data in two week blocks derived from small vessel surveys carried out by C & M-N Jenner over 1996-1998 in Exmouth Gulf.

But there were many unknown factors in assessing if this was a real effect or not. These factors included: the small sample size of the Jenners 1996 humpback sighting data (they were heavily involved in field work for this project) and the second set of aerial survey data (compounded by the timing of the first set of aerial surveys near the migratory peak while the second set were believed conducted during the tail of the migratory peak); the tendency for migratory humpback whales to temporally stagger their migrations based

on age and sex classes (Chittleborough, 1965; Dawbin, 1997); and normal yearly variability in migratory patterns. These unknowns imply that it is not possible from the data available to evaluate if this difference in habitat usage seen was real, an artefact of the sampling regime or simply within the bounds of normal variation.

The end of the S migratory body at any given point along the migratory route is usually characterised by a high proportion of cow-calf pods compared to non-cow-calf pods. The proportion of adults to calves sighted during the on-survey legs of the pre-seismic aerial surveys calculated at 9.7% (Table 14) as compared with 6.2 % for the on-survey flight legs during the *Robert* seismic survey. These were not considered greatly different (the many zero calf sightings in the during-seismic flights precluded a statistical analysis). Using all sightings data there were proportionately more calves seen during the first set of aerial survey flights (21.6% versus 10.3%), but this data includes the within Exmouth sightings, an unknown number of which were resights within the flight and which were primarily along a single transect across the Gulf.

The location of whale pods at first sighting time and their orientation when sighted (where determined) for the aerial survey and *Geco Resolution* based observer are shown on Figure 41. Many pods were deemed to be 'milling', these orientations are not marked on Figure 41. The sighting data from the pre-seismic aerial survey program suggested that there was no strongly defined 'preferred corridor' or narrow band through which humpbacks travelled S, rather the whales travelled in a broad band extending at least as far offshore as the aerial survey limits, or to 240 m water depth some 38 km off the 20 m depth contour.

The pod location-at-first-sighting from the *Geco Resolution* observer sightings appear to be similarly scattered across the NE aligned depth contours (Figure 41). Again no narrow migration corridor seemed evident during the seismic program, rather the sighting location data suggested the animals travelled S in a broad band.

To check the pod seaward distribution and hence any possible changes to the migratory pattern the range of all aerial survey and *Geco Resolution* observer pods at first sighting observed in blue water was calculated to the nearest point along the 20 m depth contour. The distribution of these ranges in 4 km bins, for the pre and during seismic aerial survey flights (15 and nine pods respectively) and the *Geco Resolution* observations (49 pods) is shown on Figure 42 (top). The depth at which each pod was located was then determined by gridding the digitised chart at a 500 m resolution and interpolating for the appropriate pod x-y co-ordinates. This distribution in 20 m depth bins is shown on Figure 42 (bottom).

It can be seen from Figure 42 that the pod locations observed during the pre and during seismic flights were scattered out to 40 km off the 20 m contour, in 200-250 m water depth. The pod sightings from the *Geco Resolution* showed a normal distribution seaward of the 20 m contour, centred at 10.6 ± 2.0 km (mean $\pm$ 95% confidence limits) off the 20 m contour. This line ran roughly through the centre of the seismic survey region. The depth distribution of the *Geco Resolution* observations was reasonably constant at 4-9 pods per 20 m depth bin. Based on these distributions there did not appear to be any evidence of gross displacement of whales seaward or inshore by the seismic survey. It should be noted though that at the writing of this document this analysis did not account for the location of the *Geco Resolution* during sightings made by the observer on board. Thus the *Geco Resolution* sighting data was not normalised for effort relative to the direction of the prevailing depth contours, whereas the aerial surveys were of uniform effort at right angles to the prevailing depth contours.

Combining the aerial survey and Geco Resolution results gave a mean pod range from the 20 m contour of

13.4 ± 2.23 km in a water depth of 96 ± 11.0 m.
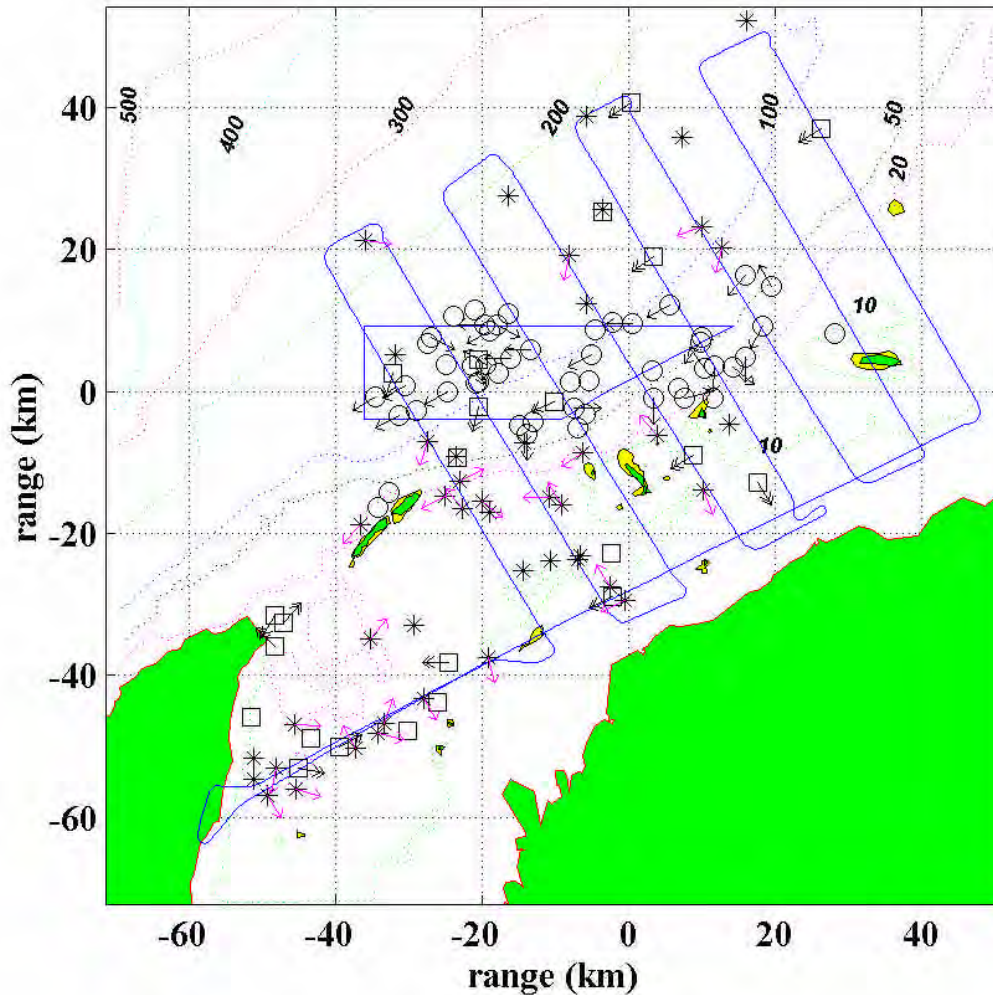
Figure 41: The locations of humpback whale pods at first sighting from pre-seismic (asterix) and during seismic (squares) aerial surveys, and from the *Geco Resolution* during the *Robert* seismic survey (circles). Where they could be determined the whale orientation or direction of travel at sighting is shown by the heavy arrows for the aerial surveys (one feather for pre-seismic, two feathers for during seismic) and the light arrows for the Geco Resolution observations. A zero reference point of 21° 30' S, 114° 40' E has been used. A representative aerial survey flight track is shown (flight 4).
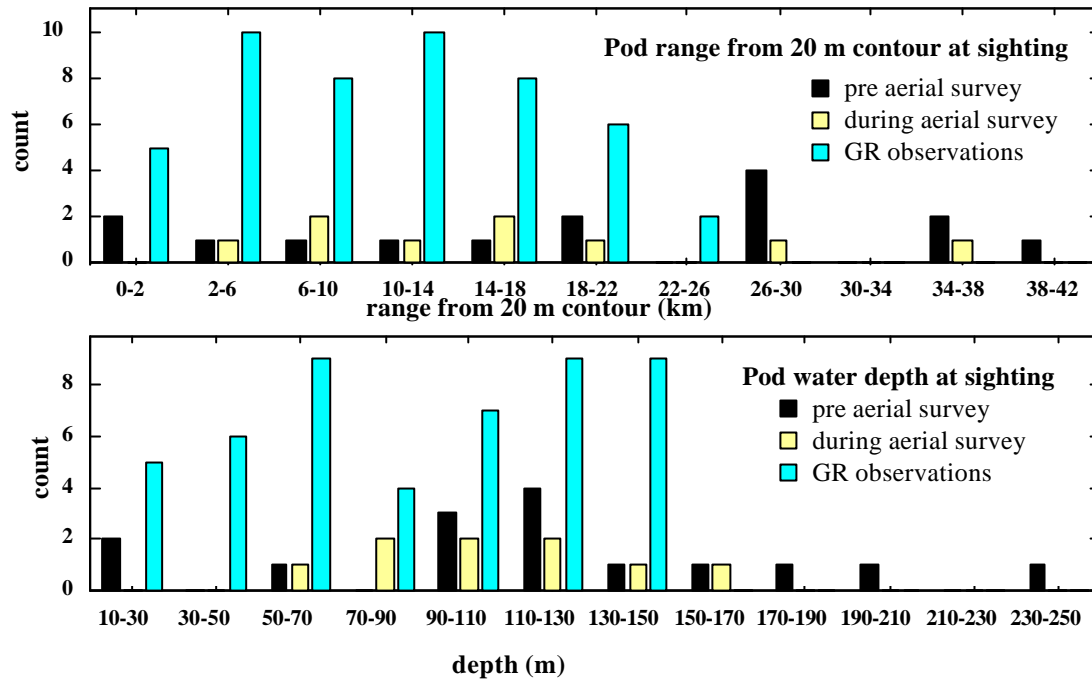
Figure 42: (**top**) Distribution of pods seen in blue water, from the 20 m depth contour, for: pre-seismic aerial surveys (flights 1-4, black bars), during seismic aerial surveys (flights 5-8, light stippled bars); and the *Geco Resolution* observations (dark stippled bars). (**bottom**) Distribution of water depths at pod first sighting, displayed as for the top plot in 20 m depth bins.

The orientation of pods observed from the "blue water" portion of the aerial surveys (seaward of 20 m depth contour) and of pods at-first-sighting, observed from the *Geco Resolution* (where they could be determined) are shown on Figure 43. The orientation data has been split into pre-seismic aerial surveys, during seismic aerial surveys, all *Geco Resolution* data, *Geco Resolution* with air-guns on during observation block, *Geco Resolution* with air-guns off during observation block, *Geco Resolution* with air-guns switched on/off during observation block and *Geco Resolution* with air-guns off/on during observation block. Circular statistics using the Watson-Williams test to compare angular means were applied to this data set to test if headings were different between observation sets. No significant differences were found in headings between any groupings, reinforcing the observation of the positional data above that there was no gross evidence for changes to the whales migratory route. Given that there was no significant differences in the mean heading for each data set, the data were lumped to give a mean swimming direction of 217° or approximately SW.

The pre-seismic aerial surveys and the *Geco Resolution* sighting observations also indicated that after swimming generally SW in the blue water, whales tended to cross into the shallower water to the E of the island chain running NE of NW Cape, mostly between Bessieres Island (@ ~ 10, -2 km E & N coordinates, Figure 41) and North Murion Island (@ ~ -30, -15 km E & N coordinates Figure 41). Sightings inside the 20 m depth contour show scattered movement patterns based on the orientations observed from the air (Figure 2), but it was believed most animals tended to head SW to end up in Exmouth Gulf. In the shallow water (< 20 m) only two pods were sighted to the E of Bessieres Island, suggesting most animals did not utilise the shallow water habitat E of 114° 45' E.
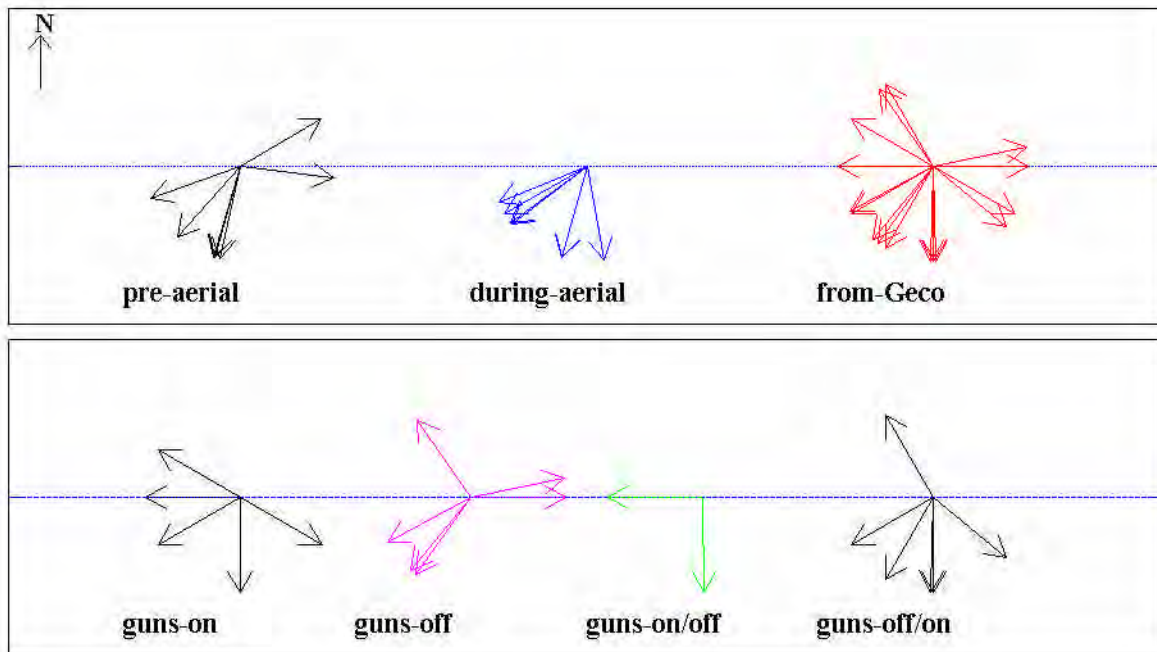
Figure 43: Pod orientation for blue water portion of aerial surveys and *Geco Resolution* sightings (at first sighting).

The *Geco Resolution* observer was aboard the ship for 43 days. As stated, during the time spent in the survey area 51 whale pods comprising 95 animals (86 adults, 9 calves/juveniles - not distinguished) were sighted. Details of sightings per 40 minute observation block with the air-gun array operating the entire observation block, off the entire block, or on/off or off/on during the block are listed in Table 15.

guns	Effort - # observation blocks	# pods	# whales	# adults	# juveniles/calves
on	142	27 (0.190)	49 (0.345)	44 (0.310)	5 (0.035)
off	86	11 (0.128)	19 (0.221)	18 (0.209)	1 (0.012)
on/off	42	13 (0.309)	27 (0.643)	24 (0.571)	3 (0.071)
total	**270**	**51 (0.189)**	**95 (0.352)**	**86 (0.318)**	**9 (0.033)**

Table 15 Number of units of effort (40 min sighting blocks), pods, total whales, adults, and juvenile/calves, seen from the *Geco Resolution*, broken up by whether the air-gun arrays were on, off or some combination of on and off. Bracketed values are sightings-counts per unit sighting block.

From the values in Table 15 there appeared to be little difference between pod sighting rate for the air-gun arrays continuously operating for the observation block compared with those when the arrays were continuously off for the observation block. If anything there were slightly more pods seen during blocks with the air-guns on (0.190 pods/block), than blocks with the air-guns off (0.128 pods/block). Assuming an equal chance of sighting pods for blocks with the guns-on and guns-off and using a $\aleph^2$ goodness of fit test, revealed no significant differences in the ratios of total pods observed between *guns-on blocks* and *guns-off blocks*. For the mean sighting rate of 0.167 pods/block to get the expected number of pods gave a $\aleph^2$ value of 1.24, with $v=1$, which is not significant or using the guns-on sighting rate only to get the expected number of pods (0.190, Table 15) gave a $\aleph^2$ value of 1.7518 which is also not significant.

There did appear to be a higher sighting rate (almost double) for observation blocks when the air-guns where turned *on* or *off* during the block (0.309 pods/block) compared with the air-guns *continuously-on*

or *continuously-off*. Lumping the guns-on and guns-off data and comparing the observed pods with the *guns-on*, *off* or o*ff/on* observed pods using all data to get the mean sighting rate (51/270=0.18889 pods per observation block) and using a goodness of fit test, gave a $\aleph^2$ value of 3.8319 with $v=1$. This gave $0.05 < p < 0.1$ level. Using the lumped continuously on and continuously off data to get the expected number of pods (0.1667 pods per observation block) gave a $\aleph^2$ value of 5.1429 ($v=1$) which was significant at the level $0.01 < p < 0.025$.

To further investigate the sighting rates recorded during air-guns *on*, *off* or *on/off* observation blocks, the sighting rates with range were plotted. The number of sightings per block which fell within the range brackets of 0-750 m, 750-1500 m, 1.5-3 km, 3-6 km and > 6 km (14.2 km being the horizon for the height of eye) were summed. This plot is shown in Figure 44 - top, for the *guns-on* versus *guns-off* sightings. A trend for more sightings at shorter range for *air-guns off* blocks exists out to 1.5 km, then at > 3 km relatively more pods were sighted during *guns-on* periods. Normalising the number of pods per category for actual area searched, to give pods/(block*km^2), shows this trend is for slightly more than three times the sighting rate at < 750 m from the survey vessel during *air-guns continuously off* blocks compared to *air-guns continuously on* blocks (Figure 44 - bottom). The blocks during which the air-guns were switched on or off show consistently higher normalised sighting rates (pods/(blocks*km^2)) out to the 3-6 km range bracket than for the *air-guns on* or *air-guns off* groups.
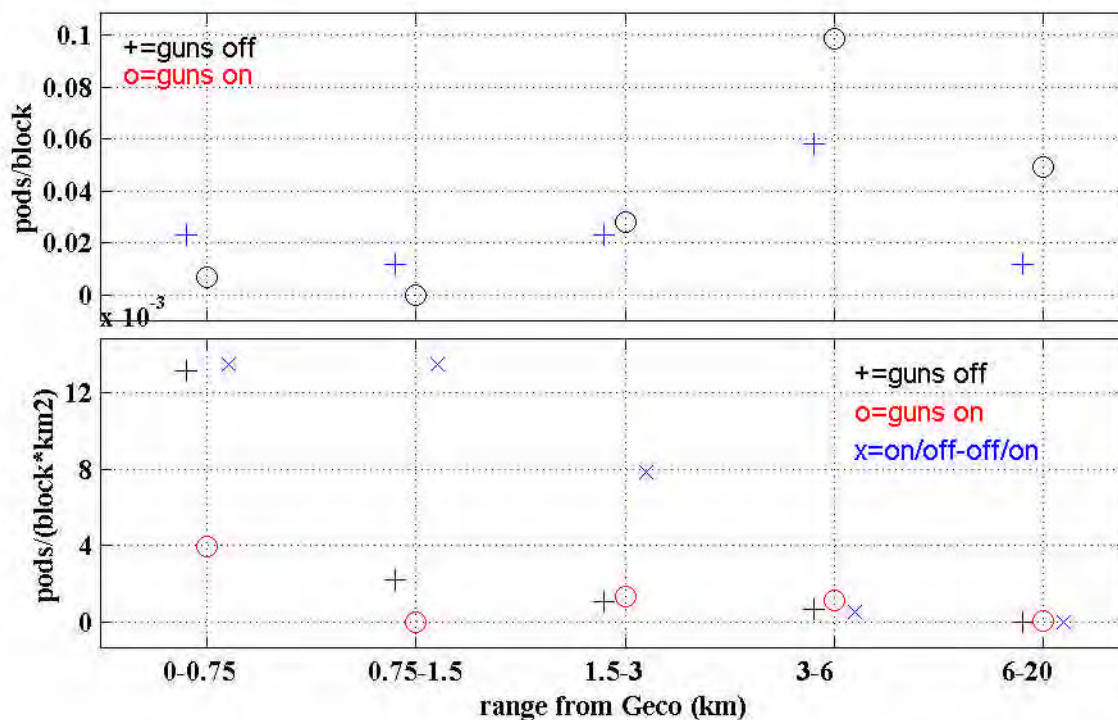
Figure 44 (**top**) Sighting rate (at first sighting) of whale pods seen from the *Geco Resolution* per 40 minute observation block summed forfive range categories. (**bottom**) Sighting rate per observation block normalised for the search area of each range category.

In summary the aerial surveys and Geco Resolution observations showed that:

- Humpback whales swam SW in blue water (seaward of the 20 m depth contour) to the NE of North West Cape in a broad band extending to the limits of observations at 40 km off the 20 m depth contour, in 200-300 m of water. They were distributed normally across this range with a mean range from the 20 m depth contour of 13.4 ± 2.2 km in a mean water depth of 96 ± 11 m.

- After travelling in the blue water whales tended to cross into the shallow waters of Exmouth Gulf mostly between North Murion and Bessieres Island. Once in the shallow waters their behaviour shifted from a directed SW swimming to a more meandering course, indicative of a shift in behaviour from migrating to resting or socialising.
- There was no evidence of any gross changes to this migratory pattern which could be attributed to the presence of a 3D seismic survey which straddled the migration path.
- Observations made from the seismic vessel showed that there was a trend for more humpback sightings within three km of the seismic vessel when the air-guns were turned *off* as opposed to when they were *operating*. Beyond three km the opposite trend was observed, more whales were seen when the air-guns were *operating* than when they were turned *off*.
- There was consistently more whales observed out to three km during observation periods when the air-guns were switched *on/off* or *off/on*, as opposed to being continuously *on* or *off* for the observation period.

2.2.2 *Geco Resolution* **humpback whale 'follows'**

Four pods were located to the N of the *Geco Resolution* by the *Blue Horizon* and followed as they approached the operating seismic vessel on interception tracks. Details of the methods used throughout the follows are given in section 1.4.2. The intention of this work was to observe the response of animals as they approached an intercepting operational seismic survey vessel. To do this required finding whales to the N-NE of the seismic vessel which were on closing tracks. A considerable amount of vessel searching time was thus required to locate suitable pods. Of six days available for searching, four suitable pods were located and tracked over three days, with one day lost to bad weather (no seismic operations) and no suitable pods sighted on two days. Given that all available time was spent in locating and following the four pods on suitable interception headings and the fact that the *Geco Resolution* operations were in no way controlled by the researchers on the *Blue Horizon,* then it was not possible to do control follows. These could have entailed follows towards the *Geco Resolution* steaming with its gear out but air-guns off and follows of whales on SW courses only. Given the search time available and the paucity of pods on suitable interception courses it was not possible to carry out these controls. During follows all efforts were made to operate the *Blue Horizon* gently and to keep a 200-500 m follow range so as to minimise any observation vessel influence. Any influence of the *Blue Horizon* on the pod behaviour or movement patterns would have been consistent over the follow duration.

During follows track details, dive times and blow rates were determined for focal animals within observed pods. Details of follows are given in Table 16. The track plot, pod to air-gun array range, pod speed, pod heading, air-gun array and pod interception range, air-gun array and pod time to interception, and estimated air-gun level for a receiver at 30 m depth are shown for the four follows on Figure 45.

Interception details were calculated for the followed whale pod and the air-gun array. These used the extrapolated course of the pod and air-gun vessel to find the closest interception range of the two extrapolated tracks, and the travel time to this, for specified points in time along the whales track. This was done for all pod track observation points (the time the pods position was noted in the field) and for the interpolated pod position, during air-gun operations. Interpolated positions were calculated at one minute intervals using a 2nd order running polynomial technique, as per methods section 1.6.2. The interception analysis was done at discrete points in time (observed or interpolated whale position) by firstly extrapolating forward along the pod and air-gun respective track headings in regular range steps using the appropriate pod or air-gun vessel speed. For the air-gun vessel travelling along a steady course the extrapolated track was straightforward. For extrapolating the whale course the heading and course between the selected and following point (observation or interpolated) were used to extrapolate the course.

Range steps were calculated for two hours ahead at five s increments. The minimum interception range and the time at which this occurred was then calculated from the extrapolated courses. This was then iterated for all observation or interpolated target pod positions over the air-gun operation period. For diverging courses the calculation returned a time one s ahead of the point in question and an interception range equivalent to that at the observation time. For nearly parallel courses the calculation returned a time to interception of 120 minutes. In the track plots (Figure 45) the time to intercept is shown on a log scale in minutes. The time to interception for diverging courses was set to the maximum scale of the plot.

Date/time	Observations
20 Oct 96 10:05-11:46	spotted at 4.5 km NNW from W heading GR milling; whale suddenly bolted heading 8-12 knots at surface across bows GR @ 1500 m closest approach maintaining a 40 s blow time and swimming at surface; slowed at 3 km S GR hence continued to make a SW course to >10 km from GR; eventually met 2nd pod; animal submerged and commenced singing, observation terminated because of proximity of 2nd pod, long down times and large range of GR
21 Oct 96 11:24-15:30	spotted heading SW with operating GR @ 6 km SE heading E; GR stopped operating @ 11:58 and commenced turn; pod stopped @ 12:20 and rested at surface to 13:10 then resumed SW course; GR commenced W line 3 km S of previous line @ 13:09 @ 10 km from pod; pod stopped and rested at surface @ 14:30; GR passed to N @ 3 km minimum range @ 15:10 with pod still resting at surface; pod remained at surface until 15:30 with GR range steadily increasing, observation ceased
22 Oct 96 10:10-12:43	spotted heading SW @ 23 km NE of E heading GR; pod maintained steady interception course with GR until @ ~ 5-8 km, then slowly adjusted speed and course such that pod would pass behind GR; GR stopped operating @ 11:54 with pod @ 4 km NNE heading slow SSW
22 Oct 96 14:18-16:22	spotted heading WSW @ 8 km N of W heading GR; pod course initially roughly tracking GR; pod slowed speed and veered S to pass behind GR tailbuoys (3 km behind GR); GR stopped operating @ 16:06 with pod @ ~ 3.2 km astern

Table 16: Details of 'follows' made from *Blue Horizon*. GR= *Geco Resolution*.]

Following four pages:

Figure 45 For the four Blue Horizon follows: (**left hand side**) Track plots for the follow pod (hollow circles, all plots), *Blue Horizon* (small crosses track plot) and the 3D air-gun array (dots). Times are given on the track plot for the interpolated whale position (in italics) and the matched air-gun array position. (**right hand side**) From top to bottom are the follow pod to array range, speed, direction of travel, target-pod to array interception range, target pod to array interception time, and estimated received sound levels. The circles represent the whale details at each observation point, the lines are values for the appropriate measure at the pod's interpolated position. Crosses are the observation vessel details. The interception plots were calculated by looking forward along the pod and array track at each whale observation point, for two hours in five s increments, and calculating the minimum approach range and the time at which this occurred. For the pod/array on converging courses the intercept range fell within one minute to 120 s. For the pod/air-gun on diverging courses the intercept range was as for the time of observation. For clarity the time to interception for diverging courses was set to the maximum value on this plot and a different symbol has been used.

Whale (o), Blue Horizon (+) and Geco Resolution (.)
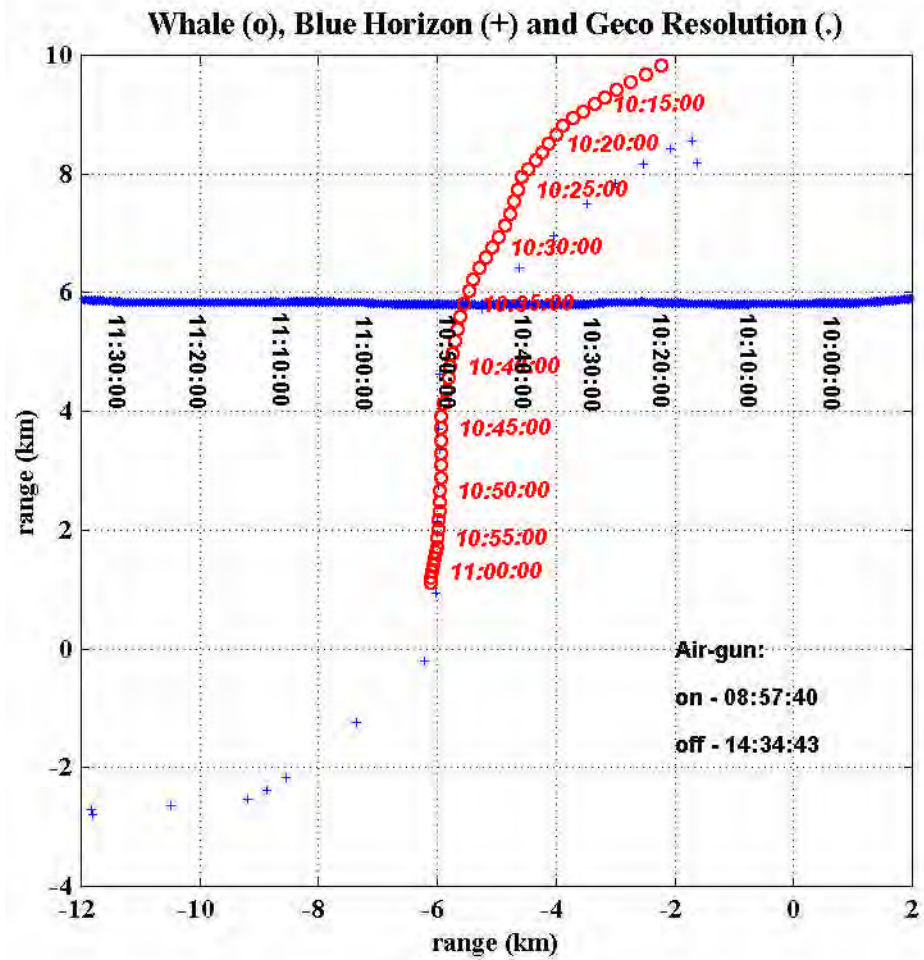
Run 1 20 Oct 96 10:00:00-11:56:00

Whale (o), Blue Horizon (+) and Geco Resolution (.)
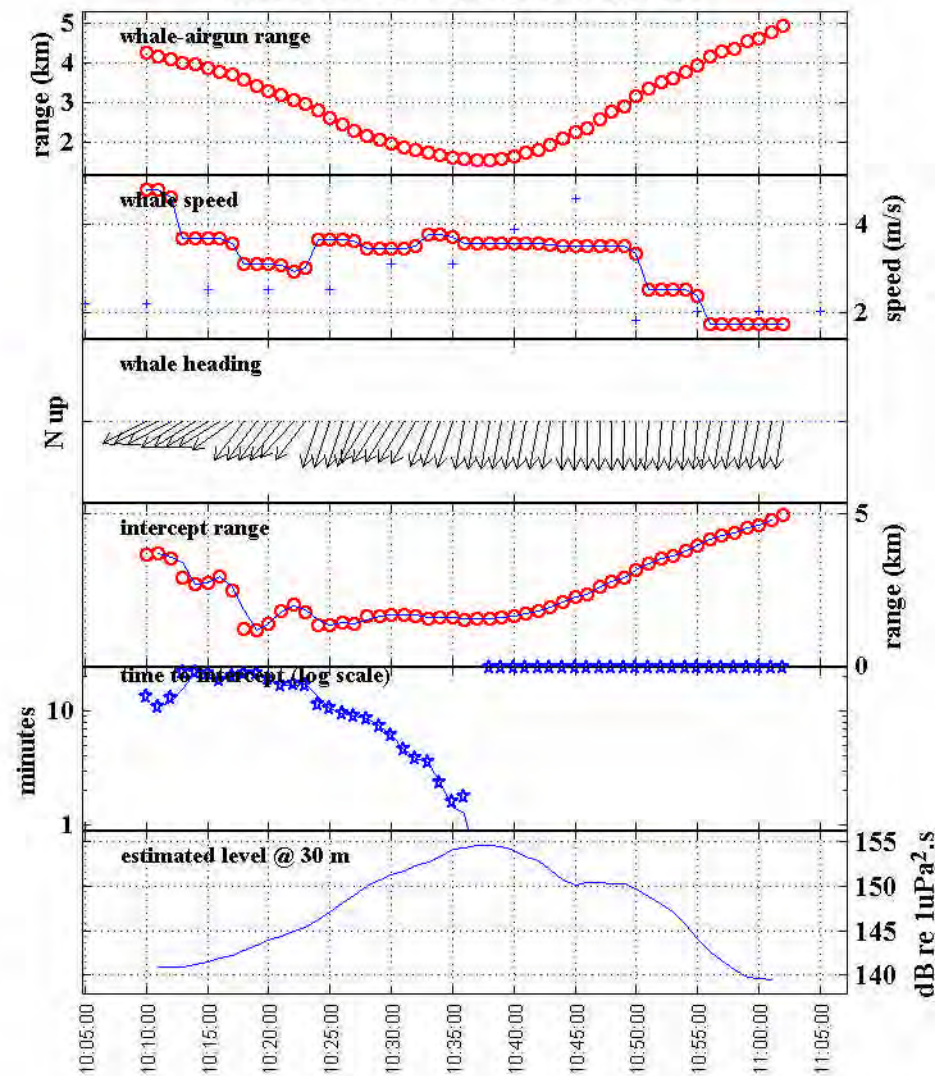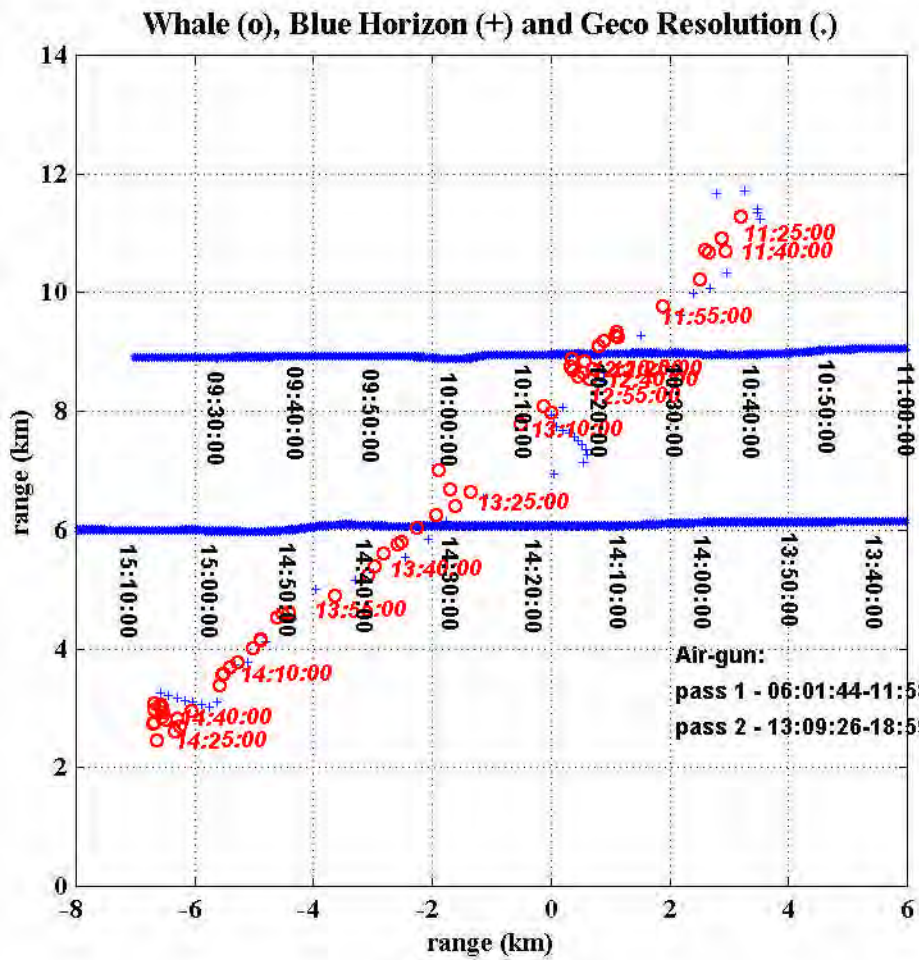
Run 2 21 Oct 96 11:20:00-14:59:00

Whale (o), Blue Horizon (+) and Geco Resolution (.)
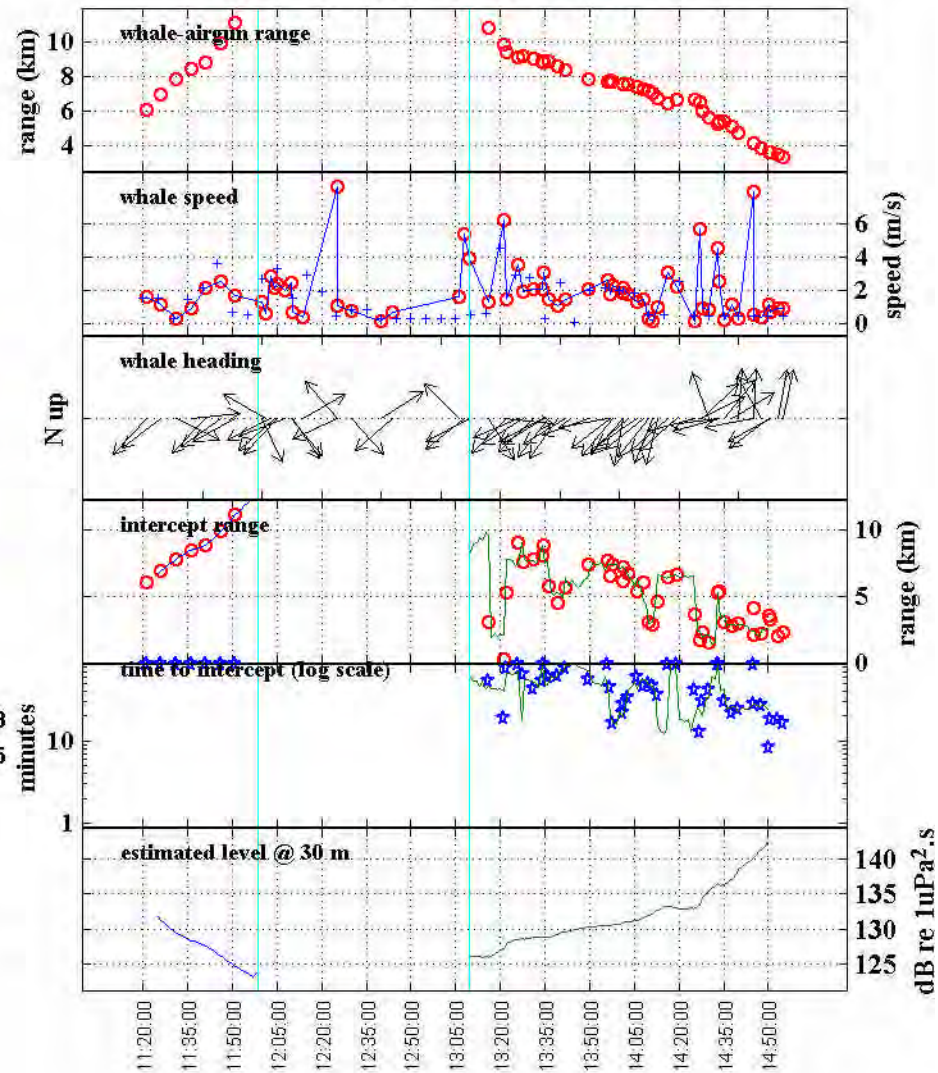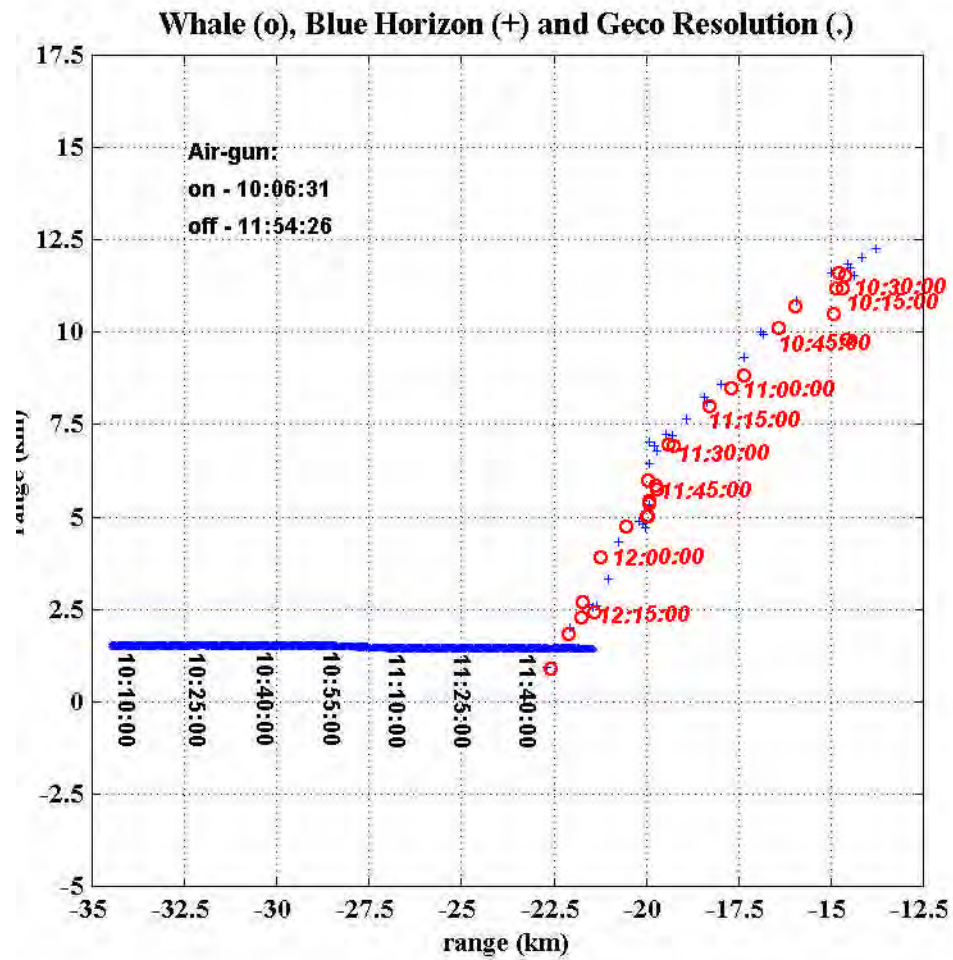
Run 3 22 Oct 96 10:10:00-12:42:00

Whale (o), Blue Horizon (+) and Geco Resolution (.)
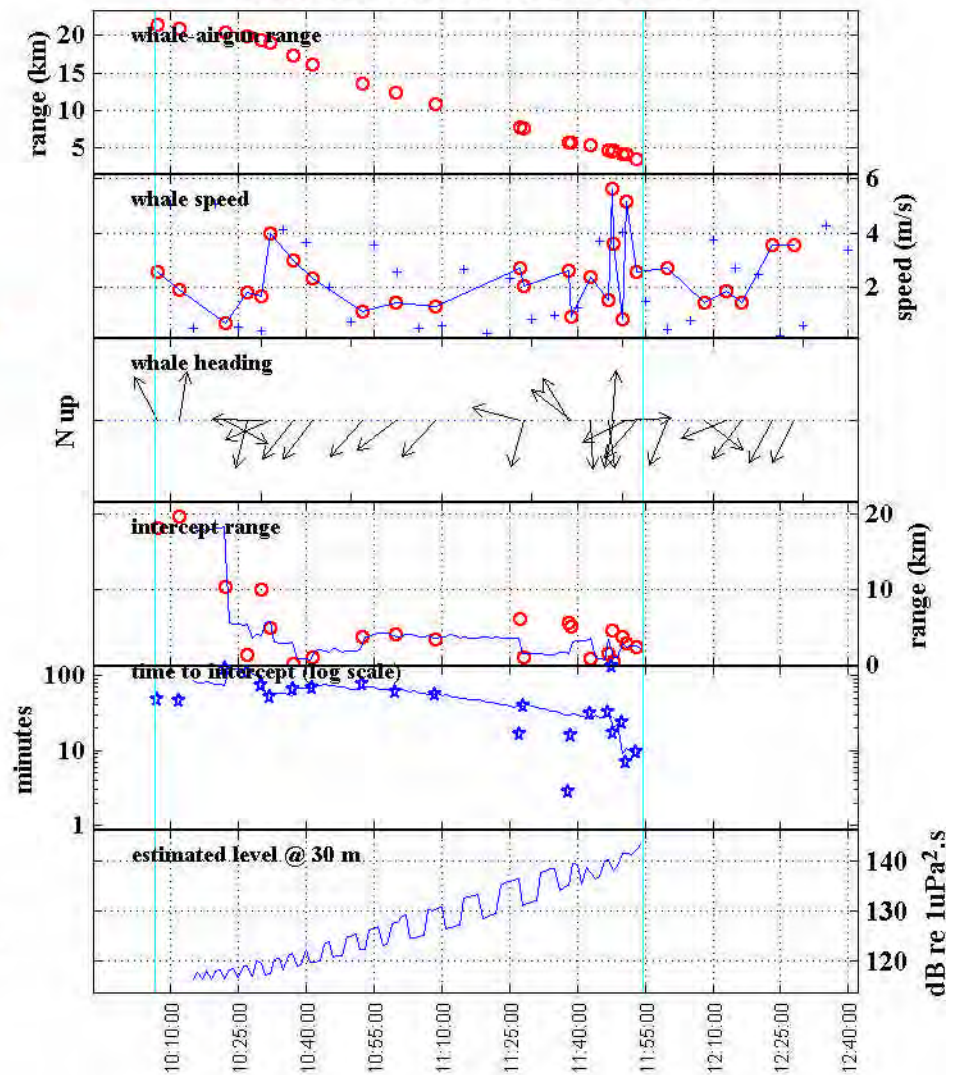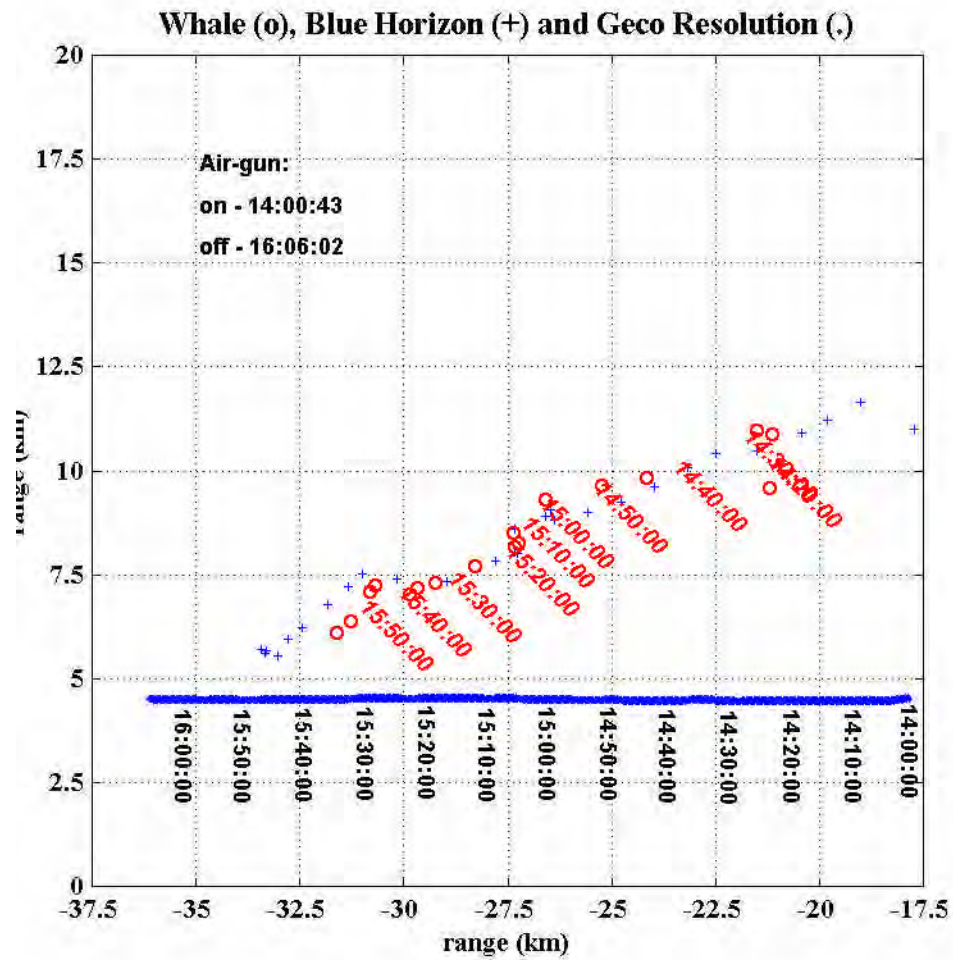
Run 4 22 Oct 96 14:10:00-16:29:00
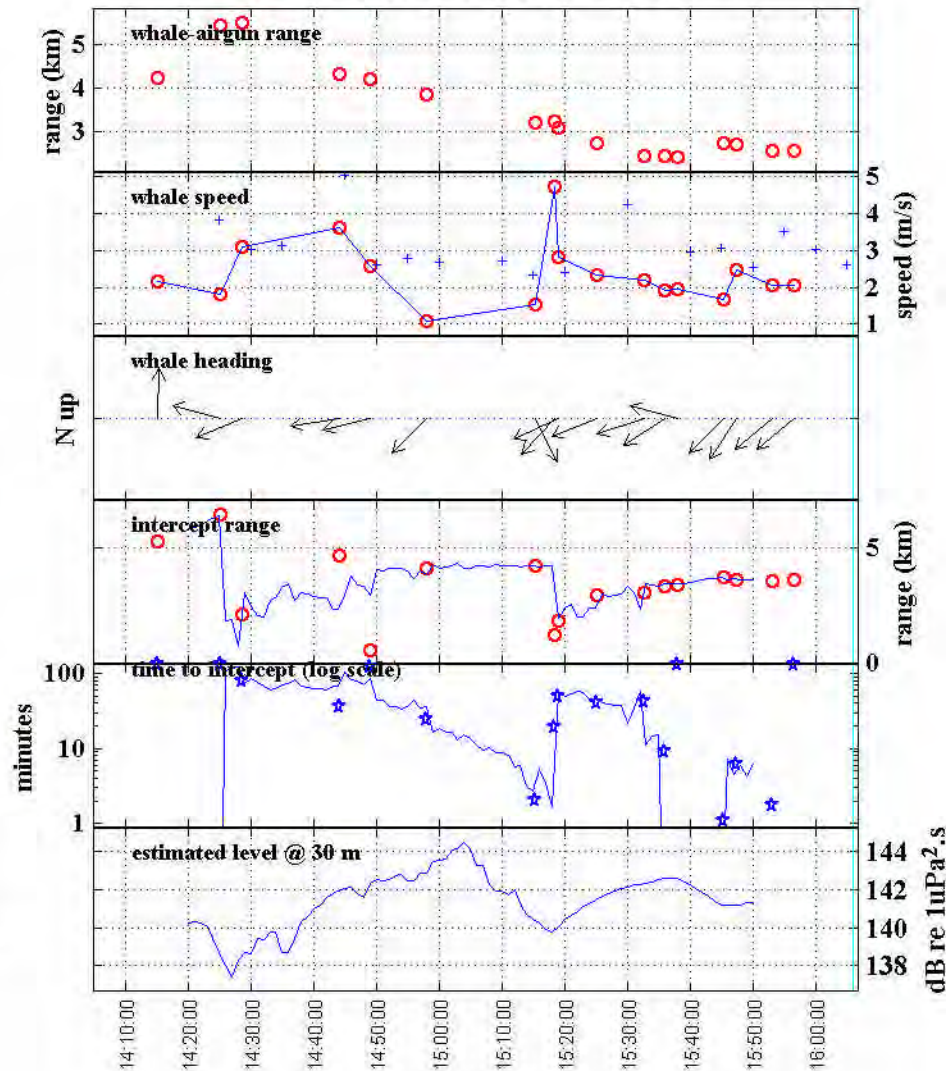
The estimated air-gun array level was derived using the fit of range to all the 3D array measures (5352 points, mean receiver depth of 32 m) given in Equation 9. This curve was adjusted for azimuth (angle of receiver from array tow direction) by using the curve displayed on Figure 23 for the modelled source level with azimuth as a template. The empirical measures showed that the pattern of the modelled broadband source level curve with azimuth, became distorted at range from the source, such that frequency dependent propagation effects enhanced the curves overall scale. This enhancement was depth dependant with a greater dB range measured as the receiver depth shallowed (eg. Figure 15). Thus the curve shown on Figure 23 for the 3D array was adjusted from empirical measures to the trend seen at 32 m depth, and this correction added to the range dependant form of Equation 9. Hence it should be realised that the levels shown on Figure 45 are estimates and given for a fixed depth. If an animal dived substantially deeper the received level could increase by as much as 10 dB, or if it moved to within very close to the water surface the received level could decrease by as much as 10 dB.

The first follow, shown on Figure 45 - 1 was the most radical, with the single whale first spotted moving slowly 500 m N of the shut down *Blue Horizon*, at 4.2 km NNW of the operating *Geco Resolution*. At 11:10 the whale suddenly took off (with the observation vessel shut down 500 m S) with an initial burst that was estimated to be at 10-15 knots. It then settled down to around 8 knots on a course which veered from SW to S to take the animal across the bows of the operating *Geco Resolution* at a closest range of 1500 m (estimated received level at 32 m depth 155 dB re 1 μPa^2.s, probably considerably less at the surface). During this period of high speed swimming the animal remained at the surface, with the tail flukes often breaking the water, with an approximate 40 s blow interval. It maintained a S course at speed until three km S of the *Geco Resolution* trackline whence it began to slow but did not stop, began diving again and slowed its blow rate. After swimming six km S of the *Geco Resolution* trackline it then resumed a SW course (still without stopping) until it met up with two pods in close vicinity at 11:40 approximately 9 km S of the still operating *Geco Resolution*. The animal then commenced singing. The long down times associated with singing and the proximity of two other pods made following the original animal difficult, so at 12:10 the observation ceased. At this point the *Geco Resolution* was receding, heading W at slightly over 9 km NNW of the pod (estimated received level at 32 m depth 128 dB re 1 μPa^2.s).

In the second follow a cow-calf pair was first spotted at 11:21 6 km NW of the E heading *Geco Resolution* slowly swimming SW. At this point the received air-gun level was 132 dB re 1 μPa^2.s at 32 m depth, and receding as the array moved to the W. The Geco Resolution stopped air-gun operations at 11:58 around 11 km E of the pod and began a 180° turn to the south, so as to begin another W heading trackline. The pod continued moving SW until 12:10 at which it stopped and lay quietly at the surface making slow way against the NE heading current. The Geco Resolution resumed operating on the W heading at 13:09, approximately 11 km E of the pod (received level at 32 m depth 126 dB re 1 μPa^2.s) on a close interception course. The whale immediately began swimming SW again, with in an initial increase in speed which suggests it was moving to cross the oncoming air-gun trackline. The pod crossed the array trackline, moved to approximately three km S of it and began resting, again with cow and calf always at or very close to the water surface. They maintained their position into the NE current (with sporadic short bursts of SW swimming) as the operating *Geco Resolution* passed to the N, at a closest range of 3 km and received level at 32 m depth of 151 dB re 1 μPa^2.s. At 15:30 the pod were still resting near the surface and the observation was ceased as drifting gear had to be recovered. At this point the pod was 4.3 km SE of the operating *Geco Resolution* with a received air-gun level at 32 m depth of 140 dB re 1 μPa^2.s.

To check for any apparent stress in the cow-calf during follow 2, the mean blow increments of cow and calf were calculated in 15 minute blocks. As the animals were nearly continuously near to the sea surface

and not involved in significant dive / swim / surface cycles, blow rates were not differentiated into blocks of when the animals were at the surface, but rather calculated continuously within each 15 minute period. Increased blow rates are believed to correlate with stress (Richardson et al, 1995). These blow increments, with 95% confidence error bars are shown plotted at the central time of each 15 minute block, for the cow and calf, on Figure 46. There was no indication of any significant change in these rates throughout the observation period for either animal. The animals were constantly near the surface so down times could not have been used as a second stress indicator. During the observation period the animals did not seem to be under any duress, if anything they seemed to be resting quietly during the idle periods despite the nearby passage of the air-gun vessel.
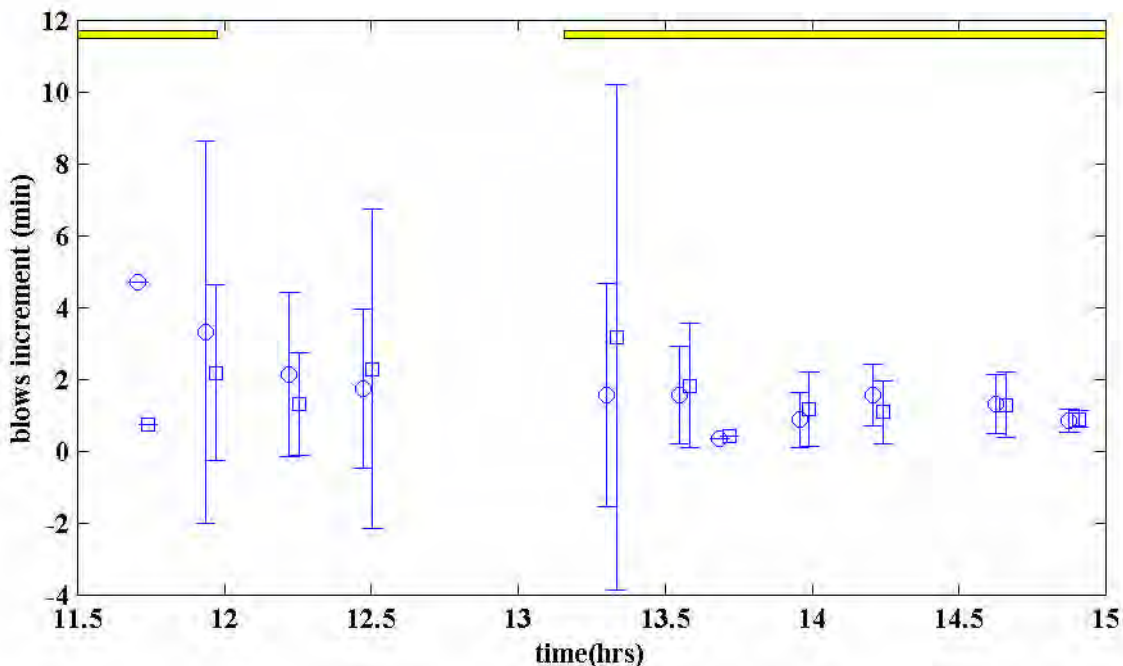
Figure 46: Mean blow intervals (minutes) calculated in 15 minute blocks for the cow (circles) and calf (squares) of follow 2 with 95% confidence limits shown. The cow values are plotted at the central time of the 15 min block, the calf measures have been slightly offset to the right for clarity. The bars at top represent times of air-gun operation.

In the third and fourth follows pods on interception courses with the operating *Geco Resolution* altered course, speed or both at some range between 4-5 km (5 km follow 3, 4.2 km follow 4) to pass behind the operating *Geco Resolution* at 3-4 km. For a receiver at 32 m depth these course changes occurred at 140 dB re 1 μPa^2.s. For follow 3 an approximately linear increase of level at 3 dB every 11 minutes was experienced prior to this course change. For follow 4 the beam pattern of the array meant that the received level at 32 m depth had peaked before the course changes had been made. The *Geco Resolution* was engaged in 'filling in' gaps in previous tracklines, thus started and stopped operating at frequent intervals. In each of these follows the array shut downs coincided with the follow pod about to pass astern the hydrophone streamer tailbuoys. In follow 3 at around 5 km one animal was seen to change behaviour from a steady SW swimming/diving cycle to a hunting or zig-zagging pattern near the surface, resulting in a slight shift in course and speed to take the animal astern the E travelling *Geco Resolution*. The calculated received level for follow 3 shows a steadily increasing but oscillating curve. These variations were due to the different alignments of the port and starboard arrays with the receiver (the arrays were separated by 80 m). The approach towards the beam of the array meant that small differences in alignment resulted in the approximate 5 dB swing in received levels seen.

In summary the four follows showed:

- That a probable single male whale made a radical manoeuvre to pass an operating seismic vessel at comparatively short range;
- There was evidence that a cow-calf pod responded to an intercepting air-gun array at 11 km range (126 dB re 1 μPa^2.s at 32 m depth) such that it moved to a position 3 km S of the oncoming array;
- On two occasions pods on closing courses with the operating air-gun array changed course at 4-5 km to avoid the intercepting array (140 dB re 1 μPa^2.s);
- On three of four occasions pods maintained an approximate three km standoff range, at which the received air-gun level at 32 m depth would have been in the range 144-151 dB re 1 μPa^2.s;
- On all occasions it was believed pods used the sound shadow near the surface to reduce the received sound loading, with this particularly emphasised when a single male whale crossed the bow of the operating air-gun array and for a cow-calf which stood off drifting at three km while the vessel passed by;
- There was no indications of increased stress on a cow-calf pair which allowed the operating seismic vessel to pass three km to the N.

2.2.3 Exmouth Gulf exposure trials

In total sixteen trials involving approaching humpback whale pods with the single operating Bolt air-gun were conducted in Exmouth Gulf. Trials were carried out to determine any movement or behavioural responses by humpback whales to an approaching operating air-gun. Whale tracklines are shown for all trials on Figure 7 (bottom). Seven trials were carried out in October 1996 and nine in October 1997. Details of the trial dates, times, start, minimum-approach and interception ranges, are given in Table 17.

Run	date	observation on - off. hh:mm	Obs. duration (hrs). hh:mm	air-gun on - off hh:mm	firing duration hh:mm	start range (km)	min. intercept range (km) / time to intercept (min) / time	closest approach (km) / time
1	26/10/96	12:11-15:18	3:07	13:20-14:36	1:16	3.8	0.68/24/13:39 i	1.9 (13:53)
2	27/10/96	09:42-12:37	2:55	10:58-12:01	1:02	4.6	0.02/49/11:02 i	1.6 (11:38)
3	27/10/96	13:10-15:45	2:35	13:54-15:15	1:20	7.2	0.17/93/14:54 i	6.5 (15:00)
4	28/10/96	10:05-12:57	2:52	10:59-12:25	1:25	7.5	diverging i & o	5.8 (12:00)
5	28/10/96	14:30-16:31	2:01	14:59-16:06	1:06	6.3	0.03/44/15:44 i	1.8 (16:06)
6	29/10/96	09:50-13:15	3:25	10:35-12:30	1:54	6.2	0.25/20/12:20 o	5.0 (12:30)
7	29/10/96	15:10-17:05	1:55	15:35-16:20	0:44	4.0	0.25/30/15:40 o	1.0 (16:05)
8	16/10/97	13:54-17:18	3:24	15:22-16:41	1:19	5.0	0.50/43/15:35 i	1.3 16:35
9	17/10/97	11:56-16:00	4:04	13:21-13:33 13:53-15:11	0:12 1:18	5.8	0.40/63/13:32 o	0.8 14:39
10	18/10/97	12:22-16:10	3:48	13:45-15:20	1:35	4.7	0.40/35/14:24 i	1.1 15:01
11	19/10/97	14:03-17:15	3:12	15:39-16:30	0:51	4.4	0.70/18/15:43 o	0.9 16:04
12	20/10/97	09:19-12:00	2:41	10:12-11:10	0:58	4.2	0.005/4/10:52 i	0.1 10:56
13	20/10/97	13:04-15:20	2:16	14:12-14:43	0:31	4.2	0.005/28/14:24 i	0.8 14:42
14	21/10/97	12:01-15:30	3:29	13:26-14:34	1:08	4.4	0.12/99/14:10 i	1.9 14:21
15	22/10/97	09:26-12:35	3:09	10:38-11:43	1:05	4.5	0.06/25/11:05 i	1.3 11:22
16	23/10/97	10:30-13:30	3:00	11:42-12:40	0:58	3.7	0.10/34/11:46 i	1.0 12:18

Table 17 Details of times of observations, times of air-gun operations, start range and minimum range and time for each humpback whale exposure trial. Note that minimum air-gun to whale range or intercept-range and associated times were as given by the lowest of interpolated or observed pod tracks (differentiated by i or o for interpolated or observed track, for the intercept information).

The full methods are detailed in section 1.5. Briefly each trial involved observers aboard the vessel

WhaleSong choosing a target pod which was followed for ideally an hour to ascertain movements and general behaviour. Once a suitable pre-exposure observation period had elapsed a second vessel, the *Flying Fish* would position itself at nominally a 5 km start range, begin air-gun operations and approach the pod on ideally an interception course. Approaches with the operating air-gun were carried out within permit guidelines (see Appendix 2 for conditions) until the pod was deemed to have shown some evasive response or had reached a position where it was unlikely to show any apparent response. Following the air-gun shut down an hour post exposure observation was made. All trials were carried out under rigorous permit conditions. Although not required as part of the permit system, the behaviour of target pods was video taped for all trials and is available for perusal.

The general behavioural patterns of humpback whales in Exmouth Gulf over the trial month (October) played a major role in dictating the trial outcomes and the selection of suitable target pods. There was a general dichotomy of humpback whale behaviours in the Gulf during October. Cow-calf pairs were predominant and seemed to use the region as a resting area, showing gentle behaviours involving slow swimming/diving cycles or long periods idle at the surface, often in pods of cow-calf and escort. In contrast what were believed to be sexually active males spent much of the time swimming singly or in groups at high speed around the Gulf searching for receptive females. Often cow-calf pods also involved several active males, with the movement of the cow-calf pair dictating the overall pod movement. On several occasions cow-calf pods were accompanied by many apparently competing males involved in vigorous surface activity.

Given that pods of males tended to swim at high speed and rather erratically within the Gulf, they were extremely difficult to follow so as to set up an approach trial. Thus trials were strongly biased toward pods containing cow-calf pairs. Of the 16 trials 12 involved cow-calf pairs. At least one female was believed present in three of the other four trials (trials 1, 3 & 5), with only one trial believed to involve a male only pod (trial 12, based on singing behaviour). The bias towards cow-calf pods was considered to be reasonable in conducting the trials, as from an ecological effects perspective the breeding females with young would be considered the most vulnerable group, and so that which any regulation should be based around.

The tracks of whales, the *WhaleSong* and the operating air-gun are shown on Figure 49 - 1 to 16 for all trials. Also shown with each set of tracks are details of the target pod range to the operating air-gun, target pod speed and heading and target pod and air-gun interception details. Interception courses were calculated as for the *Blue Horizon - Geco resolution* humpback pod follows, discussed in section 2.2.2.

General details of pod composition and summaries of pod behaviour for each trial as seen from the observation vessel *WhaleSong* (entire observation) and from the air-gun vessel *Flying Fish* (air-gun on periods only) are given in Table 18.

To ascertain if an avoidance response based on movement patterns had occurred in response to the approaching air-gun, required interpreting through time the target-pod and air-gun range, their interception range and time to interception, and comparing this with the pod's speed and heading over this period. If the animal was to show avoidance to the approaching noise source then one would expect that as the pod range to air-gun and/or interception range and time to interception, decreased, then either a detectable speed, heading or speed plus heading change would be evident. The shift of time-to-interception from a converging time (1 min < time < 120 min.) to a diverging time (set to maximum time scale on plots of Figure 49) was a good first indication of where avoidance changes were made. But is must be realised that this shift may have been as much an artefact of the tracks involved and unless correlated with a speed or

heading change was not in itself deemed a correlator with avoidance behaviour.

The resultant track plots, as given by Figure 49 were assessed for speed or heading changes which correlated with the whale air-gun range, interception course and time-to-interception. These assessments are shown on Table 19.

In trials three (two adults, one a singer), four (cow-calf) and six (cow-calf) the minimum air-gun to whale range was greater than five km. In these trials no discernible effects on movement patterns can be seen in the track plots. The approach courses chosen in each of these trials was not an interception course. In trial five a N travelling pod of cow-calf was approached from the SW. The pod crossed the air-gun vessel track at 4.5 km ahead then moved into the lee of a shallow shoal with respect the air-gun vessel noise, where it remained until the air-gun was stopped at 1.8 km. The air-gun was stopped before the vessel cleared the shoal in order to avoid a possible startle response from the whale as the vessel suddenly cleared the shoal at short range. In trial 13 a fishing trawler approached and began circling the target pod at short range with the air-gun at 800 m off. The presence of two vessels near the whale and the approaching air-gun were deemed to breach the approach guidelines so the air gun was stopped immediately it became apparent as to the trawlers intentions. Thus five trials were deemed inconclusive.

Of the other 11 trials only one involved a confirmed all male pod, trial 12 of single male as evidenced by singing behaviour. The results of this trial as compared to those with cow-calf pairs and observations made from the air-gun vessel (ie Table 19), determined that there were two almost completely opposite responses to the approaching air-gun. The first response involved pods containing cow-calf pairs or if no calves were present, pods which were believed to contain a female whale. These included trials one and 15 (two adults), two and 11 (cow-calf, escort), seven (five adults, calf), and eight, nine, 10, 14 and 16 (cow-calf). All these trials were conducted with the air-gun vessel on an interception course. In each trial there is repeated evidence of course and speed changes by the followed pod so as to keep the air-gun vessel no closer than 0.85-1.9 km off (Table 19). These changes can be seen in all appropriate track plots (Figure 49).

In trial nine the air-gun was temporarily shut down when a cow-calf pod (non target pod) approached the operating air-gun to ~ 500 m (Table 18). This pod was rapidly drifting N at the surface in a strong ebbing tidal stream while the air-gun vessel was steaming S at 1.46 ms^{-1} (2.9 knots). The pod passed the shut down vessel at 300 m closest approach, still at the surface, with the cow seen to be actively pushing the calf away from the vessel. When this pod had moved to > 1500 m astern the Flying Fish the air-gun was started again. At this point the target pod was 3.18 km away but on a direct interception course (Figure 49). When the air-gun resumed the target pod immediately reversed direction from a general N drift to a S course and increased its speed. The pod then allowed the vessel to cross its intended N trackline and pass by, then at the point of closest approach began moving N again at a steady speed, putting itself and the air-gun on a diverging course.

Thus in this trial a cow-calf pair (non target pod) did allow the air-gun to approach to 500 m. Significantly for the sound exposure received, this pod seemed to be consistently at the surface, thus reducing the received air-gun signal (see section 2.1.4). In contrast the target pod showed a similar response to the other cow-calf pod trials in its closest allowable approach. The target pod also displayed what appeared to be a startle response to the air-gun when it resumed operating at 3.18 km on a direct interception course, after being temporarily shut down

.

Table 18: For each trial: air-gun operation times; summary data of *WhaleSong* observations giving target pod (**TP**) and interacting pod composition, a general behavioural summary and specific incidents with time; and summary of incidental sightings from the air-gun vessel *Flying Fish* during times of air-gun operations, indicating whales which appeared to investigate the operating air-gun and sightings of other fauna near the operating air-gun. Codes are: aff. = affiliate; disaff. = disaffiliate.

#	gun on-off times	WS time	WhaleSong observations	FF time	*Flying Fish* Sighting
1	**13:20-14:36** **26/10/96**	13:10-13:22 13:40-13:50 14:30-15:00 15:15	**TP = 2 adults**, but up to 8 adults & unattached calf present at times 2 pods aff., give pod of 8 animals, follow TP pods disaff., form TP and pod ws2 nearby very surface active group of TP & ws2, calf still present another pod converging		
2	**10:58-12:01** **27/10/96**	11:57-12:30 12:33 12:34-12:36	**TP = cow-calf escort**, singers active nearby, initially surface passive, other pods affiliate becomes very active, ends with 5 adults 2 calves pod ws2 approach (2 adults & calf) from NE, TP & ws2 aff. become very active, chasing, pec & fluke slapping pod ws3 approach rapidly from E (1 adult) all aff. very active & some aggressive		
3	**13:54-15:15** **27/10/96**	14:52	**TP = started 4 adults & calf, disaff. to 2 adults (TP)** and cow-calf & escort singer heard under hull	15:16	single whale @ 300 m
4	**10:59-12:25** **28/10/96**		**TP = cow-calf**, surface passive whole session, no other whales nearby, large tiger shark sighted nearby	12:07 12:09-12:10 12:12 12:15-12:18 23:22	Bottlenose dolphins @ 200 m single whale (ff1) approaches starboard beam to 100-150 m ff1 300 m starboard quarter ff1 400-450 m starboard beam ff1 400 m port quarter
5	**14:59-16:06** **28/10/96**		**TP = cow calf**, TP follows steadily NW course, moves into lee of Coopers Shoal (with respect air-gun)	15:41 16:02 16:06	single whale (ff1) @ 300 m starboard beam approaching ff1 150 m astern air-gun shut off before vessel emerges from behind Coopers Shoal

#	gun	WS time	*WhaleSong* observations	FF time	*Flying Fish* observations
6	**10:35-12:30 29/10/96**	12:39	**TP = cow calf**, surface passive very surface active pod (3 adults & calf) 1000 m off	10:58-11:00 11:54 12:25	Bottlenose dolphins 150-200 m port beam milling school baitfish active on surface @ 70-100 m, ahead bottlenose dolphins @ 400 m off port bow
7	**15:35-16:20 29/10/96**	15:23 15:57 16:05 16:33 16:35-17:05	**TP = 4 adults & calf**, dynamic pod much surface activity, jostling entire observation 1 adult approach from behind, aff. TP = 5 adults & calf 1 adult disaff.(pod ws1) moves toward FF singer starts up very close ws1 returns to 10 m off stern WS TP continues high surface activity	16:05 16:07-16:10 16:13 16:33	single whale (ff1) approaching dead ahead from WS direction ff1 approached bow of FF to 150 m, then turned swam back to WS ff1 @ 500 m in WS direction (port quarter) ff1 surfaced immediately astern WS
8	**15:22 -16:40 16/10/97**	14:03	**TP = cow-calf**, meandering slowly S at first then E, then NE, surface passive tail-sailing whale drifts by	16:18	dolphins 200 m ahead, 2 sightings
9	**13:21 -13:32** **and** **13:53 -15:11** **17/10/97**	13:08 13:53	**TP = cow-calf**, short periods surface activity (fin slapping, few breaches) mixed with long periods resting pod of 2 adults @ 1000 m NE appear to approach but no contact TP rapidly moves off away from air-gun when turned back on	13:29 13:32 13:38 13:48 13:53 13:55 14:05 14:07-14:14 14:17 14:34-14:58	cow calf (pod ff1) within 500 m off starboard bow, drifting N in strong current (FF heading S) stopped air-gun, pod ff1 @ 4-500 m; FF maintains course pod ff1 ~ 300 m abeam, at surface, cow seen actively pushing calf away from FF (gun still off) pod ff1 1500 m astern; FF still heading S gun back on, pod ff1 still drift N large blow spotted astern 2 large adults (pod ff2) approaching from stern pod ff2 approach at speed, circle vessel at 100-200 m (gun on) pod ff2 begin moving to S pod ff2 move to ~ 6-700 m off, maintain distance ~ halfway towards WS
10	**13:45 -15:20 18/10/97**	13:38-13:45	**TP = cow calf**, long periods resting then swimming pod approaches to 500 m but no contact	14:17	school small fish at surface within 50 m
11	**15:40 -16:30** **19/10/97**	14:28	**TP = cow-calf & escort**, mostly swimming, little surface activity pod ws2 of 2 adults & calf approach. to 300 m, moves off	15:54 16:01 16:03 16:06 16:17 16:20	single whale (pod ff1) @ 300 m, approaching port bow pod ff1 close abeam pod ff1 @ 100 m astern pod ff1 moved away rapidly to E (starboard), lost sight of pod ff1 appears off starboard bow @ 200 m pod ff1 @ 200 m astern moving off

#	gun	WS time	*WhaleSong* observations	FF time	*Flying Fish* observations
12	**10:13 - 11:10** **20/10/97**	 09:42 10:52 10:56 10:59 11:13-12:00	**TP = single adult male**, moves quickly, affiliates with pod ws2 believed male & female, TP sings and male of ws2 pod sings TP dives, stays down and commences singing pod ws2 of 2 adults observed to cross bows FF move to WS ws2 affiliate with TP who keeps singing, some surface activity TP & ws2 move away and towards each other TP & ws2 stay affiliated, much surface activity towards end observation	10:17 10:18 10:20 10:21 10:22 10:46 10:50-10:54 10:56 10:58-11:03	single large adult appears @ 100 m off port quarter second large adult appears @ 100 m off port quarter, merges with other animal to form pod ff1 pod ff1 @ 250 m off port quarter separate single animal (pod ff2) appears @ 150 m off starboard bow pod ff1 moves WSW (away, FF heading NE) then doubles back, pod ff2 moves to vicinity nearby moored housing pod ff1 approach rapidly - up to 7.4 kn (3.7 ms $^{-1}$), @ 10:46 560 m off starboard quarter pod ff1 approaches rapidly from stern, circles vessel clockwise (port side first) @ 100-200 m, WS target pod 500 m E pod ff1 astern @ 400 m pod ff1 heads north @ 600 - 1000 m from FF
13	**14:12-14:43** **20/10/97**		**TP = 2 adults & calf**, moving slowly with much resting and surface passive	14:43	Air-gun shut down as trawler deliberately approached TP closely and began circling, put TP in position boxed in by vessels with air-gun approaching @ 800 m.
14	**13:26-14:34** **21/10/97**	 13:35 13:44 13:48 14:00 14:33 14:40 15:12	**TP = cow calf,** regular resting, swimming, some course changes, pass by several other pods, surface passive pod of 2 adults = ws2 ~ 200 m off, keep separate ws2 ~ 200 m from TP, then head S pod ws3 sighted NNE @ 1500 m pod ws4 sighted 2 km dead ahead ws4 500 m dead ahead TP, identified ws4 as cow-calf ws4 & TP within 100 m each other, pass by TP passes by fish trial cage in 10 m water	13:29 13:33 13:37 13:46 13:50 14:10 14:13-14:34	pod ff1, single adult @ 500 + m off port bow, approaching ff1 250 m off port beam, passing ff1 125 m directly astern ff1 moves off to NE, @ 2 km off starboard quarter pod ff2, single adult @ 900 m off starboard bow, approaching ff2 120 m astern ff2 follows FF @ 100 - 400 m astern
15	**10:38-11:43** **22/10/97**	 09:30	**TP = 2 adults**, travel fast in large loop, little surface activity but steady swimming just below surface and resting pod ws2 passes @ 100 m swims away	11:05 11:08	pod ff1 700 m ahead, single adult pod ff1 500 m off starboard bow moves away
16	**11:42-12:40** **23/10/97**		**TP = cow-calf** 2nd cow-calf pair close by early in obs. resulting in much confusion with behaviour calling on TP up to 11:41, both pods surface passive	12:10 12:15 12:20 12:25	pod ff1 500 m dead ahead, single adult brief sight on ff1 300-400 m ahead ff1 starboard bow @ 250-300 m ff1 circled, directly astern @ 300 m moves away to N

Table 19: Assessment of humpback whale exposure trials for speed and/or heading changes which correlated with an approaching or intercepting operating air-gun. Abbreviations are: @ time/air-gun range (km); veer - go clockwise; back - go anticlockwise; CA - closest approach, AG - air-gun; TP - target pod; meand. - meandering;

run	pre air-gun	during air-gun approach	post air-gun
1	backs course N-SW, stays SW; variable speed	backs course from WSW to SE away from incoming AG @ 13:38 / 2.85; speeds up @ 14:10 / 2.05, after AG CA; pod altered course then speed to move off closing air gun	veers to ESE course, slows then speeds up
2	meandering pod, changed from SE to N just before AG on; variable speed	on direct approach of AG first slows @ 11:30 / 1.97; then reverses course to S direct away AG @ 11:36 / 1.66 km; remains moving slowly away from AG which is circling;	30 min after AG off resumes N course
3		CA=6.5 km; inconclusive	
4		CA=5.8 km; inconclusive	
5		pod moved into sound shadow of shoal ; AG shut off to avoid possible startle as vessel cleared shoal; inconclusive	
6		CA=5 km; inconclusive	
7	head SW - S; steady speed	veer to W at AG on @ 15:35 / 3.92; speed up @ 16:10 / 1.22 to increase diverging range back to SW @ 16:14 / 1.96 after CA	revert to S course 10 min after AG off; steady speed
8	initially S then backs to SE / E	course backs to general E over AG on; speed increase @ 16:06 / 2.00 increases intercept range; speed increases @ 16:36 / 1.3 puts pod on diverging course	backs to ENE after AG off; maintains comparatively high speed until near end observation
9	meandering course with mostly S component; strong ebb tide to N, so N course is mostly drift for whole observation	AG stopped started due to 2nd cow-calf; at AG 2nd on (13:53 / 3.18) TP immediately sets course speeds up to increase intercept range; rests 14:20-14:44 whence AG goes to diverge course; speeds up swims S again @ 14:44 / 1.02 to increase AG range	stops swimming immediately AG off, rests goes to N drift; @ 15:35 heads E
10	slow swimming; meandering; goes almost nowhere; strong N ebb tidal stream	speeds up @ 13:48 / 4.64, just after AG on, heads E; backs to N @ 14:18 / 2.90 but moves slow with some meandering; sets direct N and speeds up @ 14:40 / 1.29; course sets as diverging 14:58 / 1.12; maintains slow N head	maintains slow N course
11	general SE course, slow swimming	TP maintains direct intercept course on S head until 15:57 / 1.38 when veers WNW to put AG onto diverging course at 15:59; then resumes S course @ 16:13 / 1.42 with AG diverging	swims slowly S until 16:52 then starts meandering with large speed increase towards end of observation
12	whale heading S at speed; stops to sing @ 09:42; not seen again until 10:51	assume TP maintains constant course while submerged singing; directly approaches AG for CA @ 10:56 / 0.10; Immediately after CA steers SW at high speed	slows after AG off, switches course to NW; @ 11:45 backs to S increases speed
13		trawler interrupted; trial aborted; inconclusive	
14	steady NNW heading with some meandering; mostly constant speed	speeds up at AG on @ 13:26 / 4.4; course allows TP to clear AG by 1.9 km; little meandering over AG on period	maintains N head; some meandering in course; speeds up

run	pre air-gun	during air-gun approach	post air-gun
15	SSW course some meandering, slowly decreasing speed; possible drifting on S flood tidal stream	maintains S course until 17:16 / 1.75 when reverses course to NW to take it away from incoming AG; @ 11:22 / 1.36 course switches to diverging	maintains N course and speed
16	mostly slow meandering on NE course; speed burst at end; S set flood tidal stream	sharp speed increase and course change to S away from AG @ 11:54 / 3.08; begins N course again @ 12:11 / 1.68 which maintains intercept range; slows speed while AG passes; resumes N swim @ 12:33 / 1.79 with AG diverging	swims slow N until 13:10; then drifts S with tide

For the exposure trials containing cow-calf or female humpbacks, ranges and received air-gun levels at which speed or heading changes which resulted in avoidance of the approaching air-gun and closest approach ranges are given on Table 20. Range values are as given in Table 17 for minimum approaches, or as determined from Figure 49 for course deviations. Air-gun levels (equivalent energy) were derived from the fitted curve equations given in Table 11 using the appropriate range. Curves for the specific trial were used or if no measurement set was available for that trial the curves from the nearest trial (in space) carried out during that year were used. Given the vertical sound intensity profiles present in the water column (section 2.1.4) these values represent maximum levels in the water column, levels would be lower nearer the surface.

Using these ranges, pods of cow-calves or containing females, made some detectable avoidance manoeuvre from the approaching air-gun at 1.22-4.4 km from the air-gun, with the mean range for first response at 2.47 $\pm$ 0.702 km (n=10, unless otherwise stated all $\pm$ errors are 95% confidence limits). The closest these pods allowed the operating air-gun (standoff range) was over 0.85-1.9 km, with the mean at 1.29 $\pm$ 0.282 km (n=10).

run	range at which course or speed change evident (km) / air-gun level at that range (dB re 1 μPa^2.s)	closest approach (km) / air-gun level at that range (dB re 1 μPa^2.s)
1	2.85, 2.05 / 124, 128	1.89 / 129
2	1.97, 1.66 / 128, 130	1.62 / 130
7	1.22 / 126	0.95 / 129
8	2.00, 1.30 / 120, 126	1.30 / 126
9	3.18, 1.02 / 97, 124	0.85 / 126
10	2.9, 1.29 / 124, 132	1.10 / 134
11	1.38 / 125	0.92 / 130
14	4.40 / 97	1.90 / 116
15	1.75 / 122	1.32 / 126
16	3.08 / 108	1.01 / 128

Table 20: Summary of response and closest approach ranges and respective received air-gun levels for pods containing cow-calves or females, during humpback whale exposure trials.

The distribution of received air-gun levels at which avoidance responses were initiated and at standoff ranges are shown on Figure 47. Decibel statistics for each set of values are given in Table 21. These values can be approximately converted to peak-peak level by adding 30 dB or to mean square pressure units by adding 14.4 dB (Table 8, Table 9 respectively).

	value range	mean	95% confidence limits	median
avoidance	97 - 132	126	122 - 128	124
standoff	116 - 134	129	123 - 131	128

Table 21: Decibel statistics (dB re 1 μPa^2.s) of the air-gun equivalent energy at which avoidance was noted and the standoff ranges for 10 trials listed in Table 20.

Although the tracked pods containing cow-calf pairs or females, and on interception courses with the air-gun, tended to maintain a mean 1.3 km standoff range during trials, in nine of the 16 trials (runs 3, 4, 5, 7, 9, 11, 12, 14 and 16), 11 separate pods (other than target pods) approached the operating air-gun to 100-400 m. Of these 11 pods nine were single adults only and two were of two adults. All appeared to be large mature animals. None involved calves. Many of these animals were seen to head directly for the air-gun vessel, would stop at some range then circle or partly circle the vessel, then would move off. On several occasions the directly approaching pods were moving at high speed with large bow waves evident.

In trial 12 one such incoming animal was tracked using sextant angles below the horizon to gauge range, with the pod position normalised to the air-gun vessel shown on Figure 50. This pod clocked an approach speed of 3.7 ms[1] or 7.4 knots on one occasion. In trials 12 and 14 two pods followed the operating air-gun for some time. During trial seven a single animal was seen to break off from the main pod being tracked, swam directly towards the air-gun, approached the bow of the air-gun vessel to 150 m, then swam back to the main pod, appearing off the *WhaleSong* stern (Table 18).

**Exposure experiments - distribution of avoidance and standoff levels**
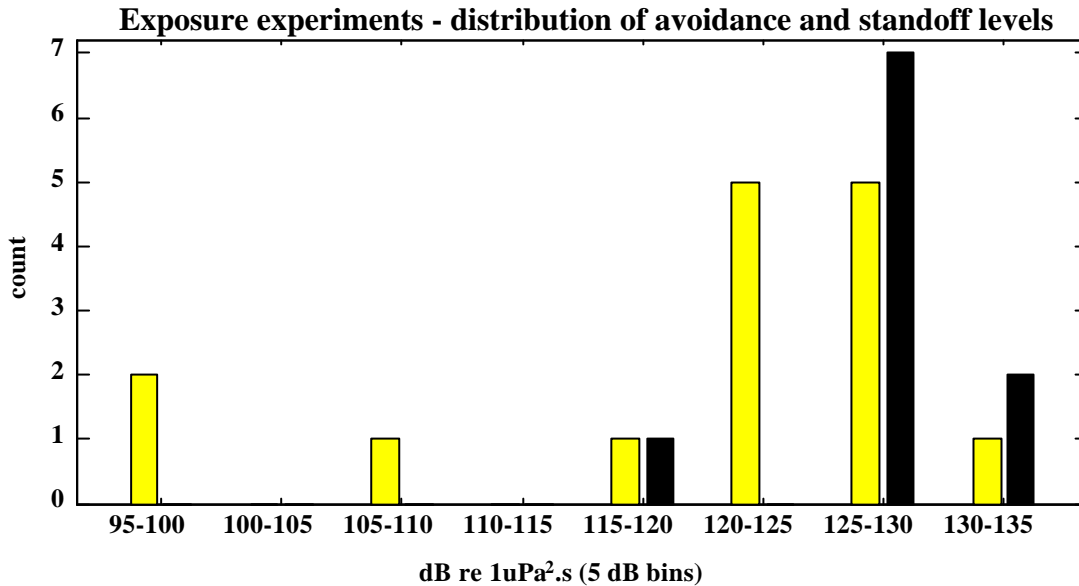
Figure 47: Distribution of received air-gun levels at which avoidance of the approaching air-gun was noted (stippled bars) and at the minimum allowable approach range (standoff range or minimum range whales allowed air-gun to pass, black bars), in 5 dB bins.

Although the only evidence we have is of behavioural patterns, it was believed that most if not all of these deliberate approaches to the operating air-gun involved mature male whales.

During trial 12, the only trial containing a male only pod, the singing whale largely ignored the oncoming air-gun, allowing it to approach to 100 m (Table 17, Table 18) on a closing course over the entire approach (Figure 49 - 12). Only once the air-gun reached 100 m did the whale alter course and speed to take it away from the air-gun.

Between 10 and 18 m depth the received level of the single Bolt air-gun at 100 m was estimated to be in the range 150-156 dB re 1 μPa^2.s (equivalent energy) and at 400 m 140-146 dB re 1 μPa^2.s, using the type B and C sediments from the modelling runs in Exmouth Gulf (section 2.1.4). Thus the male whale of trial 12, and the whales which deliberately approached the operating air-gun, would have received maximum air-gun levels in the range 140-156 dB re 1μPa^2.s

After the first two trials had been conducted, the general standoff range of 1.3 km observed, trials 3-6 were inconclusive, and given that available field time was limited, it was decided to concentrate all efforts on obtaining successful trials with target pods on good interception courses. It was deemed that to carry out a set of control trials, in which the air-gun vessel approached the target pod with air-gun deployed but not operated (it would have needed to be charged to avoid flooding) was not necessary due to virtually no vessel cues available to the whale at 0.85-1.90 km range from the approaching vessel.

The approaching, passing and departing acoustic signature of the air-gun vessel, *Flying Fish*, was measured in Exmouth Gulf during trial 6 (set 2185, 1996) over the reflective bottom and during trial 8 (set 2254, 1997) over a bottom without the reflective layer. These correspond to "good" and "bad" sound propagation conditions respectively (see section 2.1.4). Using a mid-water hydrophone (where the sound field was greatest) from set 2185 in 1996 (with reflective layer), the approaching vessel was not audible at 650 m, just audible at 600 m and only became distinct above the background noise at 450 m. At its closest approach (170 m) the vessel noise was low, reaching a maximum level of 108 dB re 1 μPa over the 630-1000 Hz 1/3 octave's or about 20 dB above background levels at these frequencies for 10 knot wind conditions. The departing vessel was not audible at 500 m. The measured 1/3 octave frequency content of the approaching and passing *Flying Fish* as measured during trial 6 is shown on Figure 51, and the spectral level of the background noise (no vessel noise, vessel at 1800 m) and the *Flying Fish* abeam the receiver at 170 m during the same trial, on Figure 52. The 1/3 octave measurements were made from 5 s 1/3 octave averages taken between air-gun shots (15 s fire rate). There was little energy from the vessel at low frequencies, so this plot is shown over the 1/3 octave range 100-10000 Hz to enhance the colour scale and remove low frequency flow noise from the moored mid-water hydrophone. Two whales were calling nearby, their signals show up as the occasional blips at 500-1000 Hz. The high frequency band above 2500 Hz is snapping shrimp noise. A similar analysis for the approaching and departing *Flying Fish* during trial 8 gave similar ranges of audibility and frequency content. The mean vessel speed during all trials was low (1.41 ± 1.18 ms^{-1}). At this speed there was no wake from the vessel and very little propeller cavitation, which is the major source of noise for a vessel underway, hence the low measured vessel signature.

From the authors experience humpback whales do not normally avoid a 7.5 m vessel approaching at 1.41 ± 0.18 ms^{-1} (2.8 ± 0.4 kn, mean *Flying Fish* speed during all approach trials) at 0.85-1.9 km range. Indeed during the trial period the *Flying Fish* regularly passed humpback pods at 50-100 m (with little obvious response from the whales) while steaming about the Gulf at 6-15 knots with the air-gun gear on deck (the air-gun was only deployed for a trial and recovered immediately after). On one occasion (discussed below) a cow-calf pair of its own accord approached the shut down *Flying Fish* to 100 m.

Thus at the range over which cow-calf responses occurred to the operating air-gun there was no underwater acoustic cue evident from the air-gun vessel. Visual cues were limited due to the low profile of the vessel. The cabin top was at 2.5 m above sea level. At 1000 m this represents 8.6' of arc for the visual field, which would be difficult for a submerged whale to see. The vessel did not blow excessive smoke and airborne noise was not considered to be high. The authors believe that given these factors and that normally humpback whales will allow most slowly moving small vessels to approach to at least within a few hundred m before showing some sign of response, then control approaches, although possibly desirable, were not necessary in the trials carried out.

There was some indications that the air-gun vessel did become known to pods resident in the Gulf over the trial periods. The cow pushing the calf away from the vessel with shut down air-gun as its drifted by during trial nine indicated that this animal had associated the vessel with the air-gun which had been shut down six minutes previously.

The trials were conducted with the observation vessel *Whale Song* as a constant presence throughout the trial. Thus any behavioural effects due to the vessels presence were consistent within and between trials. The laminated timber vessel was operated by experienced whale observers at slow speed using a 50 HP outboard motor to minimise possible behavioural effects. The observation periods before the air-gun began operating ranged in length from 25 minutes (trial 7) to 1:36:00, with a mean time of 1:05:15 ± 0:11:24

(from Table 17). Thus the mean pre-air-gun observation period of just over an hour was considered as the 'control' period for each trial.

Following trial 12, the air-gun was recovered and the vessel moved off to a nearby deep rock outcrop to catch fish for fish-air-gun trials which were being carried out concurrently. Two singers were heard nearby and a cow-calf were resting 500 m off to the S. Approximately 15 minutes after the vessel began fishing the cow-calf swam to within 100-200 m of the vessel, approaching directly. The cow, and occasionally calf, then began full-body breaching (jumping clear of the water), gradually moving away from the vessel. Over 22 minutes the cow did seven breaches, with the last estimated at 600-1000 m off the vessel. It was not uncommon to observe breaching events in Exmouth Gulf, and generally breaching whales could be followed or approached slowly. But in the authors experience it is extremely rare for humpback whales to deliberately approach shut down vessels (as opposed to vessels underway at speed) and to begin breaching at short range. Although completely speculative, this observation raised the question that perhaps the cow had associated the vessel with air-gun noise through previous trials (the air-gun was on deck during this event) and was responding in some fashion.

The short range breaching by the cow was recorded with a hydrophone at 12 m depth deployed from the *Flying Fish*. The range to cow could only be determined visually, the animal was in the vessels radar shadow, and had gently sloping land behind it making sextant measurements difficult. A full analysis of the breaching event and signals is not presented in this document. But, a breaching signal, as recorded at 100-200 m from the whale, and a comparative air-gun signal (matched primarily on equivalent energy) are shown on Figure 48. The breaching signal had a peak-peak level of 160 dB re 1 μPa, and an equivalent energy measure of 133 dB re 1 μPa^2.s. It can be seen that although not identical, the breaching and air-gun signal waveforms are similar. The signals were also audibly similar. This audible similarity has been observed from several other sets of recordings containing breaching whale signals made in northern Australia by the author. In some instances the audible similarities are striking. Several examples of breaching events sound startlingly like air-gun signals.
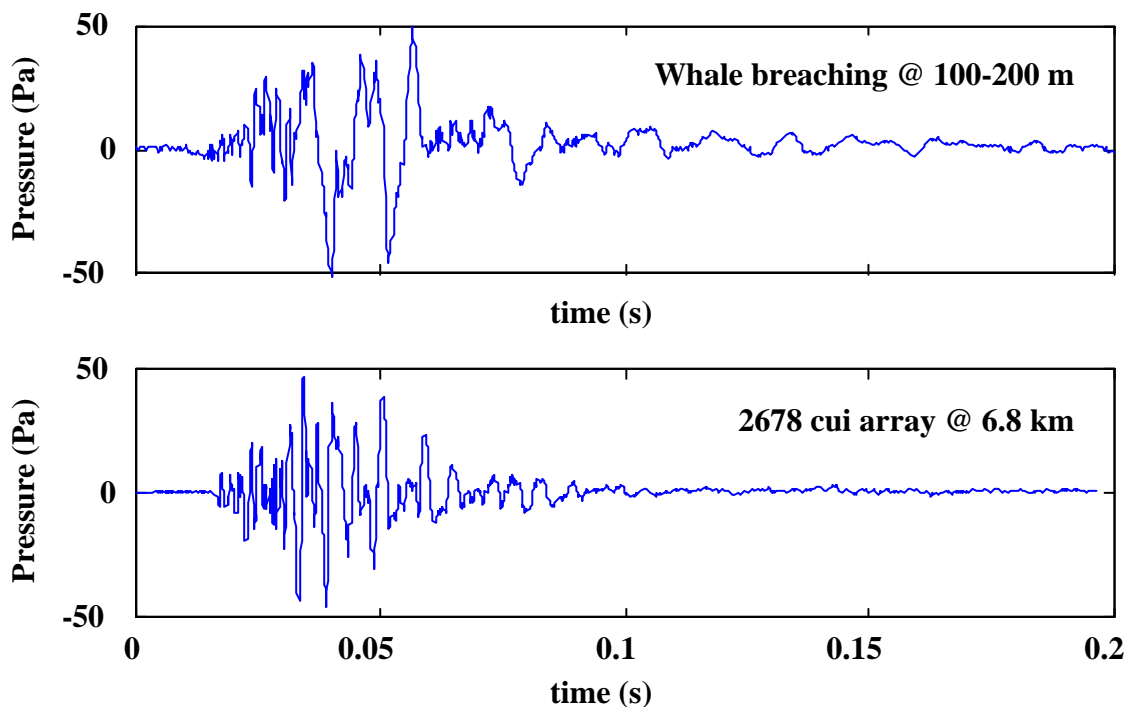

Figure 48: Comparative waveforms for a large mature humpback cow breaching at 100-200 m from a hydrophone at 12 m depth in 17 m of water (top) and a matched air-gun signal as received at 20 m depth, 6.8 km from a 2678 cui, 3D air-gun array (bottom).

We speculate that this similarity of air-gun signals and humpback breaching signals was a major factor in the deliberate whale approaches to the single operating air-gun during the Exmouth trials. One could argue that given the variability inherent in breaching sounds and the erratic timing of them as compared to consistent and regular air-gun signals, it is probable that humpbacks do not definitively mistake air-gun signals for breaching signals. But we argue that there is enough similarities between them that air-gun signals "interest" humpbacks, particularly mature males, and that this "interest" often translates to an investigative response. This could offer an explanation for the observed attraction of what were believed to be mostly mature male animals, to the single operating air-gun and the observations from the *Geco Resolution*, in which humpback sightings at ranges > 3 km from the vessel were higher during times of air-gun operations than during times with the air-guns shut down.

Thus the humpback whale approach trials with the single operating Bolt air-gun resulted in two opposing sets of results, which can be summarised as:

- for pods containing cow-calf pairs or possibly mature females - consistent avoidance manoeuvres beginning at 1.22-4.40 km (mean air-gun level of 126 dB re 1 μPa^2.s) to allow the air-gun to pass at a mean range of 1.3 km (mean air-gun level of 129 dB re 1 μPa^2.s), with a startle response seen in one trial at 3.18 km (97 dB re 1 μPa^2.s);
- consistent deliberate approaches to the operating air-gun by mostly single mature whales believed to be males, with animals approaching often at speed, circling or partly circling the air-gun vessel at 100-400 m range then swimming off (maximum received level of 165 dB re 1 μPa^2.s);
- the possibility that this deliberate approach by mature humpbacks to the single air-gun was related to 'acoustic competition' from the air-gun or the air-gun similarity to signals produced by whales during breaching events.

Five instance of small pods of dolphins passing near to the operating air-gun were also noted. In one instance (trial 6) a pod remained within a 500 m range for 30-35 minutes. The closest range at which dolphins were observed to the single air-gun was approximately 150 m in run 6. The estimated received air-gun level during this run at 150 m would have approximated 148 dB re 1μPa^2.s (equivalent to 178 dB re 1μPa peak-peak or 162 dB re 1μPa mean squared pressure from Table 8 and Table 9 respectively)

Following 16 pages:

Figure 49: For the 16 exposure trials: (**left hand side**) Track plots for the target pod (hollow circles, all plots), *WhaleSong* (small crosses track plot) and the *Flying Fish* (dots). Times are given on the track plot for the interpolated whale position (in italics) and the matched air-gun position. (**right hand side**) From top to bottom are the target-pod to air-gun range, speed, direction of travel, target-pod to air-gun interception range, target pod to air-gun interception time, and estimated received sound levels. The circles represent the whale details at each observation point, the lines are values for the appropriate measure at the whales interpolated position. Crosses are the observation vessel details. The interception plots were calculated by looking forward along the target-pod and air-gun vessel track at each whale observation point, for two hours in five s increments, and calculating the minimum approach range and the time at which this occurred. For the target-pod/air-gun on converging courses the intercept range fell within one minute to 120 s. For the target-pod/air-gun on diverging courses the intercept range was as for the time of observation. For clarity the time to interception for diverging courses was set to the maximum value on the plot and a different symbol has been used.

Whale (o), WhaleSong (+) and Flying Fish (.),
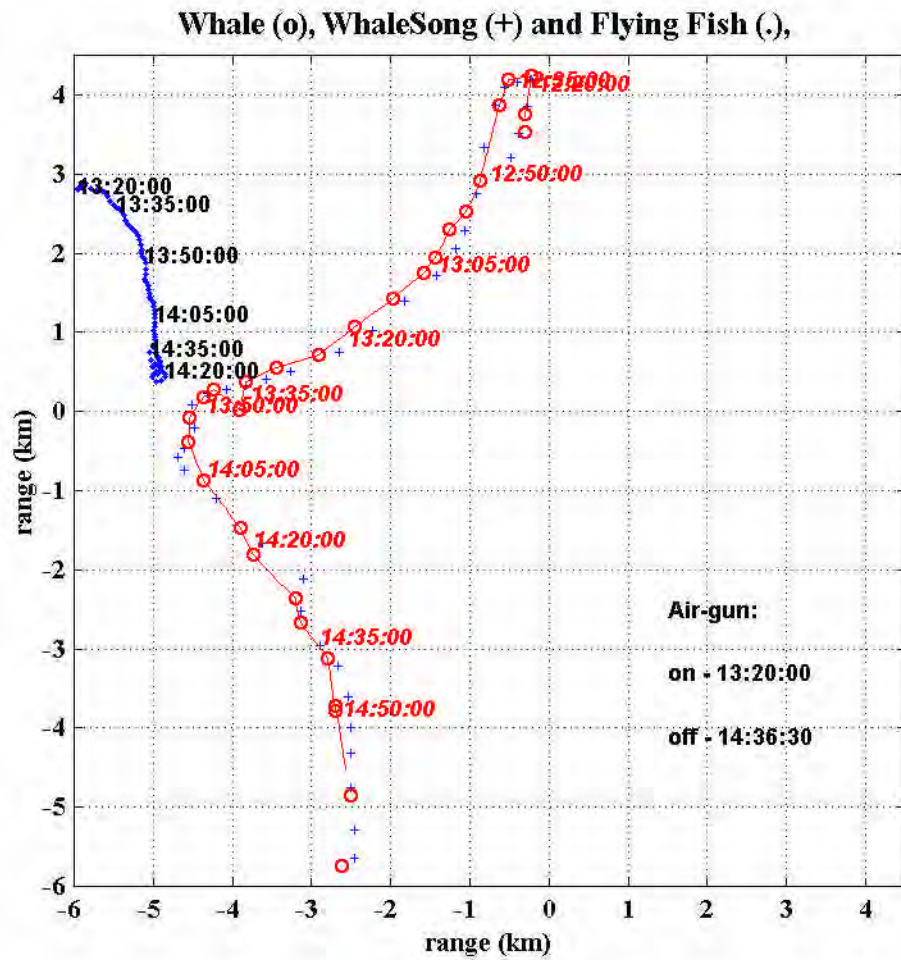
Run 1 26/10/96, 12:10:00-15:19:00

Whale (o), WhaleSong (+) and Flying Fish (.),

Run 2 27/10/96, 09:42:00-12:39:00

Whale (o), WhaleSong (+) and Flying Fish (.),

Run 3 27/10/96, 13:10:00-15:44:00

Whale (o), WhaleSong (+) and Flying Fish (.),

Run 4 28/10/96, 10:05:00-12:59:00

Whale (o), WhaleSong (+) and Flying Fish (.),

Run 5 28/10/96, 14:30:00-16:30:00

Whale (o), WhaleSong (+) and Flying Fish (.),

Run 6 29/10/96, 09:50:00-13:14:00

Whale (o), WhaleSong (+) and Flying Fish (.),
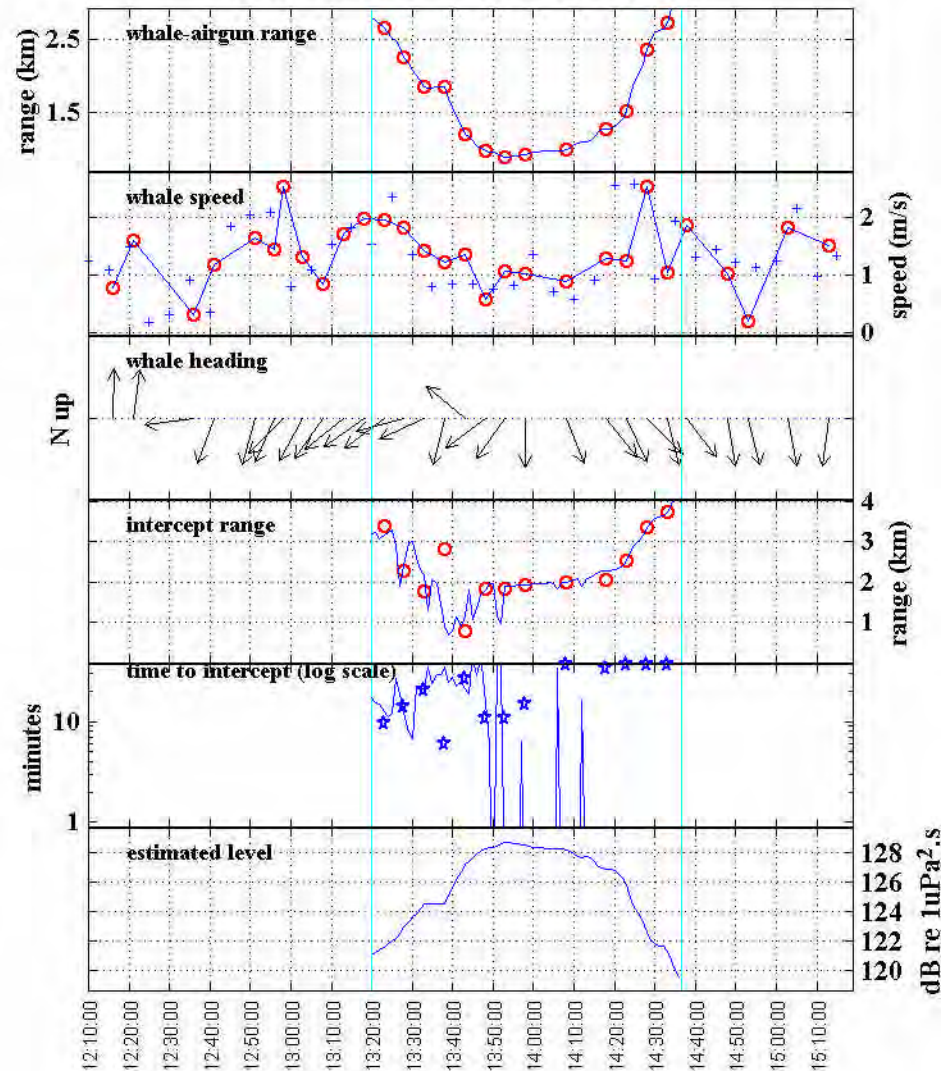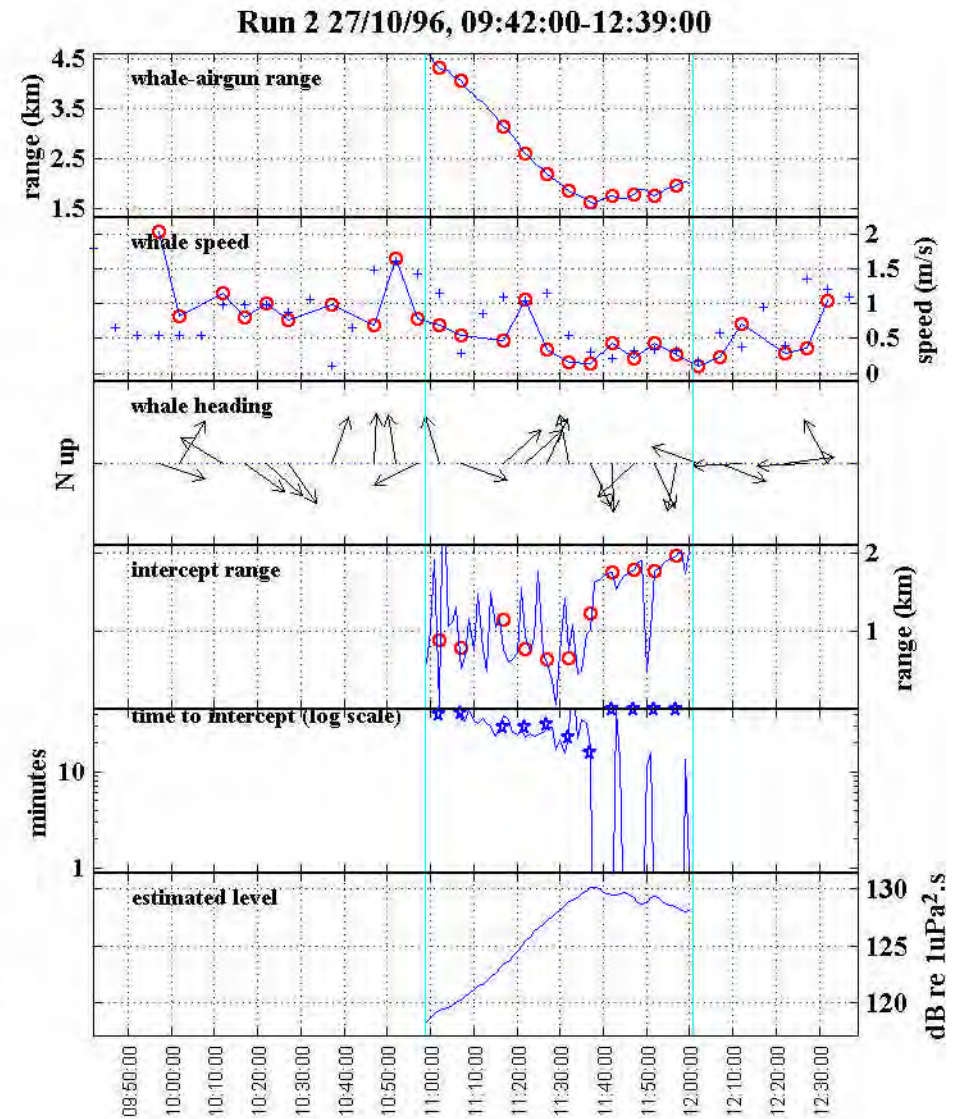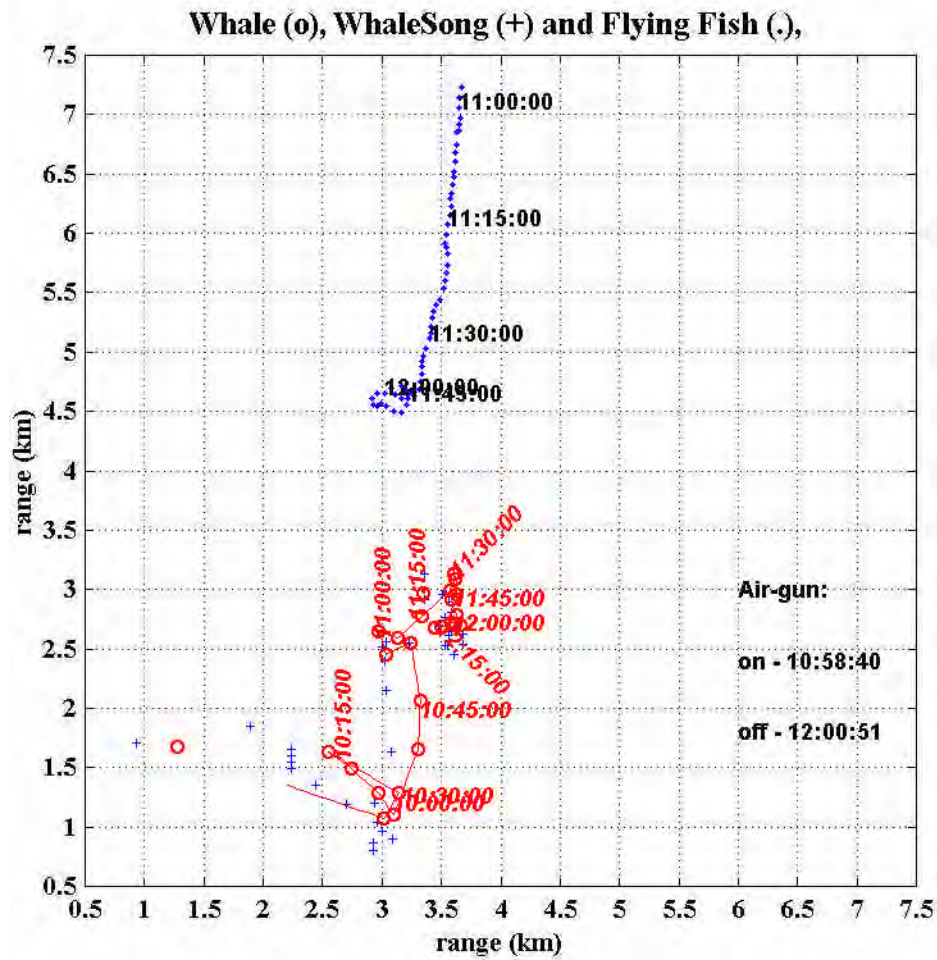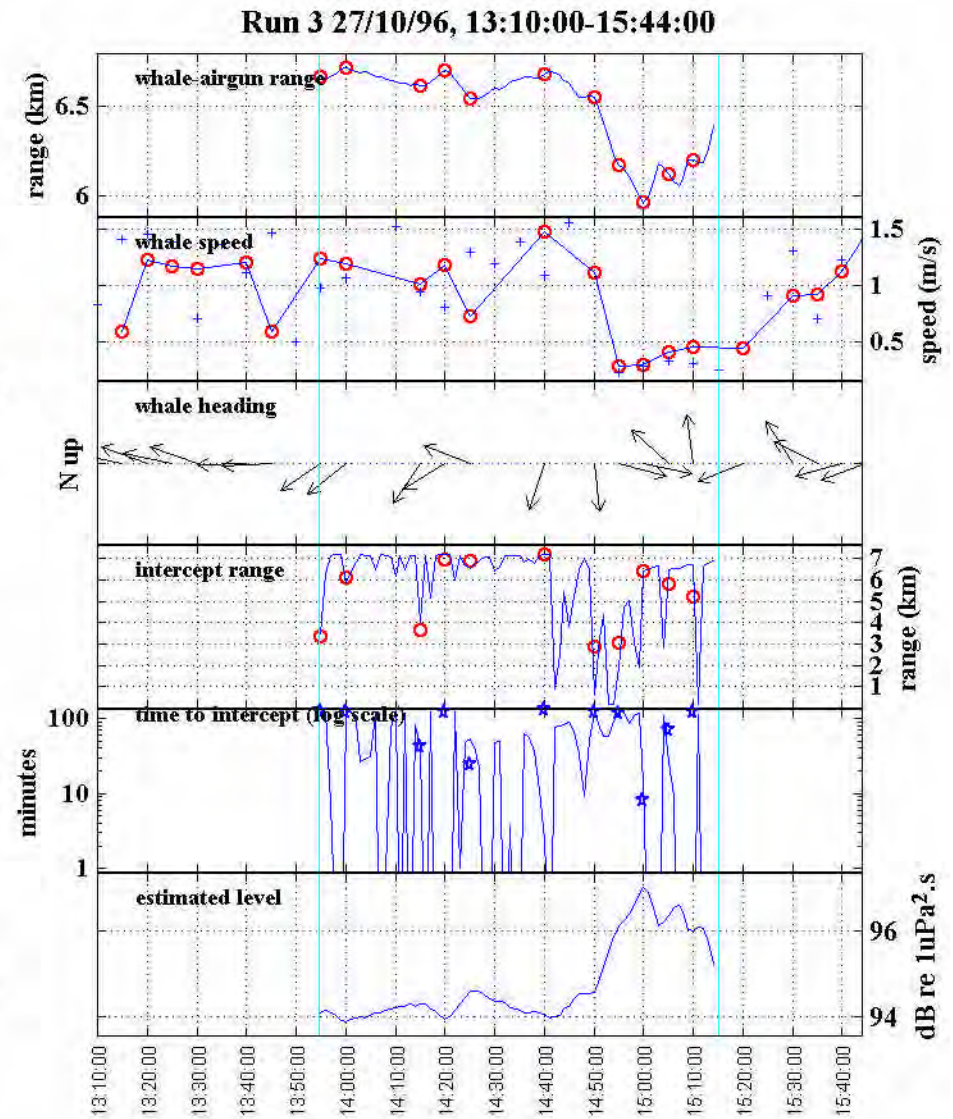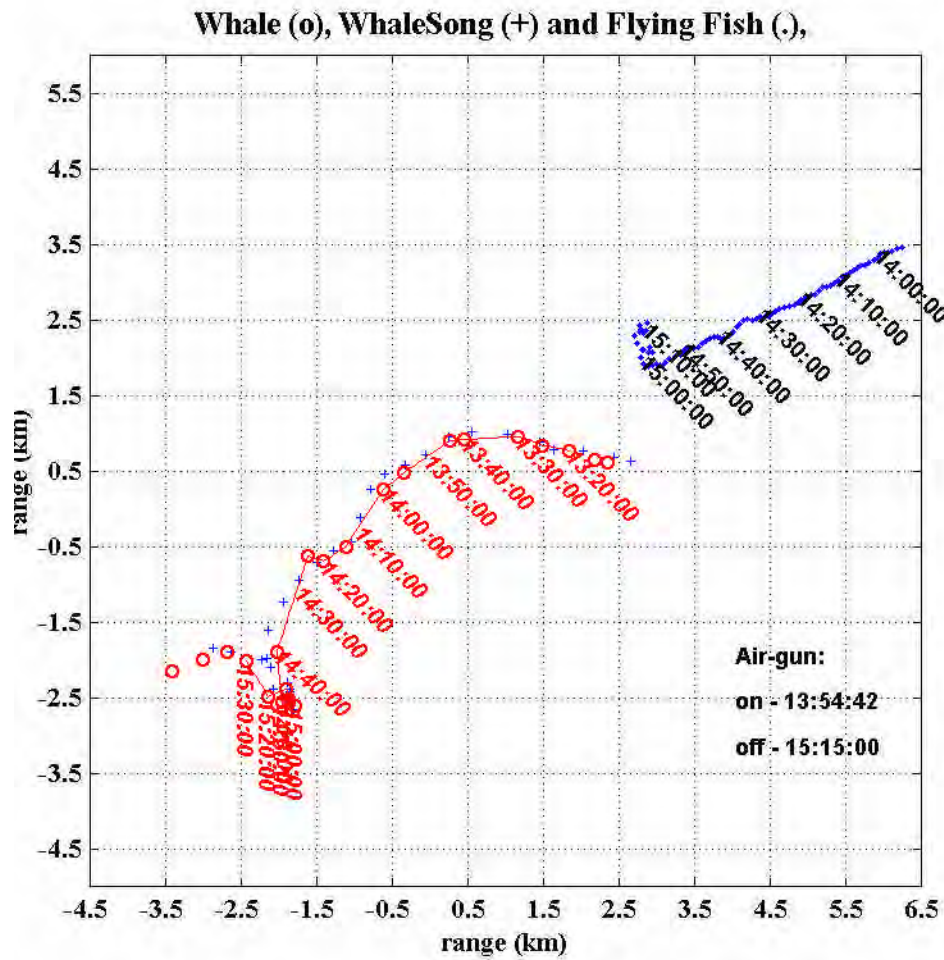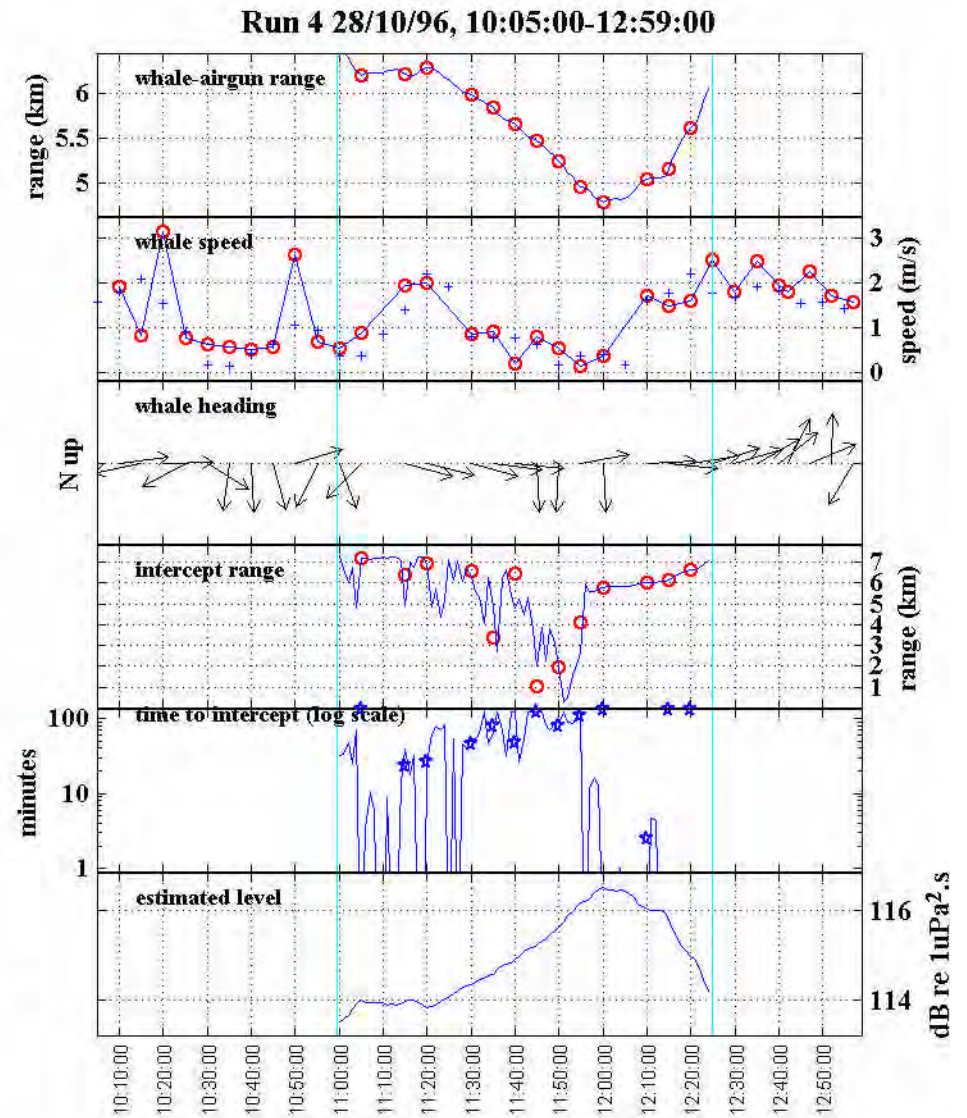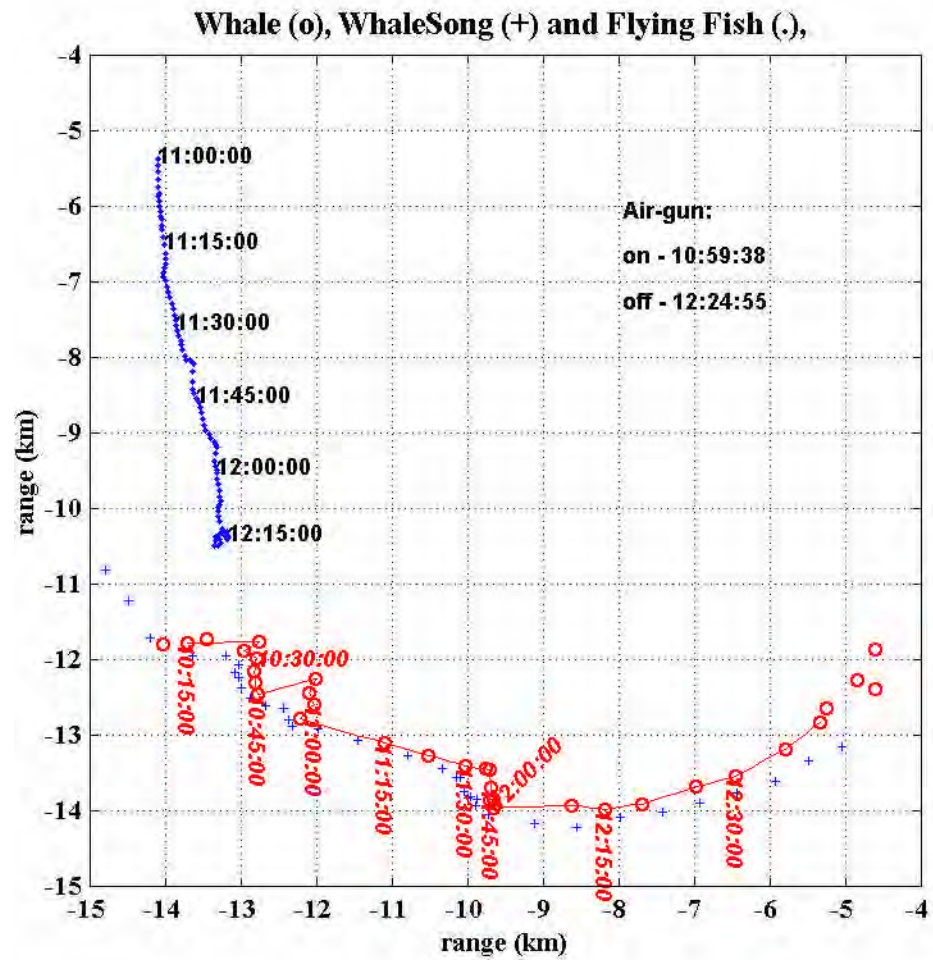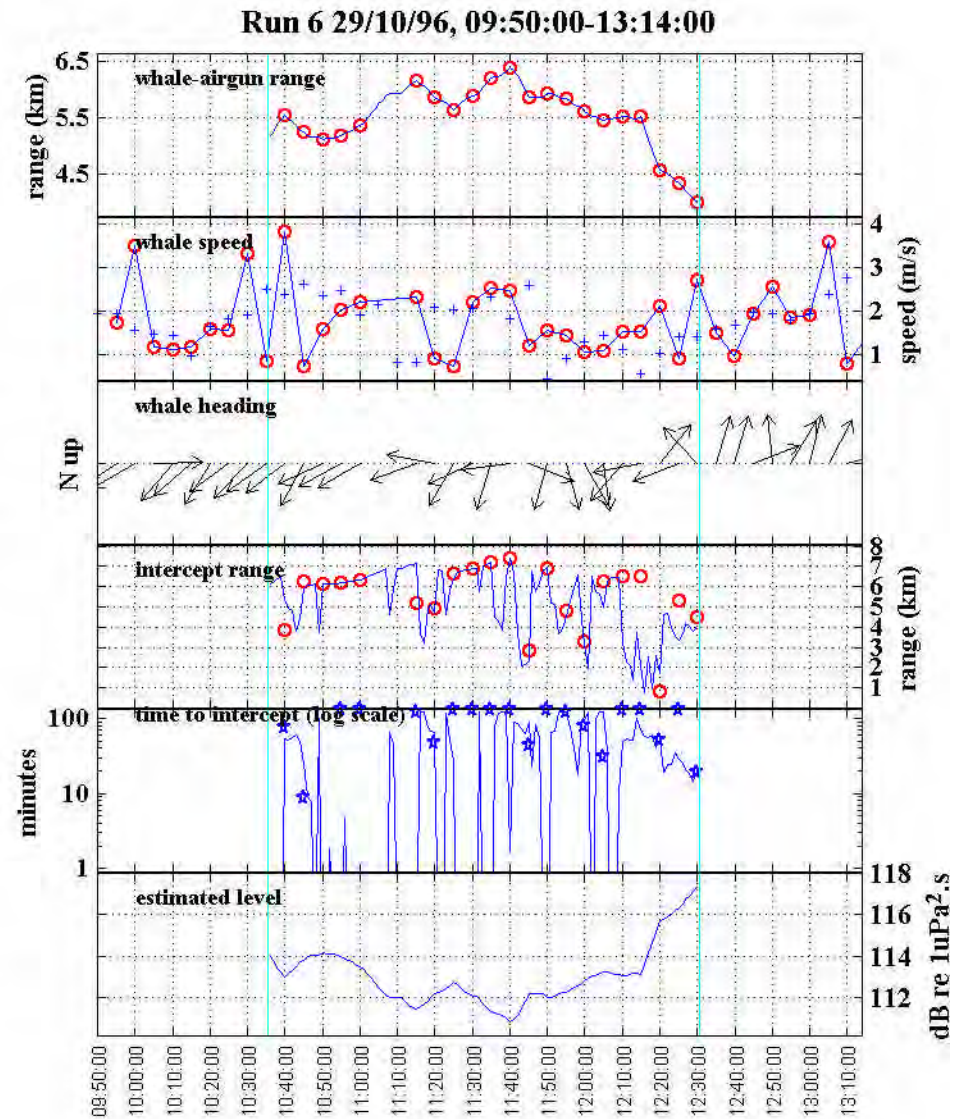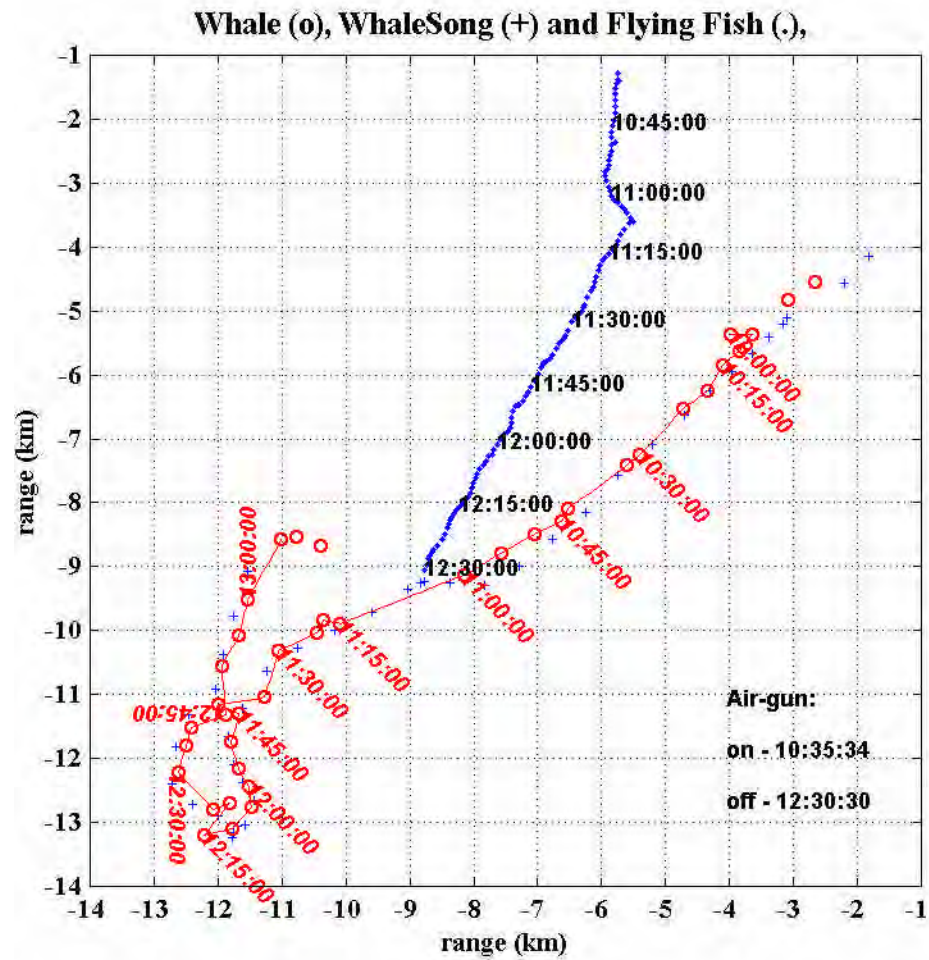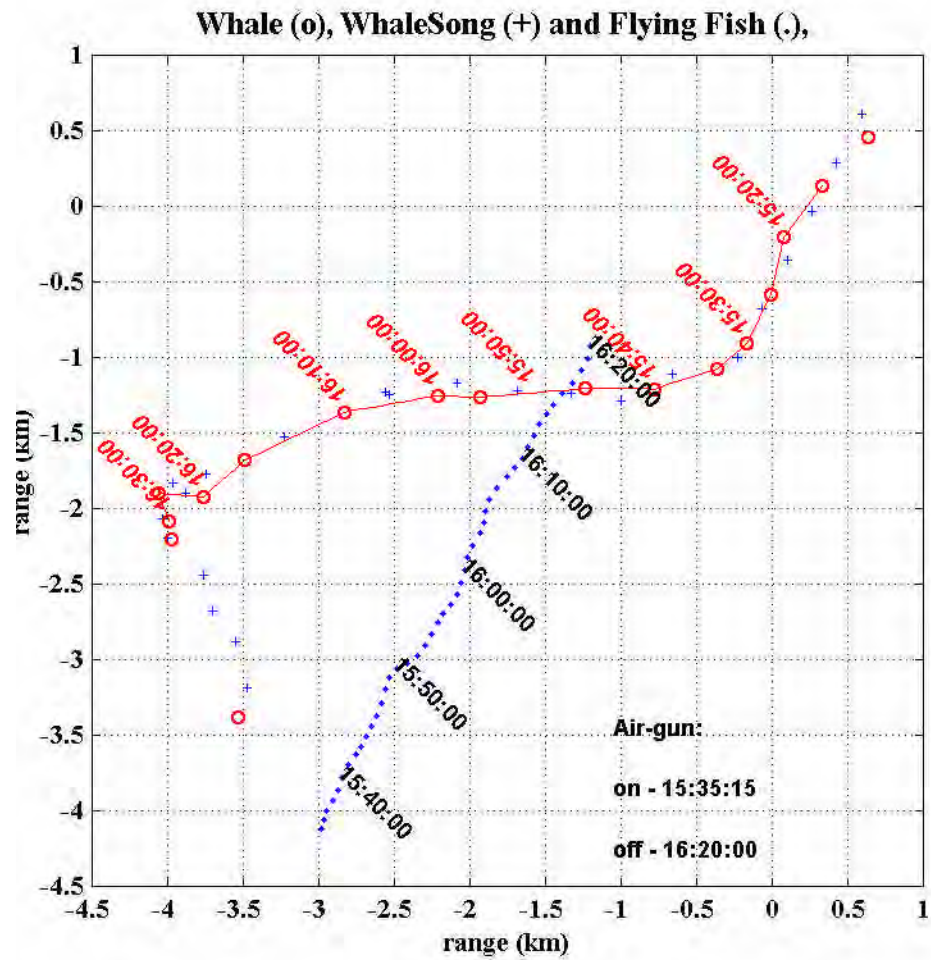
Run 7 29/10/96, 15:10:00-17:04:00

Whale (o), WhaleSong (+) and Flying Fish (.),
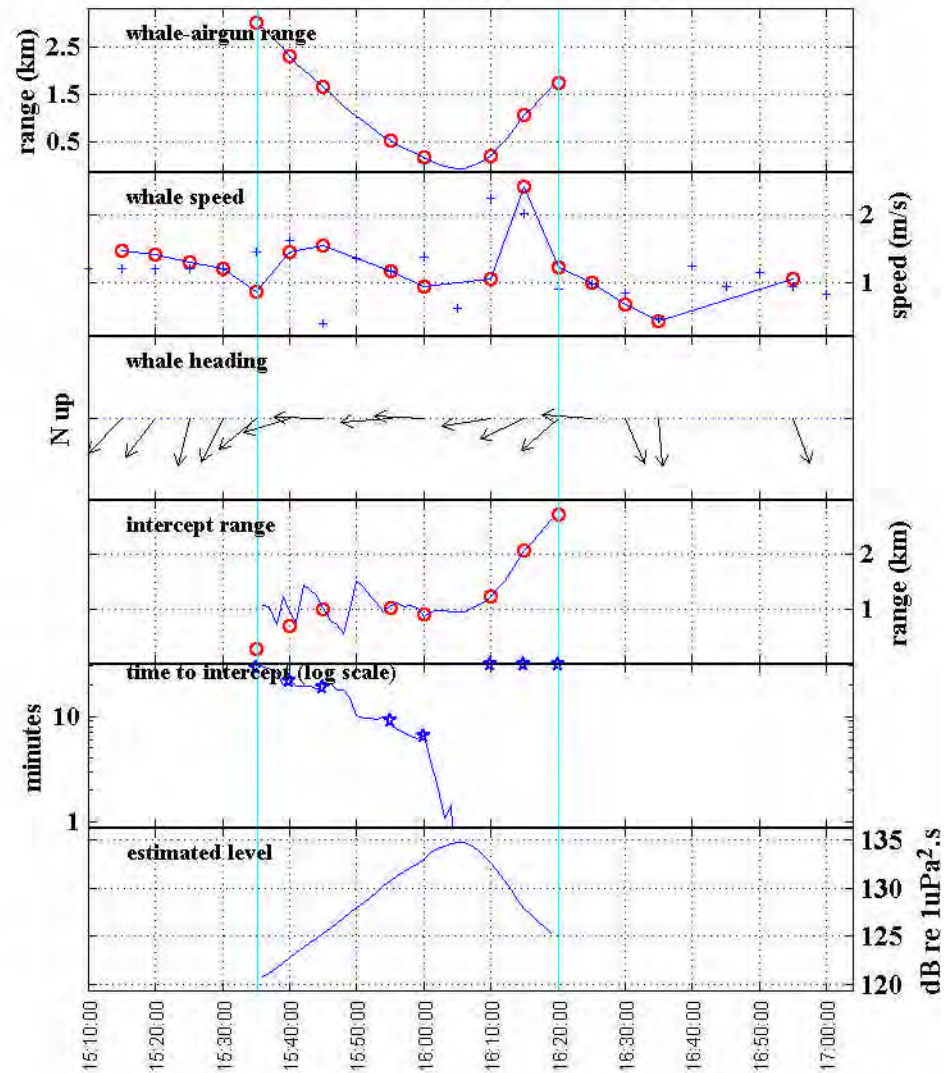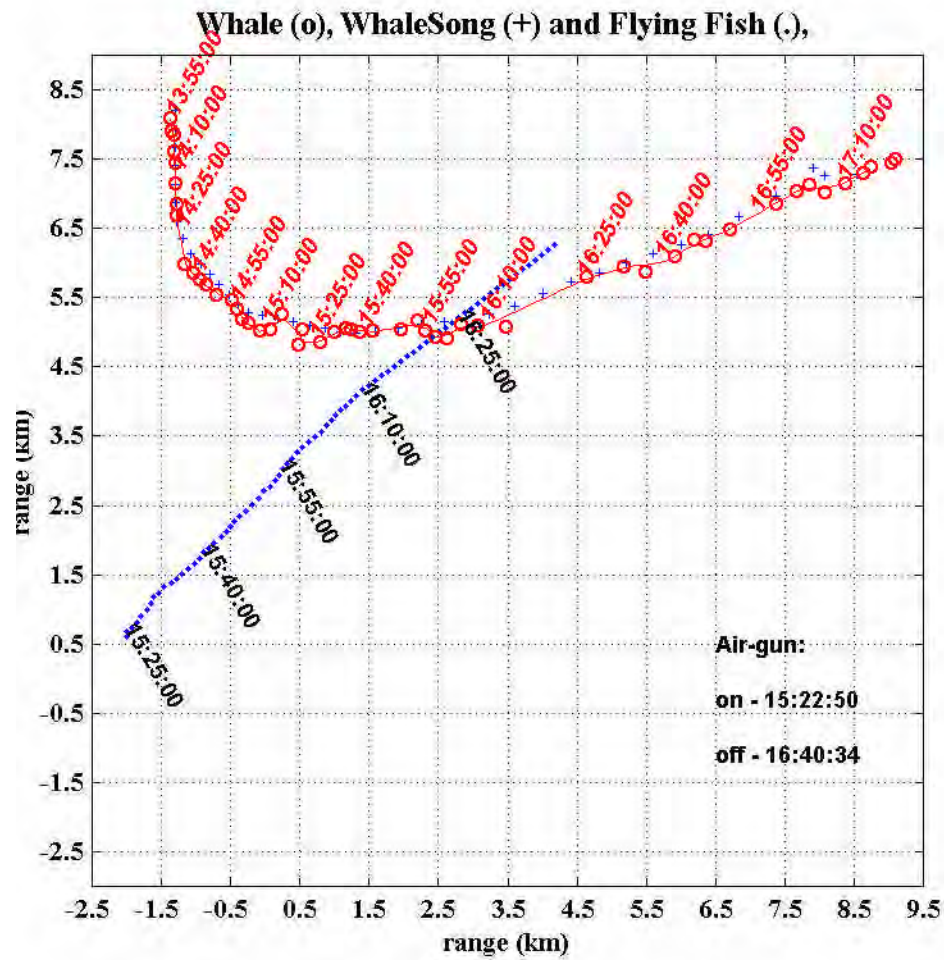
Run 8 16/10/97, 13:54:00-17:17:00

Whale (o), WhaleSong (+) and Flying Fish (.),

Air-gun:
on 1 - 13:21:21-13:32:38
on 2 - 13:53:12-15:11:17

Run 9 17/10/97, 11:56:00-15:59:00

whale-airgun range

whale speed

whale heading

N up

intercept range

time to intercept (log scale)

estimated level

Whale (o), WhaleSong (+) and Flying Fish (.),
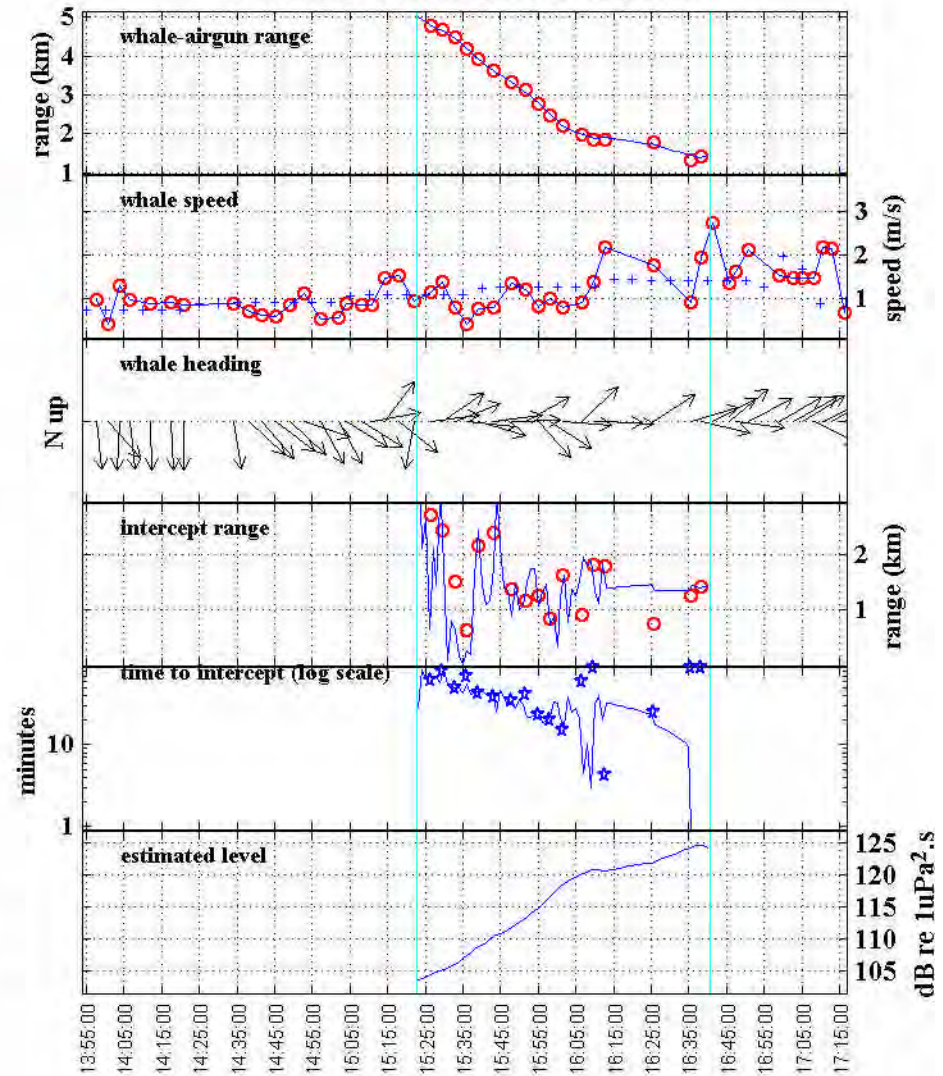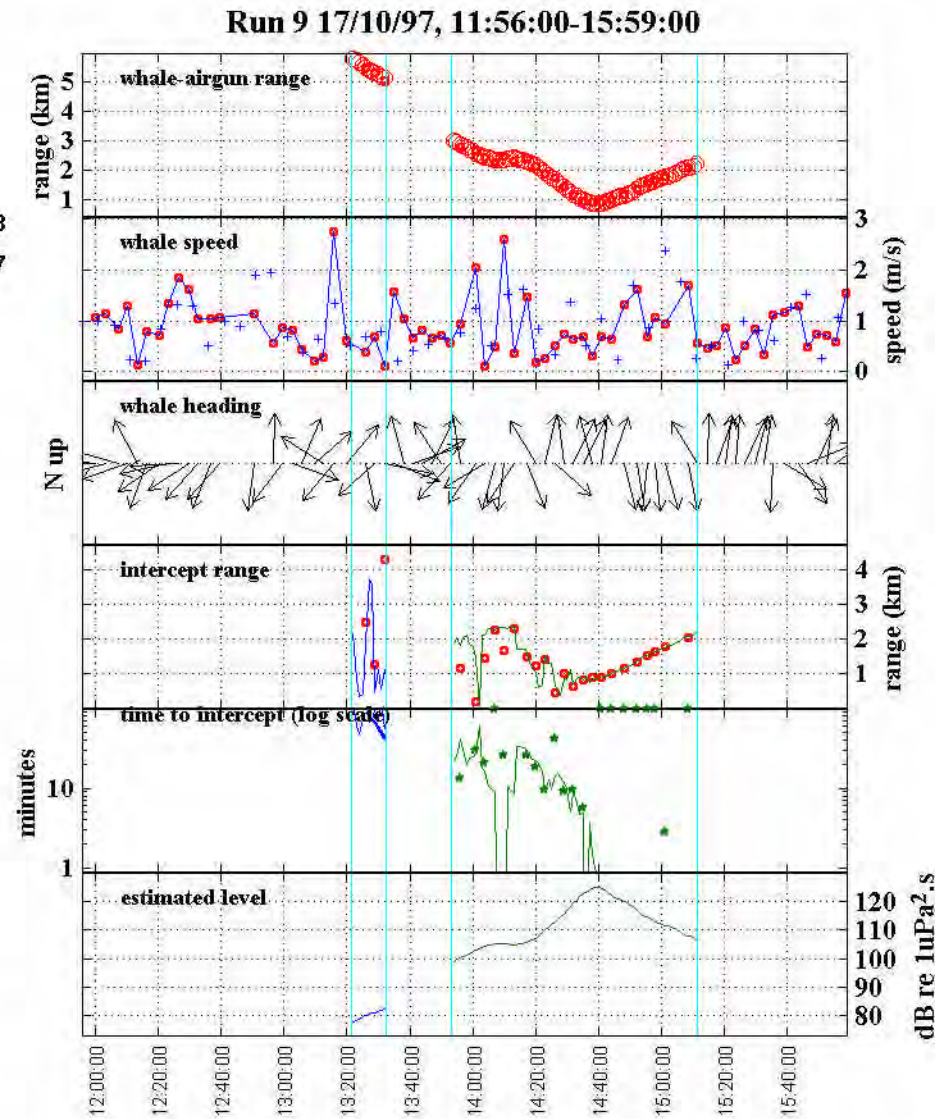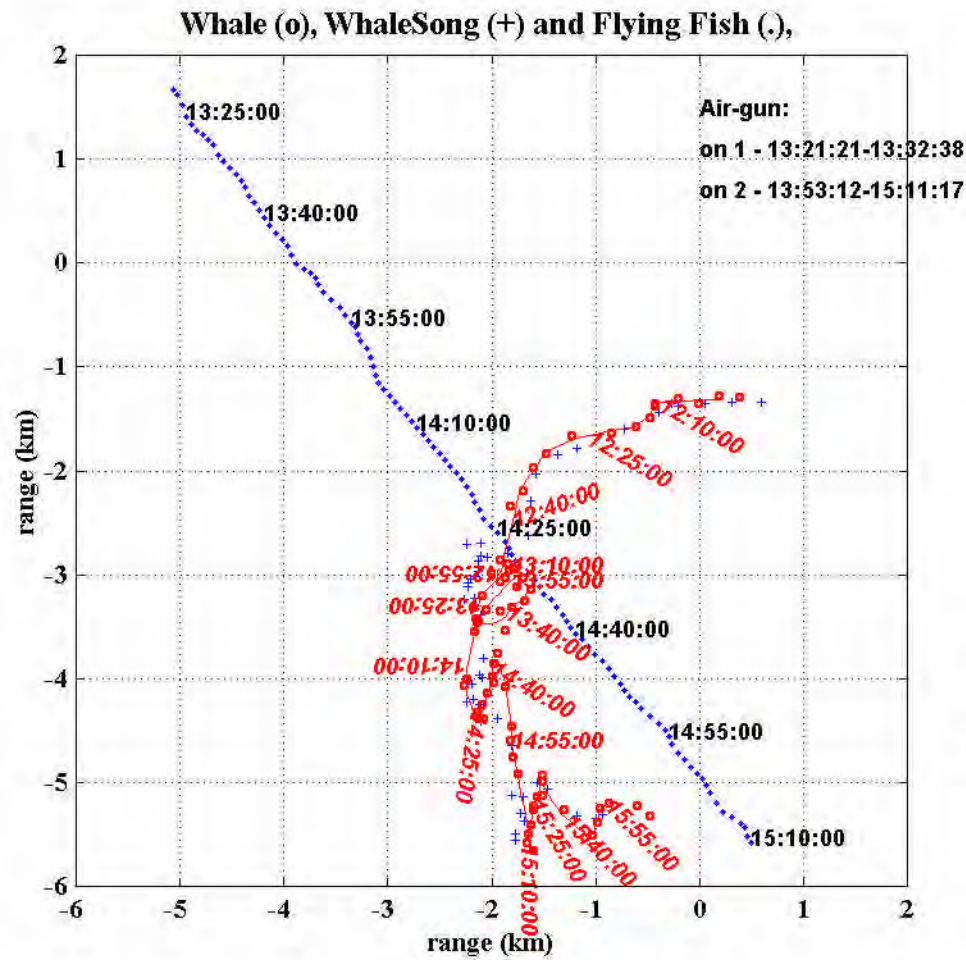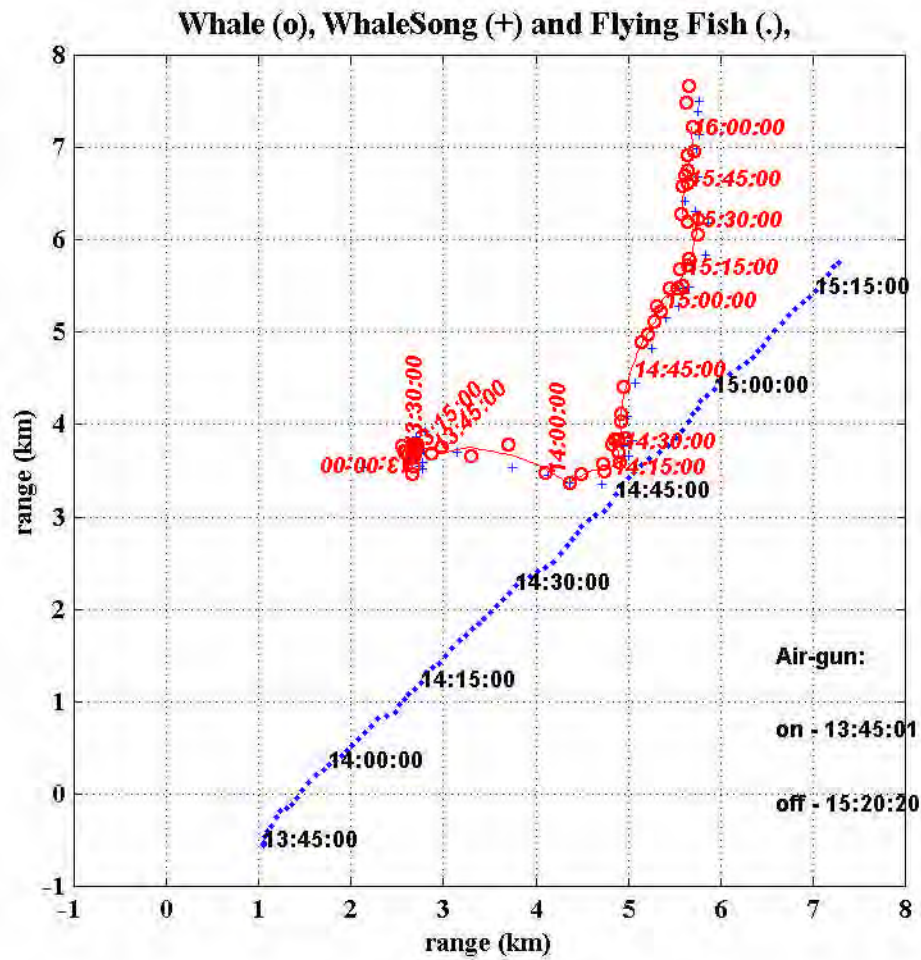
Run 10 18/10/97, 12:46:00-16:09:00

Whale (o), WhaleSong (+) and Flying Fish (.),

Air-gun:

on - 15:39:48

off - 16:30:25
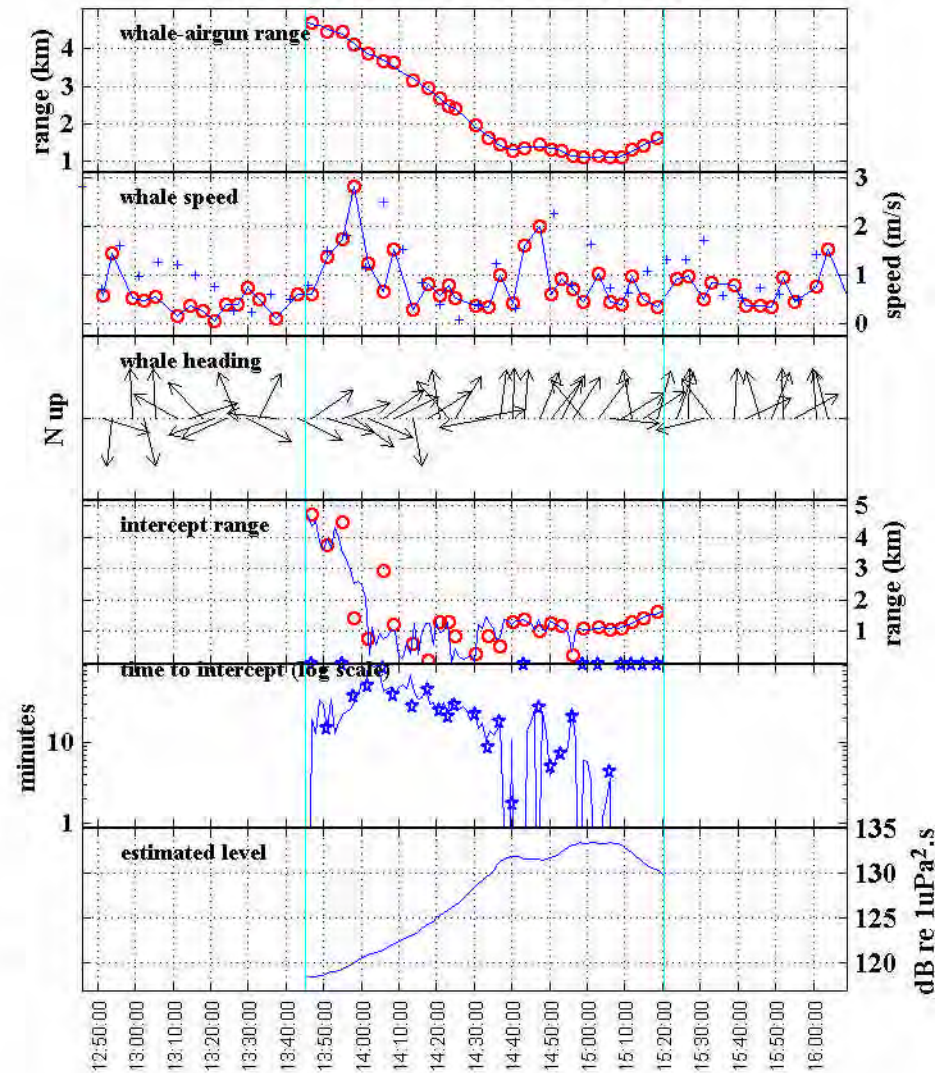
Run 11 19/10/97, 14:03:00-17:14:00

Whale (o), WhaleSong (+) and Flying Fish (.),

Air-gun:

on - 10:12:47

off - 11:10:24

Run 12 20/10/97, 09:19:00-11:59:00

whale-airgun range

whale speed

whale heading

intercept range

time to intercept (log scale)

estimated level

Whale (o), WhaleSong (+) and Flying Fish (.),

Air-gun:

on - 14:12:20

off - 14:43:00
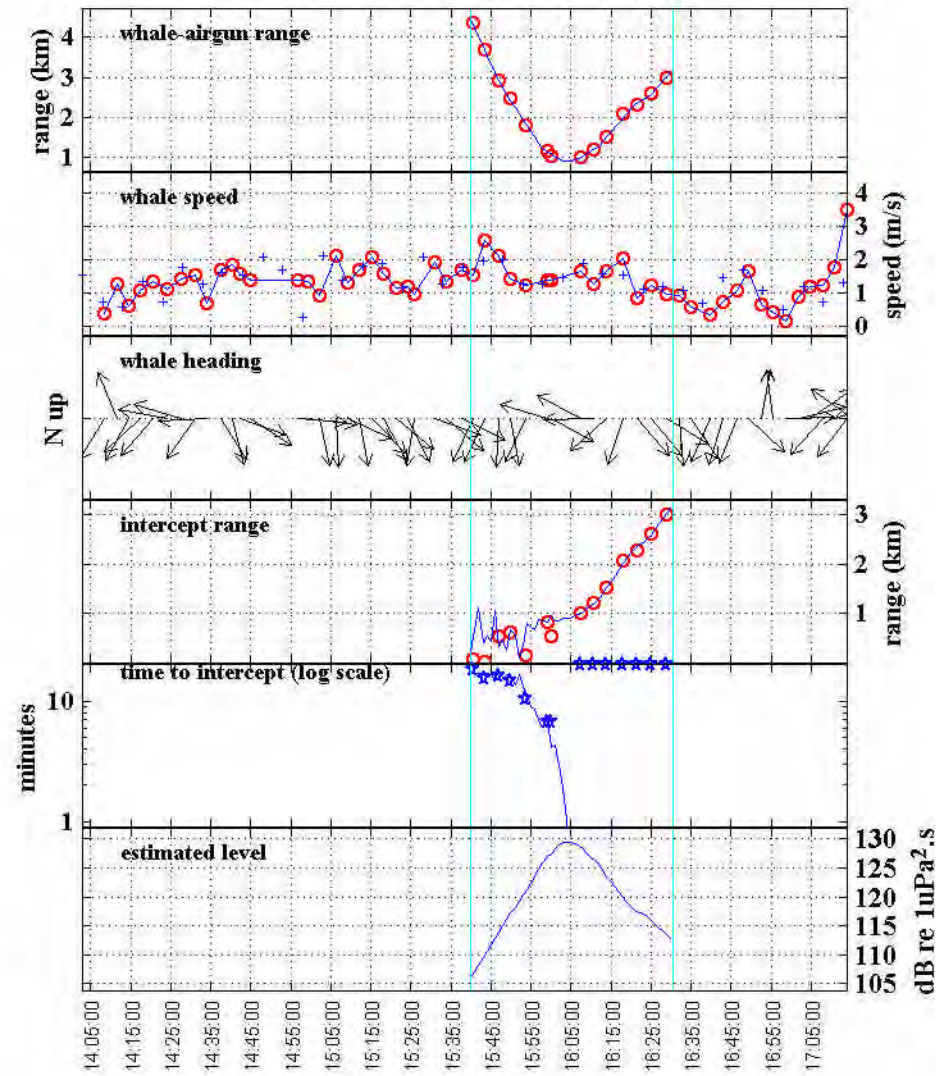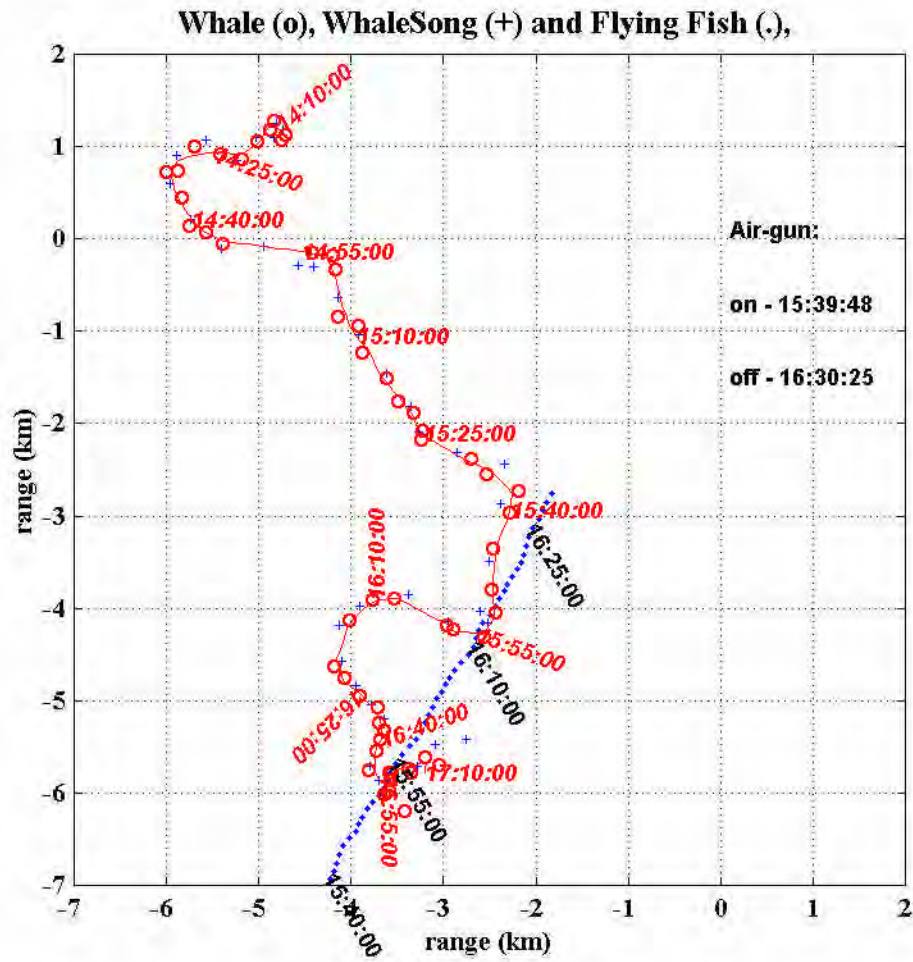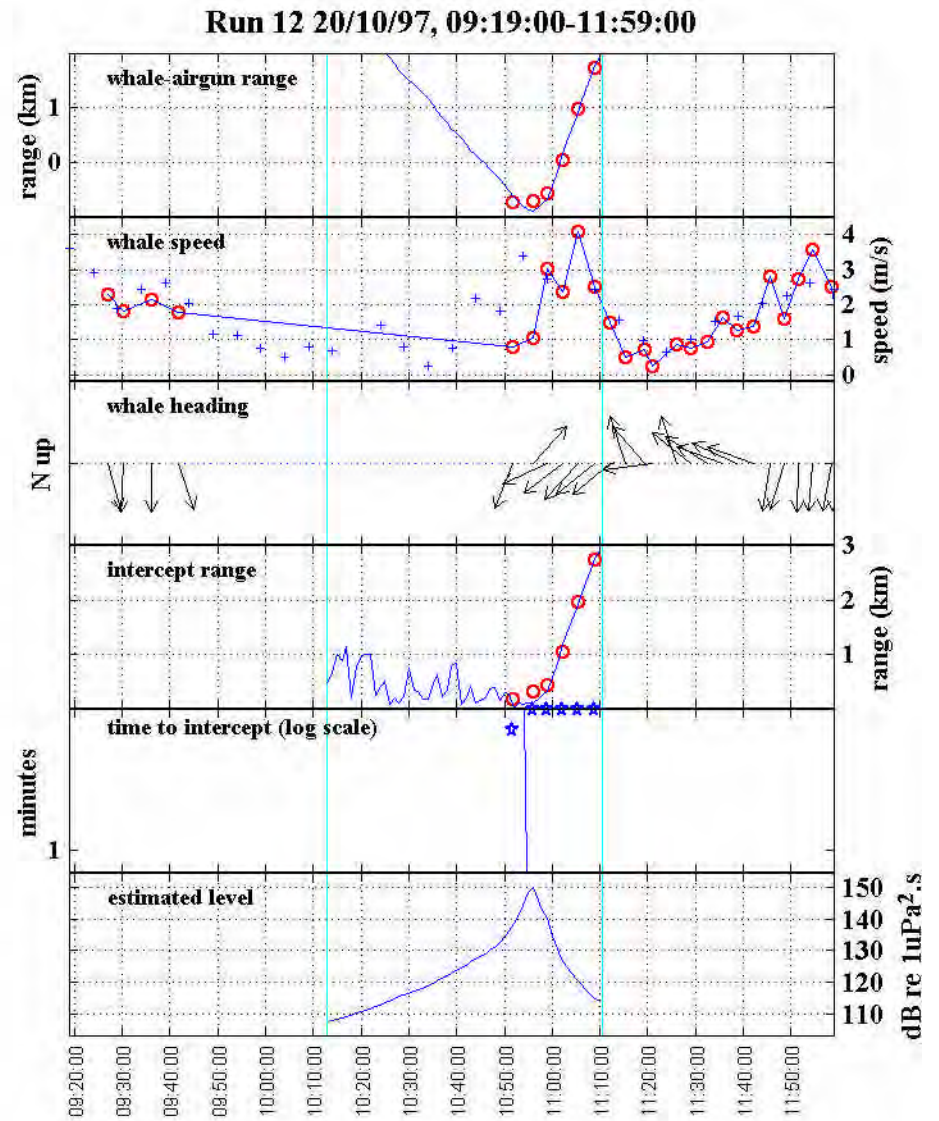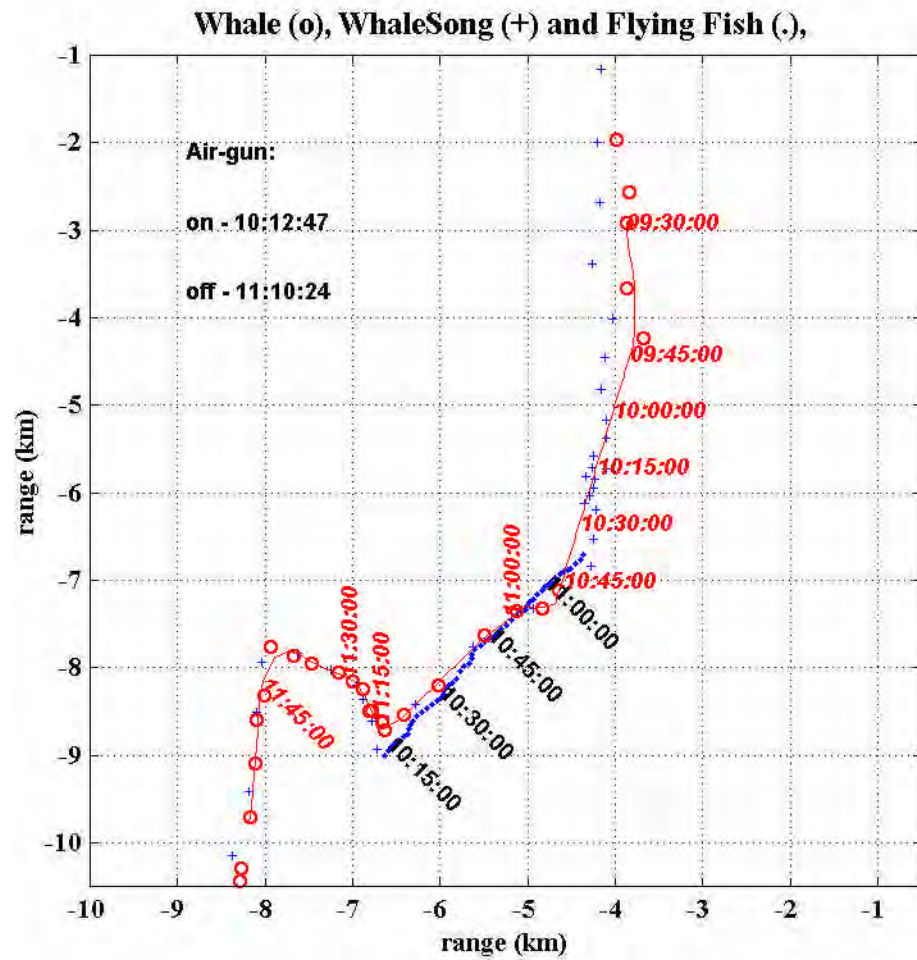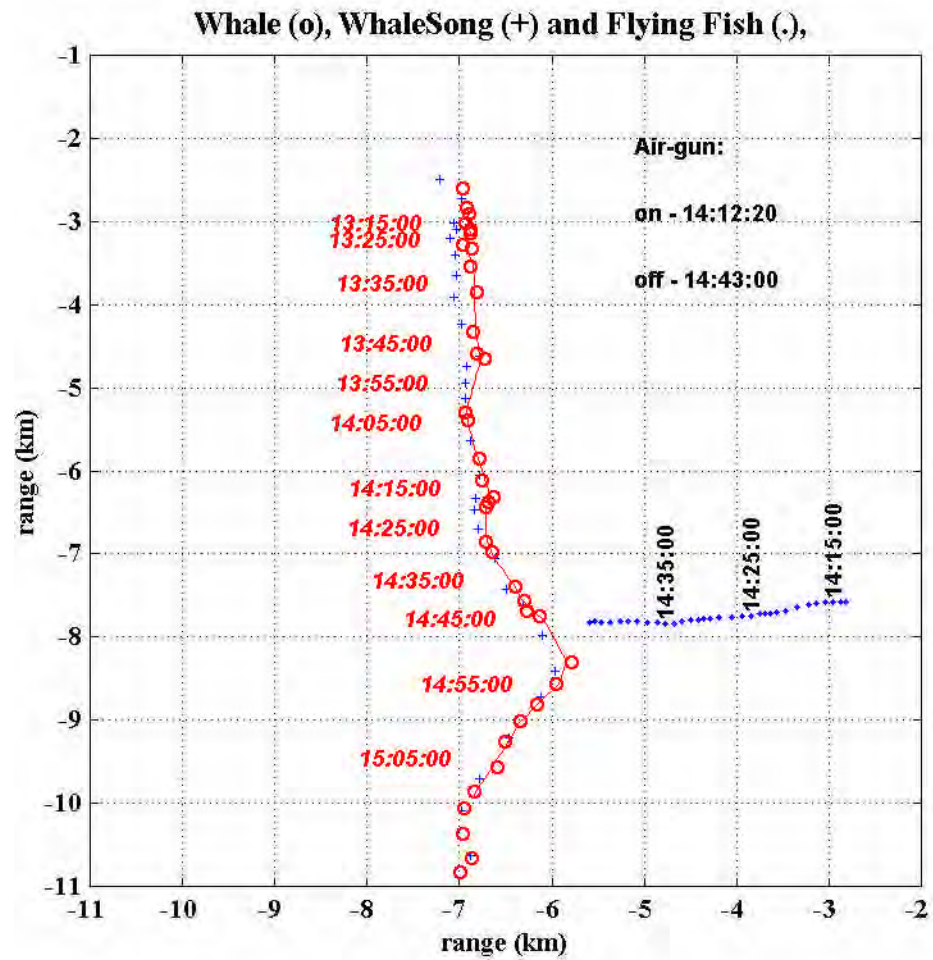
Run 13 20/10/97, 13:04:00-15:19:00

111

Whale (o), WhaleSong (+) and Flying Fish (.),

15:05:00
14:50:00
14:35:00
14:20:00
14:05:00
13:50:00
13:35:00
13:20:00
13:05:00
12:50:00
12:35:00
12:20:00
12:05:00

14:20:00
14:05:00
13:50:00
13:35:00

Air-gun:

on - 13:26:10

off - 14:34:17

Run 14 21/10/97, 12:01:00-15:29:00

whale-airgun range

whale speed

whale heading

N up

intercept range

time to intercept (log scale)

minutes

estimated level

112

Whale (o), WhaleSong (+) and Flying Fish (.),

Run 15 22/10/97, 09:25:00-12:34:00

Whale (o), WhaleSong (+) and Flying Fish (.),

Air-gun:

on - 11:42:15

off - 12:40:01

Run 16 23/10/97, 10:30:00-13:29:00

whale-airgun range

whale speed

whale heading

intercept range

time to intercept (log scale)

estimated level

114
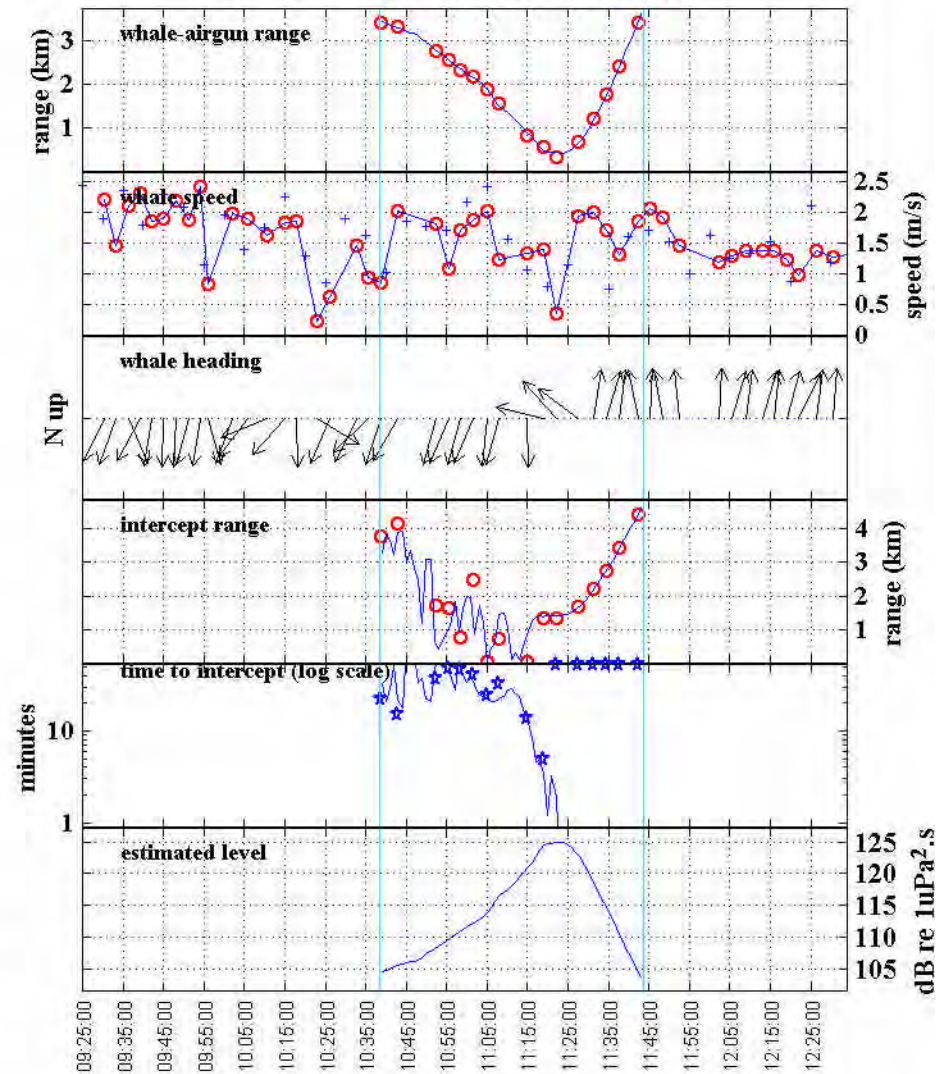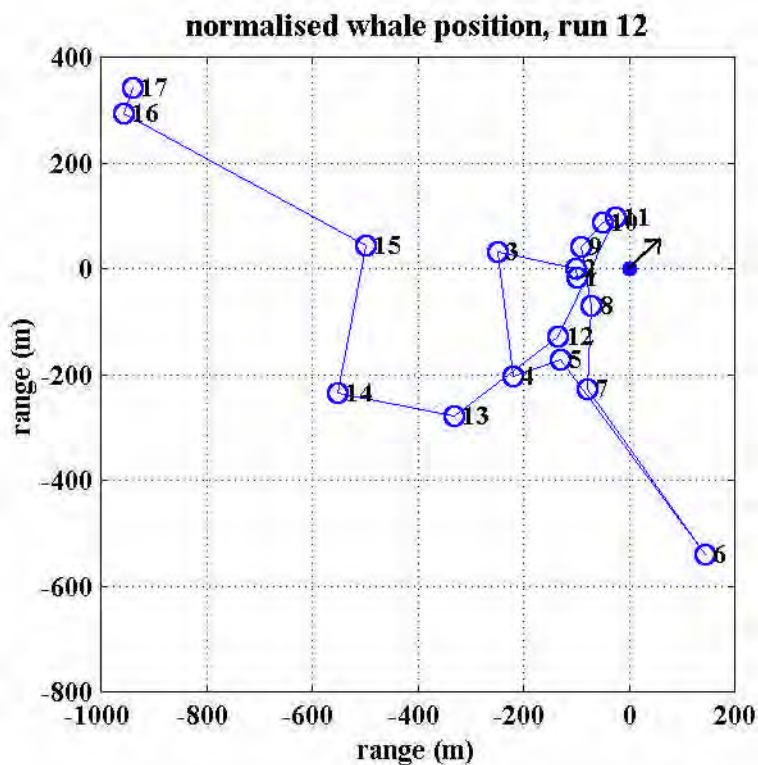
Figure 50: Track of whale pod which approached the air-gun vessel during trial 9, normalised to the vessels position. The vessels position is given by the filled circle with the direction of travel shown
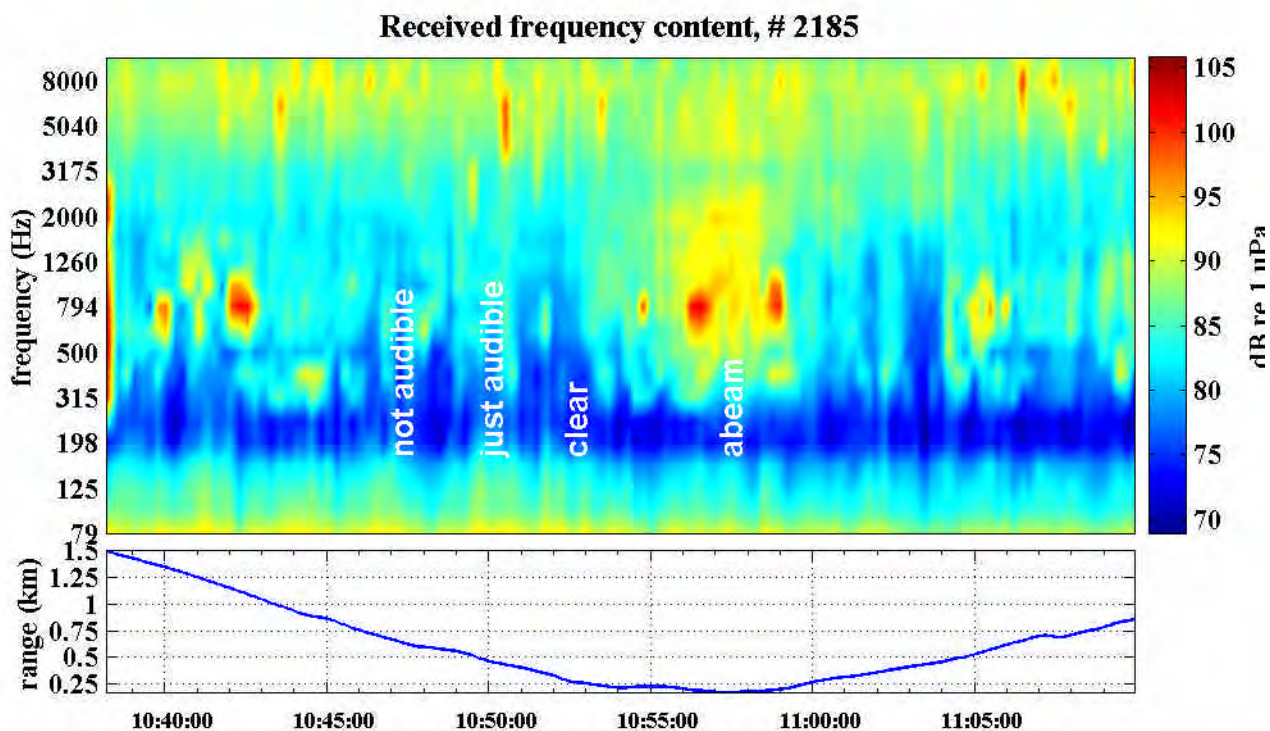
Figure 51: Frequency content with time and range, for the approaching passing and departing air-gun vessel, *Flying Fish*, as measured between air-gun shots during trial 6, 1996 over the reflective bottom type (best sound propagation). Some whale calling is evident over 250-1000 Hz and shrimp noise can be seen above 2500 Hz. Presented as 1/3 octave levels in units dB re 1 uPa. Points at which the vessel became audible on the approach leg are highlighted.
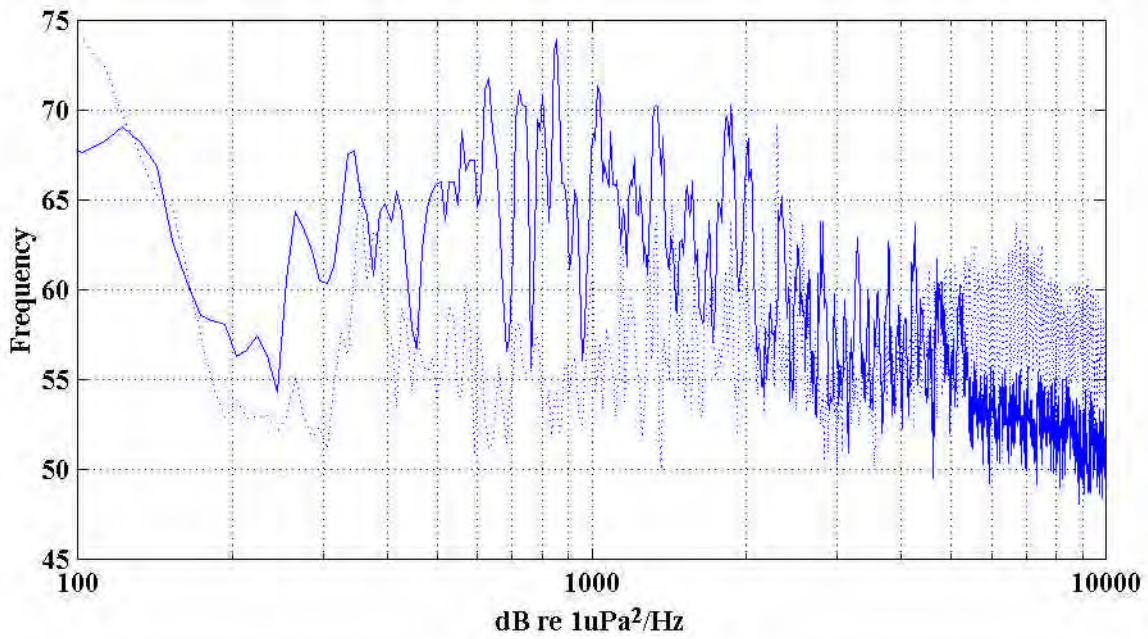
Figure 52: Spectral content of background sea noise (dotted curve) taken during run 2185 (as for Figure 51) with the *Flying Fish* not audible and at 1800 m range and spectral content of Flying Fish at point of closest approach (170 m abeam). Whale calling (20-1000 Hz), flow noise (< 200 Hz) and snapping shrimp (> 2 kHz) are also present in each curve. Spectra taken with 10.17 Hz bandwidth, Hanning window and 10 averages from midwater hydrophone.

2.3 Sea turtle response to nearby air-gun exposure (R.D. McCauley, R.I.T. Prince, J. Fewtrell)

Two trials were conducted at the Jervoise Bay site (Figure 3 for site, Table 4 for trial details) with the same set of a loggerhead and green turtle. These trials involved two, one day trials. The first trial (6, 18/08/97) used three sets of approach - departures with the single Bolt 600B air-gun, the second trial (7, 20/08/97) two sets of approach departures. The times of acclimation, trial observation, air-gun exposures and the feeding and cage cleaning regimes are given in Table 22. Trial numbering is as per Table 4.

Date	Time	Air-gun CA (m) / level (dB re 1 μPa^2.s) / time	Note
05/08/97	11:30		turtles placed into cage
06-17/08/97			turtles fed daily & cage cleaned, turtles usually in bottom portion net, green often swam in response to diver
18/08/97	09:55		**trial 6** observation begins
	11:23-12:28	~ 10 / 177 / 11:45:33	single approach depart of air-gun; 10 s cycle
	12:28-13:21		observation period
	13:21-13:51	~ 10 / 174 / 13:40:14	single approach departure of air-gun; 10 s cycle
	13:51-14:18		observation period
	14:18-14:47	~ 5 / 180 / 14:37:55	single approach departure of air-gun 10 s cycle
	14:47-15:15		observation period
19/08/97	11:42-14:07		observations from dinghy
20/08/97	10:23		**trial 7** observation begins
	11:59-12:31	~ 10 / 174 / 12:17:40	single approach depart of air-gun; 10 s cycle
	12:31-13:36		observation period
	13:36-14:05	~ 10 / 176 / 13:55:08	single approach depart of air-gun; 10 s cycle
	14:05-14:41		observation period
22/08/97			turtles recovered and returned to aquarium

Table 22: Details of dates and times of turtle acclimation and trials and air-gun exposures (CA = pontoon closest approach, ranges are given to the outside edge of the centre of the E cage side, note that the pontoon closest approach may not coincide with the closest air-gun shot, given the 10 s fire rate).

The turtles were normally housed at a commercial aquarium facility in the northern Perth suburbs. Each turtle was a rehabilitated animal, which had been washed ashore during or after a storm, recovered by the Western Australian Conservation and Land Management Authority and maintained in the commercial aquarium. The turtles were returned to the aquarium after the trial, where they still reside.

The turtles were: a 12.5 kg green (*Chelonia mydas*) with curved carapace length 475 mm and width 450 mm; and a 38.5 kg loggerhead (*Caretta caretta*) with curved carapace length 670 mm and width 605 mm. Turtles were placed in the cage and recovered using a cradle and lifting davit from a dinghy.

Over the period of acclimation and the two trials, the water temperature in Jervoise Bay was 16° C (as determined by diver held thermometers). This is at the low end of the temperature range for these turtles. Thus the animals would have physiologically been in a low metabolic state.

The detailed conduct of trials was described in the methods, section 1.3. The cameras for trial 6 were placed at the E corners of the cage at 2.5 - 3 m depth. The black and white camera (termed camera 1) was placed at the S cage end, the colour camera at the northern end (camera 2). During trial 7 the colour camera was shifted to the NW cage corner in an attempt to reduce backscatter from particulate matter. The cameras were set to view the bottom section of the cage. The fields of view of each camera did not overlap thus camera behavioural observations results can be considered as separate samples. The cage used was 10 x 6 x 3 m dimensions (length, width, depth respectively) and aligned roughly NW-SE (see

Figure 3). Heavy ply, 40 mm mesh, trawl net lagged the cage with a 10 mm light ply liner fitted inside. The air-gun was deployed from a 6 x 2 m pontoon which was towed by a 4.3 m dinghy lashed on the port quarter. The air-gun used a 10 s fire rate and was supplied by three GM nitrogen bottles. During trial 7 the pontoon's GPS position was logged to computer. A GEC-Marconi SH101-X hydrophone was set at 3 m depth in the cage centre to record air-gun signals. All cameras and hydrophones cabled ashore where an observer monitored the gear and video images. The pontoon and shore observer were in UHF radio contact throughout each trial.

At the time of trials the observers perception was noteworthy for the apparent low response by each turtle to the close approach of the air-gun. Levels of the air-gun were analysed as per the methods and section 2.1.1. The air-gun tape for the third approach departure of trial 6 stopped midway through the trial. The levels used in the behavioural analysis for this missing portion were estimated from similar runs using the known points of closest approach.

The video tapes were scored for behavioural types and corresponding times, as described in the methods and Appendix 1. The second tape of camera 2, trial 6, jammed in its VCR during the trial and would not play on analysis. Behavioural types fell into several categories listed below. These behaviours and the codes used on plots, were:
1. vertical position in the water column (lower [lo] ; mid-water [md]; top [tp]);
2. vertical swimming movements (moving bottom-middle [bm]; bottom-top [bt]; middle-bottom [mb]; middle-top [mt]; top-middle [tm]; top-bottom [tb]);
3. speed of swimming (idle [id]; slow [ss]; fast [fs], very fast [vf]);)
4. horizontal swimming movements (right-left [rl]; left-right [lr]; circling [cc]; change-of-direction [cd]);
5. specific behaviours (green nipping loggerhead [np]; turtles approach each other [ap]; green riding on loggerheads back [at]; flipper movement [fm]; head flick [hf]; front flippers facing backwards [bw]; front flippers facing forwards and against head [fw]; front flippers sideways [sw]; and turtles next to each other [nx]).

Other codes scored included housekeeping (eg. time calibrations); air-gun operations; boat noise; diver presence; and for the appropriate turtle, a code for out-of-view.

Behaviours were scored separately for each turtle. Thus the data could be split between turtles, cameras and trials. Trial 6 involved four observation periods and three periods of air-gun operations, trial 7 involved three observation and two air-gun operation periods. All analysis has been carried out independently for turtles, cameras and trials, and summed as stated.

The general behaviour of turtles during the pre trial acclimation period was that they were sluggish, spending long periods resting on the bottom of the cage often alongside each other, and tending to locate themselves more towards the middle-S cage end. The northern cage end was partly shaded by the net, thus the tendency to locate themselves towards the middle-S portion of the cage. The green turtle often reacted to the diver in the tank by swimming about, with the loggerhead swimming less often.

A graphical representation of the behavioural analysis through time from camera 1 (black and white camera, S cage end) for the green and loggerhead turtle during trial 6, along with the received air-gun levels, is shown on Figure 53.

Following page:

Figure 53: Movement patterns, specific behaviours, time turtles in-view and air-gun exposure (equivalent energy) for lumped turtle data from camera 1, trial 6 (black and white camera, S cage end). The time limits of camera operations are shown by the dashed lines (tapes were changed) and of air-gun operations by the dotted lines. The air-gun recording tape deck stopped during the third approach departure. For behavioural representation, from top down; 1) dots represent turtle vertical location in cage; 2) large head arrows show vertical movements; 3) small head arrows, small shaft shows slow swimming, two headed arrow fast swimming, dots idle; 4) left slanted arrows show swimming right to left, right slanted left to right, circles represents animal swimming in circles, cross represents change-of-direction; 5) specific behaviours of square - turtles next to each other, diamond - turtles approach, triangle - flipper movement, very small headed arrow - left slanted arrow was flippers facing forward over head, right slanted arrow was flippers facing backward

Trial 6 camera 1 green and loggerhead turtle
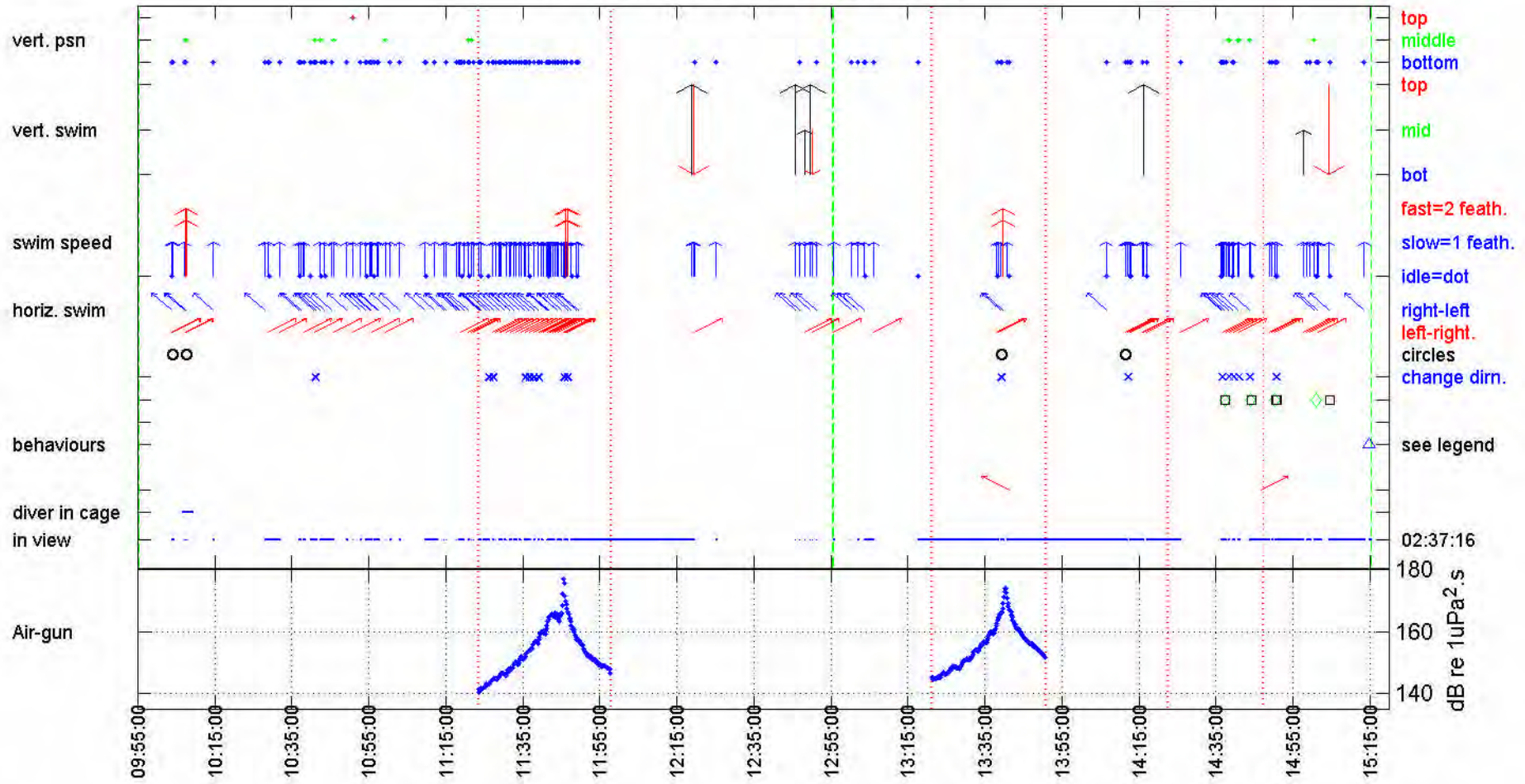
The time each animal was in view was calculated from the sum of time segments beginning with a behavioural or movement note and ending at the next out-of-view score for the appropriate turtle. In the initial analysis times-in-view were calculated for air-gun-on and air-gun-off periods for the appropriate turtle. Where in-view/out-of view scores spanned an air-gun-on/air-gun-off boundary, an appropriate in-view/out of view score was carried forward to the next boundary limit.

Considering all trial data (two turtles, two cameras, two trials), several behavioural types were associated almost entirely with periods of air-gun operations. Indicative behaviours were periods of fast swimming and changes of direction during swimming (Figure 53 double headed arrows and crosses respectively). Fast swimming was also recorded outside of air-gun operation periods in trial 6, but this correlated with a diver in the tank adjusting the camera positions and was believed a response to the diver presence.

The ratio of the *sum of recorded counts* divided by the *minutes-animals-in-view* for specified movement or behavioural types for periods of air-gun-on and air-gun off periods, using all data (two cameras, turtles, trials) is shown on Figure 54.
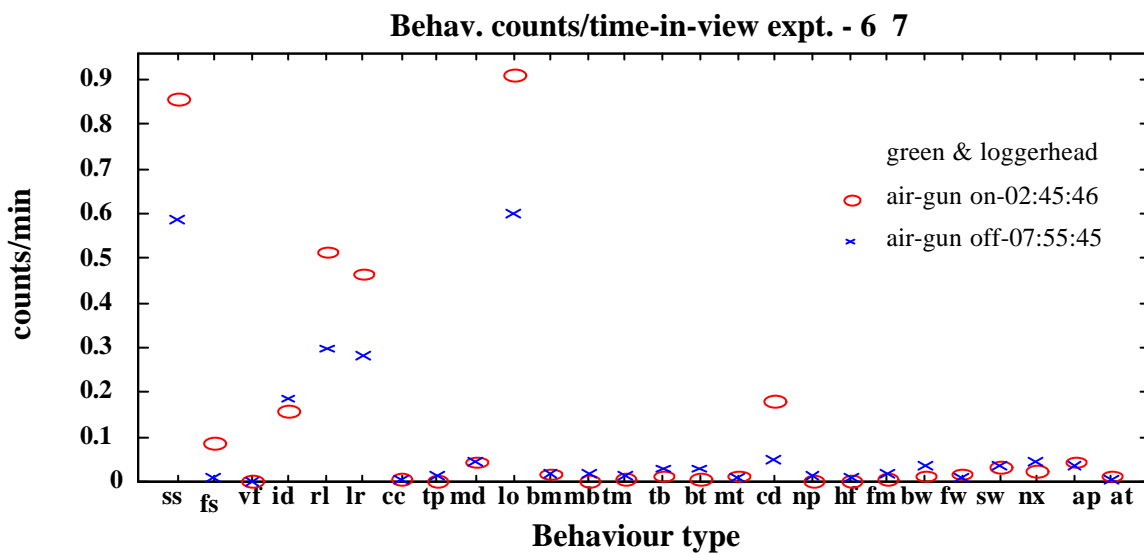
Figure 54: Ratios of number of times appropriate movement pattern or behaviour recorded per time animal in view, for air-gun on and air gun off periods (combined data for both turtles, cameras and trials). The cumulative times (hh:mm:ss) the animals were in view are also given (note that times have been calculated for each turtle separately then summed).

The combined data suggests the turtles spent more time swimming during air-gun operation periods since proportionately more swimming scores were recorded (slow -ss- and fast -fs- swimming, swim direction) and that this swimming was more erratic (proportionately more changes of direction -cd). The values given on Figure 54 are scores per minutes in view. To remove any possible bias due to the detail of scoring when comparing air-gun-on versus air-gun-off periods (the air-gun could be heard on the video tape during behavioural scoring), the data was recalculated to give the ratio of *sum of individual scores* divided by *the total number of all movement or behavioural scores*, for the appropriate period. This is shown on Figure 55. Comparing air-gun on and air-gun off periods this analysis showed: similar slow swimming scores between periods; greater fast swimming in air-gun on periods; slightly greater periods of no swimming in air-gun off periods; more movement scores in air-gun on-periods (swim direction); and more changes of direction in the air-gun on periods. This suggested that the ratio of swimming/not swimming scores may not have differed greatly between air-gun on versus air-gun off periods, but that again the instances of fast swimming and more erratic movements predominantly occurred during the air-gun on periods.

As opposed to the number of scores, the times spent swimming and idle were then calculated for each turtle, period (observation, air-gun-on, observation, air-gun-on, etc), camera and trial. This measurement was considered not biased by the presence of the audible air-gun signal during video scoring since the turtle was unambiguously in one of two states, swimming or not swimming (idle). The time swimming was calculated by firstly combining all behaviours indicative of swimming into a single variable, then for each period determining for each time-in-view-segment within the period the swimming/idle codes. The time between alternating codes (swimming/not swimming) was then calculated within the time-in view-segment and these summed for the period. For time-in-view segments which spanned the period boundaries (air-gun-on or observation) and for which no swimming code was assigned at the segment start, the initial code was set as idle (a conservative setting). These results were summed for the two cameras and air-gun-on and air-gun off periods, and are presented for each turtle and trial, on Figure 56.
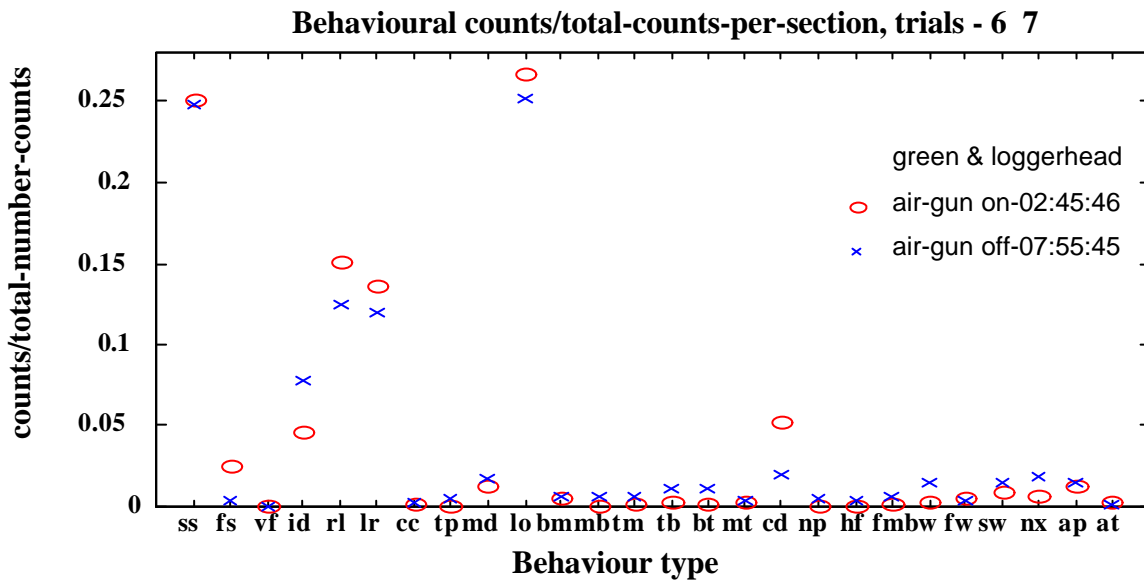
Figure 55: Ratio of sum of behavioural counts per total counts per air-gun-on or air-gun-off, for all data.

This analysis revealed only slight variations between the proportion of time spent swimming during the air-gun-on periods as compared to air-gun-off periods.

The period boundaries for the above analysis were all calculated using the beginning and end of observations (start and finish time of video tapes) and the time of first and last air-gun shots for each period of consecutive air-gun operations. That is the air-gun on period encompassed all of the time the air-gun was operating irrespective of the level received at the turtle. To investigate the effect of increasing air-gun level on the swimming time versus idle time comparisons, the analysis was carried out using sliding air-gun on/off time boundaries. The boundaries of air-gun-on periods were set at the times of a specified air-gun level on the approach and departure leg of each pass. This decreased the times of air-gun operations to only those above the specified level. The time boundaries were defined by the 150, 155, 160 and 165 dB re 1 μPa^2.s (equivalent energy) air-gun levels for each approach-departure. To display the results the ratio of time spent swimming during the control period (no air-gun operations) was subtracted from the similar ratio calculated for the period where the air-gun signal was above the specified threshold. That is the difference ratio (d_t) was calculated as:

Equation 12 $$d_t = \frac{t_{sp}}{t_{vp}} - \frac{t_{sc}}{t_{vc}}$$

where

t_{sp} = time swimming for the period > threshold

t_{vp} = time in view for the period > threshold

t_{sc} = time swimming for the control period (no air-gun operations)

t_{vc} = time in view for the control period (no air-gun operations)

The results of this analysis are presented on Figure 57.

Ratios of time turtles swimming / not swimming for air-gun on verus air-gun off trials 6 & 7
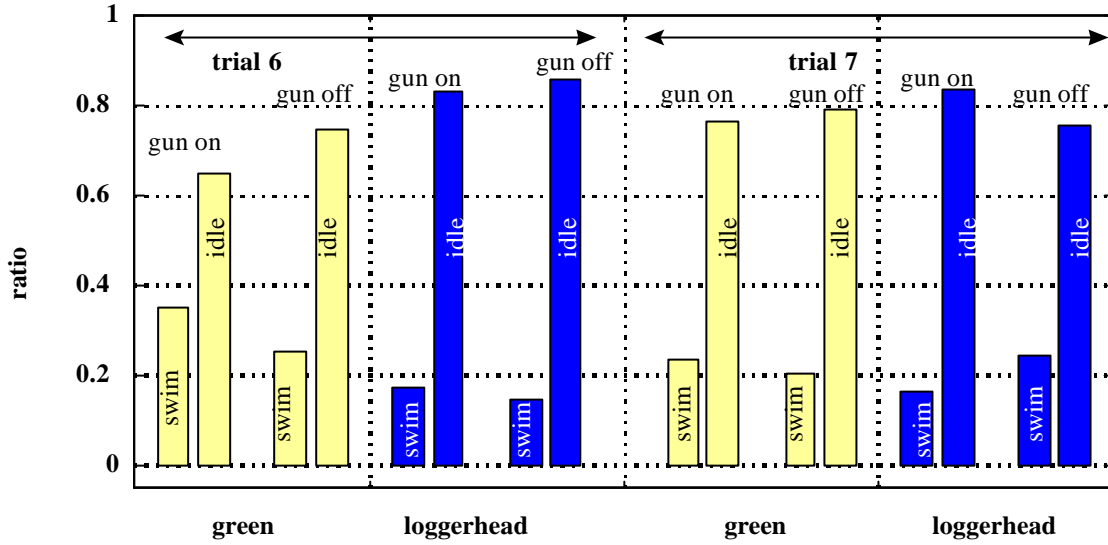
Figure 56: Swimming/idle ratios for each turtle and trial (camera results summed) during air-gun-on and air-gun-off periods.

It can be seen from Figure 57 there is a consistent trend for the green turtle, such that as the air-gun threshold increased above 155 dB re 1 μPa^2.s the turtle spent increasingly more time swimming. The loggerhead showed a similar trend in trial 6 but for the period of received air-gun level > 165 dB re 1 μPa^2.s in trial 7, reverted back to almost no difference between swimming ratios as compared with the control period. This was possibly due to the small time available above this air-gun level for observations and a correlating lack of observations (eg. the turtle out of camera field of view). Using a two tailed t test to compare the mean of the control period *time-swimming-ratio* ($\dfrac{t_{sc}}{t_{vc}}$ with variables as listed for Equation

12, period of no air-gun operations) with the *time-swimming-ratio* ($\dfrac{t_{sp}}{t_{vp}}$ with variables as per Equation

12) for each of the five periods displayed on Figure 57 (defined by times as set using all-air-gun on, > 150, > 155, > 160 and > 165 dB re 1μPa^2.s) for each turtle and each trial (giving four data points compared with four control points for each period), then the mean ratios are statistically different for the grouping of air-gun level > 160 dB re 1μPa^2.s ($0.02 < p < 0.05$, $v=6$). The critical value for the > 165 dB re 1μPa^2.s grouping calculated at $0.10 < p < 0.05$, with the lack of observations of the loggerhead turtle in trial 7 believed to bias the result down. Using the four periods of air-gun noise > 150, > 155, > 160 and > 165 dB re 1μPa^2.s, combining the green and loggerhead data and fitting a linear regression to the *time-*

swimming-ratio, $\dfrac{t_{sp}}{t_{vp}}$ versus air-gun threshold (in 5 dB steps), gave a statistically significant a regression

using the two tailed F distribution ($0.02 < p < 0.05$, F = 7.447 df. =1/1 4, $r^2 = 0.3472$). The correlation coefficient and significance of the regression increased substantially for the green turtle data only ($0.002 < p < 0.005$, F = 25.893 df. =1/6, $r^2 = 0.8119$).
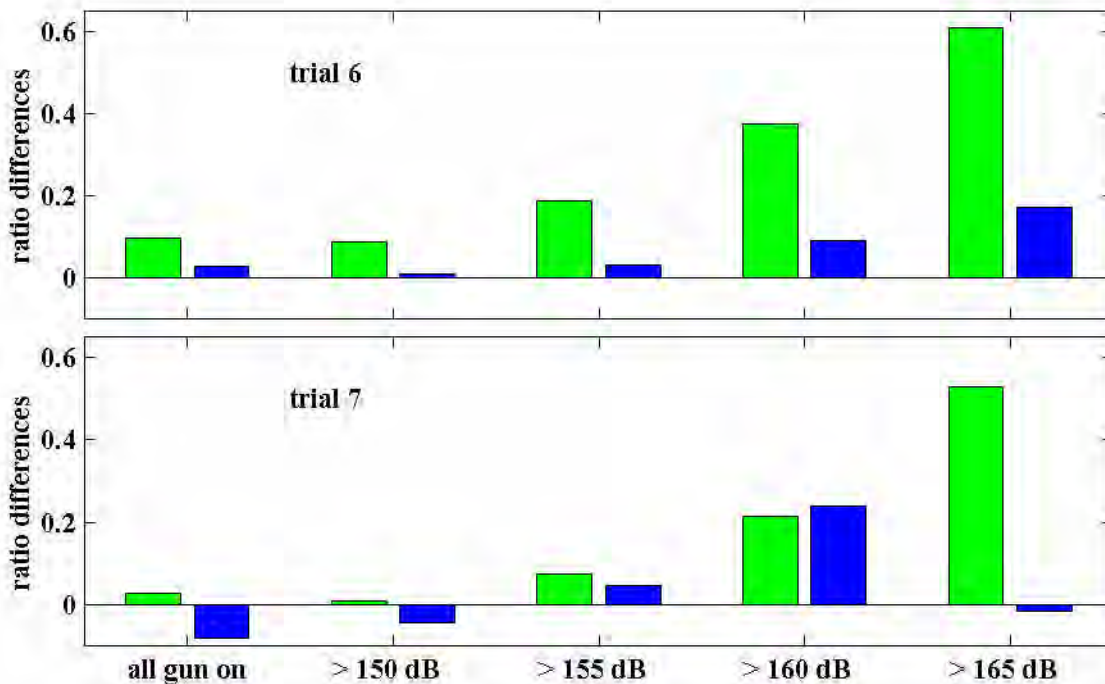
Figure 57: The difference of the *ratio of turtle swimming time for period of air-gun on or above the specified threshold* minus *the ratio of swimming time for air-gun off or below the specified threshold*, for the green (stippled bars) and loggerhead (filled bars) turtles during trials 6 and 7. Positive values imply that for that trial the turtle spent proportionately more time swimming during the time above the specified air-gun level, as compared to the time comprised of observations where the air-gun level was below the specified threshold. Units are dB re 1 $\mu Pa^2.s$

As indicated above the air-gun-on periods appeared to be correlated with what could be constituted as erratic swimming, with what appeared to be proportionately more changes of direction and periods of fast swimming recorded during periods of air-gun operations than during the observation only periods. To check this, for each of the *fast-swimming* and *change-direction* observations, the ratio (b_r) was calculated as:

Equation 13
$$b_r = \frac{b_o}{n_o} \times 100$$

where
b_o = number of incidences of specified behaviour per period
n_o = total number of behavioural scores per period
for the periods of all *air-gun off* and all *air-gun on*. This ratio normalised the specified behavioural count for the total number of counts in that period, thus removing some of any bias in scoring (behavioural scoring was done with the air-gun signal audible, see section 1.3.2). These ratios were then determined for each turtle (summing camera data) and each trial for times of *air-gun-on* and *air-gun-off*. This then gave a matrix of normalised ratios which allowed a simple t test comparison of the mean normalised ratio between air-gun operation periods and control periods. The normalised data for the two behavioural types is given in Table 23.

turtle	air-gun on		air-gun off	
	fast swimming	change direction	fast swimming	change direction
green trial 6	2.88	6.47	0.78	1.57
loggerhead trial 6	1.84	4.15	0.71	2.14
green trial 7	4.44	4.44	0.30	1.21
loggerhead trial 7	0.93	7.48	0.0	1.24

Table 23: Normalised ratios (according to Equation 13) for fast swimming and change direction behaviours.

Using the t statistic and reducing the degrees of freedom to account for the use of ratio data, then each behaviour was significantly greater in the periods of air-gun operations, with the significance at $0.02 < p < 0.05$ for the *fast-swimming* coding, and at $0.01 < p < 0.02$ for the *change-direction* coding.

The mean air-gun levels at which these events occurred was determined, with the distribution of levels shown on Figure 58 (calculated for 4 dB bins). The change-of-direction events were recorded over an air-gun level range of 143-176 dB re 1 μPa^2.s, with a mean at 162 dB re 1 μPa^2.s (conventional mean), while the fast swimming events were recorded over a range of 151-176 dB re 1 μPa^2.s, at a conventional mean of 167 dB re 1 μPa^2.s.

Thus the turtle trials, carried out at a water temperature of 16° C, showed two types of responses:

- above an air-gun level of approximately 155 dB re 1 μPa^2.s the turtles began to noticeably increase their swimming activity;
- and above approximately 164 dB re 1 μPa^2.s they began to show more erratic swimming patterns, possibly indicative of them being in an agitated state.
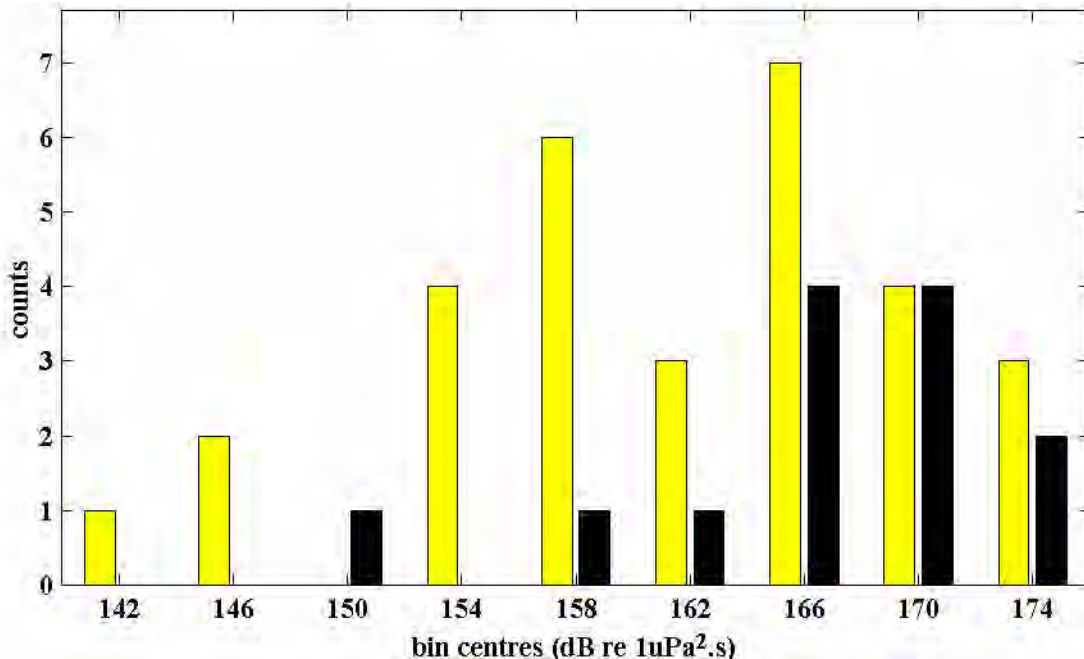
Figure 58: Distribution of received air-gun levels at which change-of-direction (light coloured bars) and fast-swimming (dark bars) events were recorded, from all data (two cameras, two trials, two turtles, 4 dB bins).

2.4 *Fish response to nearby air-gun exposure (R.D. McCauley, J. Fewtrell, A. Adhitya)*

Ten trials with caged fish were carried out to gauge their behavioural response and any physiological and pathological effects to nearby air-gun exposure. Details of the methods used are given in section 1.3. Only general details of methods are presented below. A full listing of the species used in trials, exposure regimes and result types are listed in the methods, Table 4. Eight trials were carried out in Jervoise Bay and two in Exmouth Gulf. Water temperatures for the Jervoise Bay trials ranged from 16-20° C, and in Exmouth Gulf 21-23° C. The Exmouth Gulf cage was moored in a persistent tidal stream with maximum currents to 1 knot, thus fish held in the cage were forced to swim or seek refuge in crevices in the net. The Jervoise Bay site was completely sheltered.

Trials were carried out primarily to ascertain the air-gun exposure required to produce significant behavioural changes in selected fish species. The intention was that this level could then be input into an exposure model, as per section 2.1.5, to give a predictive aid for interpreting the ecological scale of seismic surveys. An argument as to the respective advantages and disadvantages of carrying out caged trials versus field observations of wild species is presented in the discussion.

2.4.1 Caged trial seismic source

The single Bolt 600B air-gun with 20 cui chamber operated at 10 MPa gun pressure and a ten second fire rate was used as the source for all fish trials. Although commercial seismic survey arrays are much larger, it was intended that the 20 cui air-gun would achieve the same effect as the larger array's, but on a smaller geographical scale. Figure 4 (methods) displayed the waveform and frequency spectra of matched air-gun shots from a 2678 cui array at 1.5 km range with that of the 20 cui Bolt air-gun, as measured at Jervoise Bay at 115 m range. The signals have similar waveforms and frequency spectra suggesting that this 'scaling' assumption is valid.

To provide a comparison of a commercial array with the Bolt air-gun as used at Jervoise Bay an air-gun signal matching program was developed. This used a reference signal (Jervoise Bay air-gun shot) and a table of signals to be searched for to find a match (lookup signals). A matrix was built, comprising the difference of the normalised reference and lookup signals (normalised to the lookup signal range), for the values of equivalent energy, mean-squared-pressure, peak-pressure and signal length. A weighting matrix was applied, the values summed for each lookup signal, and the minimum value found so as to give the matched signal.

Using a weighting biased towards equivalent energy, signals from the Bolt air-gun as used in Jervoise Bay were compared with levels received at two water depths for a 2678 cui array off Exmouth (run 2090 Figure 13). The matched array range for signals from the Bolt air-gun as received in Jervoise Bay are shown on Figure 59. Thus at 200 m in Jervoise Bay the single air-gun was equivalent to the 2678 cui array at 1.5-2 km, this depending on the receiver depth (and the weighting used to match signals).

It could be argued that the frequency content of the single Bolt air-gun during trials would not match that of a 'large array' at some ranges, even though the frequency content displayed in Figure 4 for the two selected signals were similar. It should be pointed out that there is no such thing as a 'standard' air-gun array. Each seismic survey has a sound source designed for the purpose required. Each will have its own peculiarities with respect to frequency content and frequency patterns with aspect and elevation. To compound this the frequency content received at some range from the source will be a function of the array configuration and

the sound propagation characteristics of the region (ie. Figure 18 for large frequency differences from same source), which may change with range. Thus in any given commercial seismic survey the frequency content received at a given range is not 'standard' but a function of the particular source array and propagation regime. Hence it is not realistic to argue that any experimental setup should have a frequency content exactly matching some 'standard'.

Matched samples, Jervoise Bay - 2678 cui array, weights [1 0.2 0.05 0.05]
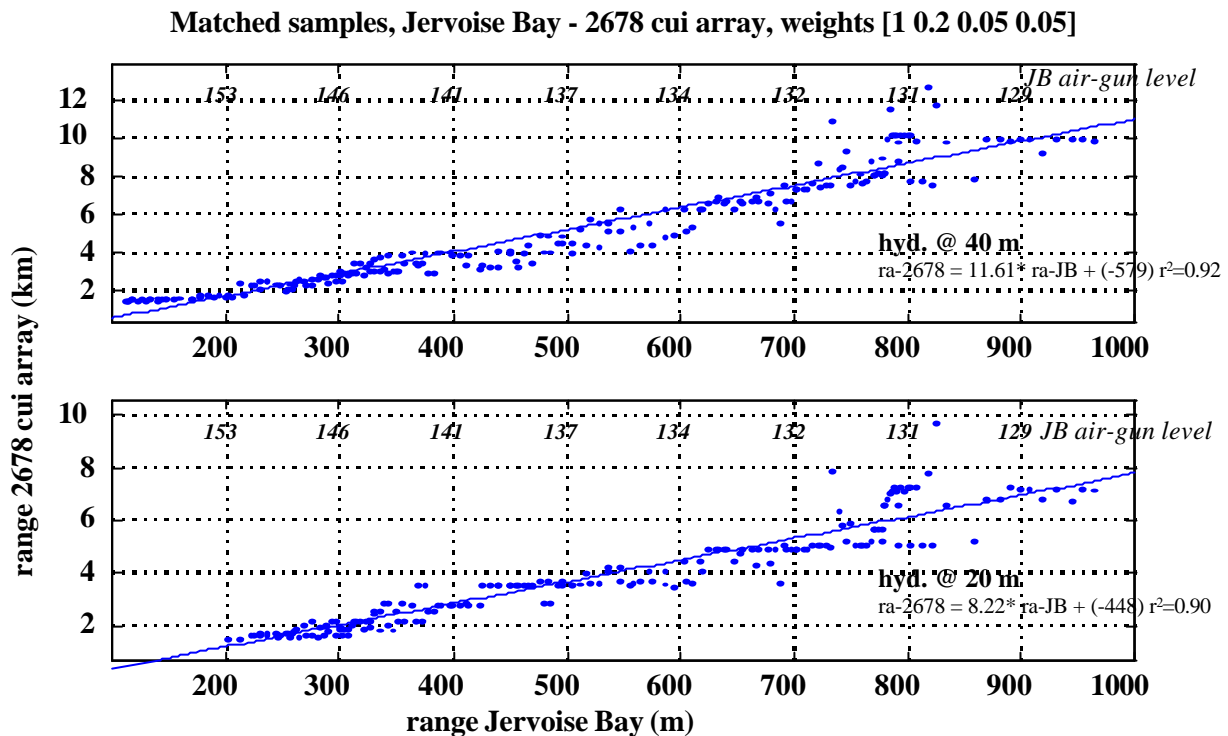
Figure 59: Comparative ranges for the single Bolt 600B air-gun as used in the Jervoise Bay trials, with a 2678 cui array as measured at two water depths off Exmouth. Signals have been matched using a weighting system comprising a matrix of the [equivalent-energy mean-squared-pressure peak-peak-level signal length] as described in Table 6. The weighting matrix was set to bias primarily on equivalent energy. The equivalent energy of the Jervoise Bay air-gun at each range step is shown in italics at the top of each plot.

2.4.2 Behavioural response

Behavioural data was worked up for nine of the ten fish trials. Trial 1 (Table 4) was a pilot run to test equipment and the air-gun configuration. All behavioural data was scored at the species level, thus trials 2 to 5, 8, 9 and 12 resulted in multi-species data sets. Observations were made on individual animals and the general school behaviour. It was found that trials with single species in moderate sized schools were simpler and more reliable to score during the behavioural coding process (see methods or appendix 1 for codes). Although a wide variety of species were present during trials, limitations on each camera's field of view meant that data sets suitable for analysis were available only for the most numerous species. Spot observations of the behaviour of less numerous species were available.

Data was thus available for different species between and within trials and for different cameras within a trial. The fields of view for each camera did not overlap, thus each camera has been considered a separate sample within a trial and results summed accordingly.

The numbers, standard length, acclimation period in the large sea-cage, and collection source, for animals used in the behavioural observations are given in Table 24. Other animals were kept in smaller cages (0.5 - 1 m^3) for physiological and pathological measures. Details of these are not included in Table 24.

The presentation format of behavioural results has been standardised, and the raw data is shown for representative species and trials in Figure 60. This format shows the air-gun level as received at the cage, a representation of the movement and behavioural patterns of the fish and periods for which the species was in and out of camera view through time.

Trial	Species	Number of fish	Mean fish size (mm)	acclimation days in large cage	fish source
1	*Acanthopagrus butcheri* (silver bream)	13	120 - 150	3	aquaculture
2	*Acanthopagrus butcheri* *Pelates sexlineatus*[1]	12 ~ 50	120 - 150 50-55	7 - 17 wild fish	aquaculture wild
3	*Acanthopagrus butcheri* *Pelates sexlineatus*[2] *Chrysophrys auratus* (pink snapper)	20 ~ 50 9	152 ± 4 50-55 149 ± 8	13 wild fish 13	aquaculture wild aquaculture
4	*Acanthopagrus butcheri* *Mugil cephalus* (mullet) *Nematalosa vlaminghi* (herring)	30 24 5	167 ± 10 212 ± 33 147 - 187	20 7-13 7-13	aquaculture purse seine purse seine
5	*Acanthopagrus butcheri* *Chrysophrys auratus* *Nematalosa vlaminghi* *Sepioteuthis australis* (squid) cuttlefish	9 10 23 12 2	159 ± 6 241 ± 23 186 ± 10	5 5-10 5-10 7-18 16	aquaculture purse seine purse seine jigging jigging
8	*Epinephelus fasicatus* *E. rivaltus* *Pelates octolineatus* *Pentapodus vitta* *Stethojulis strigiventer*	3 13 20-40 20-40 15-20		3 3 3 3 3	hook hook bottom trawl bottom trawl bottom trawl
9	*E. quoyanus* *E. rivaltus* *Lethrinus laticaudis* *Lutjanus carponotatus* *Pelates octolineatus* *Pentapodus vitta* *Stethojulis strigiventer*	1 10 3 10 20-40 20-40 15-20		2-3 2-3 2-3 2-3 6 6 6	hook hook hook hook trial 8 trial 8 trial 8
12	*Pseudocaranx dentex* (trevally) *Glaucosoma hebraicum* *Epinephelus armatus* goatfish wrasse	15 1 3 2 3	200-350[3]		hook hook hook hook hook
13	*Chrysophrys auratus*	50	230 ± 24	24	aquaculture
14	*Chrysophrys auratus*	42[4]	250 ± 8	70	trial 13

Table 24: Numbers, size (mean standard length ± 95% confidence limits where available), acclimation history and source of animals held in large sea-cage for the ten behavioural trials (fish held in smaller cages for physiological and pathological measures not included). See Table 4 for a full list of species names. Superscripts are:- 1) *P. sexlineautus* could enter and leave cage of own accord as 40 mm mesh size cage used during acclimation and trial; 2) *P. sexlineautus* could enter and leave cage during acclimation but were trapped using 16 mm mesh liner during trial; 3) All fish escaped from the sea-cage during recovery of the liner, thus all sizes are estimates; 4) Pink snapper (*Chrysophrys auratus)* from previous trial used, believed missing fish taken by fisherman.

The hydrophone was located at three m depth at the cage centre (trials 2-5), cage apex (trials 8-9), or at the centre of the cage's E side (trials 12-14). Two air-gun exposure types were used in trials (Table 4),

with the pontoon fixed near the cage and moved from 10-30 m off the cage (trials 1-5), or with the air-gun towed on the pontoon or vessel and a start range from 300-1200 m off the cage (trial numbers > 5). The difference in exposure types can be seen in Figure 60 - 1 & 6, by comparing air-gun levels in trials 3 and 14 (which had the greatest air-gun signal range). It should be noted that vertical differences in sound intensity within the cage were measured, with the level being lower near the water surface than at the cage bottom (Table 10). These measurements agree with theory and modelling (eg. Figure 27). Details of the air-gun level received at the start, minimum and maximum values, and at the end of each period, for consecutive air-gun operations are given in Table 25.

The types of behavioural results observed can be generally classified as obvious 'startle' responses (classic C-turn response), alarm responses (darting movements, flash school expansion, fast swimming) or less obvious behavioural changes which often led to 'huddling' in the cage centre. These are discussed below.

Following six pages:

Figure 60: Summary of behavioural scoring for selected fish species, cameras and trials, through time. Given are results of trial 3, camera 1, silver bream; trial 3 camera 2, *Pelates sexlineatus*; trial 9, camera 2, all fish; trial 12 camera 1, trevally; trial 13 camera 1, pink snapper; trial 14, camera 1 pink snapper (same fish as used in trial 13). From top to bottom are: **fish vertical position** - dots ; **fish vertical movements** - shown by arrows; **swimming speed**; dot = idle, small arrow = swim slow, larger arrow two feathers = swim fast, largest arrow three feathers = swim very fast**; horizontal swim direction** - left slant and right slant arrows moving right-left or left to right respectively; circle for **swimming in circles**; **field of view** square for in LHS field of view; diamond for in RHS field of view; **alarm responses** - small one feathered arrow = dart, larger two feathered arrow = part, larger three feathered arrow = flash expansion of school, circle = 'jerk', cross = change direction; **school formation** - circle = loose school, plus sign = tight school, dot = most animals with dot below = some animals; **specific behaviours -** arrow one feather = approach camera; **time in view** - given by bars; **air-gun level** given for each shot fired during trial. The **vertical lines** which run through the whole plot delineate the periods of air-gun operations, the vertical lines in the top plot only delineate the operation times for each video tape.

Trial 3 camera 1 Jervoise Bay sb
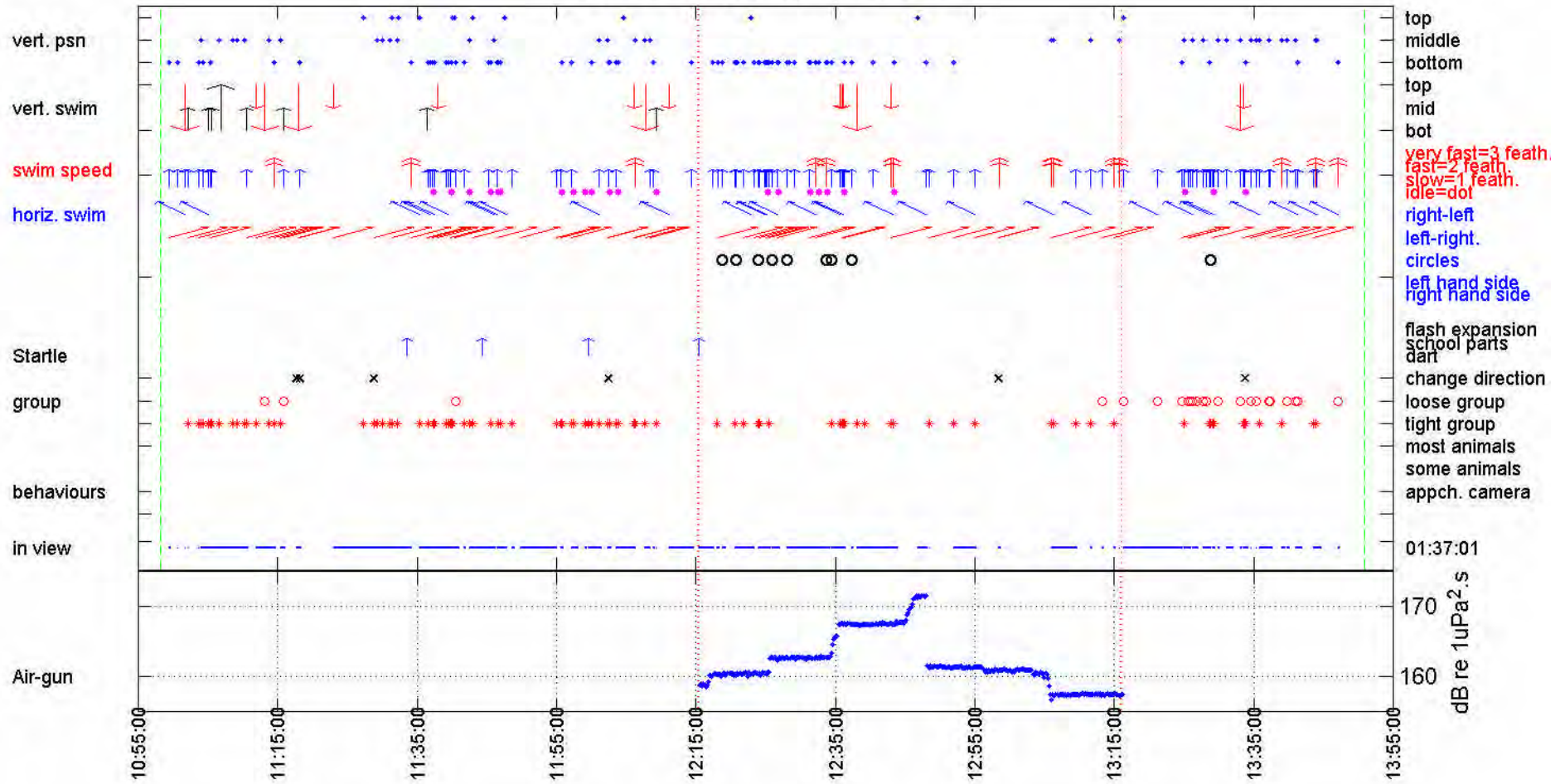
Trial 3 camera 2 Jervoise Bay sx

131
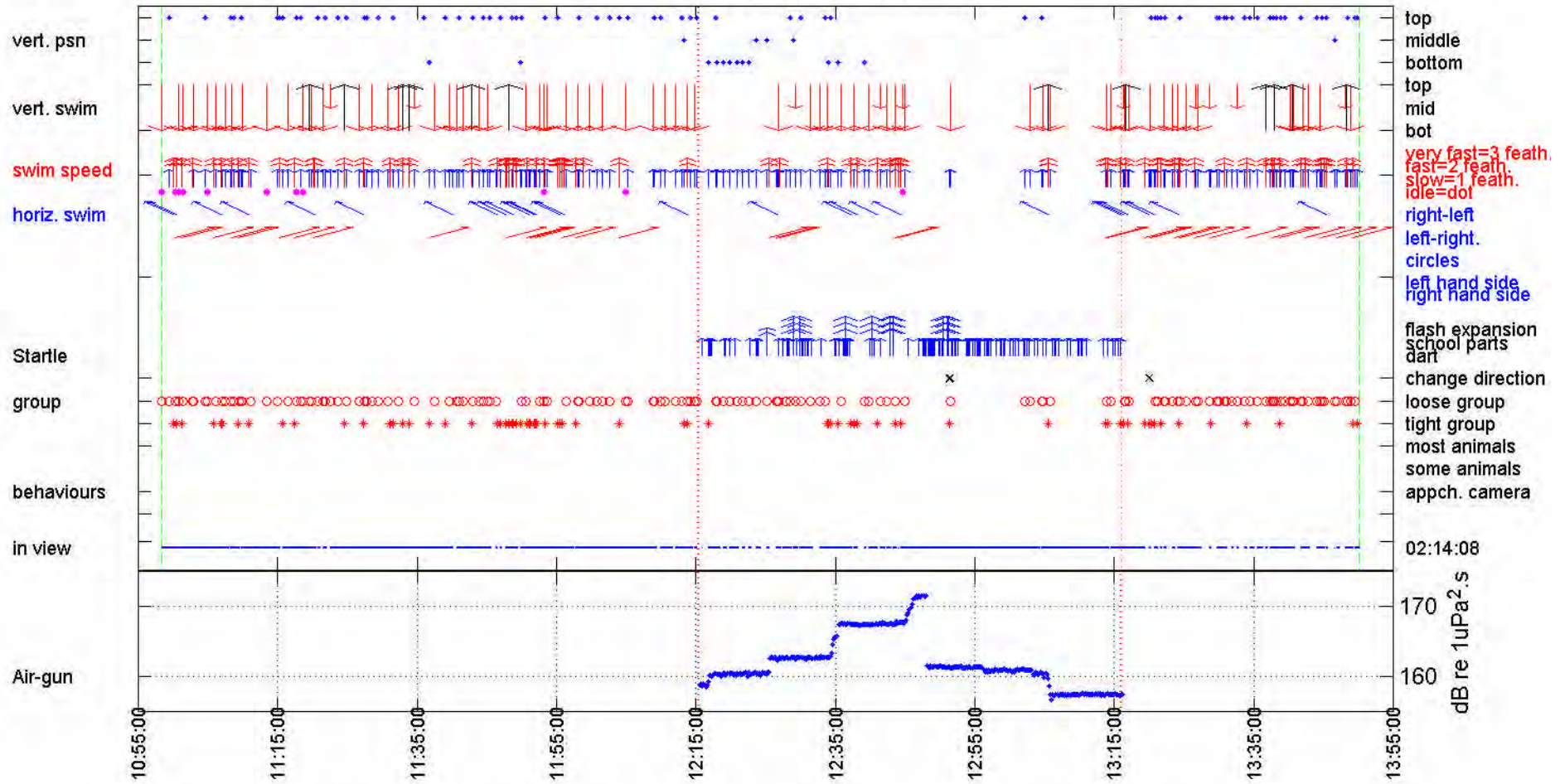
Trial 9 camera 2 Exmouth all
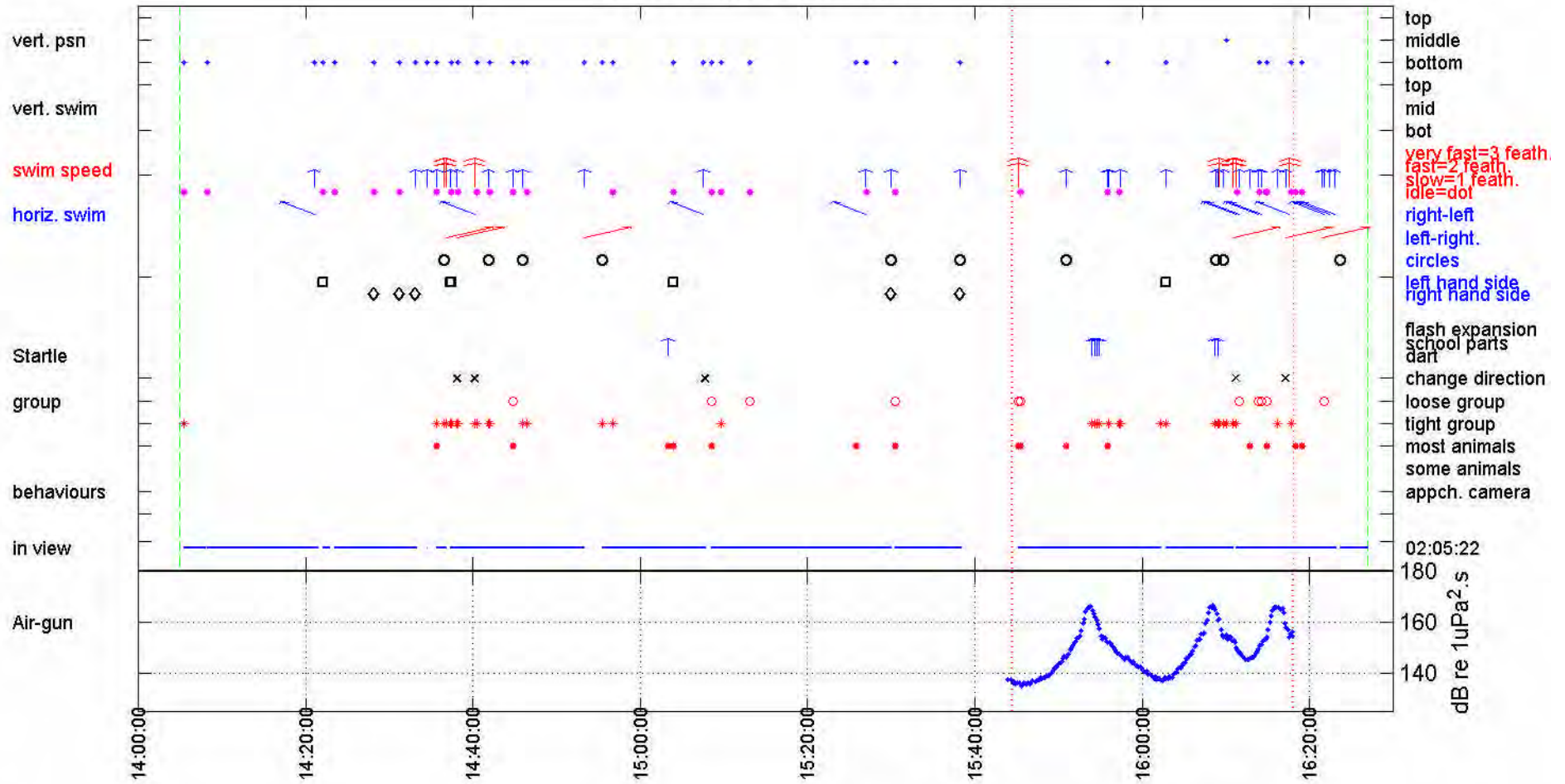
Trial 12 camera 1 Mixed all
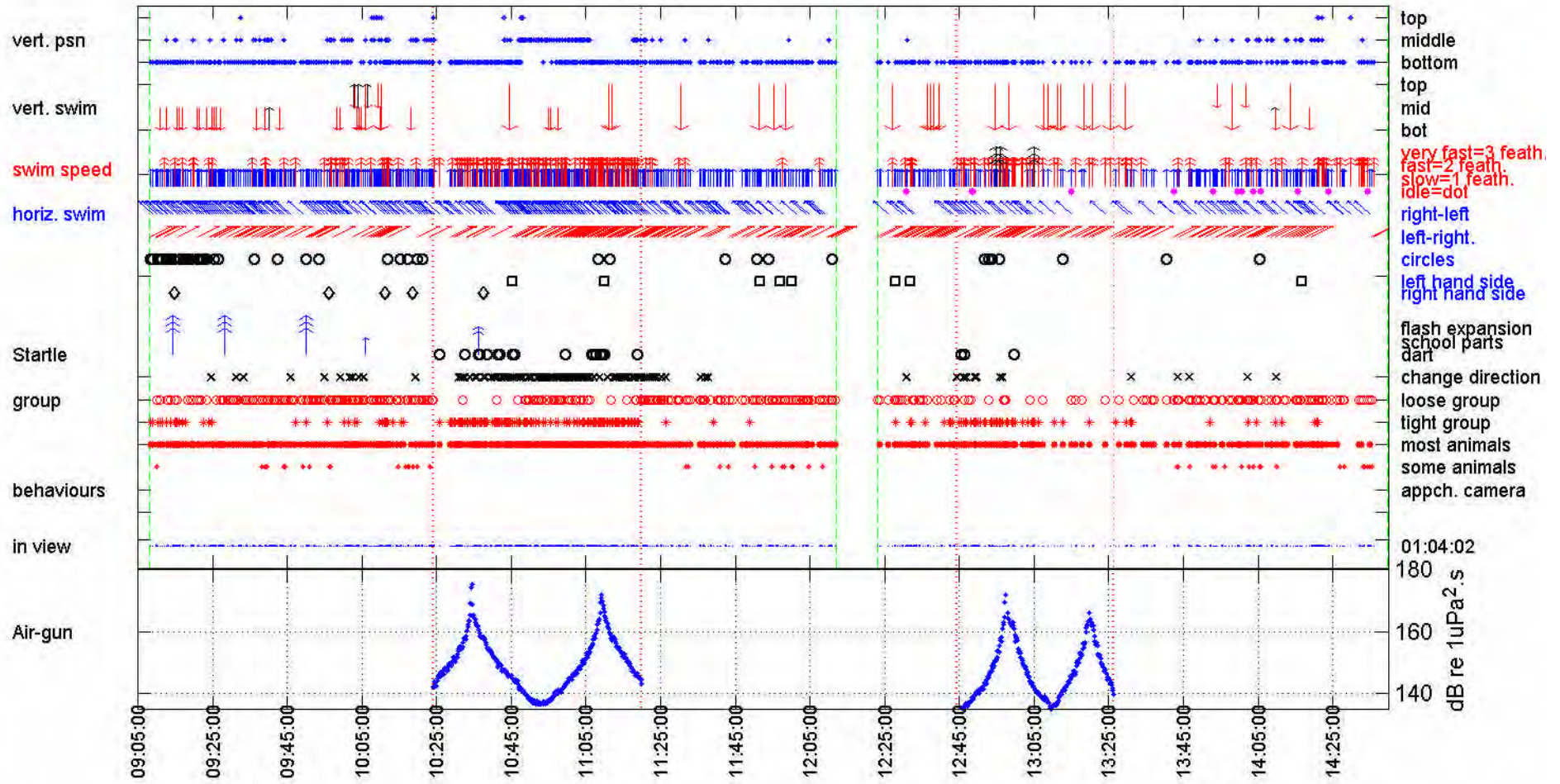
Trial 13 camera 1 pink snapper all
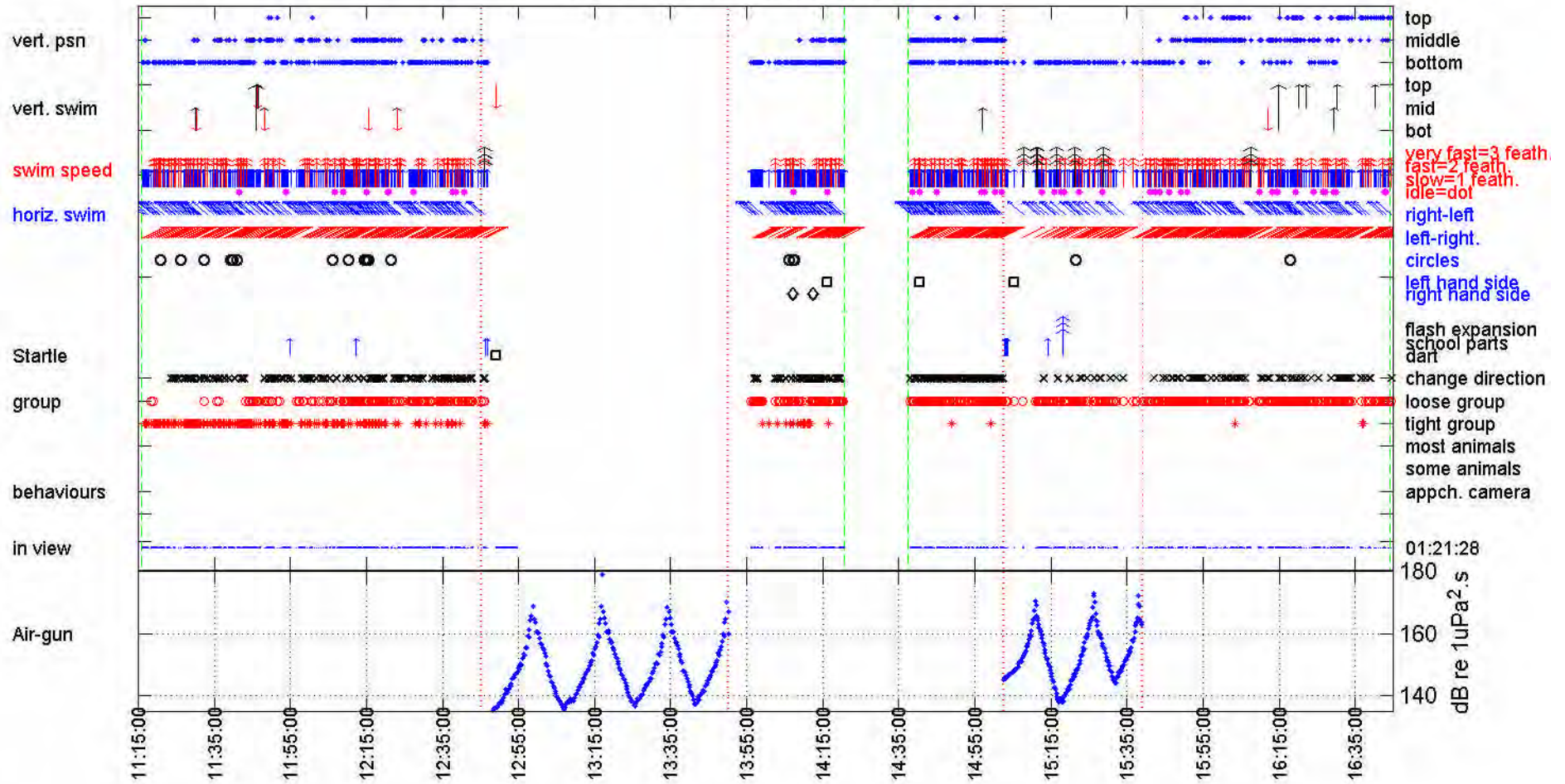
Trial 14 camera 2 pink snapper all

135
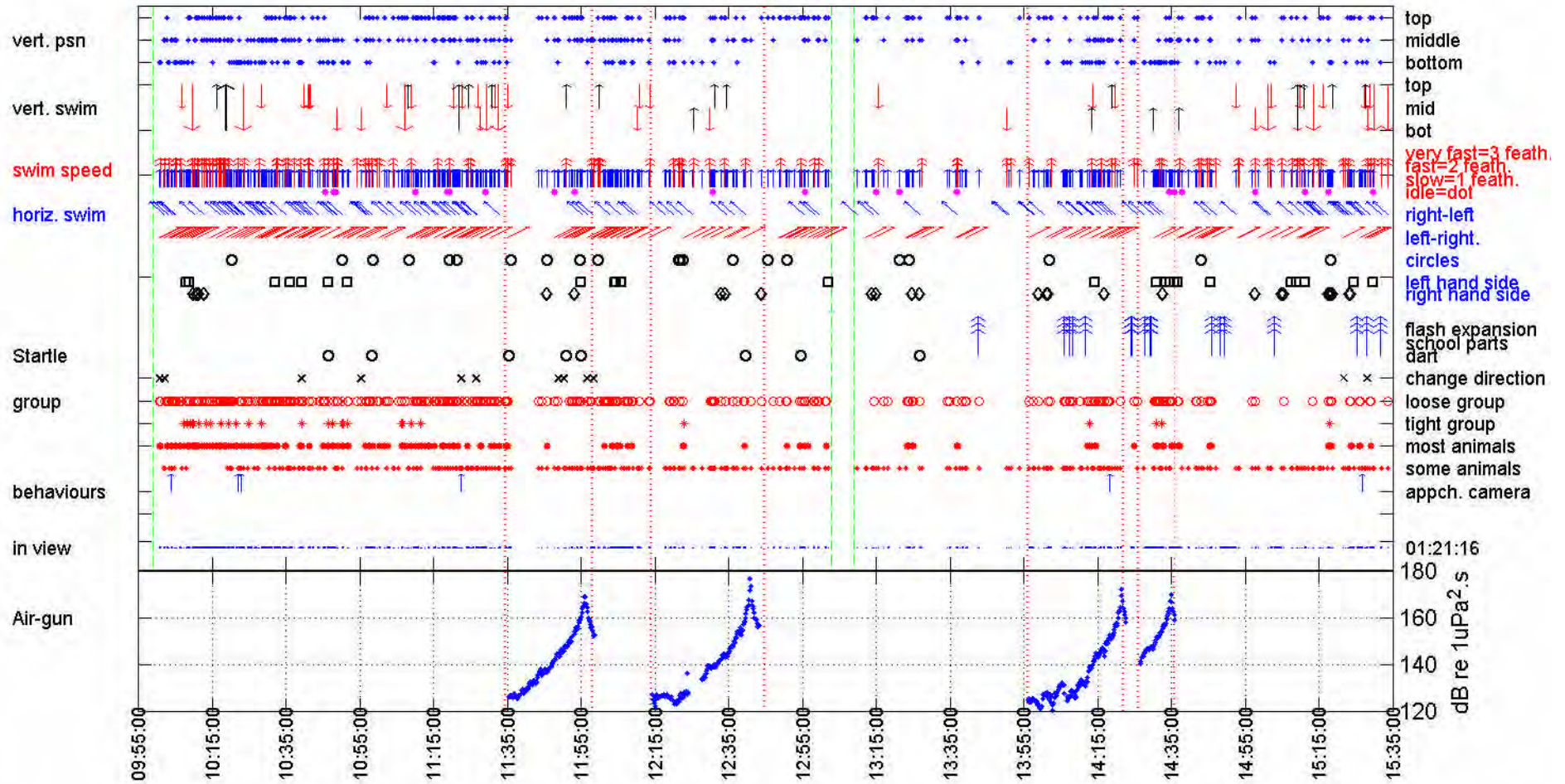
| Trial	run	start level / time	minimum level / time	maximum level / time	end level / time
1	1	172 / 11:10:44	166 / 11:14:14	174 / 11:12:44	168 / 12:10:49
2	1	159 / 10:24:18	158 / 10:33:18	165 / 11:06:18	164 / 11:24:17
3	1	159 / 12:15:35	157 / 13:05:58	172 / 12:47:37	157 / 13:16:08
4	1	163 / 11:52:52	160 / 12:42:51	170 / 12:24:31	161 / 12:53:00
5	1	163 / 11:29:03	159 / 11:29:23	170 / 12:02:11	163 / 12:27:59
	2	163 / 13:54:24	161 / 14:45:21	168 / 14:24:52	162 / 14:54:01
8	1	121 / 16:31:27	120 / 16:56:52	170 / 17:29:42	149 / 17:33:22
9	1	137 / 15:43:54	135 / 15:45:33	167 / 16:08:24	155 / 16:17:58
12	1	142 / 10:24:02	137 / 10:52:56	175 / 10:34:26	143 / 11:19:59
	2	125 / 12:44:15	123 / 12:45:05	172 / 12:57:19	140 / 13:26:12
13	1	131 / 12:45:14	131 / 12:46:06	182 / 13:49:59	167 / 13:50:19
	2	145 / 15:02:31	138 / 15:17:53	173 / 15:26:23	163 / 15:38:52
14	1	126 / 11:35:25	126 / 11:37:46	169 / 11:55:57	153 / 11:58:37
	2	127 / 12:14:18	122 / 12:14:58	177 / 12:40:47	157 / 12:43:08
	3	125 / 13:56:05	120 / 14:02:46	172 / 14:21:25	158 / 14:22:35
	4	140 / 14:26:26	140 / 14:26:26	170 / 14:34:46	159 / 14:35:46

Table 25: Details of air-gun exposures for each set of consecutive air-gun operations during fish trials. Air-gun units are equivalent energy, dB re 1 μPa^2.s.

Startle / alarm responses

Where observed, startle and alarm responses of individual animals to a given air-gun shot were evident along a continuum from the classic 'C-turn' startle response, in which the animal contracted the lateral body muscles along one side of the body to rapidly shoot away from the stimulus, to small 'jerking' motions coincident with air-gun shots. In some instances flash expansion of schools occurred. In these instances the school structure broke down as individuals darted in all directions.

The most notable startle responses occurred for schools of juvenile *Pelates sexlineatus* during trials 2 and 3. For these trials the cage was permanently set up with a 40 mm mesh net. This was large enough for the small fish to enter and leave the cage at will. The school of small fish used the cage as a refuge during the acclimation period. For trial 2 no liner was put inside the cage, thus the fish were free to leave the cage during the trial. Before trial 3 a 16 mm liner was fitted to the inside of the 40 mm mesh net, and the *P. sexlineatus* captured, thus they could not escape during the trial.

In trials 2 and 3 classic C-turn startle responses were observed from all members of schools of 50 or so *P. sexlineatus* from almost every air-gun shot for which the animals were in view. Air-gun levels received by these fish ranged over 159-172 dB re 1 μPa^2.s. For the first 6.5 minutes of air-gun exposure during trial 3 the *P. sexlineatus* were in the foreground of camera 2. This enabled the number of body lengths individual *P. sexlineatus* moved during each air-gun induced startle response to be estimated by analysis of each video frame from before to the cessation of the startle response (video frames about each air-gun shot were looked at sequentially and the movement of the school could be monitored). After the 6.5 minute period the animals moved into the background field of view and the distance moved per frame could not be accurately estimated. The startle response is shown in Figure 61 as the mean number of body lengths per frame (five fish per sample) moved during the video frame immediately after the air-gun shot, as compared with body lengths moved per frame from just prior the air-gun shot. A reduction in the response over the six minutes period was evident, indicating habituation, although the startle response was still evident at the end of this period. A sigmoid curve was fitted to the mean startle body lengths/frame (Figure 61), to give Equation 14. This gave a correlation coefficient (r^2) of 0.80 and was significant at $p \ll 0.001$ using the F statistic.

Equation 14
$$b_f = \frac{(2 \cdot 4225)}{1 + \left(\dfrac{x}{2 \cdot 224}\right)^{1.888}} + 0 \cdot 2025$$

where

b_f = body lengths moved per frame after each air-gun signal

x = the time from the first air-gun signal in minutes.
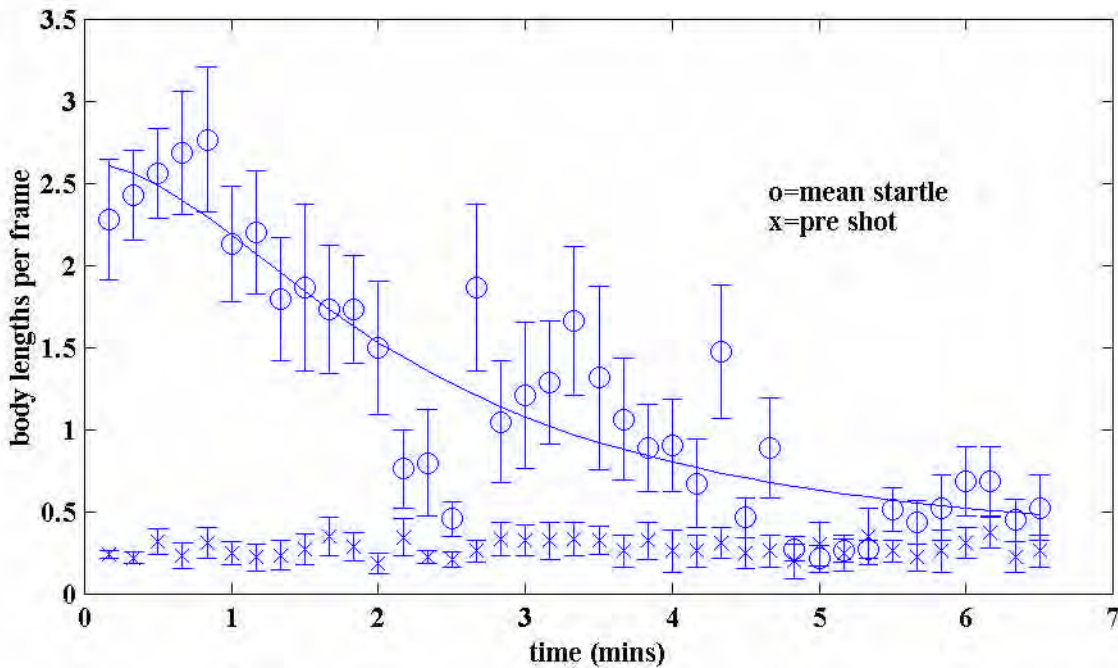
Figure 61: Number of body lengths per video frame moved by *P. sexlineatus* during control periods and the air-gun induced startle response, over a six minute period (error bars are 95% confidence limits).

Of the behaviours scored (Appendix 1), those considered alarm responses for finfish included: flash expansion; parting; darting; or jerking. These events were also recorded outside of the periods of air-gun operations. Often this was at the beginning of trials and coincided with the presence of a diver in the cage setting or adjusting the camera location. The incidence of startle/alarm events occurring is summarised in Table 26. Included in this table is the ratio of the number of alarm events recorded per period (all of air-gun off or all of air-gun on respectively), divided by the total number of all behavioural counts for the respective period (see Equation 13 in the turtle analysis). These ratios have been calculated from the sum of values using both cameras per trial and for the species indicated. The total number of counts per period was used as opposed to the total time in view per period, so as to try to reduce any bias in scoring from listening to the air-gun during video scoring (see section 1.3.2). The air-gun signal, although clipped to a set maximum level, was audible during playback of the video tapes (providing a useful time reference and allowing correlation of behaviours with each air-gun shot) but may have increased perception and detail during the scoring process.

Simply comparing the mean values of the alarm response ratios between *air-gun-on* periods and *air-gun-off* periods (Table 26) using the *t* statistic and reducing the degrees of freedom by one to allow for the use of ratio data, gave a *t* value of 1.73, which is just not significant at the 95% level, with $0.05 < p < 0.20$. But the calculation of this ratio using data from the entire air-gun on periods, includes times of low air-gun

levels when the fish were less likely to respond and is biased in that for several experiments the fish moved into the lower portion of the cage during air-gun passages, where they were mostly out of view of the cameras (trial 13 particularly eg. Figure 60-5). This greatly reduced the number of observations which could be made. Trial 14 also used fish which had been previously exposed to air-gun noise in trial 13, hence the issue of habituation or sub-lethal damage to hearing systems which may have reduced the behavioural response (see section 2.4.4) arose.

Trial	Species	No air-gun period	During air-gun operations
2	*Acanthopagrus butcheri*	none	**yes** - (0.012) flash expansion @ 162 dB
	P. sexlineatus	none	**yes** - (0.438) startle at every shot in view
3	*Acanthopagrus butcheri*	**yes** - (0.007)	no
	P. sexlineatus	**yes** - (0.007)	**yes** - (0.341) startle at every shot in view
4	all species	none	**yes** - (0.010)
5	all species	**yes** - (0.002)	**yes** - (0.004)
8	all species	none	**yes** - (0.007)
9	all species	**yes** - (0.004)	**yes** - (0.074) marked increase as level ↑
12	*Pseudocaranx dentex*	**yes** - (0.001)	**yes** - (0.011) marked increase as level ↑
13	*Chrysophrys auratus*	**yes** - (0.015)	**yes** - (0.018) mostly out of view during air-gun on
14	*Chrysophrys auratus*	**yes** - (0.004)	**yes** - (0.008) possibly influenced by previous (trial 13) exposure

Table 26: Incidence of startle/alarm response for finfish observed from video cameras. Numbers in brackets are *startle/alarm-counts-per-period* divided by *total behavioural counts per period* (period = air-gun off or air-gun on, respectively).

Although when averaged over all trials and all air-gun operation periods there was only weak evidence of an increase in alarm response during air-gun operation periods, for specific trials there was strong evidence of increased alarm responses in air-gun operation periods (eg, trials 2 & 3). In trials 9 and 12, which had a 32 and 49 dB air-gun signal range respectively, the proportion of startle/alarm responses increased by 18 and 11 times during the air-gun operation periods as compared to the control periods.

During trials 9 and 12 the proportion of startle/alarm responses also increased as the air-gun signal increased. To present this trend sliding time boundaries were used to compare the ratio of startle/alarm counts per total number of behavioural counts, for different time periods. The time boundaries were set by the air-gun signal level as received at the cage (as similarly calculated for the sea turtle time spent swimming). Thus an air-gun signal level could be specified and a program calculated various ratios or times from the coded data, for the trial times where the received air-gun signal was above and below the specified threshold. This was calculated for trials 9 and 12 (summed for cameras each trial, and for species trial 9). For presentation the difference between the ratio: *startle-counts-per-period / total-count-per-period*, calculated for the period above threshold minus the similar ratio calculated for the control period (air-gun off), are shown on Figure 62. This difference ratio (*d*) was then:

Equation 15 $$d = \frac{s_p}{S_p} - \frac{s_n}{S_n}$$

where
d = difference ratio
s_p = startle/alarm counts period above threshold
S_h = total behavioural counts period above threshold
s_n = startle/alarm counts period with no air-gun operations
S_n = total behavioural counts period with no air-gun operations

The air-gun thresholds chosen to delineate different periods were 100, 140, 145, 150, 155 and 160 dB re 1 μPa^2.s. The initial threshold of 100 dB re 1 μPa^2.s was below any received air-gun signal thus compares times with all air-gun on with all air-gun off (control).

All values shown on Figure 62 are positive implying that the startle/alarm response occurred more frequently in the period of air-gun operations. As the air-gun level increased so did the relative proportion of recorded startle/alarm events, with this increase more marked for air-gun signals above 145 to 150 dB re 1 μPa^2.s. When fitted with a second order regression, each set of data shown in Figure 62 showed a strong correlation ($r^2 = 0.97$ both trials) was significant (each trial $p < 0.01$ using the F statistic), indicating that as the air-gun level increased so did the probability of an increase in alarm responses. This is as suggested in Table 26.
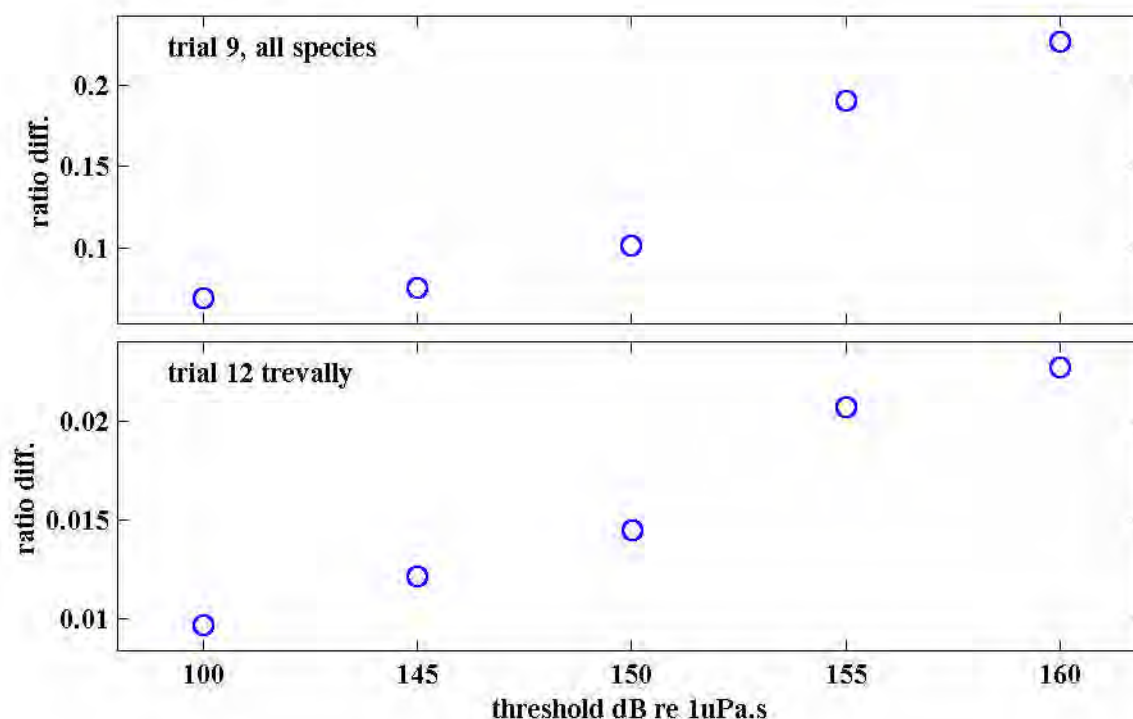
Figure 62 Difference between ratio of *startle/alarm response per total counts*, for periods above specified thresholds, minus the similar ratio for the control (no air-gun) period. The trial 9 data was calculated using all species in the trial, the trial 12 data using trevally (*Pseudocaranx dentex*) only and each trial used the sum of the two camera data sets.

Of other trials with a sufficient air-gun dynamic range to carry out similar calculations (trial numbers ≥ 8): in trial 8 there was insufficient numbers of startle/alarm responses recorded; in trial 13 the fish moved out of the field of view of each camera during air-gun operation periods; and trial 14 gave all positive ratio differences but with a less clear trend as the air-gun level increased. Thus the data presented above for trials 9 and 12 was the only data set suitable for this analysis.

Changes in movement patterns and swimming behaviour
Aside from the obvious startle/alarm responses, more subtle behavioural responses to air-gun exposure included: a tendency for the fish to spend more time at the bottom of the cage during air-gun operations; changes in swimming speed with air-gun operations; and the fish tending to use different portions of the cage than normal, particularly huddling in the cage centre.

The shift in vertical position in the cage can be seen on Figure 60 - 1, 2, and 5, (trials 3, 3 & 13) with the

fish tending more to the bottom of the cage during periods of air-gun operation. To analyse this depth trend the difference ratio of times (d_t):

Equation 16:
$$d_t = \frac{t_p}{T_p} - \frac{t_n}{T_n}$$

where:
d_t = difference ratio
t_p= time species in lower portion cage for period above specified threshold
T_p = time species in view for period above specified threshold
t_n = time species in lower portion of cage for no-air-gun period (control)
T_n = time species in view for no air-gun period (control)

was calculated for all periods above the air-gun thresholds. These used results at the species level summed for the two cameras per trial. Similar calculations were carried out for the times spent fast or slow swimming and the formation of loose or tight groups. The resulting difference ratios comparing periods of air-gun level > 150 dB re 1 μPa^2.s with the no air-gun periods are given in Table 27. Mean difference ratios were calculated with 95% confidence limits assuming each species-trial as a single sample.

Trial	Species	difference ratio - time lower	difference ratio - time fast swim	difference ratio - time tight group
2	*A. butcheri* (sliver bream)	nd	- 0.599	0.008
2	*P. sexlineatus*	nd	- 0.123	0.423
3	*A. butcheri*	0.386	- 0.023	- 0.022
3	*P. sexlineatus*	0.217	0.673	- 0.022
4	unidentified fish	- 0.006	0.106	- 0.007
4	*A. butcheri*	0.381	- 0.073	0.097
4	*Mugil cephalus*	nd	- 0.150	0.166
4	*Nematalosa vlaminghi*	- 0.024	0.071	0.019
5	unidentified fish	0.388	0.001	- 0.163
5	*A. butcheri*	0.307	0.316	0.434
5	*Mugil cephalus*	0.140	0.098	0.043
5	*Nematalosa vlaminghi*	0.026	- 0.006	- 0.080
12	*Pseudocaranx dentex* (trevally)	0.111	0.278	0.528
14	*Chrysophrys auratus*	0.043	- 0.067	0.008
mean		**0.179 ± 0.11**	**0.036 ± 0.164**	**0.102 ± 0.121**

Table 27: Difference ratios calculated for fish in bottom section of camera field of view, fish fast swimming, or fish in tight group, calculated as per Equation 16 for periods above an air-gun threshold of 150 dB re 1 μPa^2.s compared with no air-gun periods (nd = no data).

Trials 8, 9 were excluded from Table 27 as the fish were continually swimming into a strong current and were thus either hiding in pockets within the net or were already stationary in a tight group in the cage centre before air-gun operations began. Trial 13 was excluded from calculations as the fish moved out of camera view during most of the periods of air-gun operations. Trial 14 was carried out on pre-exposed fish which may have shown habituation or suffered physiological hearing damage in the previous trial (see section 2.4.4) and thus exhibited a lessening of behavioural response. The inclusion of trial 14 made little difference in the mean calculations.

Using the *t* statistic to compare the difference ratios between the observed set of data shown in Table 27 and the expected set (zero for no difference), then the fish utilised the lower portion of the cage significantly

more during periods of air-gun operations (p < 0.01). Although in some other trials several species, showed a significant trend to increase swimming speed and tighten their school structure during the periods of higher air-gun levels (eg. silver bream trial 5, trevally trial 12), averaged over all trials these trends were not significant (95% confidence limits of mean value for all trials encompass zero, Table 27).

Trials 8, 9, 12, 13 & 14 were fish trials carried out with the air-gun started at > 300 m, thus had an air-gun signal at trial start of < 150 dB re 1 μPa^2.s. As indicated above, trials 8 & 9 were biased due to the strong currents forcing fish to seek refuge or swim constantly into the current, in trial 13 the fish simply moved out of view during the period of air-gun operations and trial 14 used pre-exposed fish. Thus trial 12, using the trevally (*Pseudocaranx dentex*) was the only trial with a large signal dynamic range, the animals consistently in view throughout the trial and previously unexposed fish. The difference ratios (Equation 16) for the trevally's use of the bottom portion of the cage, time spent bunched up as opposed to in a loose school and time spent fast swimming (as opposed to idle or slow swimming) using the five air-gun level thresholds, are shown in Figure 63. It can be seen that these behaviours became increasingly more prevalent as the air-gun threshold increased. The trend for use of the lower portion of the cage is significant for all periods above an air-gun threshold of 145 dB re 1μPa2.s (two tailed *t* test, gives 0.02< *p* < 0.05, v=5), while the trend for the trevally forming a tighter group and swimming faster were significantly greater during periods of all air-gun operations (two tailed *t* test, gives *p* << 0.001, v=7, each behaviour).
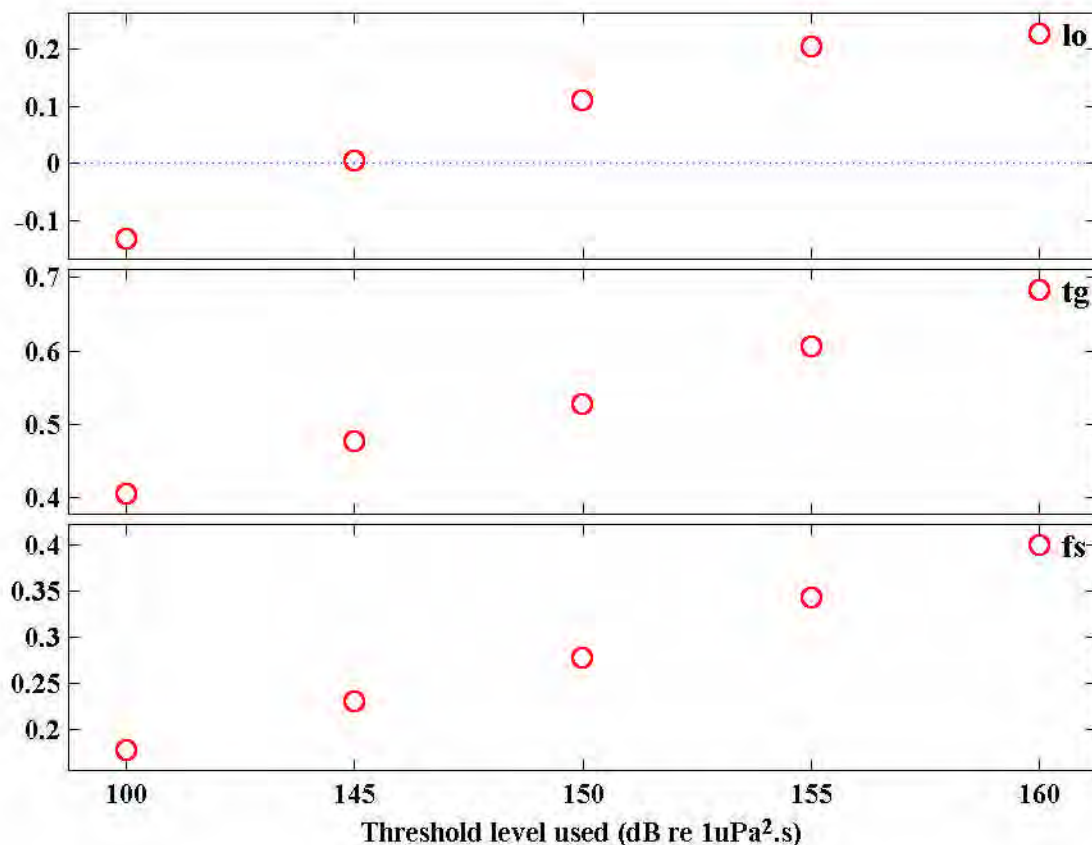

Figure 63: Difference ratios from trial 12 for trevally (*Pseudocaranx dentex*) use of lower portion of cage (top), schooling behaviour (middle) or swimming speed (lower) with increasing air-gun thresholds. Difference ratios are of times, as calculated by Equation 16.

The significant trend for fish to utilise a different portion of the cage as the received air-gun level increased

was emphasised by the trials in which animals left the fields of view of the cameras during periods of air-gun operations. Cameras were positioned at the beginning of trials according to the swimming patterns observed during the acclimation period. During the air-gun exposure period it was common for fish to alter this pattern so that they moved out of, or were barely in, the camera field of view. This can be seen in Figure 60 - 5, for the pink snapper of trial 13, camera 1. The same trend was observed in the second camera of this trial. Before the air-gun operations began the fish displayed a slow circling behaviour (no preference for clockwise or anti clockwise swimming), using the mid-lower portion of the cage, in a loose school. During the first approach of the air-gun the fish remained in view until the air-gun level reached 151 dB re 1 μPa^2.s whence they moved into the very lower centre portion of the cage, mostly out of the field of view of each camera, until five minutes after air-gun operation had ceased. They then began circling the full extent of the cage again. In camera 2 of this trial the fish moved out of camera view very shortly after the first air-gun shot for each of the two periods of consecutive operations, and remained mostly out of view until each period of air-gun operations ceased. Thus the behavioural observations were strongly biased as the fish response had been to huddle in the lower cage centre during the air-gun passages, where they were not in view of the cameras.

This 'huddling' behaviour where fish aggregated in the lower centre of the cage during air-gun operations was observed in trials 3 (silver bream and *P. sexlineatus*), 5 (herring), 12 (trevally) and 13 (pink snapper). Moving to the bottom of the cage would have increased the received air-gun level as compared to fish which moved to near the water surface (eg. Table 10).

Recovery
In trials 3, 12 and 13 the time taken for the fish to move back into the field of view of the camera or to resume using the full cage extent could be determined. These times are summarised in Table 28

Trial	camera	pass	species	time to return to view (minutes)	time to return to normal vertical cage usage (minutes)
3	2	1	silver bream	4	17
12	1	2	trevally	in view whole period	31
13	1	1	pink snapper	5	18
		2	pink snapper	4	11
13	2	1	pink snapper	9	29
		2	pink snapper	9	29

Table 28: Times taken for fish to return to field of view and to resume normal position in water column (pass = period of sequential air-gun operation during trial, time rounded to nearest minute).

Thus resumption of the fish's normal behavioural pattern took between 4-31 minutes after the cessation of air-gun activities.

In summary the caged-fish behavioural response to nearby air-gun operations was:

- startle response to short range start up or high level air-gun signals for some fishes
- greater startle/alarm response from smaller fishes and with an increase of received air-gun level above 145-150 dB re 1 μPa^2.s
- lessening of severity of startle/alarm response through time (habituation)
- increased use of lower portion of cage during air-gun operation periods
- tendency in some trials for faster swimming and formation of tight groups correlating with periods of high air-gun levels
- general behavioural response of fish to move to bottom, centre of cage in periods of high air-gun

exposure when the level approximately reached or exceeded 145-150 dB re 1 $\mu Pa^2.s$

2.4.3 Physiological response

Blood samples were taken from fish in trials 2, 3, 4, 5 and 13, for analysis of blood plasma glucose and/or cortisol levels. Cortisol is a primary stress hormone, released immediately on application of a stressor. Cortisol measurements were analysed from trials 3, 4, 5 and 13. Amongst other things, blood plasma glucose is a secondary stress indicator, produced in response to the release of primary stress hormones. Plasma glucose levels were analysed from trials 2, 3 and 13. It was intended that measurements of cortisol and blood glucose levels would give an indication of the severity of air-gun exposure as a stress event.

All fish sampled for physiological measures were kept in 0.5, 0.64 or 1 m³ cages at the sea cage site. Stocking densities during the few days prior trials were either five (any cage) or ten fish per cage (0.64 or 1 m³ cages only). All control samples were taken from undisturbed cages immediately prior to trials. As their was often not sufficient fish available, control samples were not always available for all species. The methods for fish husbandry, cage locations, cage movements after control sampling, collecting blood and analysing samples were outlined in section 1.3.3. To obtain statistically significant samples, the cortisol or glucose means of a minimum of five fish (same cage) were considered a single sample. Where sufficient fish were available control fish were sampled before trials, moved into regions of Jervoise Bay sheltered from the air-gun passage before air-gun exposures commenced, then returned to the vicinity of the sea cage after trials. No fish were re-sampled before a minimum six day interval had elapsed. The sampling periods are outlined in Table 29, the exposure regimes in Table 4 and Table 25, and the fish source and acclimation history were as given in Table 24 for the fish used in behavioural experiments.

Trial	species	Control samples	sample time from maximum air-gun exposure	measure
2	*Acanthopagrus butcheri*(silver bream)	taken	2 hrs	gluc
3	*A. butcheri*	taken	1.5-2 hrs, 3 , 6, 9 & 12 days	cor/gluc
	Chrysophrys auratus (pink snapper)	not taken	1.5-2 hours, 6 & 12 days	cor/gluc
	Pseudocaranx dentex (trevally)	not taken	1.5-2 hours, 6 & 12 days	cor/gluc
4	*A. butcheri*	taken	1.5 hours, 1 & 2 days	cor
	A. butcheri, mullet	not taken	1.5 hours, 1 day	cor
	Nematalosa vlaminghi (herring)	not taken	1.5 hours, 1 day	cor
5	*A. butcheri*	taken	3, 3.5, 4, 4.5, & 5 hrs, 2, 4, 6, & 8 days	cor
	Mugil cephalus (mullet)	not taken	"	cor
	P. dentex	not taken	"	cor
13	*C. auratus*	taken	0.5, 1.5, 2.3, 4.5, 22.2 & 24.5 hrs	Cor/gluc

Table 29: Sampling regimes for physiological samples (times are given from time of maximum air-gun signal in first air-gun pass, cor = cortisol analysed, gluc = plasma glucose analysed).

Mean blood plasma glucose levels from silver bream of trial 2 were: 52.8 ± 12.0 mg/dl for exposed fish as compared to 29.3 ± 5.6 mg/dl for control fish (± 95%confidence limits). Using a two tailed *t* test to compare sample means these measures are significantly different ($p \approx 0.002$), implying that blood glucose had increased immediately after the trial. But, as stated, blood glucose levels are a secondary stress indicator. They may also vary according to a host of other physiological factors (eg. time of last feed). Thus without a corroborative set of cortisol measurements to indicate a primary stress response they cannot be

used to indicate an increase in stress levels.

Mean cortisol and glucose levels as measured from trial 3 for silver bream, pink snapper and trevally are shown on Figure 64 (using a log scale for the cortisol levels). There were no significant trends in the cortisol levels for any species. The silver bream blood glucose did peak at 6 days after the trial, but as the cortisol levels did not rise significantly before this, the rise in glucose level was not believed to indicate a secondary stress response.

The mean cortisol levels for silver bream taken during trials 4 and 5 are shown on Figure 65. Again there is no clear trends which could relate an increase in stress levels with the air-gun exposure. The mean value shown for the sample taken at the point of maximum air-gun exposure (run 1, trial 5) was entirely due to one of the five fish sampled. Four fish showed no detectable cortisol levels with the fifth showing a reading of 762.5 ng/ml. The error range for this sample set encompasses the zero trend for all other samples. The rise in cortisol level seen at 10 days after the completion of trial 5 was believed due to bottlenose dolphins investigating the cage. A small school of dolphins was seen in the cage vicinity prior the physiological sampling.
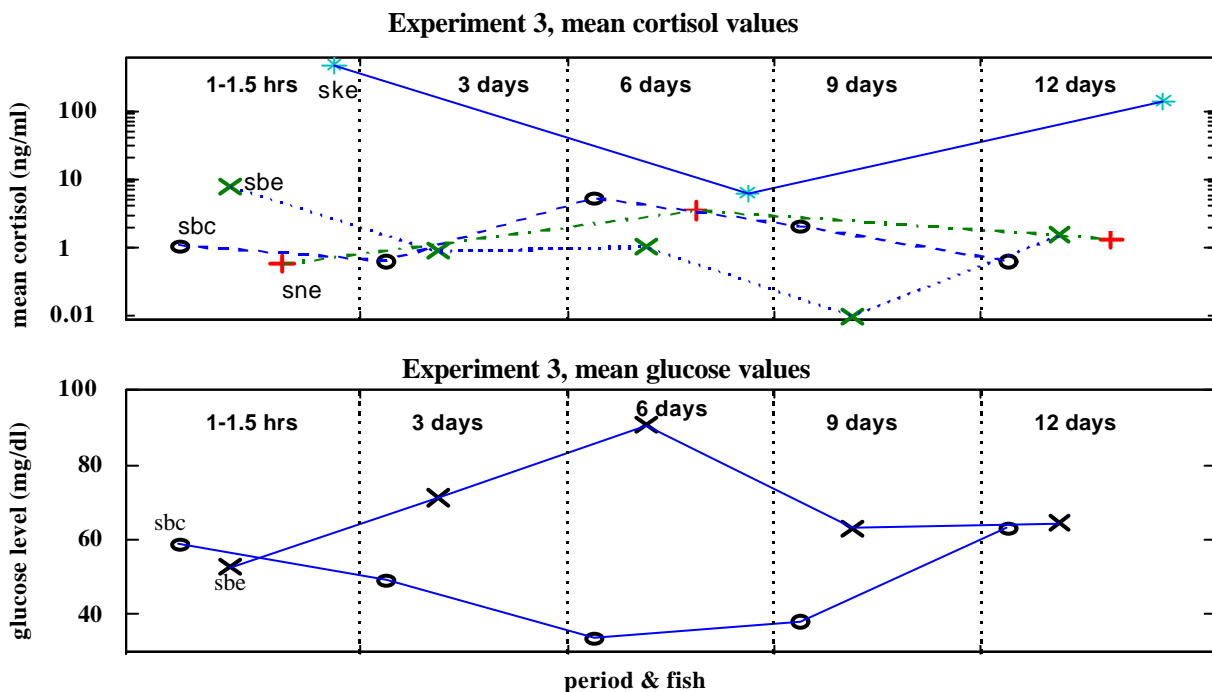

Figure 64: Mean cortisol levels for silver bream, pink snapper and trevally as measured from trial 3. There were sufficient control fish for silver bream only. Abbreviations are: sbe - silver bream experiment; sbc - silver bream control; sne - pink snapper experiment; ske - trevally experiment.
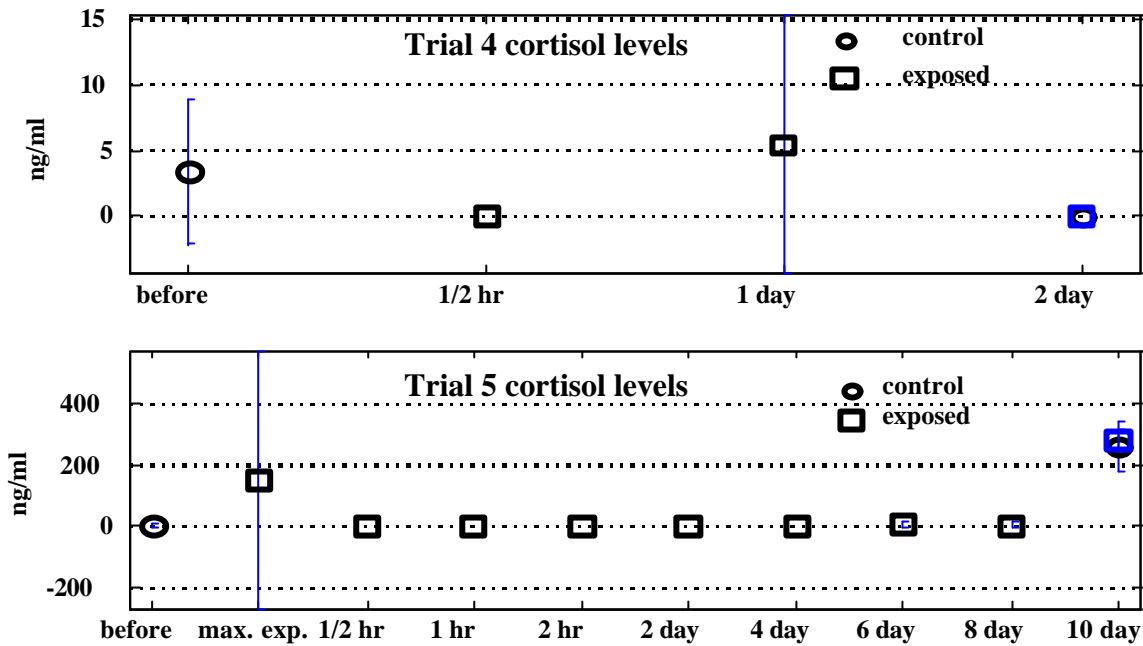
Figure 65: Mean cortisol levels for silver bream of trials 4 and 5 with 95% confidence limits for non-zero means.

In summary the physiological measurements showed no significant increases in stress measurements which could be definitively associated with air-gun exposure.

2.4.4 Pathological effects to hearing systems

Fish utilise their inner ear labyrinth systems to perceive sound. For a review of fish hearing see Popper and Fay (1993) or summary chapters in Fay and Popper (1999). These systems comprise laterally paired sets (ie left and right ears) of end-organs, with each set containing calcareous, elaborately shaped stones termed the sagittal, utricule and lagena otoliths. Although in most bony fishes the sagittal otolith and its sensory epithelium is primarily responsive for sound transduction, each end-organ is believed to contribute to hearing sensitivity and in selected fish species one of the other end organs may be the primary transducer (Popper and Fay, 1999). Each otolith is contained in a fluid filled cavity and supported by connective tissue but free to respond to applied forces. Each otolith has a sensory epithelium, termed a macula, which lays along one surface of the otolith. For the species described below, the pink snapper, the sagittal macula lay along a section of the inner side of the otolith. This macula is lined with sensory hair cells similar to vertebrate type II hair cells (several hair cell types may be present). These hair cells produce an electrical response proportional to bending of the protruding hairs which stimulates a nervous response from innervating neuron's. The macula is coupled to the otolith by a gel, such that movement of the otolith results in forces applied against the macula, some of which may produce relative shear between macula and otolith thus bending the hair cells and so producing a nervous response.

An impinging sound wave sets the bulk of the fish's body tissues into motion at the same phase as the sound wave, since the density of the fish's body tissues are approximately the same as the surrounding sea-water. But the otoliths' are approximately three times as dense as the surrounding tissue so their motion will lag that of the sound wave. Thus the macula sensory hair cells will experience shearing forces proportional to the movement pattern of the otolith and the degree to which the macula is driven by the sound wave, as opposed to dragged by the otolith-macula coupling. Fish are able to translate the relative otolith and sensory epithelium motion, and using this information from all otolith end organs can determine information

145

about impinging sound waves, including direction and possibly distance.

A schematic diagram of the layout of the sagittal otoliths is shown on Figure 66 for *Terapon theraps* a species which has a specialised swimbladder with anterior muscles attached and a cartilaginous 'membranous window' overlying the otolith. This 'membranous window' can range from being absent completely (otolith overlaid by bone), through various densities of cartilaginous material to a fine membrane. In the pink snapper (*Chrysophrys auratus*), the primary species for which results are presented below, this 'membranous window' was absent although the arrangement of the sagittal otolith was similar.

Over-stimulation of the macula-otolith system could produce mechanical damage to the macula and its sensory hair cells. Before trials were undertaken it was not known if this would occur. To check if any pathological damage had occurred samples were taken from control and exposed fish used in the behavioural trials and scanning electron microscopy (SEM) used to search the hair-cell populated portion of the fish's sagittal macula for possible damage. The full methods are given in section 1.3.4. It must be stressed that the trials were designed primarily to obtain behavioural results and not to determine the level or duration of nearby air-gun exposure required to produce any pathological damage. Although the air-gun exposures received at the cage were known, the ramped nature of the received air-gun signals meant that the exact level which potentially produced damage could not be determined. Given the preliminary nature of this examination and the fact that the techniques were new to the authors, only the sagittal otoliths were examined for possible damage.

Pathological samples were taken from trials 5 (silver bream, *Acanthopagrus butcheri*), 9 (*Lutjanus carponatatus, Epinephelus rivaltus, E. fasciatus*), 11 (squid *Sepiotuethis australis*), 13 (pink snapper, *Chrysophrys aurata*) and 14 (pink snapper). Trial 14 was carried out with the previously exposed pink snapper from trial 13 with 58 days elapsed from the end of trial 13 to the beginning of trial 14. There is evidence that fish can re-grow damaged hair cells (eg. Lombarte et al 1993), thus trial 14 involved sampling fish at intervals of 0, 11, 28 and 44 days from the end of air-gun operations.

At the stage of writing this report the pathological examination of specimens available was not complete. The results presented below are mainly for pink snapper used in trial 13 and 14 and must be considered preliminary.

a) Cut away view of *Terapon theraps*

b) Lateral view of ear region
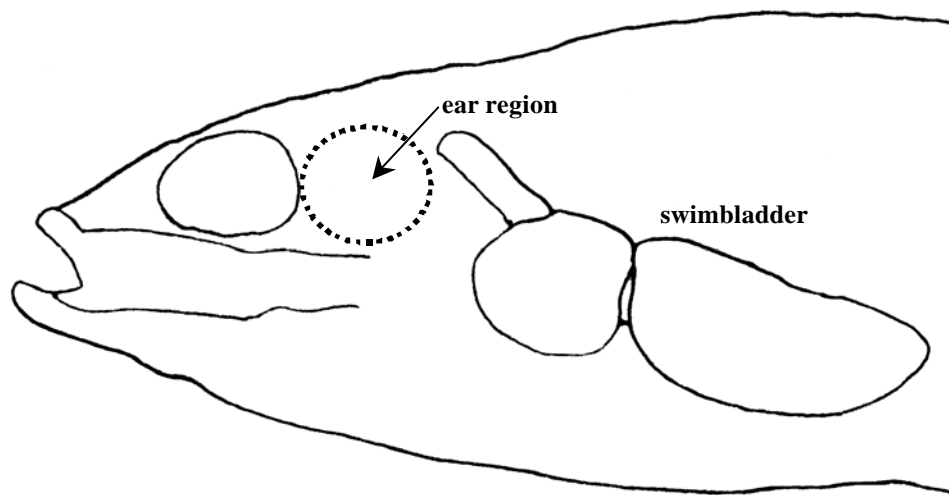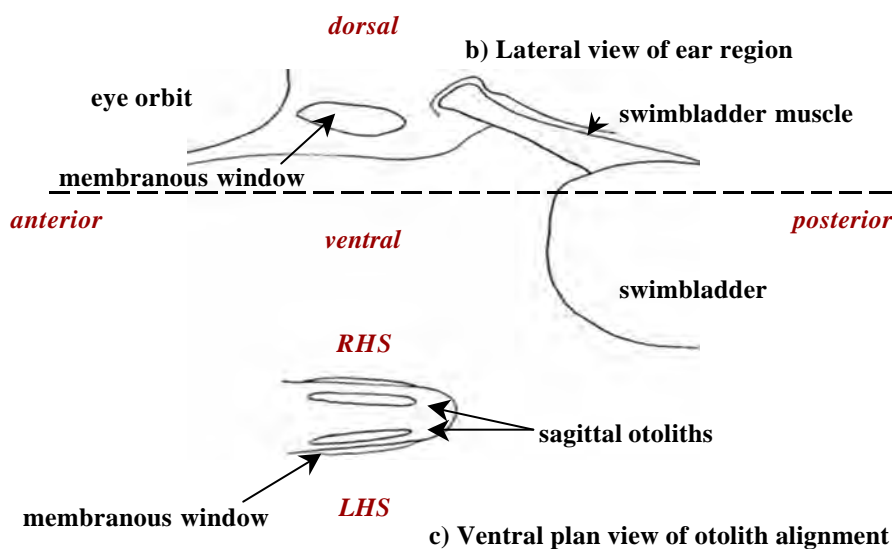
c) Ventral plan view of otolith alignment

Figure 66 (**a top**) Cut away view of *Terapon theraps* showing location of ear structures. This species has extrinsic sound producing muscles at the anterior swim bladder end.; (**b middle**) Lateral view of forward end of swim bladder and 'membranous window' which overly otolith; (**c bottom**) Ventral view of sagittal otolith layout. The otolith-macula compartment is filled with watery fluid. For the pink snapper discussed below the hair-cell populated portion of the macula lay along the long axis of the otolith on the inner side.

A full sagittal macula taken from a pink snapper is shown on Figure 67 (top). The hair cell populated region lies across the centre of the image, as shown by the outline (containing boxes) in the lower plot of Figure 67. To ascertain the extent of any damage a grid of 23,500 μm^2 squares was established across the hair-cell populated region, as shown in Figure 67 (bottom). Each square was scanned for possible damage to hair-cells and surrounding stem cells.

The pink snapper macula fitted into a groove along the inner edge of the otolith. An image of this groove is shown on Figure 68 (top). A higher magnification of a section within this groove is shown on Figure 68 (bottom). The crystalline structure of the otolith can be seen.
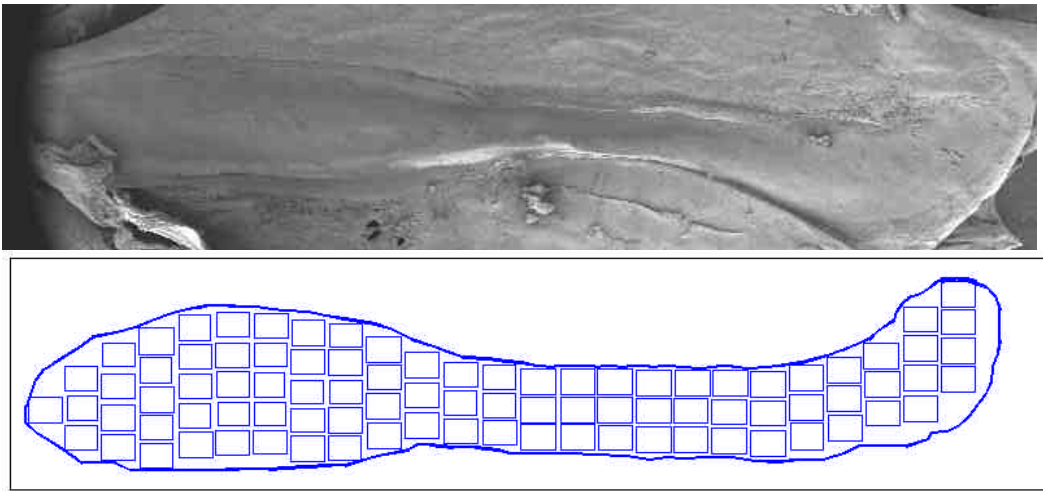
Figure 67: (**top**) SEM image of whole macula with hair cell populated region lying within boxed region (pink snapper *Chrysophrys auratus*); (**bottom**) Layout of grids setup to sample for damage.

Several configurations of hair cell bundles were present on each macula (as described by Popper and Fay, 1999). Obvious differences were the length of the ciliary bundles, with hair-cells on the periphery of the populated region having long stereocilia, while those on the inner portion of the populated region were much shorter. An SEM image from a control *Epinephelus fasciatus* of trial 9 (no previous air-gun exposure), with un-damaged hair cells and a region of the macula showing a junction between edge hair cells with long stereocilia and hair cells with intermediated length stereocilia is shown on Figure 69 (top). These were typical images of control hair cells, which appeared mostly erect with the ciliary bundles lying in a neat line.

We were initially unsure if damage would occur to the hair cells. Consequently we did not know how we could quantify any hair cell damage. Upon examination of several exposed specimens it became apparent that the presence of what appeared to be completely ablated cells was a suggestion of a damaged region of the macula. A SEM image of macula regions showing ablated cells are shown on Figure 70 for pink snapper of trial 13. It appears that several hair-cells have been completely removed from the macula. Surrounding hair cells also appear to be damaged. Many look 'squashed' with the ciliary bundles flattened against the macula, or the ciliary bundles having a 'ragged' look. Given the difficulty of quantifying the damage to hair-cells still present on the macula but which appeared to be damaged, it was decided to simply count the presence of ablated cells and use this as an indication of damage across the macula. This was comparatively easy to do and enabled an entire macula to be scanned using the grid pattern of Figure 67 (bottom). It must be realised in this analysis that the counts of ablated hair-cells given below are potentially indicative of wider damage to that particular macula region, in that hair-cells which remained in that region may not have been fully functional.

Counts of the presence of ablated cells in the 23,500 μm^2 grid configuration shown on Figure 67 (bottom) were made using five control sagittal macula and five exposed sagittal macula from pink snapper of trial 13. Each set of five macula used three fish, with a left and right macula used from two individuals and a left macula only used from the third specimen. A comparison of the mean value per grid location, for control and exposed ablated cell counts is shown on Figure 71. The sample grid is shown at the figure top, the ablated cell counts from the control group in the middle and the ablated cells from the exposed group on the bottom, with the colour scale for middle and bottom plots at the very bottom. It appears that the macula of exposed fish have considerably more regions of damage, in that localised regions of ablated hair

cells occur. It is possible that in these regions remaining hair-cells have suffered damage and may be functionally impaired. The damage seems to be localised to the narrow 'neck' of the hair-cell populated stripe.

There were some ablated hair cells present in the control fish, although the maximum count per grid was low. Descriptive statistics of the ablated cell counts for the five control and five exposed macula are given on Table 30. After this analysis was completed exposed fish macula were found with up to 30 pits per 23,500 μm^2 block.

	range	mean ± 95% confidence	median
control	0 - 3	0.1124 ± 0.0391	0
exposed	0 - 9	0.5775 ± 0.1252	0

Table 30: Descriptive statistics of ablated hair cell counts per grid, from control and exposed pink snapper of trial 13.

Using a two tailed t test to compare the number of ablated cells per 23,500 μm^2 grid (89 sections) between control and exposed fish, gave a highly significant result with $p \ll 0.001$, implying that the number of ablated cells on the exposed macula was significantly greater than on the control macula. Although the maximum number of ablated cells per grid shown on Table 30 is low (maximum of 9 cells per 23,500 μm^2 in the five exposed macula) it must be realised that the presence of ablated cells is believed indicative of wider damage.

As stated above, the trials were run as approach departures of the operating air-gun with the intention of elucidating behavioural changes at a given air-gun level. Thus the precise level or time of exposure required to produce the damage seen, could not be determined.

The maximum air-gun level received by fish in trial 13 was 182 dB re 1 μPa^2.s (Table 25), which is equivalent to 193 dB re 1μPa mean squared pressure or 212 dB re 1μPa peak to peak level. The distribution of air-gun shots received at the cage is shown on Figure 72. At this stage, assuming the damage is real, then the exact level and/or number of shots through time required to produce the damage seen, is not known.

The pink snapper used in trial 14 were those previously exposed in trial 13. The behavioural results of trial 13 differed substantially from those of trial 14. From Figure 60-5, (trial 13 behavioural data) it can be seen that shortly after the first presentation of air-gun noise the pink snapper went completely out of view of the cameras, as they moved to the bottom of the cage. On the second presentation of air-gun signals they stayed in view but were exclusively in the lower portion of the cage. During trial 14 (Figure 60-6), 58 days later the same pink snapper showed virtually no reaction to three presentations of air-gun noise to similar maximum levels. This apparent lack of response may have been due to either habituation or possible damage to hearing structures. Although the examination of the ears from fish of trial 14 was not complete at the time of writing this document, all trial 14 fish examined, including controls (with controls being those exposed in trial 13 but sampled before trial 14 exposures) showed evidence of the pits similar to those of Figure 70. Unlike all other fish examined, all trial 14 fish sagittal macula viewed had some evidence of a 'meshwork' of fine filaments across it. An example of the filaments of this 'meshwork' is shown on Figure 73 from a pink snapper sampled immediately after the completion of trial 14. The filaments are believed to be too fine to be fungal or bacterial (rods) contamination and are speculated to be a part of an inflammatory repair response.
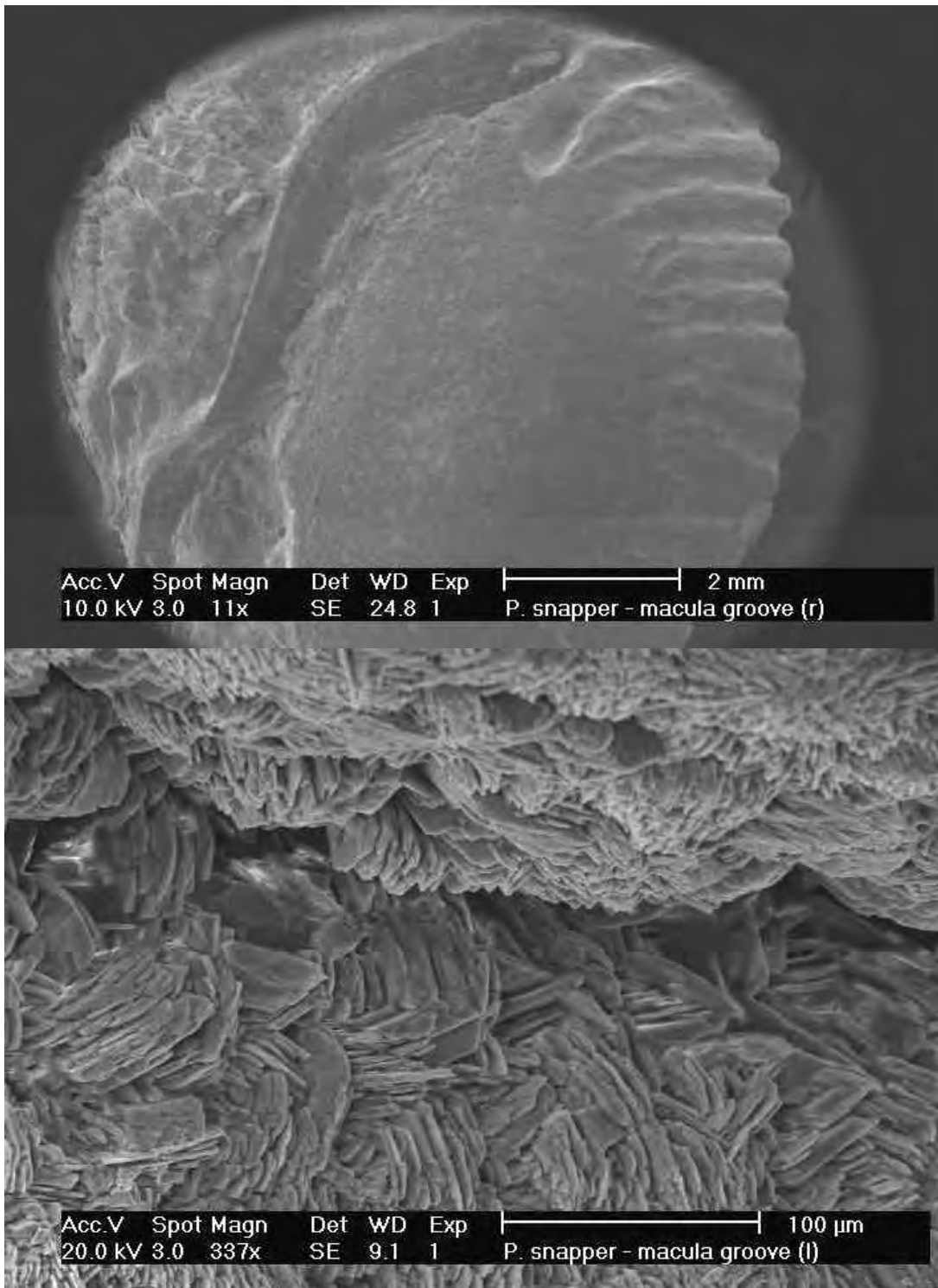
Figure 68: (**top**) Inside edge of pink snapper sagittal otolith showing groove in which macula lies. (**bottom**) Close up of the otolith surface showing the inner groove edge and the crystalline structure.
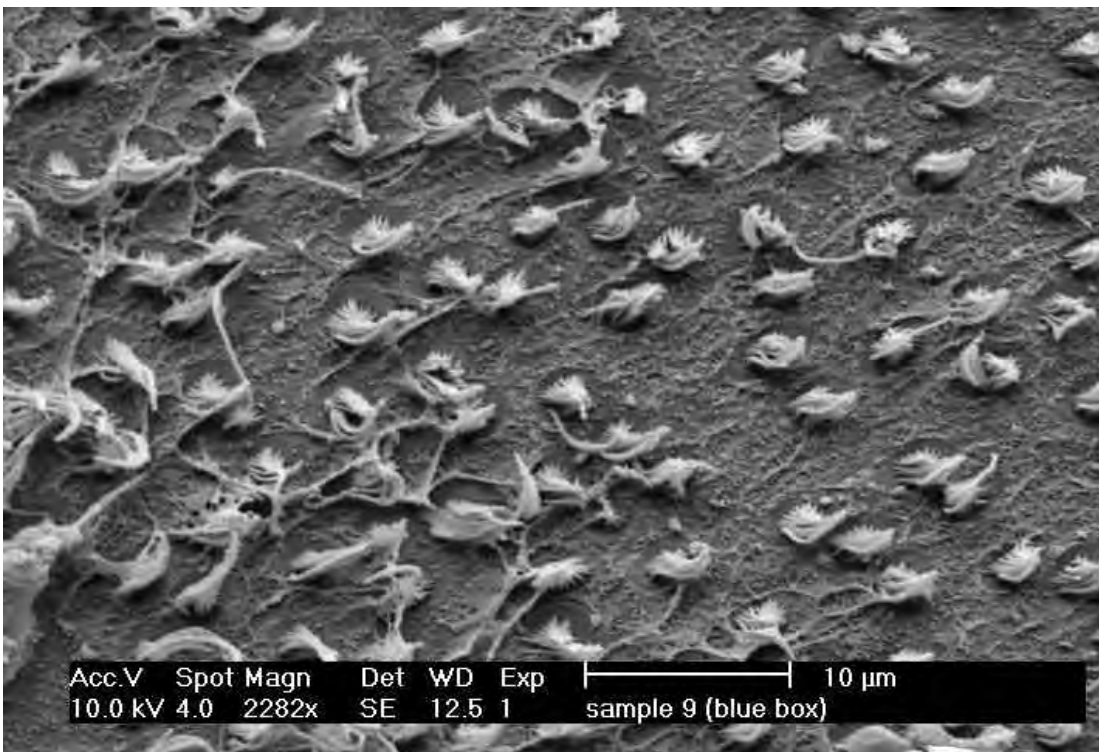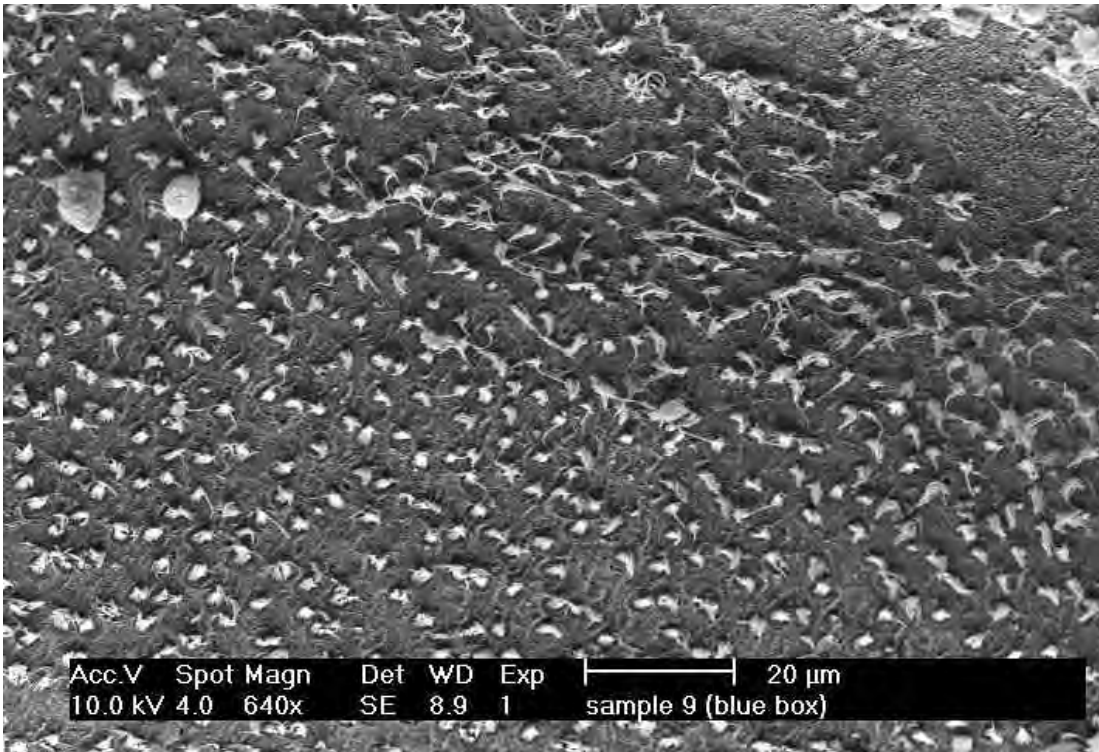
Figure 69: (**top**) Control fish macula (*Epinephelus fasciatus,* from trial 9) showing macula edge with change of hair cell types from medium to long primary cilia with no damage evident. (**bottom**) Close up of area of macula with medium length primary cilia, again with no damage evident.
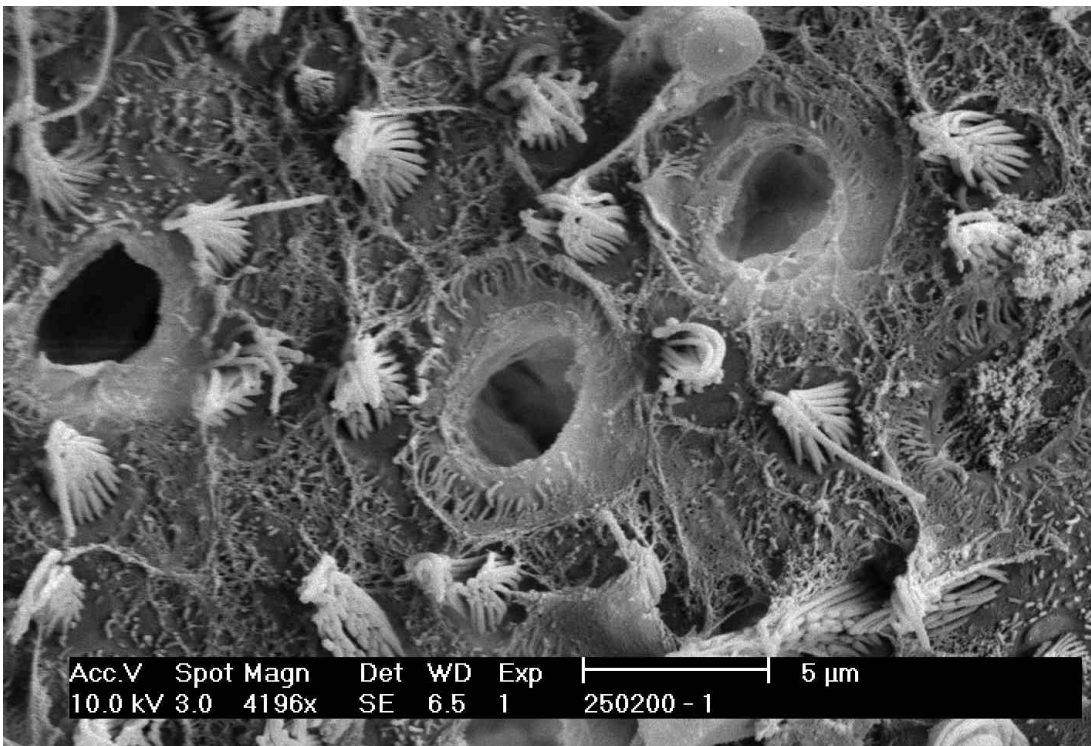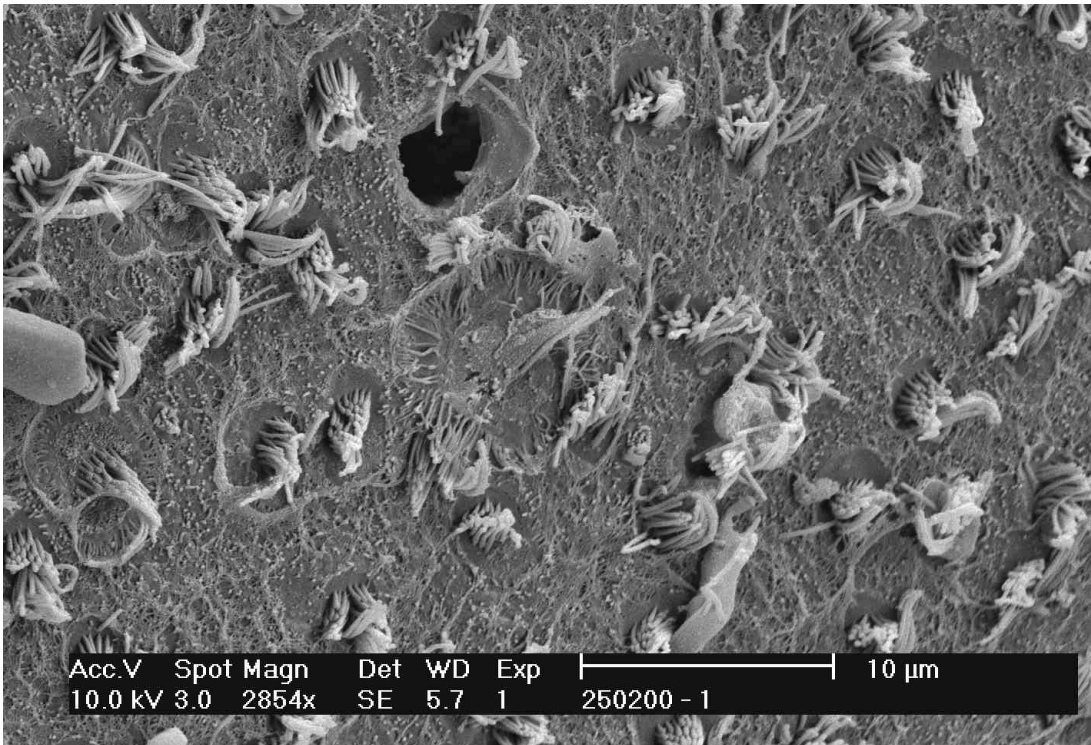
Figure 70: (**top**) Damaged region of macula showing pit and 'squashed' hair cells from exposed pink snapper (*Chrysophrys auratus*, sampled immediately after exposure). (**bottom**) Higher magnification of several pits, from same sample as top image.
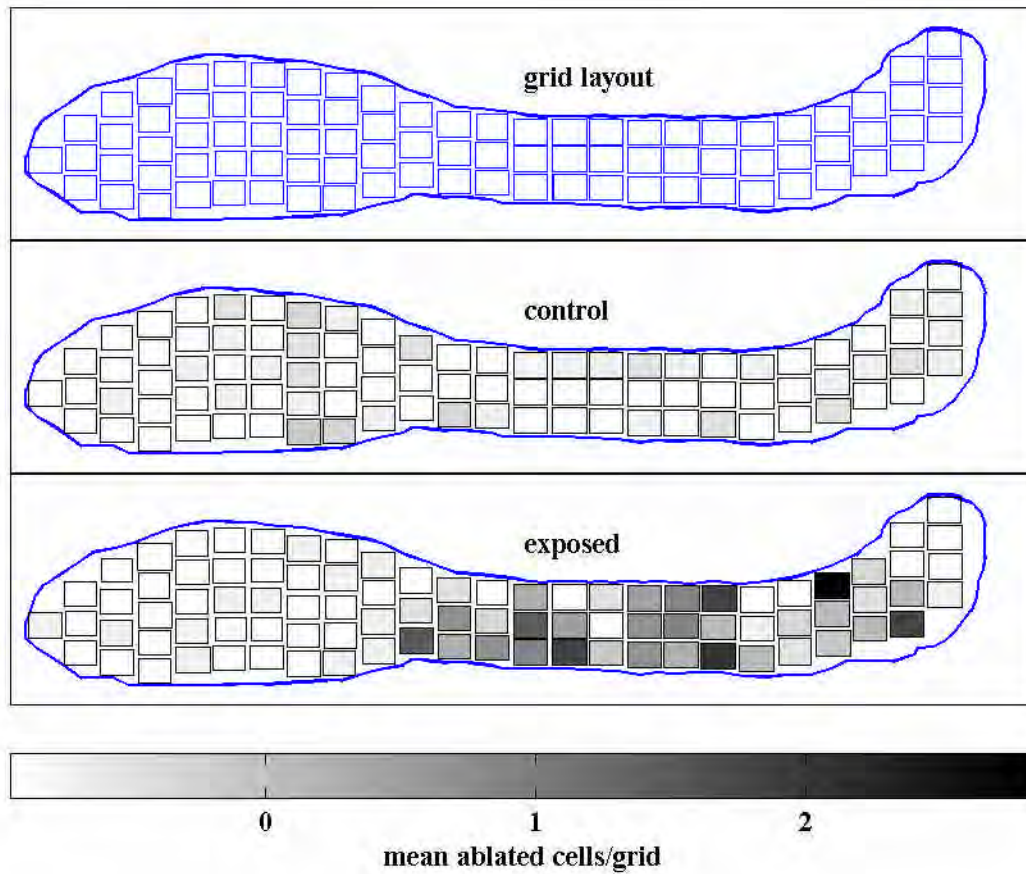
Figure 71: (**top**) Grid of macula regions scanned for ablated hair cells; (**middle**) Grid showing colour coded mean number of ablated hair-cells per grid for control pink snapper (*C. auratus*); (**bottom**) Grid showing colour coded mean number of ablated hair cells per grid for exposed pink snapper. All specimens were from trial 13, control and exposed ablated cell counts shown used mean of five macula each. Colour bar at bottom for middle and bottom plots.
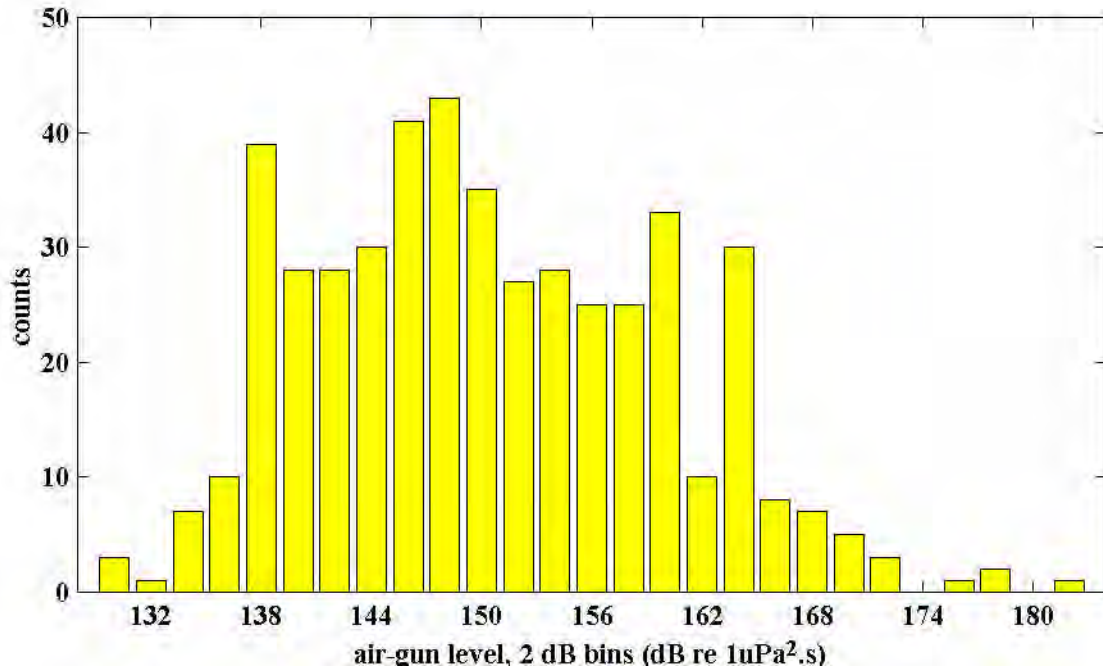
Figure 72: Distribution of received air-gun levels as received at the cage for trial 13, using hydrophone at the centre of the cage side facing the air-gun passage and at 3 m depth.
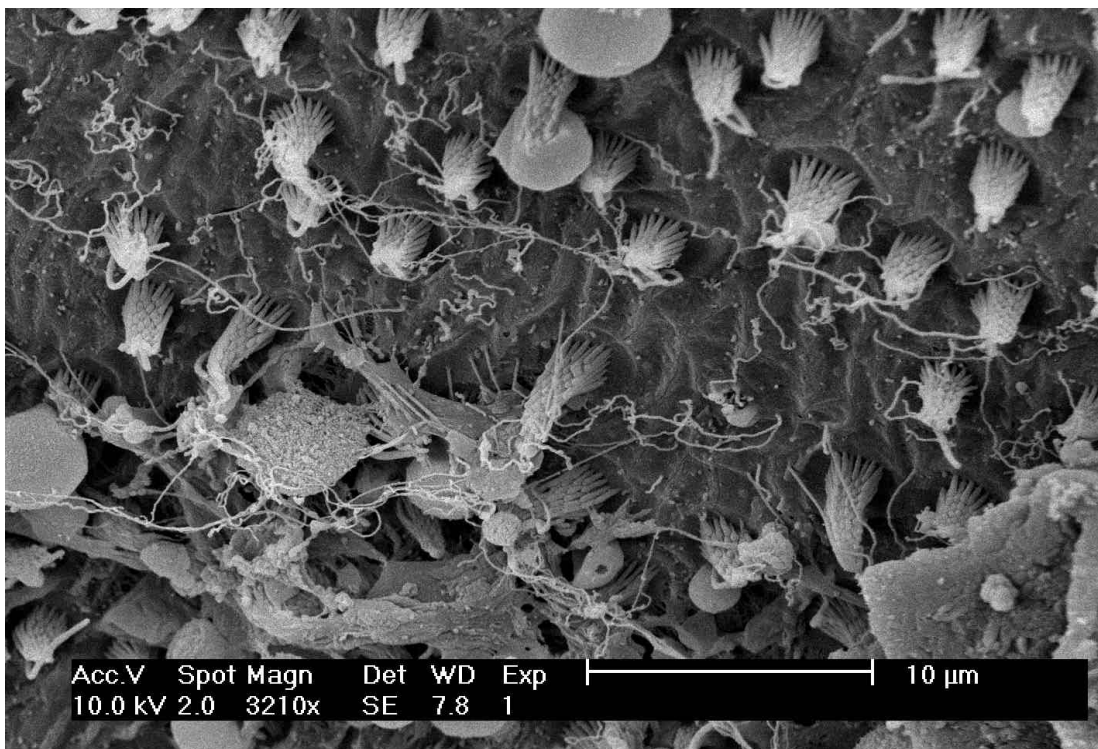
Figure 73: Pink snapper macula sampled immediately after trial 14, and which had also been exposed 58 days previously in trial 13, showing a light covering of fine filaments ('meshwork') believed to be a part of an inflammatory repair process.

2.4.5 Otolith motion modelling

The response of fish hearing systems was modelled using a simple harmonic oscillator equation to describe otolith motion. Equations and constants were derived primarily from De Vries (1950), Kalmijn (1988), Karlsen (1992) and Fletcher (1992). The modelling was done to provide some insight into how a range of different sized otoliths respond to applied air-gun signals of varying amplitude and frequency content. These results could then be compared against the experimental exposures carried out.

The model produced and discussed below considers the otolith response to the directly impinging sound wave only. For those fish with a swim bladder present but not directly coupled to the otolith, some energy from the impinging sound wave may be re-radiated by the swim bladder back to the otolith. This will depend on the distance between otolith and swimbladder and any mechanical systems between the two for enhancing or blocking the re-transmitted otolith signal. For most of these fishes and fish without a swimbladder it would be expected that the mechanical response of the otolith would be dominated by the directly impinging sound wave. Fishes with specialist hearing systems physically couple their swim bladders or a gas bubble to an otolith pair, usually with significant mechanical gain (see Rogers et al 1988 or Schuijf and Buwalda 1980). These specialist fishes may be far more responsive to sound waves than those non specialist fishes with no swim bladder-otolith coupling. Hence the following argument does not apply to specialist hearing fishes. The model also does not consider the relative volume of the otolith compared to the volume of the chamber in which it is housed, or the shape of the otolith. The volume difference between the otolith and its surrounding chamber (which is filled with fluid) may range from very small, allowing the otolith little scope for movement, to very large. The shapes of otoliths also vary enormously and this may have some bearing on the otolith motion as the effective otolith spring constant (k below) may differ between spherical otoliths and flat otoliths aligned with the flat face facing the impinging sound wave. But, given these caveats, the model presented below is believed to give a first approximation of the response of fish otoliths to applied air-gun signals for many fishes.

To a first approximation, the movement of the otolith relative to the macula can be modelled as a simple harmonic oscillator with an elastic restoring force (spring) and damping (de Vries 1950, Kalmijn 1988, Karlsen 1992). An outline of this configuration with the frame of reference is shown on Figure 74.

Using the simple harmonic oscillator approach results in a second order differential equation of the form:

Equation 17 $\qquad m_e x'' + b x' + k x = -F(t)$

where

Equation 18 $\qquad F(t) = m_o \left[\dfrac{(\mathbf{r}_o - \mathbf{r}_w)}{\mathbf{r}_o} \right] u'$

and:

m_o = otolith mass

$\mathbf{r}_o$ = density otolith (assumed 3000 kg/m^3)

$\mathbf{r}_w$ = density sea water (assumed 1000 kg/m^3)

u' = particle acceleration (differential of particle velocity)

m_e = effective mass of the otolith plus the inertia of the water [otolithic membrane] which must also be accelerated when the otolith moves; with m_e approximately 1.3 m_o (de Vries, 1950). Note that Karlsen (1992) uses m_e as the effective mass of the otolith and entrained endolymph fluid.

b = viscous drag force on the moving otolith, per unit velocity

k = restoring spring force per unit displacement

x = relative otolith-macula displacement
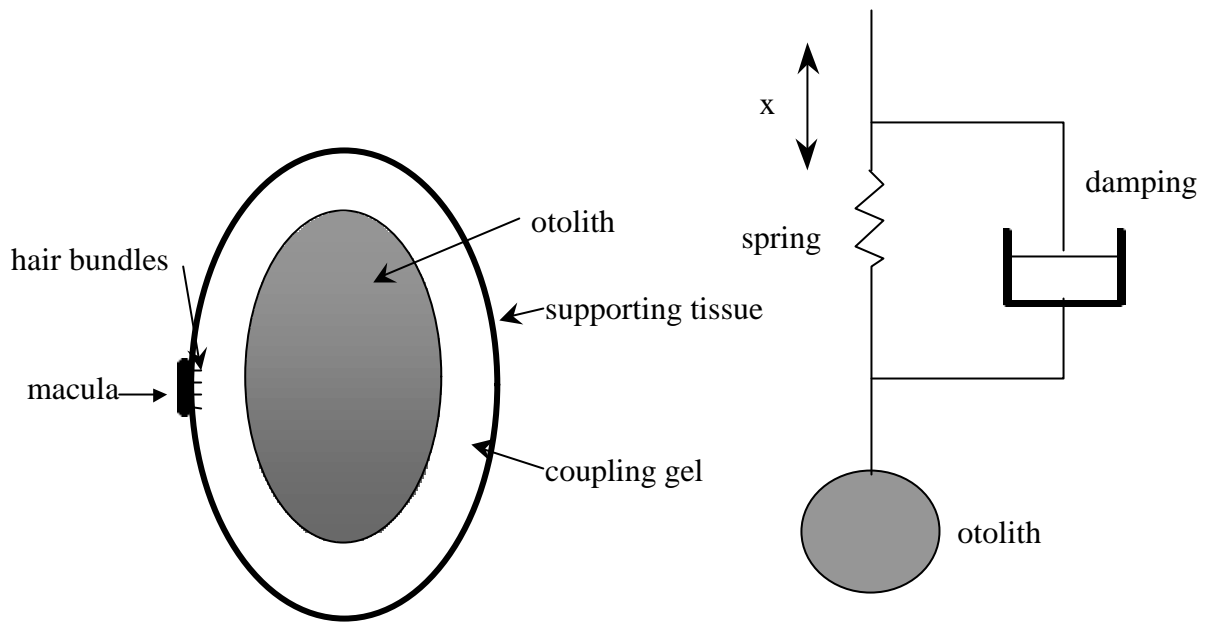
Figure 74: Schematic diagram of fish otolith, macula with representative hair cells (left), and approach used in modelling otolith motion (right).

The derivation of the otolith equations of motion (Equation 17, Equation 18) are given in Appendix 4. The second order differential equation can be rearranged to form a system of two first order equations, as per:

Equation 19 $\qquad x_1{}' = x_2$

and

Equation 20 $\qquad x_2{}' = \left(\dfrac{-k}{m_e}\right)x_1 - \left(\dfrac{b}{m_e}\right)x_2 - \dfrac{F(t)}{m_e}$

These were solved numerically in the Matlab environment, using 4th or 5th order Runge-Kutta iterative methods, to give otolith displacement and velocity as functions of time. Otolith acceleration was determined from the otolith velocity output vector.

Constants used were

b 0.015 kg/s (0.15 cgs units, de Vries;1950)

k 1.3 N/m (1300 dyne/cm, de Vries; 1950)

m_e 1.3 m_o (de Vries; 1950)

m_o ranged from 5 - 155 mg in 10 mg steps. These values encompassed the otolith mass range of fish species tested.

Air-gun signal inputs:

Air-gun signals were recorded and captured as per methods (section 1.6.1), then fed to the model program as time versus pressure files. Pressure values were used to obtain particle velocities versus time, by using the relationship:

Equation 21 $$z = \frac{P}{u} = \boldsymbol{r}.c$$

where P = pressure (Pa)
u = particle velocity (m/s)

ie $u = P/z$
and $z = 1 \cdot 48 \times 10^6$ Pa.s/m for water

Differentiation with respect to time then gave particle acceleration versus time. In order to use this to obtain the driving force in the simple harmonic oscillator differential equation, linear interpolation was used to evaluate acceleration at a given time.

A sequence of input air-gun shots were chosen from Jervoise Bay approach trials. These were taken from trial 13 (Figure 60- 5) and were each 4096 samples at 192×10^{-6} s sample rate (5208 Hz). Shots 80-130 were used These represented an approach from 13:05:05-13:18:13 (12:28 min) with the signal level starting at 139 dB re 1 μPa^2.s, peaking at 179 dB re 1 μPa^2.s (shot 126), and dropping to 161 dB re 1 μPa^2.s.

Model output

The model predicted that smaller otoliths were more easily driven than larger otoliths and tended to track the input signal better. Figure 75 displays this by comparing the pressure waveform of an input air-gun signal with calculated otolith displacement for the extremes of otolith mass used in the modelling, 5 and 155 mg. For the different otolith masses there are considerable differences in displacements and response time. The heavier otolith can be seen to continue oscillating once set into motion, whereas the lighter otolith quickly returns to the rest position.

Inputting the air-gun signals to the model resulted in maximum otolith displacements (of the absolute value of displacement) as shown in Figure 76. It can be seen that although there are some peaks in maximum displacement below an input signal of approximately 160 dB re 1 μPa^2.s, probably due to resonances in the otolith response, the most dramatic response occurs for all otolith sizes at levels above approximately 160 dB re 1 μPa^2.s. Above this level the maximum otolith displacement rapidly increases, with the mean maximum displacement increasing 11 fold over the range of input signals 160 - 179 dB re 1 μPa^2.s. Thus it appears that above a threshold the fish otolith response to an applied air-gun signal can be expected to rapidly increase.
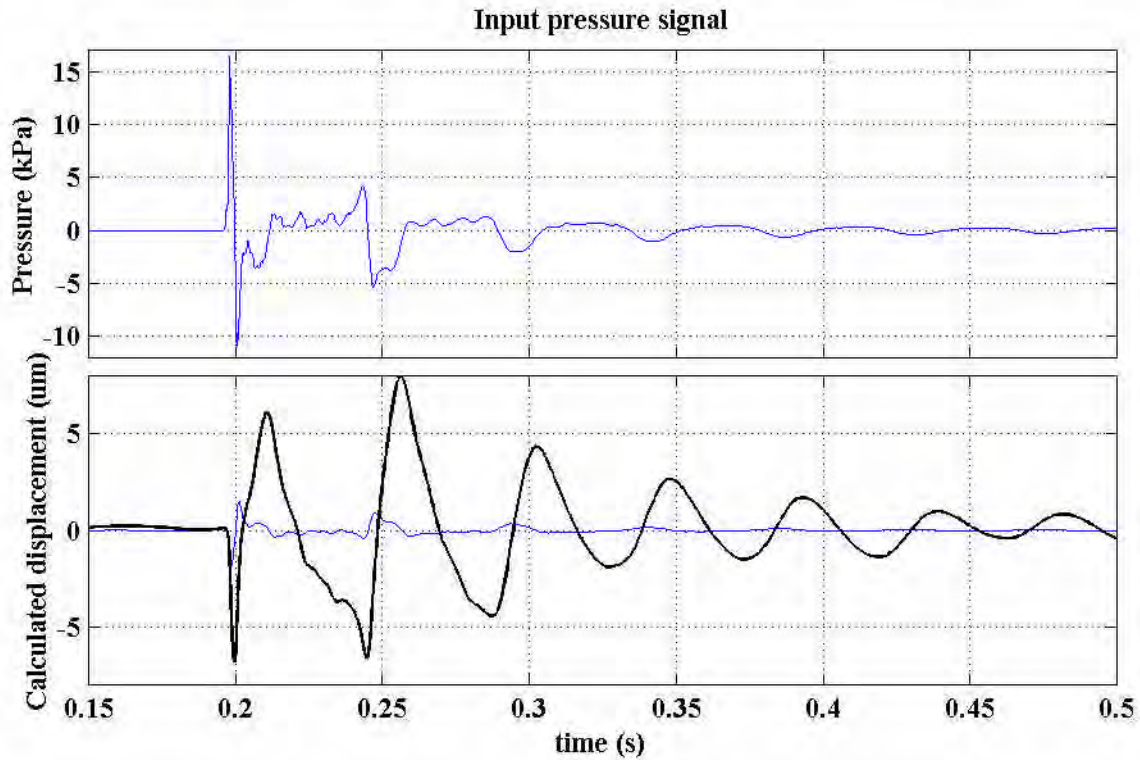
Figure 75: (**top**) Input waveform of air-gun signal. (**bottom**): Calculated otolith displacement for 5 mg (thin line) and 155 mg (thick line) otoliths.
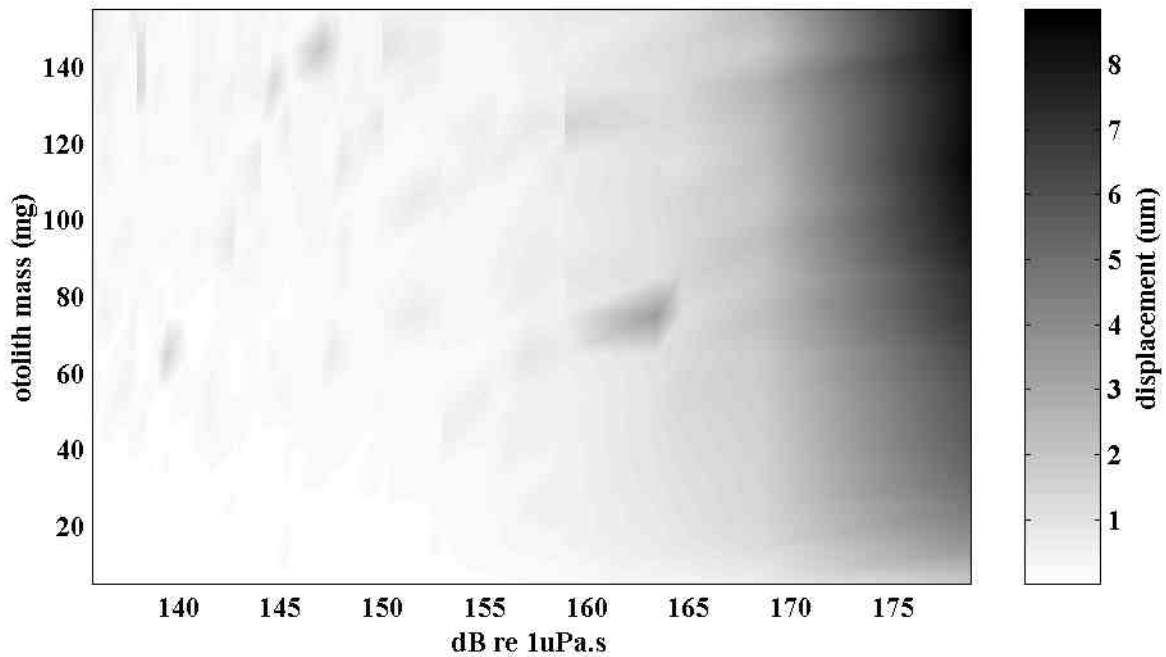
Figure 76: Maximum otolith displacement output by otolith motion model for unfiltered air-gun signals as input, for otoliths from 5-155 mg mass.

The air-gun signal level at which the otolith response rapidly increases can be seen by looking along the maximum otolith displacement curves for separate otolith masses. This is shown in Figure 77. The point at which the maximum displacement begins to rapidly increase lies between 155-160 dB re 1 μPa^2.s
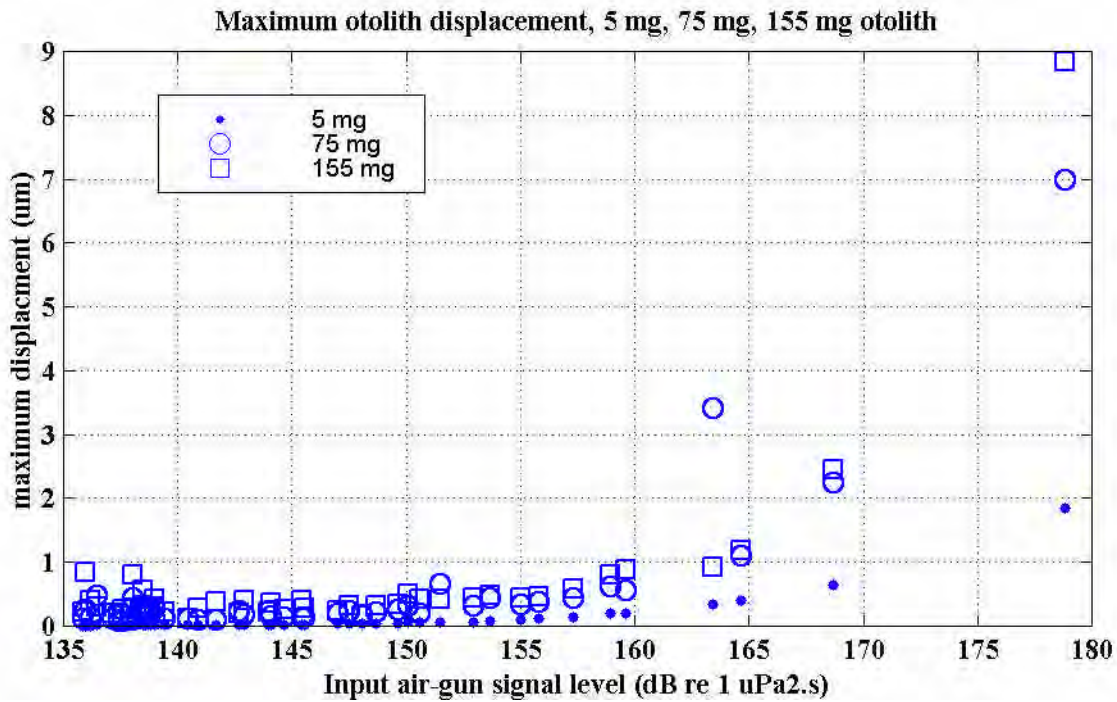
Figure 77: Calculated maximum otolith displacement for three otolith masses.

The maximum shearing forces at the at the macula sensory hairs could be expected to occur when the otolith is driven in the opposite direction to the macula (that is the otolith motion is being driven 90º out of phase compared to the macula). The greatest potential for damage may occur for this type of motion, and/or may also involve the alignment of the shearing forces along the direction of greatest sensitivity of the hair cell ciliary bundles. Hair cell bundles on fish macula are known to be polarised, with regular patterns of common ciliary bundle directions (Popper and Fay, 1999). It may be conceivable that over stimulation resulting by a sound source from a specified direction may result in damage to specific regions of the macula, these corresponding to a specific hair cell orientation pattern and perhaps hair cell type.

Highest hearing sensitivity and the potential for pathological stress would be expected at highest hair cell shearing forces. These would occur at the higher levels of the absolute value of the otolith maximum displacement, as shown on Figure 76 or Figure 77. It appears that larger otoliths are more susceptible than smaller otoliths, given the greater maximum displacements involved.

As well as the maximum displacements experienced, the time of highest stimulation would also play an important role in determining the potential for pathological damage and the behavioural response to the input signal. In most vertebrate nervous systems, input from the hearing system is normally processed in a statistical fashion, with time averaging a critical factor. To compare the amount of stimulation through time for the model output, the total time the absolute value of the otolith displacement vector (as produced by the input air-gun signal) was above a threshold was calculated. The threshold was chosen as the mean maximum-displacement value across the 16 otolith masses used, at an air-gun signal of 155 dB re 1 μPa^2.s. The resulting curve, calculated for the highest air-gun signal input to the model (shot 126 of level 179 dB re 1 μPa^2.s), is shown in Figure 78. Otoliths above 60 mg appear to be stimulated for longer periods than otoliths of lower mass.
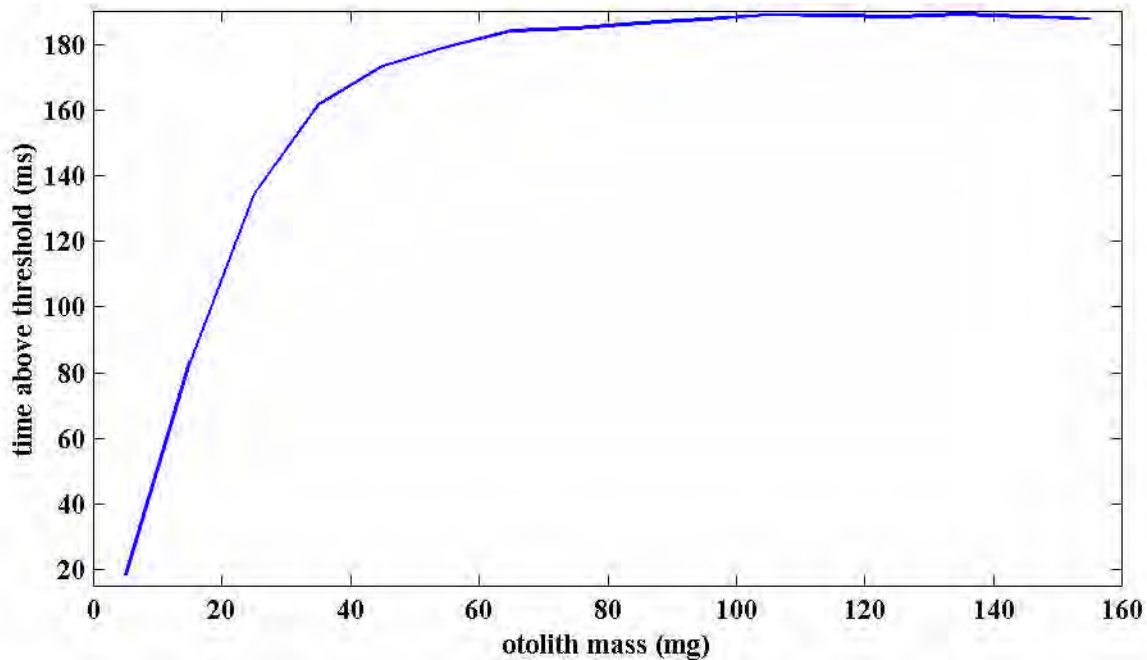
Figure 78: Time otolith above a threshold displacement value, as given by 155 dB re 1 μPa2.s air-gun signal averaged across all otolith masses, for a range of otolith sizes for an air-gun signal of level 179 dB re 1μPa^2.s

The input signals were then passed to the modelling program in a filtered form to check on the frequency response of the modelled otolith system. Signals were filtered with high and/or low pass, 5th order Butterworth filters, as per 0-150 Hz, 150-300 Hz, 300-450 Hz and 450-600 Hz. For the two model runs up to 300 Hz the results of otolith motion were similar in shape to those obtained from the unfiltered signal. For filtered signals above 300 Hz the maximum displacement values became linear with input signal level and were of much lower amplitude than the runs containing the low frequency energy. Localised spikes in the maximum displacement plots became increasingly obvious as the overall maximum displacement amplitudes decreased.

To display the effect of frequency on the modelled otolith response, the frequency content of air-gun shot 126 is displayed on Figure 79 with the maximum otolith displacement for this shot selectively filtered, shown on Figure 80. The filtered air-gun signals which pass the low frequency energy (< 150 Hz) best matched the unfiltered input signal. Thus it appears that most of the otolith response is driven by the low frequency portion of the air-gun signal.

SUMMARY

A simple model based an a damped harmonic oscillator was developed to predict fish otolith response to an impinging air-gun signal. The form of the model, derivation of, and constants were obtained primarily from De Vries, (1950); Kalmijn, (1988); Karlsen, (1992); and Fletcher (1992).The model only considered stimulation by the impinging sound wave, and did not take into account re-scattered energy from a nearby swim bladder, or direct coupling of swim bladder to ear. The model assumed that the input parameters used remain constant for different sized otolith systems (or through growth).
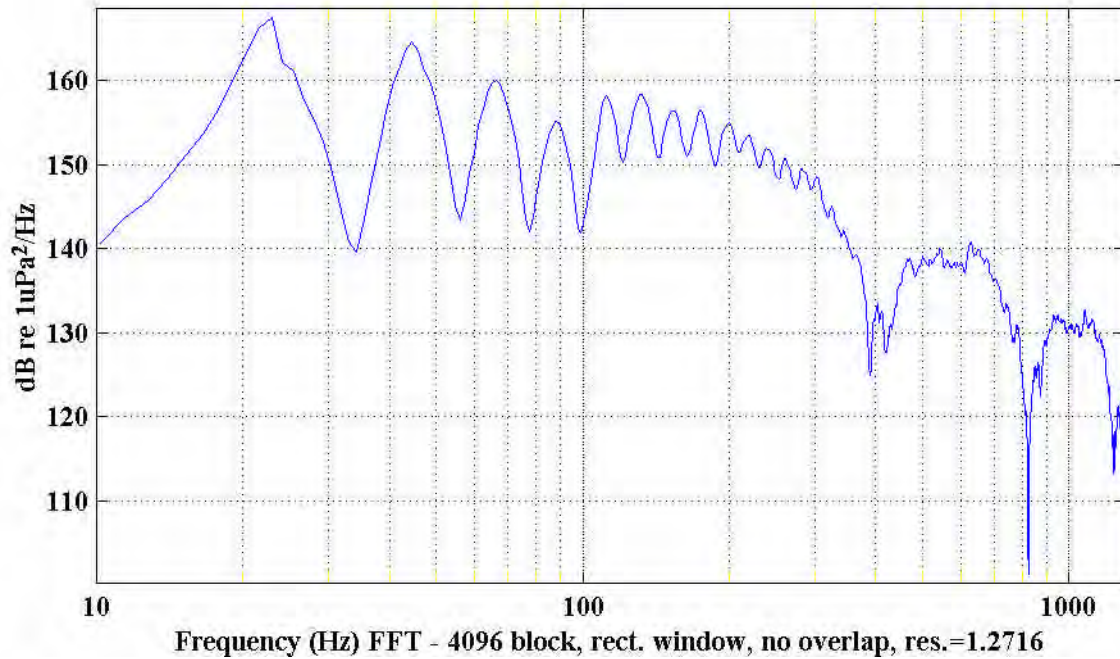
Figure 79: Spectral content of signal 126 (maximum signal fed into exposure model).

Modeled max. otolith displacment, filtered input, shot 126
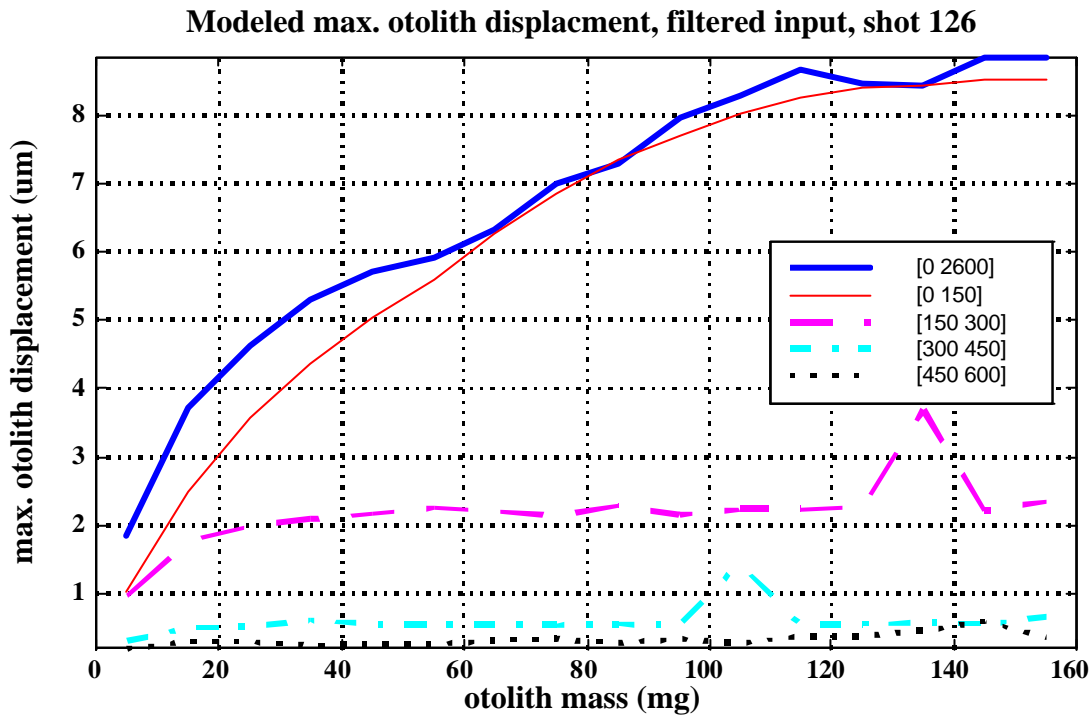
Figure 80: Calculated maximum otolith displacements for unfiltered and filtered air-gun signal from shot 126 of input file (179 dB re 1 μPa^2.s level). Legend gives lower and upper filter boundaries (Hz), 0-2600 Hz is unfiltered input signal.

The results showed that:

- The model output predicted that the otolith mechanical response to applied air-gun signals begins to increase rapidly above an input air-gun level of between 155-160 dB re 1 μPa^2.s. This implies that the fishes behavioural response and any potential for pathological damage will increase accordingly above this input signal level
- Smaller otoliths tended to track the incoming signal better than larger otoliths. In contrast, once larger

161

otoliths were set into motion they oscillated for longer periods with greater maximum displacements.

- Otolith motion was mass dependant. Otolith maximum displacement, velocity or acceleration reached higher maximum levels for longer periods for larger otoliths.
- By selectively filtering the input air-gun signals, it appears that otolith motion was driven primarily by the portion of signal energy less than 300 Hz. This corresponded to the maximum energy content of the unfiltered applied air-gun signals.

2.5 Squid response to nearby air-gun exposure (R.D. McCauley, J. Fewtrell)

Three trials were carried out at the Jervoise Bay facility with squid (*Sepioteuthis australis*) and cuttlefish, primarily to gauge behavioural effects to nearby air-gun operations. Trial methods were as per section 1.3. Trial 5 used the air-gun operated from the moored pontoon, trials 10 and 11 used the air-gun operated from the towed pontoon thus had the larger dynamic range. The squid of trial 10 were exposed again four days later, in trial 11. The source and acclimation history of animals for each trial are given in Table 31 and the details of the air-gun exposures in Table 32.

Trial	Species	Number of squid	Mean squid size (mm)	acclimation days in large cage	squid source	camera depth during trial (m)
5	squid cuttlefish	12 2	166 ± 23	7-18 16	jigging jigging	2
10	squid	19	185 ± 14[1]	7-10	jigging	2.5
11	squid	19	185 ± 14	11-14	trial 10	1.5

Table 31:Number, size (mantle length ± 95% confidence limits), acclimation history and source of animals used in squid trials. Roughly equal numbers of male and female animals were present in all trials. Superscripts: 1/ size inferred from squid recovered in trial 11.

Trial	run	start level/time	minimum level/time	maximum level/time	end level/time
5	1	163 / 11:29:03	159 / 11:29:23	170 / 12:02:11	163 / 12:27:59
	2	163 / 13:54:24	161 / 14:45:21	168 / 14:24:52	162 / 14:54:01
10	1	136 / 12:12:36	136 / 12:12:50	178 / 12:55:23	151 / 12:59:33
	2	146 / 14:10:50	144 / 14:11:29	178 / 14:18:28	149 / 14:32:54
11	1	144 / 11:21:32	144 / 11:21:50	180 / 11:47:10	147 / 12:08:09
	2	146 / 13:20:13	144 / 13:34:55	184 / 13:27:25	144 / 13:59:25

Table 32: Details of air-gun exposures for each set of consecutive air-gun operations during squid trials. Air-gun units are equivalent energy, dB re 1 μPa^2.s.

The statocyst organs of several control and exposed squid were preserved for SEM preparation. There is little in the literature to indicate that squid can hear. During the trials described below several squid made an unequivocal response to an air-gun signal in the acoustic far-field, in the form of a startle response. The most probable cue was the noise of the air-gun pulse. The most likely receptor organ in squid for a hearing response is the statocyst system, which although vastly different in detail to the fish otolith system, is roughly analogous in that the statocyst system could utilise differential motion between calcareous stones (the statocysts) and underlying hair cells, to produce a nervous response. Thus it is intended to scan the hair-cell receptor membranes of the statocyst organs for possible pathological damage. At the time of writing this work had not been carried out, thus the results of this study will not be discussed further.

During acclimation periods the squid were found to very quickly associate the noise of the 4.3 m outboard powered dinghy used to service the cage with feeding and a strong association established where the squid would appear alongside the dinghy when it pulled up to the cage. This association was seen to occur immediately after the exposures of trials 10 and 11 whence the squid were fed. A strong hierarchy also existed amongst the squid during feeding events, with smaller animals always holding back from the larger

ones.

For each trial behaviours were scored as per the methods (section 1.3.2) using the codes given in appendix 1. Codes were as per the fish trials with the addition of codes for: firing ink sacs; the direction of swimming, since squid can adjust their siphon orientation so as to swim forwards or backwards; and colouration. The scored behavioural data is shown on Figure 81 for camera 1 of each trial.

During trial 10 and after the first period of air-gun exposure, at least one of the squid deposited eggs onto the lines of camera 1 in the SE corner of the cage. The squid were seen to consistently approach firstly camera 2, beginning 13 minutes after the first air-gun exposure (approach over 13:14-13:50,), then to switch their attention to camera 1. They persisted in approaching camera 1 during the entire second portion of the trial (> 13:59 Figure 81 - 2, which was when the second tape of the trial began to the trial end), irrespective of the air-gun operations. At the trial conclusion a large deposit of squid eggs were found on the fastening lines of camera 1. A period of aggressive behaviour, seven minutes after the end of the second period of air-gun operations, and believed related to the egg deposition, was observed from camera 1 (Figure 81, 14:38-15:06).

As for the fish trials the squid behavioural response to nearby air-gun operations was considered as a 'startle' or alarm response, or a more subtle change in behaviour, position or movement. These are considered below.

Startle/alarm Response

During trial five with the air-gun at approximately 30 m range, the first shot of the trial (received level of 163 dB re 1 μPa^2.s) resulted in at least three squid firing their ink sacs and darting in the opposite direction to the air-gun (not all squid were in each camera field of view). Their was a perfect correlation with the onset of the first air-gun shot and the squid firing their ink sacs. This was only observed for the first shot of trial 5. Higher overall air-gun exposures were experienced in trials 10 and 11 as compared to trial 5 (Table 32), but the lower received level of the first shot and ramped nature of the air-gun signal approach in these trials must have reduced the degree of the startle/alarm response.

Persistent alarm responses in the form of squid jetting away from the air-gun source and corresponding with an air-gun shot were observed. The number of these observations increased with air-gun level. This was demonstrated using the difference ratio for *count-of-startle-responses-period/total-behavioural-counts-period*, for above air-gun threshold periods minus the similar ratio for periods with no air-gun operations, as outlined for fish in Equation 15. The difference ratios thus calculated for trials 10 and 11 which had the suitable dynamic range of air-gun levels, are shown on Figure 82. Using a *t* test to compare these mean difference ratios with expected ratios (zero or the same as measured in control periods), and reducing the degrees of freedom to account for the use of ratio data gave significant results for each trial and trials 10 and 11 combined, with $p < 0.005$. It can be seen that for each trial as the air-gun threshold was increased so did the relative proportion of startle responses recorded, and that this type of response was consistent between trials. In trial 5, which did not have a suitable signal range for a similar analysis, the relative proportion of startle responses recorded during the period of air-gun operations was higher than the similar ratio for the air-gun off period (0.071 air-gun on, no startle responses air-gun off).

Following three pages:

Figure 81: Representation of squid behaviour and movement patterns for camera 1 of trials 5, 10 and 11. Scoring is given as for fish behavioural plots with some squid specific behaviours. From top to bottom are: **squid vertical position** - dots ; **squid vertical movements** - shown by arrows; **swimming speed**; dot = idle, small arrow = swim slow, larger arrow two feathers = swim fast, largest arrow three feathers = swim very fast**; horizontal swim direction** - left slant and right slant arrows moving right-left or left to right respectively; circle for **swimming in circles**; **field of view** square for in LHS field of view; diamond for in RHS field of view; **startle responses** - small one feathered arrow = dart, larger two feathered arrow = part, larger three feathered arrow = flash expansion of school, circle = 'jerk', cross = change direction; square = fire ink sac; **school formation** - circle = loose school, plus sign = tight school, dot = most animals with dot below = some animals; **specific behaviours -** arrow one feather = approach camera, large dot = dark colouration, circle = light colouration, circle with cross in = whit spot present on mantle, diamond = squid attacking each other; **time in view** - given by bars; **air-gun level** given for each shot fired during trial. The **vertical lines** which run through the whole plot delineate the periods of air-gun operations, the vertical lines in the top plot only delineate the operation times for each video tape.

Trial 5 camera 1 Jervoise Bay sq
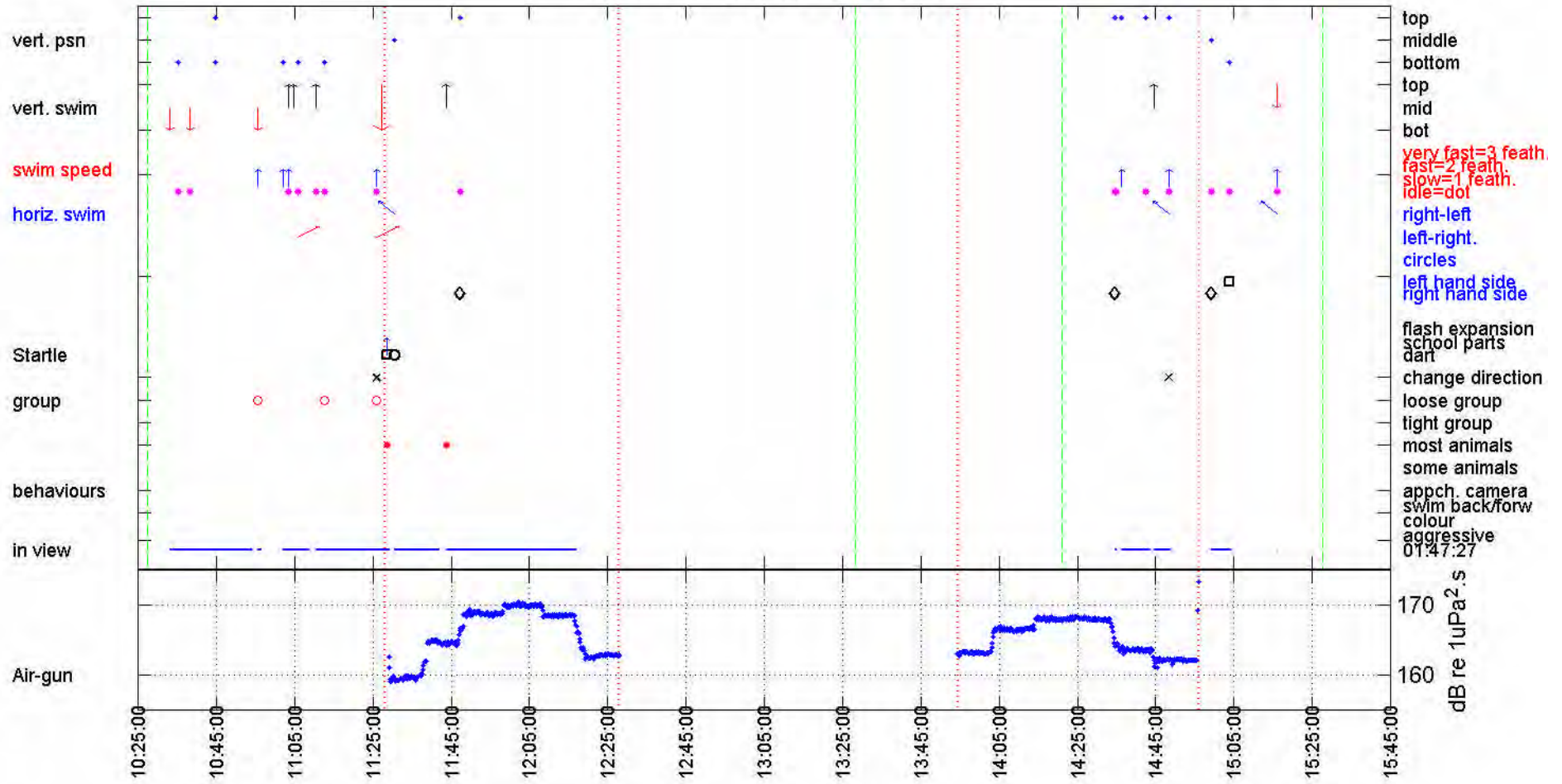
Trial 10 camera 1 squid Jervoise Bay all
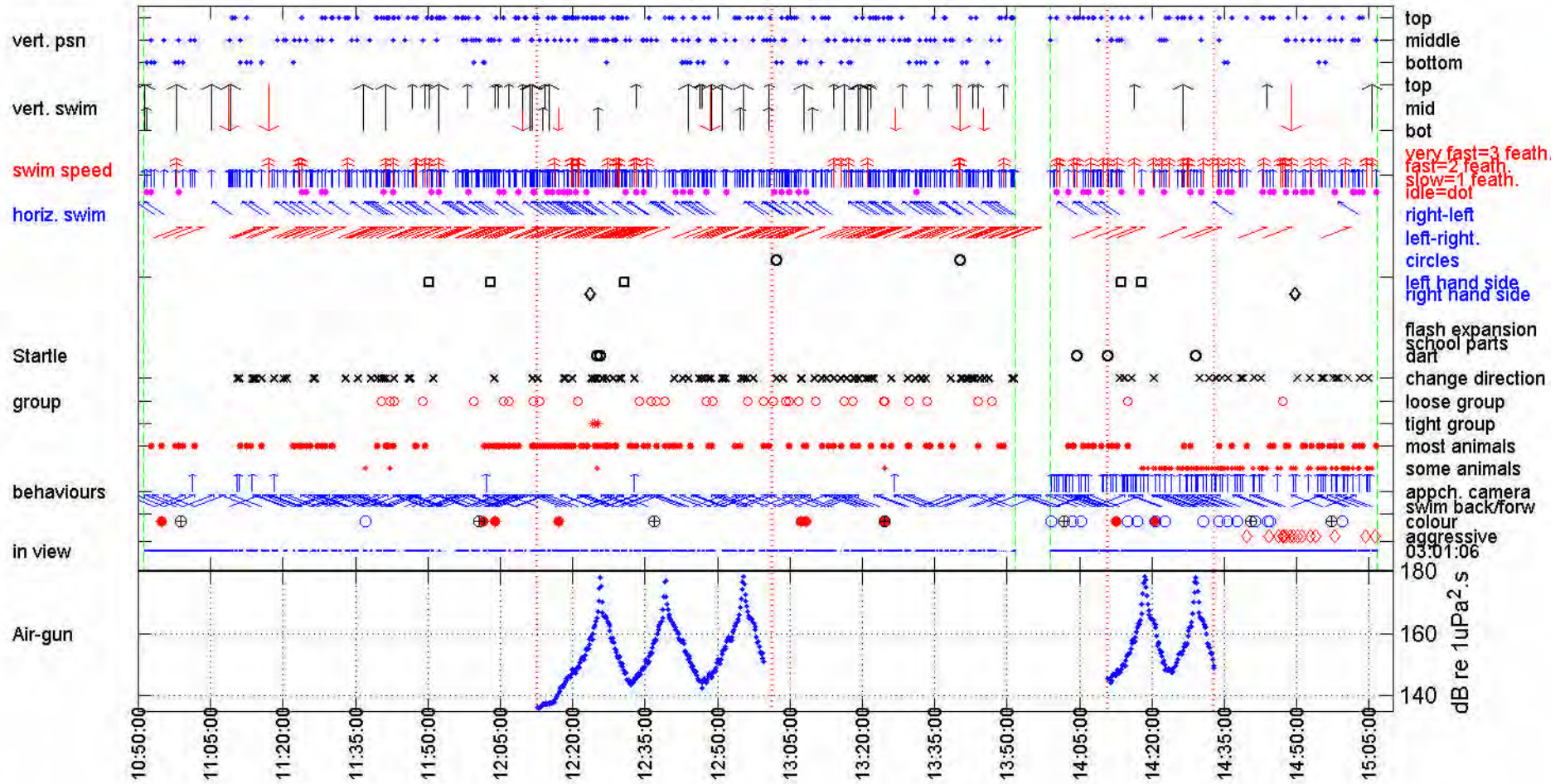
Trial 11 camera 1 squid Jervoise Bay all
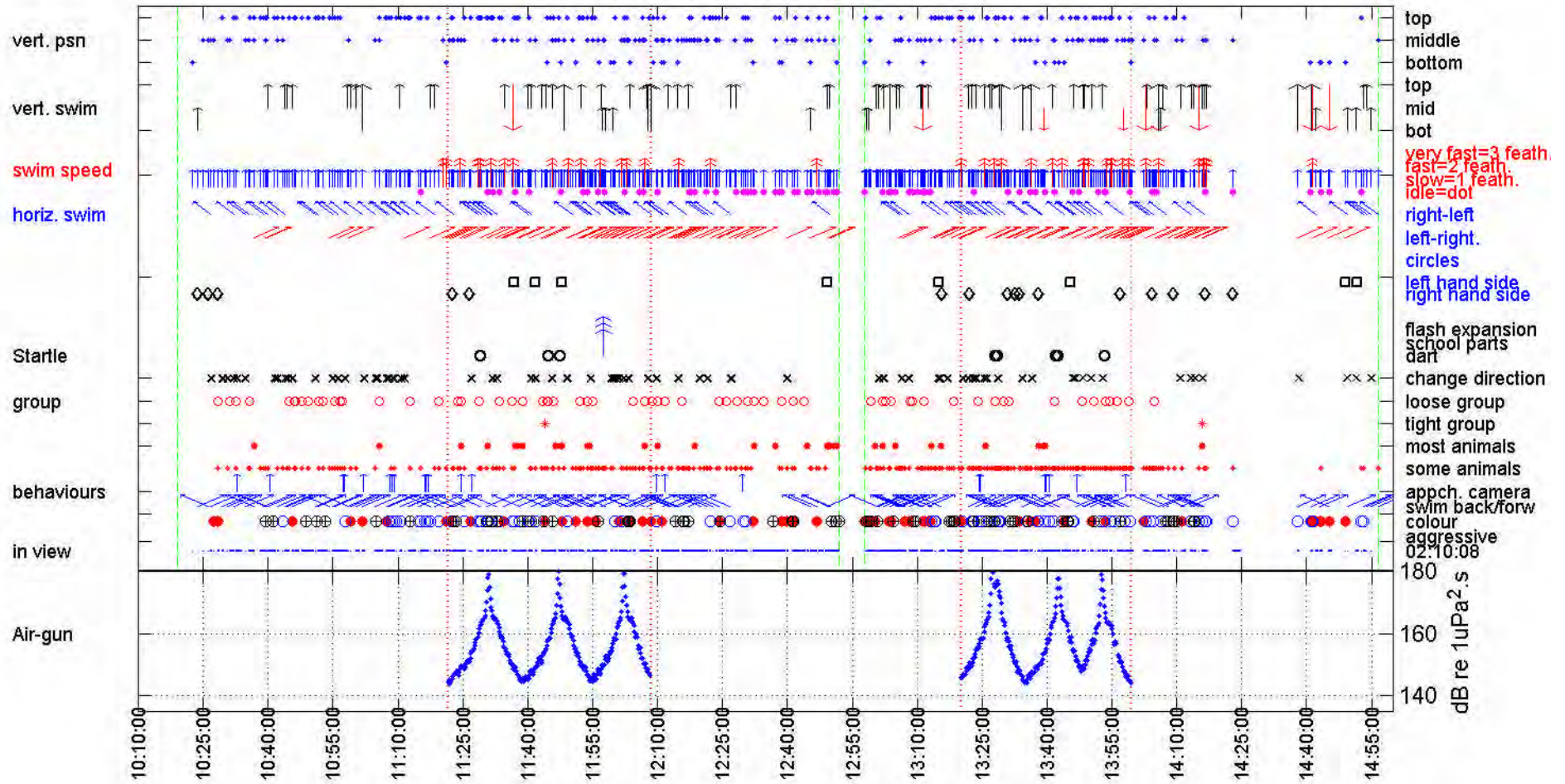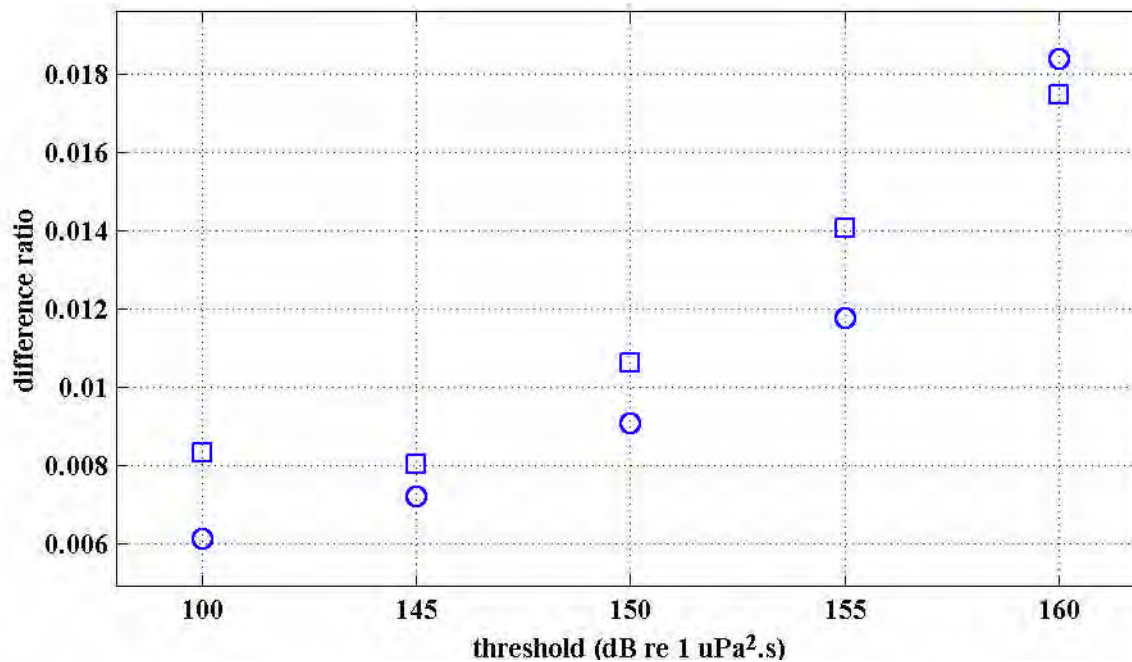
Figure 82: Difference between ratio of squid *startle response per total counts*, for periods above specified air-gun thresholds, minus the similar ratio for periods with no air-gun operations, from trials 10 (circles) and 11 (squares) . Data summed for each camera per trial.

Changes in movement patterns and swimming behaviour

Although there were perceived to be changes in the general behaviour of squid throughout the air-gun exposures there were no consistent trends apparent in the behavioural scoring results. During the first squid trial, (5) the squid went out of camera view shortly after the beginning of the first period of air-gun operations and did not return until towards the end of the second air-gun operation period (Figure 81 - 1). Observations from the dinghy revealed that most squid had moved higher into the water column within 1 m of the water surface and had aggregated towards the S end of the cage (away from the air-gun source). This was borne out by the camera observations which showed the squid moving to the surface during air-gun operation periods (Figure 81 - 1).

During trials 10 and 11 the behavioural scoring of the squid vertical position and vertical swimming patterns did not reinforce this trend of moving towards the top of the cage. Rather during the air-gun passages squid seemed to be scattered in loose groups mostly in the middle to top portion of the cage. They did consistently show a trend to firstly increase their swimming speed above the no air-gun period as the air-gun began approaching and to then slow as the signal exceeded 155 dB re 1 μPa^2.s. This can be seen on Figure 83 for trials 10 and 11 (trial 5 had insufficient air-gun signal range) using the difference ratio of *time fast swimming/time in view* during the above threshold periods minus the similar ratio for the no air-gun periods (Equation 16).

Observations made as the air-gun pontoon passed by (closest approach) during trials 10 and 11 indicated that many of the squid were within 1 m from the water surface (out of view of the cameras), and spread throughout the cage, moving slowly and aligned randomly. This supported the similar observation made during trial 5. But the camera observations during trials 10 and 11 indicated other squid were also located in the full vertical range of the camera field of view.
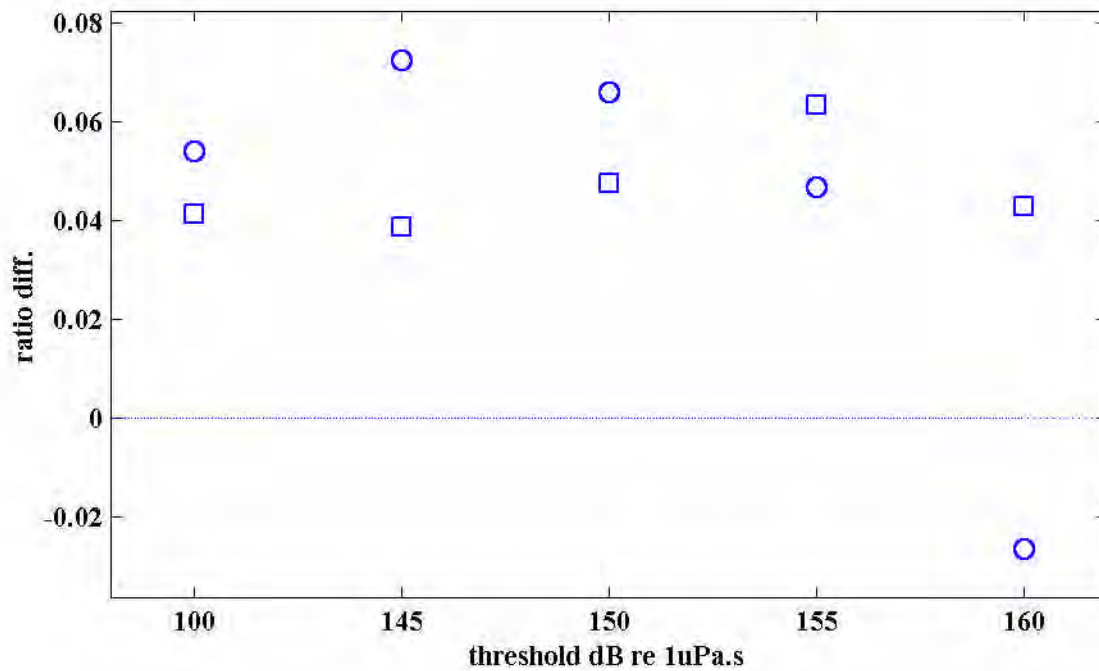
Figure 83: Difference ratio of *time spent fast swimming per time in view* for periods above the air-gun thresholds minus the similar ratio for no air-gun periods for squid trials 10 (circles) and 11 (squares), using summed camera results per trial.

In summary the squid behavioural response to the nearby air-gun operations were:

- strong startle response (firing of ink sac) to first start up observed at received air-gun level of 163 dB re 1 μPa^2.s, but not observed for similar or greater levels if signal ramped up
- increasing proportion of startle response (jetting away from air-gun shot) recorded as air-gun signal increased with effect most noticeable above 145-150 dB re 1 μPa^2.s
- possible trend observed for squid to move towards water surface as air-gun approached (air-gun signal became significantly lower nearer water surface)
- evidence of increased in squid swimming speed as air-gun approaches then slow down at air-gun signals >= 155 dB re 1 μPa^2.s

As indicated, at this stage no pathological examination of preserved squid statocyst systems has been made.

3 - DISCUSSION

3.1 - *Physical factors*

3.1.1 - Air-gun signal characterisation

Extensive sets of measurements made at ranges of 5-6000 m from a single 20 cui air-gun used in experimental trials and of a 2678 cui 3D air-gun array from 1.5-64 km range revealed that the most consistent measure of the received air-gun signal was some measure of its energy. This is as suggested in Richardson et al (1995) for pulsed sounds. Typically an air-gun signals' mean square pressure or peak pressure have been reported in the literature. It was found that under certain circumstance measurements which used time integration over the received air-gun pulse (ie. *mean squared pressure*) suffered due to factors complicating a repeatable measure of the signals start and end time, or pulse duration. Inconsistencies in the pulse length definition then biased the time integrated measure. Factors which tended to alter the measured pulse length were: the air-gun bubble pulse; headwaves for seafloor coupled hydrophones in an appropriate seabed type; or for distant air-gun signals, high background noise or biological transients such as fish and whale calling. Although air-gun arrays are designed to suppress bubble pulse signals in the downward direction they may not do this in the lateral or horizontal direction, which is of importance for biological effects studies. Headwaves are sound waves channelled along the seabed water interface. The presence of the bubble pulse or headwaves in the received signal often acts to increase the calculated signal time without contributing significantly to the total energy content of the signal. This dragged the time integrated measure down.

In the present work a standardised method based on the digitised signal was used for generating a set of parameters describing a received air-gun signal. Of these parameters the "equivalent energy" in units of dB re 1 μPa^2.s was found the best signal descriptor and was used throughout all analysis in this project. Note that this measure is not an energy unit, but since is proportional to energy has been termed "equivalent energy" throughout this document. For the different sources measured, empirically derived corrections were used to convert these equivalent energy units to mean squared pressure or peak pressure values for comparison with other workers. Converting the 'equivalent energy' units to mean squared pressur*e* values is valid since the mean squared pressure (in dB re 1 μPa) is equal to the 'equivalent energy' measure minus $10*\log_{10}$(air-gun pulse duration, in seconds). From the measurements made in this report the mean squared pressure in dB re 1 μPa was equal to the 'equivalent energy' plus 11.4 to 14.6 dB, depending on the source and local environment over which the measurements were taken. Note that the correction is positive since the air-gun signal duration was always less than one second.

Converting either mean squared pressure or 'equivalent energy' measures to peak-peak pressure units is not technically valid, but since many workers have used peak pressure units (or some derivation of), to describe sound levels in their results, there has been no option but to do this. Empirically derived correction factors from many thousands of air-gun measurements made in this report, were found to be consistent over ranges out to many kilometres. The peak-peak pressure levels from a received air-gun signal were 27.3 to 30.5 dB above the equivalent energy units. Again this varied depending on the source and local environment in which the measurements were made.

For ease of comparison with other literature this discussion preferentially presents the air-gun levels as mean squared pressure units. For the results arising from this report these units are either as measured directly from air-gun signal data sets or derived from equivalent energy measurements, for the appropriate source type and local environment.

3.1.2 - Measured and modelled air-gun signals

The sets of air-gun signals measured elaborated many of the complications inherent in describing the received level of a signal at range from an air-gun source in shallow water. These complications included:

- directionality inherent in an air-gun array;
- receiver depth;
- the seabed properties;
- the array operating state;
- the source depth;
- water depth along the propagation path.
- sound velocity profile in the water and seabed

A 2D and 3D array were each modelled for source directionality. Each showed an increase in higher frequency energy off the array beam while the 2D array also had highest levels of low frequency energy radiated fore and aft relative to the array tow axis. Measurements of the 3D array showed that the abeam directionality was enhanced at range, such that the signal level could increase by up to almost 10 dB at a given range as the receiver came abeam. This effect was greatest higher in the water column.

Measurements and modelling showed that at a specified range there were differences in the vertical sound intensity profile. A consistent trend for lower received levels on moving towards the surface was observed. For example the 3D array measured at 1.6-1.8 km range showed a 6 dB decrease in level on moving from 40 to 5 m depth. Modelling a single air-gun in 20 m water depth showed that at range from the source the maximum level extended from approximately midwater to the bottom, and that levels near the water surface could be 10 dB lower.

Seabed properties are known to be crucial in horizontal sound propagation. Sound energy from an in-water noise source may reflect directly off the bottom or may enter the bottom and subsequently be reflected or refracted back into the water. Because of its military implications a large literature base exists on sound propagation in shallow water (eg. reviews in: Jensen et al, 1994; or Medwin and Clay; 1998). Depending on the bottom type, the frequencies of interest and the water depth, it may be that a precise definition of the physical seabed parameters to at least 50-100 m below the seafloor is required to accurately define the horizontal propagation along any travel path. In Australian waters this level of detail is generally not available.

The importance of seabed parameters was emphasised during humpback whale trials in Exmouth Gulf, Western Australia. During 16 trials where humpback whales were approached with a single operating air-gun (Bolt 600B, 20 cui chamber, 10 MPa operating pressure) to gauge responses, nine sets of measurements were made of the air-gun from 0.17-6.8 km off. All measurements were made within an approximate 20 x 30 km area, in water depths of 16-20 m. It was anticipated that from these empirical measurements a single fitted curve could be derived to describe the air-gun level received by the whale. This was not the case, rather two general sets of signal loss with range curves were measured, 'good' and 'bad' propagation conditions with differences in broadband air-gun level of up to 10 dB at one km range. The 'good' propagation curves returned far more higher frequency energy (160-1000 Hz) than the set of 'bad' propagation curves. Investigation of the available literature suggested that patchily distributed cemented limestone pavements were common throughout the region. Thus sound propagation models were run using estimates of the seabed type with and without a cemented pavement. These grossly matched the

frequency content observed and the received air-gun level curves, suggesting that the two sets of curves observed were probably due to the presence or absence of a shallow cemented layer. The large differences in level observed for the same source at a given range within the bay and its patchy distribution in a relatively small space highlighted the localised importance of the seabed type in determining sound propagation.

During 3D seismic operations two air-gun arrays are towed parallel to each other and equally spaced about the tow direction. These are fired in a flip-flop fashion, alternating between port and starboard arrays. The arrays are normally identical in nature, towed at the same depth and operated at the same pressure. Measurements of port and starboard 2678 cui 3D array's revealed that although when averaged over many signals there was no net difference in received level at range between port and starboard, consecutive air-gun signals were consistently different, with up to a 9 dB variation. It was believed slight differences in the orientations of receivers to each array, alignments and depths of array components and of functioning air-guns within each array contributed to the measured differences. Again this exemplified the difficulty of predicting the received air-gun level for a specified air-gun array and the requirement for a detailed study of the source and environment.

Modelling was carried out to determine the effect of air-gun source depth on horizontal sound propagation. Source depth plays a crucial role in determining an air-gun array downward performance, since it dictates the time delay for the surface reflected signal which in turn affects the frequency content of the downward directed signal of primary interest to the geophysicist. Modelling a single air-gun in Exmouth Gulf for horizontal sound propagation found that increasing source depth consistently increased the received signal at any specified horizontal range and receiver depth. This was a function of the modal structure inherent in shallow water, such that the optimal position for placement of the source was at the apex of the primary mode at each frequency. For the predominant frequencies in the example used this mode occurred near midwater (at 10 m depth in 20 m water). In the model run used, increasing the source depth from 2.5 to 6 m resulted in a mean 8 dB signal increase for a receiver at 10 m depth over ranges of 0.15-5 km.

Differences in travel path bathymetry profiles also played an important role in determining received levels. Many sets of measurements were made of the 2678 cui 3D array from a receiver set on the bottom in 32 m of water from the array source in 100-120 m of water. These travel paths then involved up-slope propagation. Because of the increasing number of bottom-surface bounces and increasingly steeper angles involved (closer to the vertical axis) as the water shallowed, this type of propagation results in much larger signal attenuations compared to measurement sets over similar ranges but constant water depths. In one instance the signal was not audible at a receiver in 10 m of water 28 km from the source in 130 m of water. Measurements at similar ranges in deeper water returned clearly audible signals.

A model was built to predict source levels of any given air-gun array configuration for a specified azimuth (horizontal aspect), elevation (vertical aspect) and the presence or absence of the source ghost. Such models are routinely used by geophysical contractors to develop particular air-gun array configurations, but these are proprietary in nature with their details not available. The source model produced was based on a modified version of an air-gun bubble model presented by Johnson (1994) and required some source specifications from the geophysical contractor to 'tune' the output.

There are a number of numerical models available for the calculation of horizontal acoustic propagation. These include ray tracing, normal mode and parabolic equation models. Each has its own strengths and weaknesses. Some are best suited to shallow water, others to deep water, some can deal with complex bathymetry profiles, others require a fixed water depth, some return vertical sound intensity profiles through

the water column, others output for a fixed depth only, some can deal with shear waves, others cannot. The choice of horizontal propagation model thus depends on the circumstances dictated by the environment in question. All of these models run at a single frequency only. Thus to characterise a source with complex frequency components, such as an air-gun array, the chosen model needs to be run at many frequencies and the resultant energy summed to give the broadband received signal level.

Given all of the above factors and others not discussed such as sound speed profiles within the water column, it is believed that at present, predicting the horizontal sound propagation from any specified air-gun array source needs to be done on a case by case basis. There are some generalisations which can be made such as those listed above, but accurately predicting levels at specified ranges and water depths requires modelling of the source and local environment. It would be hoped that over time enough air-gun signal measurement and modelling sets would become available from different Australian environments, so that historical data sets could be used to predict received air-gun level with range. At present only the measurements described above, for two exploration regions, are available.

3.2 - Air-gun exposure modelling

Although it is a valuable exercise to model the horizontal propagation of single air-gun shots this tells us little of the exposures received through time for a constantly moving seismic source. Seismic vessels steam at around 3-5 knots (1.5-2.5 ms^{-1}) along straight tracklines in the region of the survey for weeks to months operating at an 8-15 s repetition rate. The repetition rate is determined by the hydrophone spacing in the streamers, such that optimally an air-gun pulse is fired at this spacing. A 3D seismic survey may concentrate activity in a few hundred km^2 for upwards of a month, with a trackline coverage every 100 m.

The results of studies into the response of marine animals from this study and elsewhere suggest that above threshold level air-gun signals, behavioural changes occur in many species and that with increasing air-gun level these behavioural changes become increasingly significant. Assuming one can predict the threshold level at which the behaviour of a particular group of marine animals will be altered in some fashion, suggested presenting the seismic survey exposure history as the proportion of a region experiencing levels above a specified threshold over the seismic survey duration.

Thus an exposure model was developed which for any given seismic survey source, trackline configuration and set of environmental parameters, returned an estimate of exposure through time as the number of air-gun signals exceeding a specified threshold, on a spatial grid. This exercise was carried out for an example seismic survey. The model produced a contour plot of the number of received air-gun shots at a specified receiver depth which exceeded the threshold level for the full seismic survey duration (121 days in the example used). This contour plot could be interpreted as a probability plot, showing a scale of potential disturbance for the entire seismic region over the survey duration. The model saved the data for each period of consecutive operations (ie. each period with no breaks in operations for turns, dropouts, gear failures etc.). Thus the data could be further processed and presented on a different time scale, perhaps as number of shots exceeding the threshold, per-hour, per-day.

It was intended that this exposure model could be used to gauge the potential ecological scale of biological effects. The particular exercise carried out was done post-survey, but could just as easily be done prior to any seismic survey, and thus would give some prediction of the potential scale of any effects. It is believed this type of modelling would be a useful tool for evaluating potential conflicts. With refinements and considerable computer processing power, the technique could also be used to optimise seismic survey trackline configurations so as to minimise possible environmental implications.

3.3 - Humpback Whale response to air-guns

Observations were made of southward migrating humpback whales transiting the region of a 3D seismic survey. The whales were migrating south west, while the seismic vessel ran east west tracklines straddling the migratory route. Complementary to this work 16 approach trials were carried out where humpback whales were observed for around an hour, approached with a single operating air-gun then followed for another hour. Movement patterns and behaviours were logged for any changes correlating with the air-gun approach. Preliminary results of this work are presented in McCauley et al, 1998.

3.3.1 - Humpback movements about an operating seismic vessel

The study region for the seismic survey vessel operations was north east of North West Cape, off Exmouth. Humpback whales transiting the seismic region appeared to move south from the Monte Bello Islands towards North West Cape in blue offshore water in a broad band that extended at least as far offshore as the sampling effort undertaken. This was out to 240 m of water 38 km from the 20 m depth contour. Animals seen in this region were migrating, which involved continuous swimming on a south-westerly course or south-westerly swimming interrupted by short to long resting periods. A considerable number of whales tended to cross into the shallow water inside the island chain extending north east of North West Cape between Bessieres Island and the Murion Islands. Few animals were seen in shallow water to the east of Bessieres Island, while many were seen to the west of it. After passing from the offshore region into shallow water these animals were believed to then swim into Exmouth Gulf. Animals seen inside Exmouth Gulf showed much more random swimming patterns than migrating animals seen in the blue water, and were either resting or engaged in courting behaviours. This behavioural distinction was important in assessing results. It also should be pointed out that adult humpback whales do not feed when in tropical Australian waters during their migration. The significant feeding that does occur is of cows feeding calves.

In the region of the seismic survey, the distributions of whale pods sighted during aerial surveys undertaken before the seismic survey began, during the seismic survey, and of pods sighted from the seismic survey vessel appeared to be uniformly distributed across the depth contours. There was no obvious evidence that whales were displaced inshore or offshore by the seismic survey.

Using data from all whale observations made from the seismic survey vessel, there was no discernible differences in the number of whales sighted per observation block (40 minute period) between observation blocks with the guns-on or guns-off for the entire block. When broken down by range category, the guns-off sighting rates were considerably higher from ranges near the vessel to 3 km than the guns-on sightings in the same range category.

This observation suggests localised avoidance of the operating air-gun vessel during periods with the air-guns on and agrees with published findings. These indicate that at some range most whales will avoid an operating seismic vessel. Richardson et al (1995) summarises the findings of many researchers whom have found that gray and bowhead whales generally avoid seismic vessels where the received sound level is between 150-180 dB re 1 μPa mean squared pressure. The level at 3 km from the seismic vessel from which the humpback observations were made was in the range 157-164 dB re 1 μPa mean squared pressure for a receiver at 32 m depth, which is in agreement with the standoff level given for gray and bowhead whales.

At > 3 km from the operating seismic vessel the guns-on sighting rates were considerably higher than the guns-off observations in similar range categories. The higher sighting rates observed at ranges > 3 km

during guns-on observations suggested that at these ranges some bias existed in the availability of animals for sighting during guns-on periods or that whales were attracted to the operating air-gun vessel.

A possible sighting bias was the tendency for whales to utilise the sound shadow near the sea surface to reduce the received sound loading. Four follows were made of humpback whales moving about the operating seismic vessel. Two of the 'follows' involved whales which spent an inordinate amount of time at the surface. In follow 1 a single animal swam entirely at the surface to cross 1.5 km off the bows of the operating seismic vessel. In follow 2 a cow and calf remained lying at the surface while the operating seismic vessel passed 3 km north of them. It is well known that as one approaches the sea surface the noise level of a nearby sound source will decrease substantially due to phase cancellation of the direct and surface reflected signals. This effect is exemplified for shallow sound sources (the air-gun arrays were towed at seven m depth). It is plausible that these whales were using this effect to reduce the air-gun sound loading received and thus increased their sighting availability.

It was found during experimental exposures that what were believed to be male humpbacks were attracted to a single operating air-gun possibly due to its similarity to the sound produced by humpback whales breaching (discussed below). Thus there may have been several reasons for the increased sighting rate at ranges > 3 km when the seismic vessel was operating its air-gun arrays.

The pod sighting rates observed during blocks when the air-guns were switched on/off or off/on were higher than the sighting rates during guns-continually-on or guns-continually-off observation blocks for the range categories from 0.75-3 km. These higher rates could be explained by: 1) a startle response bringing animals to the surface for air-guns turned on after being off for a protracted period; or 2) an investigative response where whales tend to come to the surface for air-guns turned off after being on for a protracted period. Startle responses to seismic survey sounds have been reported for humpbacks at levels of 150-169 dB re 1 µPa (effective pulse pressure, believed equivalent to mean squared pressure measure) by Malme et al (1985).

The first 'follow' made of whales moving nearby to the operating seismic vessel showed that on occasions whales would deliberately pass an operating seismic vessel at comparatively short range (1.5 km), albeit with a somewhat radical manoeuvre. Two follows involved pods on interception courses with the seismic vessel. These pods consistently made course and speed changes at 4-5 km to avoid the operating seismic vessel, standing off at 3-4 km at an estimated received level of 157-164 dB re 1 µPa mean squared pressure. The most consistent manoeuvre seen by intercepting whale pods from the four follows and from the seismic vessel was for the pod to alter course and speed so as to pass behind the operating vessel. During follow 2 a cow calf pair were seen to react by swimming strongly to the air-gun array starting up on an almost direct interception course at 11 km and a received level of 139 dB re 1 µPa mean squared pressure. But this pod only swam to a position 3 km south of the approaching vessels' trackline then stayed there resting quietly at the surface while the vessel passed to the north and departed. Based on blow rates the animals did not seem to be under any duress.

3.3.2 - Humpback approach trials

The 16 approach trials carried out in Exmouth Gulf revealed that humpback pods which contained females consistently avoided an approaching single operating air-gun (Bolt 600B, 20 cui chamber) at a mean range of 1.3 km. Avoidance manoeuvres were evident before standoff at ranges from 1.22-4.4 km. In one instance a startle response was observed. The mean air-gun level for avoidance was 140 dB re 1 µPa mean squared pressure, the mean standoff range at 143 dB re 1 µPa mean squared pressure and the startle

response observed at 112 dB re 1 μPa mean squared pressure. These levels are considerably less than those observed from the operating seismic vessel observations made outside Exmouth Gulf and from those published for gray and bowhead whales. More recent work on migrating bowhead whales has shown air-gun levels for avoidance less than those observed for the resting humpback whales (W.J. Richardson, LGL. Ltd. Canada, personal communication). For the observations made of humpbacks in the Exmouth region, it is believed the differences in behavioural state of the animals at the times of the respective exposures primarily accounted for the difference in response levels. Pods containing females and inside Exmouth Gulf were invariably resting or attempting to rest. Resting was a particularly important behavioural state for cow-calf pods. It is believed that whales engaged in such behaviours were more sensitive to the approaching air-gun than animals involved in the purposeful migratory swimming behaviour seen as the animals passed through the region of the seismic survey to the north east of North West Cape.

Although pods containing females kept the air-gun at some standoff range during the Exmouth Gulf trials, in nine of the 16 trials mostly single, large, mature humpbacks approached the operating air-gun to 100-400 m, investigated it, then swam off. These approaches were deliberate, direct and often at speed with one incoming whale clocked at 8 kn. These whales would have received maximum air-gun signals at 100 m of 179 dB re 1 μPa mean squared pressure (or 195 dB re 1 μPa peak-peak). This level is equivalent to the highest peak-peak source level (level at one metre) of song components measured in the 1994 humpback whale song in Hervey Bay by McCauley et al (1996), or as given by Thompson et al (1986) for humpback whale sounds in Alaska, of 192 dB re 1μPa peak-peak at one metre.

Fortuitously breaching signals produced by a large cow leaping clear or partly clear of the water and slamming back in were measured after one of the sets of approach trials. These breaching signals were measured over 0.1-1 km range. The underwater signals produced by this animal breaching were audibly similar to air-gun signals. The author has noted this before from recording sets in Hervey Bay, Queensland ('rifle' shots, McCauley et al, 1996) and from sets with continual humpback singing with breaching from the Kimberley region of Western Australia (personal observation). On analysis of the breaching signals it was found that they could be matched well with air-gun signals based on waveform, energy content and frequency spectra. As an example a breaching signal as recorded at 100-200 m matched a signal from a 3D seismic array as recorded at 6.8 km range and a 20 m depth hydrophone, based on equivalent energy levels.

We speculate that given the similarities between air-gun and breaching signals male humpback whales may identify air-gun signals as a 'competitor'. The songs mostly male humpback whales generate are possibly used to attract females and/or to signal other males as to their presence and breeding intentions. Sustained air-gun signals may present as an acoustic 'threat' to the integrity of a singer or as an event worth investigating. Thus we believe that the animals which investigated the single air-gun during the Exmouth Gulf approach trials were males, intent on investigating a potential 'competitor', or what they perceived as a breaching event. We stress that this is speculative.

3.3.3 - Management implications for large baleen whales

Cow/calf pairs are in the author's experience more likely to exhibit an avoidance response to man-made sounds they are unaccustomed to. Thus any management issues relating to seismic surveys should consider the cow/calf responses as the defining limits. Adult male humpback whales intent on mating often doggedly pursue available females. Swimming towards or around an operating seismic vessel may be a small obstacle to a male humpback whale who has sensed a sexually available female on the other side. This was borne out by the observation of a male animal swimming across the bows of the operating seismic vessel.

For management purposes the distinction is made between migratory or transiting whales versus whales which remain in a general area for socialising, resting, calving, mating, feeding or some other purpose ('key habitat' type). Migratory whales are those involved in travelling, for Australian humpbacks this is very purposeful for northerly travelling whales and more meandering for southerly travelling whales.

For the humpback whale pods migrating south outside the 20 m depth contour the major implication of the seismic survey vessel operating across their migration track seems to have been localised displacement about the seismic vessel. Animals on interception courses essentially maintained their course until at 4-5 km, whence they adjusted course and speed to pass by the operating vessel, allowing an avoidance range of around three km. Some animals approached the vessel closer, with on one occasion a single animal seen to deliberately cross the vessels bow while swimming at high speed and on two occasions the vessel stopping work when single animals were sighted within 1-2 km. There was no evidence of any gross changes in the southerly migration track in the region of the seismic survey, such as displacement inshore or offshore during times when the vessel was operating.

Given that only localised avoidance was seen by migrating whales one would conclude that any 'risk factor' associated with the seismic survey was confined to a comparatively short period and small range displacement.

The peak-peak levels of the 3D seismic array measured were of the order of 182 dB re 1 μPa at 1.6 km, which was below the source level of the highest components of humpback whale song or breaching/pec slapping sounds (eg. 192 dB re 1 μPa peak, Thompson et al 1986 for pec slapping, 192 dB re 1 μPa peak-peak McCauley et al 1996 for some song components). The breaching signal measured at 100-200 m range gave a received peak-peak level of 160 dB re 1 μPa. Using spherical spreading and a 150 m range gives a crude source level for this signal of 182 dB re 1 μPa peak-peak at one metre. Thus at 1.6 km the received 3D air-gun signal was within the range which humpback whales would be expected to cope with physiologically, since it would be difficult to argue that humpback whale song or natural breaching events can cause physiological problems to the animals. McCauley et al (1996) report on a humpback whale singing persistently within 20-50 m of other whales and during the observation in Exmouth of the cow breaching the calf was always within 20-50 m of the landing cow. This natural exposure to intense signals coupled with the fact that humpbacks were seen to be actively utilising the 'sound shadow' near the surface when in the vicinity of seismic operations, implies it is probable that humpbacks are not at physiological risk unless at short range from a large air-gun array.

Using an algorithm generated to estimate the received level of a 3D array at 32 m depth which accounted for beam patterns, the range at which the air-gun array peak-peak signal matched the known source level of humpback sounds was calculated at 0.95-1.4 km for a receiver at 32 m depth. This assumed a 30 dB correction to shift the air-gun units from equivalent energy to peak-peak pressure, and a maximum humpback song component source level of 192 dB re 1 μPa peak-peak. The generated curve with angle from the air-gun array bow is shown on Figure 84.

Given these two factors, that displacements to migratory animals were comparatively short in time and involved small range changes and the low chance of physiological effects, then there appears to be a low risk for migratory animals exposed to seismic activity.

The same could not be said for humpback whales which are not migrating, but which are relatively sedentary in an area and involved in some behavioural activity which is important from a population

perspective (key habitats). For humpback whales along the Western Australian coast such areas include at least, coastal waters of: the southern Kimberleys between Broome and the northern end of Camden Sound; Exmouth Gulf; Shark Bay; waters to the north and north east of Rottnest Island; and Geographe Bay, during the late winter-spring months. In particular Jenner et al (2000) have identified the southern Kimberley region as a calving ground used by a large portion of the Western Australian humpback whale population.
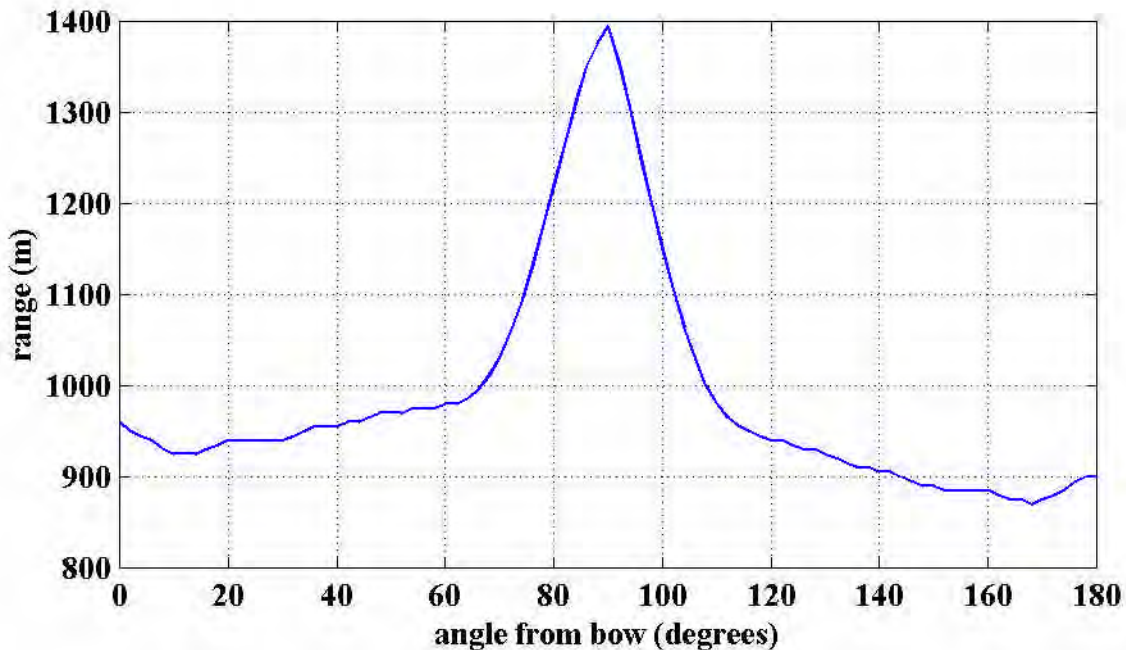
Figure 84: Calculate range at which the received air-gun level from a 2678 cui 3D array at 32 m depth matched the highest recorded level of humpback song. Note that this range will vary considerably for different air-gun arrays.

In these key habitat areas the possibly lower threshold for response to air-gun signals could be expected to result in displacement by an operating seismic survey vessel at ranges greater than observed for animals outside these habitat types. Scaling the air-gun level results of the approach trials using the single air-gun, where avoidance occurred at 1.3 km in a key habitat, to levels about the 3D array measurements described, gave a potential range of avoidance about an operating seismic vessel of 7-12 km. This 7-12 km range would only apply to whales in a key habitat type, and then may be lower given different sound propagation conditions.

Displacement by a continually operating seismic vessel in a key habitat type could have much more profound and serious effects on individual animals and the population than exposure for animals migrating or not in a key habitat type. For example Exmouth Gulf is used as a resting area by southerly travelling humpback whales, specifically by cows resting and feeding 4-8 week old calves. At this stage of their lives the calves are small, comparatively weak and possibly vulnerable to predation and exhaustion. The potential continual dislocation of these animals in a confined area would interrupt this resting and feeding stage, with potentially more serious consequences than any localised avoidance response to an operating seismic vessel as seen during their migratory swimming behaviour. Similarly any repetitive displacement or disruption of animals on their calving grounds during the time when they are present (eg. southern Kimberleys for Western Australian humpbacks during July to late September), may have serious consequences at the population level.

3.4 - Sea turtle response to air-guns

Two trials were conducted with caged sea turtles and an approaching-departing single air-gun (Bolt 600B, 20 cui chamber) to gauge behavioural responses. The trials were conducted on a green (*Chelonia mydas*) and loggerhead (*Cartetta caretta*) turtle and separated by 2 days. The first trial involved 2:04 hrs of air-gun exposure and the second 1:01 hr. Each trial used a 10 s repetition rate. Water temperature during trials was uniform throughout the water column at 16° C. This is at the low end of the temperature range these turtles are normally exposed to and may have resulted in a lessening of behavioural response due to a low metabolic rate during trials.

The two trials were consistent and showed that above an air-gun level of approximately 166 dB re 1 µPa mean squared pressure the turtles noticeably increased their swimming activity compared to non air-gun operation periods and above 175 dB re 1 µPa mean squared pressure their behaviour became more erratic possibly indicating the turtles were in an agitated state. The increase in swimming behaviour tracked the received air-gun level, in that the turtles spent increasingly more time swimming as the air-gun level increased. The point at which the turtles showed the more erratic behaviour would be expected to approximately equal the point at which avoidance would occur for unrestrained turtles.

Two similar trials have been reported in the literature. O'Hara (1990) reported that loggerhead turtles kept in a 300 x 45 m enclosure in a 10 m deep canal maintained a standoff range of 30 m from a Bolt 600B air-gun with 10 cui chamber and two Bolt 'poppers', all operating at 2000 psi (14 MPa), suspended at 2 m depth and operated at a 15 s interval. O'Hara did not measure the received air-gun levels. The paper does indicate that the Bolt air-gun produced most of the energy in the received signal. In experiments conducted in this report an identical Bolt 600B air-gun with a 20 cui chamber deployed at 5 m depth in 10 m of water using a 1500 psi (10 MPa) operating pressure produced a signal of 176 dB re 1 µPa mean squared pressure at 30 m range and 3 m depth receiver. We found that for every MPa increase in the air-gun operating pressure an approximate 1 dB increase in signal level was achieved. Thus assuming in O'Hara's experiment that the significant signal energy received was produced primarily by the Bolt air-gun only, that the increased level expected from the larger chamber size in our trials was compensated by the lower operating pressure (3-4 dB difference), and similar sound propagation for the similar water depths (a reasonable assumption at such short range), then we could expect that the level at which O'Hara saw avoidance was around 175-176 dB re 1 µPa mean squared pressure. This agrees with the value observed in our trials at which the turtle behaviour became more erratic and reinforces the view that at this level active avoidance of the air-gun source would occur.

Moein et al (1994) using loggerhead turtles enclosed in an 18 m x 61 m x 3.6 m enclosure in a river, measured avoidance behaviour, physiological response and electroencephalogram measurements of hearing capability, in response to an operating air-gun. The air-gun (s) were deployed and operated from the net ends at 5-6 s intervals for five minute periods. They quote three air-gun levels received by the turtles, 175, 177 and 179 dB, but do not give the units nor the ranges from the source at which these refer to. Details of the air-gun, its operational pressure, deployment depth and sound levels experienced by the turtles throughout the cage were not given. Considering the results from all turtles tested (11 individuals six trials each) avoidance was seen during the first presentation of the air-gun exposure at a mean range of 24 m. Further trials several days afterwards did not elicit statistically significant avoidance. The physiological measures did show evidence of increased stress but the effects of handling turtles for sampling were not accounted for thus the stress increase could not be attributed to the air-gun operations. A temporary reduction in hearing capability was evident from the neurophysiological measurements but this effect was temporary and the turtles hearing returned to pre-test levels at the end of two weeks.

The avoidance behaviour described by Moein et al (1994) is in partial agreement with the findings reported for the caged experiments described in this document. The results of the two trials reported and those of O'Hara, suggested that at some level the turtles would show avoidance of the operating air-gun. The behavioural results in our caged trials were consistent between trials two days apart using the same turtles. The results of Moein et al (1994) showed that the avoidance behaviour was not statistically significant for loggerheads receiving repeated air-gun exposures several days after their first exposure. They concluded that this was due to either habituation or a temporary shift in the turtles hearing capability.

There were differences in the presentation of the air-gun signals between these experiments. In the trials reported in this document the air-gun signal was ramped up by the air-gun approach-departure scenario used. This meant the turtles only received a small number of moderate to very high level air-gun signals. This type of exposure is similar to that which would be experienced by an approaching and departing seismic survey vessel. In contrast the experiments of Moein et al used a fixed air-gun source operated at constant range. Although the source details of the Moein et al trials were not stated, to give some idea of the levels experienced, a Bolt 600B air-gun with 20 cui chamber, 5 m gun depth, 10 MPa operating pressure for a receiver 3 m deep in 10 m water depth, produces a received level of 176 and 172-175 dB re 1 μPa mean squared pressure at 24 and 64 m respectively (24 m being the mean avoidance range for first exposure given by Moein et al, 64 m being their maximum cage length). Comparing this with the received air-gun shot levels for the first sea turtle trial reported here (trial 6, Table 22), then a full trial of the Moein et al experiments exposed the turtles to ~180 shots > 172 dB re 1 μPa mean squared pressure (assuming three five minute periods with 5 s operation rate and level at 64 m of 172 dB re 1 μPa mean squared pressure), whereas sea turtle trial 6 exposed the turtles to only 97 shots > 172 dB re 1 μPa mean squared pressure. Thus the temporary shift in hearing thresholds observed by Moein et al, which may have played a part in the lack of avoidance seen in trials repeated several days after a turtles first air-gun exposure, may have been less important in the trials reported in this document, possibly because of the different air-gun regimes used between trials.

Lenhardt (1994) reported on a swimming response from loggerhead turtles in large shallow tanks on presentation of low frequency (< 100 Hz) tones. Although the results are not directly applicable to impulsive air-gun signals they suggest that the increase in swimming behaviour seen in our trials and by Lenhardt (1994) may be a consistent sea turtle 'alarm' response.

3.4.1 Implications of seismic operations for sea-turtles

The available evidence from these trials and the literature suggests that sea-turtles may begin to show behavioural responses to an approaching air-gun array at a received level around 166 dB re 1 μPa mean squared pressure and avoidance around 175 dB re 1 μPa mean squared pressure. It must be cautioned that to date the available evidence on sea turtle responses to air-gun signals is based on very few observations, few individuals with a limited age span, few species, and at least in the trials described in this report, may not account for warmer water conditions when the turtles are physiologically and behaviourally more active.

Taking note of these cautions on the probable variability likely in sea turtle responses to air-gun signals, from measurements of a seismic vessel operating 3D air-gun arrays in 100-120 m water depth these sound levels corresponds to behavioural changes at around 2 km and avoidance around 1 km. Important sea turtle habitats mostly occur in shallower water, often less than 20 m deep. The propagation of an air-gun array in such water depths may be vastly different than that for the array measured in 120 m water depth. One would generally expect that sound propagation in water < 20 m deep would be significantly worse,

that is the signal would not carry as far. But under some circumstances dictated by the seabed properties, this may not be so.

Thus given possible variability in seismic sources, sound propagation conditions in shallow water and the limited data set to draw effects conclusions from, then these one and two km response and avoidance ranges for sea turtles are a guide only and may be more or less.

A wild card for sea turtle response to air-gun signals is the sediment borne headwave signals. These may be significant in some seabed types such as seen within Exmouth Gulf. For bottom coupled hydrophones in some areas within Exmouth Gulf an air-gun signals headwave energy exceeded the waterborne energy at a sufficient range. Conversely some seabed types will not support headwaves at all. Sea turtles are believed to have some capability of bone conducted hearing (Lenhardt et al 1983) and commonly spend long periods lying still on the bottom (personal observation). It may be that they can receive the headwave signals produced by an air-gun via bone conducted pathways. It is not known if they do this, nor if they did, what their response would be to the headwave component of an approaching air-gun.

3.5 - Fish response to air-guns

The full methods and results describing the ten fish trials carried out of the response of fish in a 10 x 6 x 3 m cage to a nearby operating air-gun, are presented in McCauley et al (2000). The results included behavioural, physiological and pathological measurements from experimental trials and the running of a simple fish otolith model using air-gun signals as the input to predict response. The experimental trials showed that the fish response to nearby air-gun operations included:

- for some fish a startle response (C-turn) to short range start up or high level air-gun signals;
- a greater startle response from some smaller fishes;
- evidence of alarm responses, with this becoming more noticeable with an increase of received air-gun level above approximately 156-161 dB re 1 μPa mean squared pressure;
- a lessening of severity of startle and alarm responses through time (habituation);
- an increased use of the lower portion of cage during air-gun operation periods;
- the tendency in some trials for faster swimming and formation of tight groups correlating with periods of high air-gun levels;
- a general behavioural response of fish to move to bottom, centre of cage in periods of high air-gun exposure (for levels approximately greater than 156-161 dB re 1 μPa mean squared pressure);
- no significant measured stress increases which could be directly attributed to air-gun exposure;
- evidence of damage to the hearing system of exposed fishes in the form of ablated or damaged hair-cells although an exposure regime required to produce this damage was not established and it is believed such damage would require exposure to high level air-gun signals at short range from the source.

The modelling work used a simple harmonic oscillator equation to model the otolith-macula relative movement, as described by de Vries (1950), Kalmijn (1988), Karlsen (1992) and Fletcher (1992) and using constants from various sources. This model only assumed the sound wave impinging directly onto the otolith system and did not include energy re-radiated from a nearby swim bladder or coupled to the otolith by mechanical linking from nearby gas bubble or swim bladder. Thus it is a first approximation and does not apply to hearing specialist fishes with morphological adaptations to enhance hearing sensitivity by adding in pressure reception. The model suggested that:

- above an air-gun level threshold of around 171 dB re 1 μPa mean squared pressure a fish otolith-macula system begins to show a rapid increase in absolute displacement parameters (displacement,

velocity, acceleration), suggesting that associated behavioural response and susceptibility to mechanical damage will increase accordingly;

- smaller otoliths tracked the input air-gun signal better than larger otoliths but showed lower absolute displacement parameters and returned to the rest position quicker, suggesting that smaller otolith systems may be at less mechanical risk from air-gun exposure than larger ones;
- the otolith system responded primarily to air-gun energy < 150 Hz, which encompassed the frequency of maximum energy of the input air-gun signals.

The behavioural experiments were consistent in that with increasing air-gun level some fishes persistently firstly increased swimming speed then moved to the lower portion of the cage then moved to 'huddle' in the cage centre. This general response is shown on Figure 85.
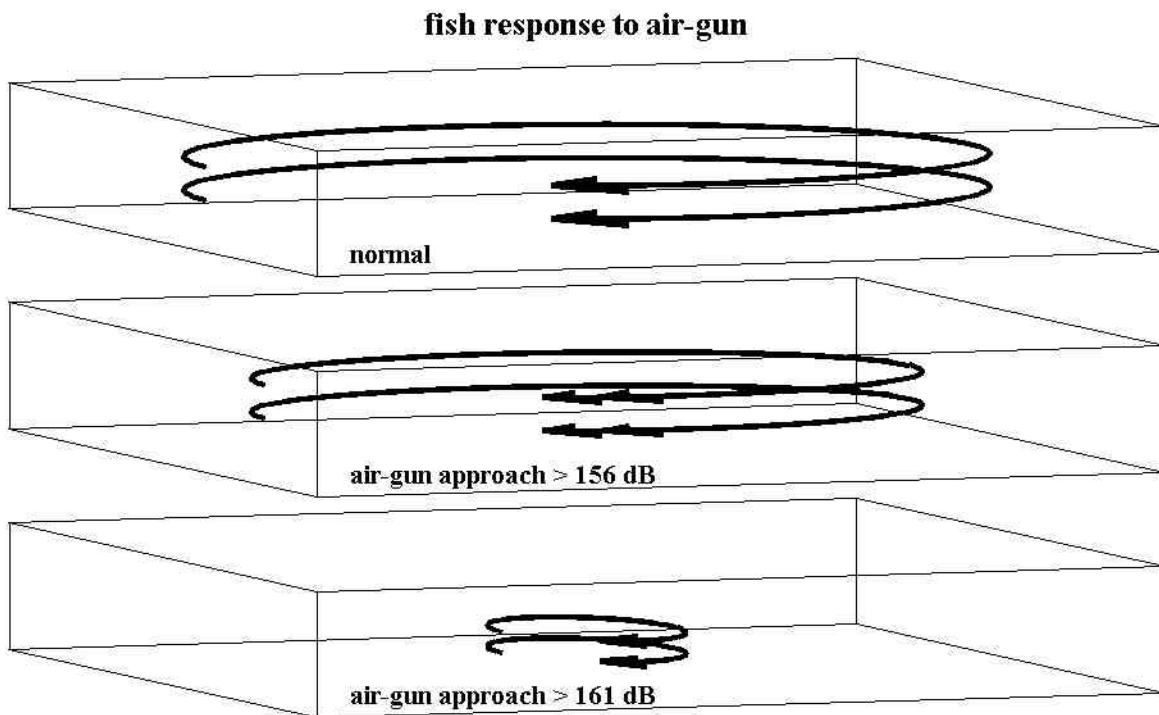
Figure 85: Generalised fish behavioural response to approaching air-gun. Units in dB re 1 μPa mean squared pressure.

A similar response to that shown in Figure 85 has been widely reported for many fishes avoiding approaching vessels (Olsen et al, 1983; Ona 1988; Misund, 1993; or reviewed in Olsen 1990).

Pearson et al (1992) carried out trials exposing captive rockfish (*Sebastes* spp.) in a 4.6 m octagonal cage 3.6 m deep deployed at the water surface to signals produced by a 100 cui (1639 cm^3) air-gun deployed at 6 m depth and operated at a 10 s rate. They observed similar behaviours to that described above, with *S. mystinus* milling in increasingly tighter schools with an increasing air-gun level, *S. melanops* schools collapsing to the bottom when air-gun operations started nearby and *S. miniatus* and *S. serranoides* schools remaining stationary near the bottom or rising in the water column on presentation of air-gun signals. They gave received levels for subtle changes in behaviour of 161 dB re 1 μPa (**mean-peak** level, defined as dB value of mean of sum of maximum positive and absolute value of minimum negative pressure values) and for the 'alarm' responses (defined as general increases in activity and changes in schooling or position in the water column) at 180 dB re 1 μPa (mean-peak level).

Using conversion factors derived from the air-gun sets described in this document for mean-peak levels,

gave levels for significant change in schooling behaviour from our experiments as 168-173 dB re 1 μPa mean-peak. This is lower than the level given for schooling changes given by Pearson et al (1992) of 180 dB re 1 μPa mean-peak, but lies within their range of 'subtle' behavioural changes at 161 dB re 1 μPa mean-peak, and their 'alarm' response at 180 dB re 1 μPa mean-peak. The lower levels of the 'alarm' responses reported from our caged trials could be because of different behavioural definitions, species differences, we used fish acclimated to the cage over many days whereas the fish in the Pearson et al trials were captured by hook and line the day prior to the trial, or because the significant trials reported in this document used an approaching and departing air-gun rather than a stationary one used in staircase fashion, as in the Pearson et al trials.

Despite the difference in levels required for similar behavioural changes between the two studies they are consistent in that at some received air-gun level the fish behavioural state became altered significantly, to the point that they displayed a consistent response of seeking shelter in tight schools near the bottom. Dalen and Raknes (1985) have also suggested that cod (*Gadus morhua*) may also respond to seismic signals by swimming towards the bottom.

Pearson et al (1992) recorded startle responses, defined as the C- turn type response (an involuntary response where all the lateral muscles along one side of the fish contract and the fish darts off in that direction, Blaxter et al 1981) at levels of 200 and 205 dB re 1 μPa mean-peak. In the trials reported in this document, the C-turn type responses were less common in the larger fishes at received levels up to 203 dB re 1 μPa mean-peak. But they were consistently observed from small (50-55 mm SL) *Pelates sexlineatus* between a received air-gun level of 182-195 dB re 1 μPa mean-peak. Alarm responses defined as faster and more erratic swimming, jerking movements concurrent with an air-gun shot or flash expansion of schools became increasingly evident above 168 dB re 1 μPa mean-peak.

In a recent study Wardle et al (in press) operated three 150 cui (2.5 L) air-guns near a small reef system in Loch Ewe, Scotland. They observed fish behaviour through an underwater video system and movements of selected individuals using an ultrasonic pinger tracking system, for 7 days before, during and for 4 days after air-gun operations. Eight air-gun exposures were used over a four day period. These ranged from 17 to 86 minutes in length with firing intervals of from 57-188 s. All exposures used a fixed air-gun (constant range).

Wardle et al observed startle responses (C-turns) from fish in camera view for every air-gun shot discharged, at levels from 195-219 dB re 1 μPa peak received at the observation camera. Again the units need conversion. The level at which C turn responses were observed from the *P. sexlineatus* in the trials reported here was 183-196 dB re 1 μPa peak, which overlapped the bounds at which Wardle et al observed similar responses.

Wardle et al did not see any significant effect other than C-turn responses to each air-gun shot. There was no shift in schooling behaviours of fish in the camera view and overall no significant change in the routine behavioural patterns of fish which transited the camera field of view or of those acoustically tracked, although there were some small aberrations. This may have been a function of the stationary air-gun source and the low number of air-gun shots discharged. The fastest repetition rate used was around once per minute which is much less than a conventional seismic survey of a shot every 5-15 s. The air-gun was also fixed in position, unlike the typical rapidly increasing signal expected from an approaching air-gun source. Thus the fact that Wardle et al did not see the 'alarm' response reported by Pearson et al (1992) or the increase in startle/alarm responses and 'huddling' behaviour seen with increasing air-gun level described in our trials, may have been an artefact of the exposure regime. The shot spacing may have been long enough

for the fish to fully recover from the alarm response which initiated the C-turn, and the fact that the source was stationary meant it would not have constituted an approaching threat.

Thus the behavioural results described from trials described in this document and from other published works show some consistency and possibly predicability. Summarised, these are that at some received air-gun level from an approaching vessel demersal fish could be expected to begin to change their behaviour by increasing speed and swimming deeper in the water column. As the air-gun level increases these fishes would be expected to form compact schools probably near the bottom in continental shelf depths (< 200 m). Eventually levels may be reached at which involuntary startle responses occur in the form of the classic C- turn. One would predict that at or near this level the fish would begin to show avoidance or for site attached fishes begin to seek refuge. Engås et al (1996) in an elegant and well carried out field trial in continental shelf waters, have displayed that avoidance by some species clearly occurs about an operating seismic vessel. In deeper water (> 200 m) any effects would be expected to lessen with increasing depth, as the air-gun signal level dropped accordingly.

The threshold for the initial increases in swimming behaviour may be of the order of 156 dB re 1 µPa mean squared pressure using the results of trials presented in this document. For the 3D array measured (2678 cui in 100-120 m water depth) this corresponds to a range of around 3 km. At levels of around 161-168 dB re 1 µPa mean squared pressure (results of our trials and Pearson et al 1992 using conversion for Bolt air-gun from mean-peak to mean squared pressure units) active avoidance of the air-gun source would be expected to occur. This corresponds to a range from the 3D array measured of 1-2 km. It must be cautioned that these ranges may differ depending on the specific air-gun array and the local environment. For risk assessment these air-gun level values can be used in exposure modelling to predict impacts for a specific survey and region, as described below.

The otolith modelling work showed that above an air-gun level of approximately 171 dB re 1 µPa mean squared pressure the response of the fish macula-otolith system increased dramatically. This suggested the behavioural response would increase accordingly. This is in line with the prediction of avoidance of the air-gun array based on the caged trial results.

The preliminary finding of pathological damage to the hearing system of pink snapper (*Chrysophrys auratus*) poses many questions. Although fish have been shown to survive very short range exposures to air-gun noise (hence high levels) for periods up to several weeks after exposure, none of these experiments or conclusions have considered the fitness of the animal from the perspective of potential sub-lethal damage. The findings presented in this document of fish exposed to very short range air-gun exposure exhibiting some damage to the hearing system, evident as ablated and damaged hair cells, implies that some fishes may have reduced fitness after exposure. This may have implications from an ecological perspective. Experimental animals held in cages are fed directly and do not face threats from predators, thus their survival after exposure to intense stimuli does not necessarily reflect what may happen to wild animals.

The fish used in trials were constrained and approached to short range with an operating air-gun, unlike fish in the vicinity of a commercial operating seismic vessel. It could be expected that avoidance would occur before air-gun signals reached levels sufficient to produce some form of hearing damage. The damage seen consisted of ablated or damaged hair cells on the macula of the sagittal otolith. Counts of ablated cells in exposed fishes were comparatively low (less than 1% of each sampling region of 23,500 μm^2 grid), although it was believed that ablated cells were indicative of wider damage to hair-cells which could not be easily quantified. It is known that fish can repair damaged hair cells (Lombarte et al, 1993). The recovery time for fish which had macula hair cells damaged by drugs was short, with recovery within 15 days

(Lombarte et al, 1993). But for greater levels of damage it is not known how long this process takes nor how effective it is. Samples were made in this set of trials of repetitively exposed fish (46 days between exposures) and regularly through a recovery period up to 44 days after exposure, but at the time of writing these were still being worked up. At this stage these pathology results must be considered as preliminary.

3.5.1 - Implications of seismic operations for fisheries

Commercial fisherman have long considered the operations of offshore seismic surveys to be disruptive to their fishery operations. This is not a phenomenon peculiar to any one country but is a view widely held by many fisherman across the world.

Engås et al 1996 have shown in an experimental regime that cod (*G. morhua*) and haddock (*Melanogrammus aeglefinus*) moved away from a 3 x 10 n mile region (5.6 x 18 km) in which seismic operations were carried out over a 5 day period. They observed reductions in fish stock out to the limit of their sampling at 33 km. Løkkeborg (1991) analysed longline catches of cod *(G. morhua)* made in the presence of seismic surveys and concluded a reduction in catch rate had occurred, as did Skalski et al (1992) in an experimental trial with rockfish (*Sebastes spp.*). These observations suggested that the fish had responded in a fashion such that they either avoided the sound field of operating seismic vessels from some range or that their behavioural state was changed such that they were no longer available to the fishing techniques tested. Conversely Løkkeborg and Soldal (1993) suggested that behavioural changes which forced fish to the bottom acted to temporarily increase catch rates of cod in saithe trawls during seismic activities. It should be noted that these studies have been undertaken in heavily fished regions and may not necessarily relate to Australian fisheries.

The literature observations support the findings presented from this study and justify the rationale on which the exposure modelling exercise was carried out. It is believed the threshold values used in the exposure modelling (161 and 166 dB re 1 µPa mean squared pressure) will give a good indication of the level at which behavioural effects to nearby fish begin to occur. This form of model would be particularly useful for interpreting the scale and probability of the potential disturbance of a given seismic survey on finfish, in time and space. The interpretation of any disturbance then needs to be considered at the commercial fisheries level and at an ecological level. The ecological level would need to be species specific and consider factors such as spawning aggregations, the proportion of a population impacted upon and flow on effects to higher level predators. These issues are discussed further in McCauley (1994).

It must be pointed out that any potential seismic effects on fishes may not necessarily translate to population scale effects or disruptions to fisheries. For many fish species any behavioural changes or avoidance effects may involve little if any risk factor. Thus a thorough understanding of fish response to seismic, proper risk assessment procedures and good communication between seismic operators and fisherman can negate any potential or perceived problems.

3.6 - Squid response to air-guns

Three trials were carried out with caged squid (*Sepioteuthis australis*) to gauge their response to nearby air-gun operations. In the first trial several squid showed a strong startle response to a nearby air-gun starting up by firing their ink sacs and/or jetting directly away from the air-gun source at a received level of 174 dB re 1 µPa mean squared pressure. Throughout this trial the squid showed avoidance of the air-gun by keeping close to the water surface at the cage end furthest from the air-gun. The air-gun level never fell below 174 dB re 1 µPa mean squared pressure throughout this trial. During two trials with squid and using a ramped approach depart air-gun signal (rather than a sudden nearby startup), the strong startle response

was not seen but a noticeable increase in alarm responses were seen once the air-gun level exceeded 156-161 dB re 1 µPa mean squared pressure. No consistent avoidance responses were seen in these trials but there was a general trend for the squid to increase their swimming speed on approach of the air-gun but then to slow at the closest approach and for them to remain close to the water surface during the air-gun operations.

Squid were particularly capable of learning to associate the dinghy used to service the cage with feeding. They retained this association immediately after the cessation of air-gun operations, coming to the dinghy to be fed, possibly indicating little hearing threshold changes.

Squid were the only animals observed during the caged trials which appeared to make use of the sound shadow measured near the water surface (an almost 12 dB difference was consistently observed between hydrophones at 3 m and 0.5 m depth in trials 13 & 14 along the side of the cage). The common fish response to the air-gun was the opposite, to go towards the bottom which because of the sound propagation peculiarities would take them into the part of the water column with the highest levels of air-gun signals.

The response of squid to air-gun signals has not been reported in the literature before. They are an extremely important component of the food chain for many higher order predators, and sustain dedicated fisheries in some parts of the world. The responses seen in the cages suggest that like the other animals observed, behavioural changes and avoidance to an operating air-gun would occur at some range. Thus it is probable that seismic operations will impact upon squid and that the exposure modelling approach using thresholds at 161-166 dB re 1 µPa mean squared pressure would give indications of the extent of disruption for specific seismic surveys.

3.7 - General synthesis

3.7.1 Unit systems

Although many authors have stressed this point, it is reiterated, there is as yet no standardised way to describe an impulsive air-gun signal. This causes no end of confusion in comparing works from different authors and is easily capable of leading to erroneous conclusions by comparing different works with different unit systems. From analysis of several measured sets of air-gun signals, it was found that the most consistent method to describe an air-gun signal was some measure of its total energy reached above the background noise. It was found measurements which required time integration over the signal were prone to certain types of biases, which may or may not be present. It was also found that many factors may cause large differences in the received level of an air-gun signal from the same source operating in the same general area. Thus air-gun signal descriptors need to be precisely stated, the situations of the measurement stated and ideally conversions for that source in that environment into different units given.

3.7.2 Experimental protocols - Cage versus field trials

There are essentially three techniques which can be used to study the implications of seismic survey noise on marine animals. These are: controlled trials with caged animals, as described here for sea turtles, fishes and squid; observations of wild animals in controlled approaches, as described for the humpback approach trials in Exmouth Gulf; or observations made during commercial seismic operations, as for operations about the *Geco Resolution*. There are arguments for and against each type of regime. Some of these issues are summarised in Table 33.

Trial type	Advantages	Disadvantages / problems
1) Caged trials	full control over air-gun exposure type accurate measure of exposures can be made fine detail on behavioural, physiological and sub-lethal responses possible relatively inexpensive thus a lot can be achieved for modest costs can mate levels for specific types of response for modelling work only way that issues such as sub-lethal effects can be accurately defined	need to be careful in way signal presented to ensure realistic exposure influence on behavioural response of artificial cage environment logistical problems of cage configuration - needs to be large in large body of water (cannot be done in tanks), issues of water quality, security, and shelter cannot be used for 'megafauna' such as whales ethical issues
2) Free ranging animals - controlled approaches	some control over air-gun exposure no bias from artificial cage environment can be used on megafauna	problems in observing animals arise - use follows, tracking, active acoustics, video little control over target species - may flee incidentally, difficult to control for age, sex etc expected to require dedicated sound measurement runs and/or modelling work to understand exposures received difficult to give precise exposure history for targeted animals ethical issues involves sea going vessels hence field costs higher than 1)
3) Free ranging animals - commercial seismic programs	if carried out thoroughly gives realistic measure of effect of commercial seismic programs can give estimate of recovery and disruption periods results of methods 1) & 2) can be used to guide trial observations and design can be used to verify trials of form 1) and 2) and hence verify exposure modelling approaches as described here (section 2.1.5)	no experimental control over exposures observation techniques difficult (use active acoustics, follows, tagging, aerial surveys etc) likely to require extensive measurements and modelling to describe exposure regime received by observed animals impossible to know exposure history for specific animals invokes problem of understanding how repeated exposures through time influence animal movements & behaviour very expensive - typical field costs from 100 k upwards for single set of observations

Table 33: Summary of various advantages and disadvantages for studying seismic effects.

The regime used in the fourteen trials with sea turtles, fishes and squid described in this document, was to approach experimental animals held in cages with an operating air-gun. A comparatively large cage size (10 x 6 x 3 m deep) was used in a large body of water (Jervoise Bay, 10 m water depth). For trials 6 and onwards a > 30 dB air-gun signal dynamic range was used. For these trials signals were presented in approach-departure scenario, which is as experienced in actual seismic surveys. This is an important issue as an approach by a moving source may represent as a greater threat to an animal (and thus elicit a greater behavioural response) than a high noise level but from a stationary source. The air-gun source used in trials was shown to be comparative to a 'real' seismic source (it was in fact a 'real' seismic source, see Figure 4, Figure 59 and section 2.4.1 for comparison). The arguments that the experimental source did not match that of a commercial seismic survey array were discounted (section 2.4.1) primarily on the basis that there is simply no 'standard' seismic source, all differ and environmental conditions will to a large extent dictate the source signature at some range and water depth. Despite the efforts to make the caged trials realistic the animals in these trials were still held in cages, thus the behavioural observations may be biased by this. Neverless there were still clear trends, such as the fish compacting in the cage centre during periods of high air-gun levels.

3.7.3 Summary and species comparisons

A table of levels (in mean squared pressure units) for various effects of nearby air-gun operations on marine animals from literature and this study is given in Table 34. Despite the different animal groups listed there are some striking similarities in the thresholds for response to a nearby air-gun. Several baleen whale species are listed as showing general avoidance of an operating seismic source at 157-165 dB re 1 μPa mean squared pressure (excluding the resting cow pods from within Exmouth Gulf of this study), sea turtles were seen to begin to noticeably increase their swimming behaviour at 166 dB re 1 μPa mean squared pressure, many fin-fishes displayed their general 'alarm' response of increased swimming speed, tightening schools and moving towards the sea floor at 156-168 dB re 1 μPa mean squared pressure, and behavioural changes in squid were seen from levels of 156-166 dB re 1 μPa mean squared pressure upwards. The hearing systems of baleen whales, sea turtles, fishes and squid are fundamentally different, yet the received air-gun level range over which responses seem to become significant is within 10 dB for these diverse groups. This raises the questions:

- is there common evolutionary pressures which have shaped the high end hearing response of a wide range of marine animals;
- or is there a common limitation to the hearing systems of marine animals.

Although the mechanisms of delivering energy to the inner ear (or statocyst system of molluscs) may differ enormously, perhaps the limitations of hair-cell mechanics may shape the behavioural response to high intensity sounds.

Source	Level (dB re 1 ■Pa mean squared pressure)	Animal group	Effects
Malme et al 1985	160	gray whales	general standoff range
Richardson et al 1995	150-180	gray and bowhead whales	general standoff range - summary of many workers results
This study (2.2.1 & 2.2.2)	157-164	humpback whales	standoff range for migrating humpbacks
This study (2.2.3)	140	humpback whales	resting pods with cows in key habitat type begin avoidance
This study (2.2.3)	143	humpback whales	resting pods with cows in key habitat type standoff range[a]
This study (2.2.3)	179	humpback whales	maximum level tolerated by investigating probable male humpbacks to single air-gun, although this possibly due to visual clues
This study (2.3)	166	green & loggerhead turtle	noticeable increase in swimming behaviour
This study (2.3)	175	green & loggerhead turtle	turtle behaviour becomes increasingly erratic
O'Hara (1990)	[b]175-176	loggerhead turtle	avoidance
This study (2.4.2)	156-161	various fin-fishes	common 'alarm' behaviour of forming 'huddle' on cage bottom centre, noticeable increase in alarm behaviours begins at lower level
Pearson et al (1992)	[c]149	rockfish (*Sebastes spp.*)	subtle behavioural changes commence
Pearson et al (1992)	[c]168	rockfish	alarm response significant
This study (2.4.5)	> 171	fish ear model	rapid increase in hearing stimulus begins
This study (2.4.2)	182-195	fish *P. sexlineatus*	persistent C- turn startle
Pearson et al (1992)	200-205	selected rockfish species	C- turn startle responses elicited
Wardle et al (in press)	[d]183-207	various wild finfish	C-turn startle responses
This study (2.4.3)	146-195	various finfish	no significant physiological stress increase
This study (2.4.4)	[e]????	fish *Chrysophrys auratus* & others	preliminary evidence of pathological damage to hearing systems of constrained fish
This study (2.5)	174	squid	startle (ink sac fire) and avoidance to startup nearby
This study (2.5)	156-161	squid	noticeable increase in alarm behaviours
This study (2.5)	166	squid	significant alteration in swimming speed patterns, possible use of sound shadow near water surface

Table 34: Summary of effects of nearby air-gun operations on a range of marine fauna from the literature and this study. Note all units are dB re 1 μPa mean squared pressure. Where appropriate conversions have been applied from empirical measurement sets presented in this document. Superscripts: **a** - standoff range is minimum range animals allow operating vessel to approach; **b** - level derived from similar air-gun used in this study, see sea turtle section above; **c** - converted from mean-peak to mean squared pressure using -12 dB correction from 7712 records from Bolt 600B air-gun; **d** correction of -12 dB applied (peak to mean squared pressure), note that lower limit to elicit C turn not determined; **e** - exposure precisely known but because of ramped nature did not allow level for damage to be determined

Appendix 1: Codes used in scoring movements and behaviour of fish, squid and sea turtles.

BEHAVIOUR	CODE
SPECIES	
butterfish	BA
whiptail	WT
spanish flag	SF
charlie court	CT
spangled Emporer	SN
unidentified fish	UF
silver bream	SB
squid	SQ
mullet	LL
herring	HE
baitfish	BF
green turtle	GN
loggerhead turtle	LD
skippy	SK
wrasse	WR
jewfish	JW
cuttlefish	CF
break sea cod	BS
goat fish	GT
Pelates sexlineatus	SX
SCHOOL/GROUP	
Loose group	LG
Tight group	TG
Animals in all directions	AD
Majority of animals	MA
Some animals	SE
STARTLE	
flash expansion (school)	FL
parting (school)	PA
Dart	DA
Change direction	CD
fired ink sac	IK
animal jerks, squid shoots backwards	JE
SWIMMING SPEED	
Idle	ID
Slow swimming	SS
Fast swimming	FS
very fast swimming	VF
HORIZONTAL MOVEMENT/POSITION	
Moving from right to left of screen	RL
Moving from left to right of screen	LR
Circling	CC
Animals on left hand side	LH
Animals on right hand side	RH
VERTICAL POSITION	
upper	UP
lower	LO
mid	MD
VERTICAL MOVEMENTS	
swimming from top to bottom	UL

swimming form top to mid	UM
swimming from bottom to top	LU
swimming from bottom to mid	LM
swimming from mid to bottom	ML
swimming from mid to top	MU
GENERAL BEHAVIOUR	
approach camera	CM
in view	IV
animals out of view	OV
unsure of numbers	UN
fish in centre of cage	CN
fish being fed	FD
swimming away from camera	AW
swimming towards camera	TW
swimming on side	SD
body pointed at surface	BP
bad visibility	VB
SQUID SPECIFIC	
backwards swimming	BW
forwards swimming	FW
dark colouration	DK
light colouration	LT
white spot on mantle	WS
animals attack each other	AK
TURTLE SPECIFIC	
nip	NP
head flick	HF
move flipper	FM
front flipper facing backwards	BW
front flipper facing forwards	FW
front flipper sideways	SW
turtles very close to each other on bottom	NX
green approaches loggerhead	AP
turtles attached to each other	AT
HOUSEKEEPING	
boat engine	XX
gun on	GN
gun off	GF
diver in cage	DV
diver out of cage	DO
video stopped working/started working	?
observation from dinghy	DG
stop clock	ZZ
moving camera	MC
moving cage	MG

Appendix 2: Permit restrictions for humpback whale exposure experiments.

Trials operated under the following guidelines which were designed to minimise any stress or unnecessary harassment. Superscripts denote years in which conditions were imposed. Tense is as per written into the permit requirements.

1. [96, 97] Each vessel will conform with approach rules as per the Australian whale watching guidelines;
2. [96, 97] Pods of adult whales without calves will be approached no closer than 100 m by the vessel with operating air-gun;
3. [97] Pods containing calves will be approached no closer than 500 m by the vessel with operating air-gun;
4. [96, 97] The air-gun vessel will start operations at 3-5 km from the target pod;
5. [96, 97] The air-gun vessel is to maintain as closely as practicable a constant heading during all air-gun operations;
6. [96, 97] For each trial the heading chosen by the air-gun vessel is to be such that it leaves the targeted whales plenty of room to move into deep water;
7. [96, 97] Trials will cease if targeted whale pods appear to be moving into water less than 5 m deep;
8. [96, 97] The vessel with operating air-gun is not to chase or pursue whales;
9. [97] Trials are not to be carried out on any whales which appear to be injured or in distress before the commencement of trials;
10. [96, 97] Trials are to cease if any of the following behavioural responses are observed: tremors or shudders from whales correlating with air-gun discharge; violent contractions; apparent stunning; or aggressive behaviour directed toward the air-gun vessel such as tail fluke slaps or sideways swishes or close (< 50 metres) breaches.

Appendix 3: 1/3 octave band limits used in analysis

Centre frequency (Hz)	lower frequency (Hz)	upper frequency (Hz)	bandwidth correction (dB)
0.49	0.44	0.55	-9.47
0.62	0.55	0.69	-8.46
0.78	0.69	0.87	-7.46
0.98	0.87	1.10	-6.46
1.23	1.10	1.38	-5.45
1.55	1.38	1.74	-4.45
1.95	1.74	2.19	-3.45
2.46	2.19	2.76	-2.44
3.10	2.76	3.48	-1.44
3.91	3.48	4.38	-0.44
4.92	4.38	5.52	0.57
6.20	5.52	6.96	1.57
7.81	6.96	8.77	2.57
9.84	8.77	11.05	3.58
12.40	11.05	13.92	4.58
15.63	13.92	17.54	5.58
19.69	17.54	22.10	6.59
24.80	22.10	27.84	7.59
31.25	27.84	35.08	8.60
39.37	35.08	44.19	9.60
49.61	44.19	55.68	10.60
62.50	55.68	70.15	11.61
78.75	70.15	88.39	12.61
99.21	88.39	111.36	13.61
125.00	111.36	140.31	14.62
157.49	140.31	176.78	15.62
198.43	176.78	222.72	16.62
250.00	222.72	280.62	17.63
314.98	280.62	353.55	18.63
396.85	353.55	445.45	19.63
500.00	445.45	561.23	20.64
629.96	561.23	707.11	21.64
793.70	707.11	890.90	22.64
1000.00	890.90	1122.46	23.65
1259.92	1122.46	1414.21	24.65
1587.40	1414.21	1781.80	25.65
2000.00	1781.80	2244.92	26.66
2519.84	2244.92	2828.43	27.66
3174.80	2828.43	3563.59	28.66
4000.00	3563.59	4489.85	29.67
5039.68	4489.85	5656.85	30.67
6349.60	5656.85	7127.19	31.67
8000.00	7127.19	8979.70	32.68
10079.37	8979.70	11313.71	33.68

Appendix 4: Derivation of the equation of motion used to model fish otolith response to applied air-gun signals.

Let $w(t)$ be the distance from fixed datum to body of fish,

        $y(t)$ be the distance from fixed datum to otolith,

        $x(t)$ be the distance from body of fish to otolith

Then forces acting on the otolith are**:**:

1)-Viscous damping (steady drag force), assume proportional to velocity (for turbulence, ie high Reynolds numbers (Re) is proportional to square of velocity, (Fletcher; 1992), but Re is low here, as per:

for conservative estimate, use largest u, largest D, smallest ν:

    estimate $u \sim 5*10^{-3}$ m/s, based on results from model

                    $D \sim 10^{-3}$ m, based on value of 0.03 cm (de Vries; 1950), where D is the distance between otolith and macula

                    $\nu \sim 10^{-6}$ m^2/s, based on value for water (smaller than ν for jelly-like membrane)

                    $Re \sim uD/\nu$

                      $= \sim 5*10^{-3} * 10^{-3} / 10^{-6}$

                      $= 5$

                which is < 2000, hence laminar flow, so proportional to velocity).

2) - Elastic / 'restoring' force, proportional to displacement (Hooke's law: $F = kx$)

3) Unsteady drag force due to acceleration of fluid relative to otolith. The acceleration reaction is given by:

$$F_{DU} = -\rho_w V_o a_{rel}$$

where a_{rel} is the acceleration of the fluid relative to the otolith (adapted from Batchelor, 1988).

The acceleration of the fluid relative to the otolith is equal to the acceleration of the fluid relative to a Newtonian (non-accelerating) frame of reference minus the acceleration of the otolith relative to a Newtonian frame of reference, so

$$a_{rel} = w'' - y''$$

which gives:

$$F_{DU} = -\rho_w V_o (w'' - y'')$$

4) 'Buoyancy force' due to the fluid displaced by the otolith. The fluid acceleration is analogous to the presence of a (time-varying) gravitational field that results in a buoyancy force equal to the weight of fluid displaced (Batchelor 1988, Fletcher 1992).

$B = m_w w''$ since w'' is the acceleration of the fluid (cf $B = m_w g$)

$$= \rho_w V_o w''$$

First, assume the fluid is stationary.
Using Newton:
$$\Sigma F = ma$$
ie. $$ma = \Sigma F$$
ie $$m_o y'' = -bx' - kx$$

Now for an accelerating fluid, it is necessary to consider both the buoyancy force (to obtain the fluid force in the reference frame of the fish's body, van Netten, 1991), and the unsteady drag force.
ie $$m_o y'' = -bx' - kx - \rho_w V_o (w'' - y'') + \rho_w V_o w''$$

Substitute $y'' = w'' + x''$,
ie $$m_o (w'' + x'') = -bx' - kx - \rho_w V_o(-x'') + \rho_w V_o w''$$
ie. $$(m_o - \rho_w V_o)w'' = -(m_o + \rho_w V_o)x'' - bx' - kx$$

But $$\rho_w V_o = (\rho_w/\rho_o)\rho_o V_o$$
$$= (\rho_w/\rho_o)m_o$$
so $$(m_o - (\rho_w/\rho_o)m_o)w'' = -(m_o + (\rho_w/\rho_o)m_o)x'' - bx' - kx$$
ie. $$(1 - (\rho_w/\rho_o))m_o w'' = -(1 + \rho_w/\rho_o)m_o x'' - bx' - kx$$
ie $$[(\rho_o - \rho_w)/\rho_o]m_o w'' = -(1 + \rho_w/\rho_o)m_o x'' - bx' - kx$$

w'' is the acceleration of the fish. But the density of the fish is similar to that of the surrounding seawater, so that w'' will be approximately equal to the particle acceleration, u' (where u = particle velocity).

Also, let $$m_e = (1 + \rho_w/\rho_o)m_o \approx 1.3 m_o$$

Substitute,
ie $$[(\rho_o - \rho_w)/\rho_o]m_o u' = -m_e x'' - bx' - kx$$
ie $$m_e x'' + bx' + kx = -[(\rho_o - \rho_w)/\rho_o]m_o u'$$

giving $$m_e x'' + bx' + kx = -F(t)$$

with all derivatives with respect to time.

Rearrangement of this second order differential equation to form a system of two first order equations then gives
$$x_1' = x_2$$
$$x_2' = (-k/m_e)x_1 - (b/m_e)x_2 - F(t)/m_e$$

AUTHOR AFFILIATIONS

Rob McCauley, Alec Duncan, John Penrose
Centre for Marine Science and Technology
Curtin University
GPO Box U 1987
Perth, Western Australia, 6845
email   r.mccauley@cmst.curtin.edu.au or rmccaule@cc.curtin.edu.au
        a.duncan@cmst.curtin.edu.au
        j.penrose@cmst.curtin.edu.au

Jane Fewtrell
Aquatic Sciences
Curtin University
GPO Box U 1987
Perth, Western Australia, 6845
email   pfewtrellj@cc.curtin.edu.au

Curt & Micheline Nicole-Jenner, Kathryn McCabe
Centre for Whale Research W.A. (Inc.)
PO Box 1622
Fremantle. 6959
email   curtmich@bigpond.com or 61418912669@mobilenet.telstra.net

Dr R I T (Bob) Prince,
Leader, Western Australian Marine Turtle Project,
Wildlife Research Centre, Dept CALM,
PO Box 51,
Wanneroo, Western Australia, 6946.
email   bobp@calm.wa.gov.au

Anita Adhitya
Department of Physics
University of Western Australia
Nedlands 6907, Western Australia
enail   aadhit@tartarus.uwa.edu.au

Julie Murdoch
Fisheries Division, Department of Primary Industry and Fisheries, Darwin
PO Box 990
Darwin 0801
email   julie.murdoch@dpif.nt.gov.au

REFERENCES

Barger, J.E., Hamblen, W.R. (1980). The air-gun impulsive underwater transducer. **J. Acoust. Soc. Am**. 68(4):1038-1045

Batchelor, G.K. (1988). An Introduction to Fluid Dynamics. Cambridge University Press

Blaxter, J.H.S., Gray, J.A.B., Denton, E.J. (1981). Sound and startle response in herring shoals. **J. Mar. Biol. Ass. UK**. 61:851-869

Chittleborough, R.G. (1953). Aerial observations on the humpback whale *Megaptera nodosa* (Bonnaterre), with notes on other species. **Aust. J. Mar. Freshwat. Res**. 4:219-226

Chittleborough, R. G. (1965). Dynamics of two populations of the humpback whale, *Megaptera novaeangliae* (Borowski). **Aust. J. Mar. Freshwat. Res**., 16, 33-128.

Collins, M.D. (1992). A self-starter for the parabolic equation method, **J. Acoust. Soc. Am**. 92(4):2069-2074

Collins, M.D. (1993). A split-step Pade solution for the parabolic equation method, **J. Acoust. Soc. Am**. 93(4):1736-1741

Dalen, J., Raknes, A. (1985). Scaring effects on fish from 3D seismic surveys. Institute of Marine Research. Rep. No. P.O. 8504, Bergen, Norway

Dawbin, W.H. Temporal segregation of humpback whales during migration in southern hemisphere waters. **Mem. Qld. Mus.** 42(1):105-138

Duncan, A.J. (1998). research into the acoustic characteristics of an air-gun sound source. Centre for Marine Science and Technology, Curtin University Western Australia, C98-18, 23 pp.

Duncan, A.J. (1999). Research into the acoustic characteristics of an air-gun sound source. Centre for Marine Science and Technology, Curtin University Western Australia, C99-12

Engås, A., Løkkeborg, S., Ona, E. and Soldal, A.V. (1996). Effects of seismic shooting on local abundance and catch rates of cod (*Gadus Morhua*) and haddock (*Melanogrammus aeglefinus*). **Can. J. Fish. Aquat. Sc.** 53(10):2238-2249

Engås, A., Løkkeborg, S., Ona. E. Soldal, A.V. (1993). Effects of seismic shooting on catch and catch availability of cod and haddock. Institute of Marine Research. Fisken Og Havet NR 9-1993

Fay, R.R., Popper, A.N, (Eds.) (1999). Comparative hearing: Fish and amphibians. Springer, New York

Fletcher, N.H. (1992). Acoustic systems in biology. Oxford University Press, New York, 333 pp.

Goold, J.C., Fish, P.J. (1998) Broadband spectra of seismic survey air-gun emissions, with reference to dolphin auditory thresholds. **J. Acoust. Soc. Am**. 103(4):2177-2184

Hall, M.V. (1996). Measurement of seabed sound speeds from head waves in shallow water. **IEEE J. Ocean. Eng.** 21(4):413-422

Hamilton, L.J. (1997). Sediments and turbidity. In (Scott, B.D. Ed). Investigation of a proposed tracking range near Exmouth. Defence Science and Technology Organisation, Pyrmont, Sydney

Jenner, C., Jenner, M-N., McCabe, K. (2000). Geographical and temporal movements of humpback whales in Western Australian waters - A prelinary report and description of a computer assisted matching system. Unpublished report by Centre for Whale Research, WA.

Jensen, F., Kuperman, W.A., Porter, M.B., Schmidt, H. (1994). Computational ocean acoustics. American Institute of Physics, New York, 612 pp.

Johnson, D.T. (1994). Understanding air-gun bubble behaviour, **Geophysics** 59(11):1729-1734

Kalmijn, A.J. (1988). Hydrodynamic and acoustic field detection. In: Atema J., Fay R.R., Popper A.N., Tavolga W.N., 1988 Sensory biology of aquatic animals. Springer-Verlag, New York.

Karlsen, H. (1992). The inner ear is responsible for detection of infrasound in the perch (*Perca fluviatilis*). **J. Exp. Biol**. 171:163-172

Lenhardt, M.L. (1994) Seismic and very low frequency sound induced behaviours in captive loggerhead marine turtles (*Caretta caretta*). In (Bjorndal, K.A., Bolten, A.B., Johnson, D.A., Eliazar, P.J. Eds.) 1994, Proceedings of the fourteenth Annual Symposium on Sea Turtle Biology and Conservation. NOAA Technical Memorandum NMFS-SEFSC-351, 323 pp.

Lenhardt, M.L., Bellmund, S., Byles, R.A., Harkins, S.W., Musick, J.A. (1983). Marine turtle reception of bone conducted sound. **J. Aud. Res**., 23:119-125

Lokkeborg, S. (1991). Effects of a geophysical survey on catching success in longline fishing. **ICES C.M** 1991/B:40, 9pp.

Lokkeborg, S., Soldal, A.V. (1993). The influence of seismic exploration with air-guns on cod (*Gadus morhua*) behaviour and catch rates. **ICES Marine Science Symposium** 196, 62-67

Lombarte, A.Y., Popper, A.N., Chang, J.C., Platt, C. (1993). Damage and regeneration of hair cell ciliary bundles in a fish following treatment with gentamicin. **Hear. Res**. 66:166-174

Malme, C.I., Miles, P.R., Tyack, P., Clark, C.W. Bird, J.E. (1985). Investigations of the potential effects of underwater noise from petroleum activities on feeding humpback whale behaviour. Report from Bolt Beranek & Newman Inc., Cambridge, Massachusetts for U.S. Minerals Management Service, Anchorage, Alaska. Var. pag. NTIS PB86-218385

Malme, C.I., Smith, P.W.Jr., Miles, P.R. (1986). Characterisation of geophysical acoustic survey sounds. OCS Study MMS-86-0032. Prepared by BBN Laboratories Inc., Cambridge, for Battelle Memorial Institute to the Department of the Interior-Mineral Management Service, Pacific Outer Continental Shelf Region, Los Angeles, CA.

McCauley, R.D. (1994). Seismic Surveys. In: Environmental implications of offshore oil and gas development in Australia - the findings of an independent scientific review, Swan, J.M., Neff, J.M. and Young, P.C. (Eds.), APEA, Sydney, pp. 19-121

McCauley, R.D., Cato, D.H., Jeffery, A.F. (1996). A study of the impacts of vessel noise on humpback whales in Hervey Bay. Report for the Queensland Department of E & H, Maryborough Office, from the Department of Marine Biology, James Cook University, Townsville, 137 pp.

Medwin, H. (1975). Speed of sound in water: A simple equation for realistic parameters. **J. Acoust. Soc. Am**. 58(6):1318-1319

Medwin, H., Clay, C.S. (1998). Fundamentals of acoustical oceanography. Academic Press, Sydney 712 pp.

Misund, O.A. (1993). Avoidance behaviour of herring (*Clupea harengus*) and mackeral (*Scomber scombus*) in purse seine capture situations. **Fish. Res.** 16:179-194

Moein, S.E., Musick, J.A., Keinath, J.A., Barnard, D.E., Lenhardt, M., George, R. (1994) Evaluation of seismic sources for repelling sea turtles from hopper dredges. Report for US Army Corps of Engineers, from Virginia Institute of Marine Science, VA USA

O'Hara, J. (1990). Avoidance responses of loggerhead turtles, *Caretta caretta*, to low frequency sound. **Copeia** 1990(2):564-567

Olsen, K. (1990). Fish behaviour and acoustic sampling. **Rapp. P.-v. Reun. Cons. int. Explor. Mer**. 189:147-158

Olsen, K., Angell, J., Petterson, F., Lovik, A. (1983). Observed fish reactions to a surveying vessel with special reference to herring, cod, capelin and polar cod. **FAO Fish. Rep.** 300:131-138

Ona, E. (1988). Observations of cod reaction to trawling noise. Fisheries Acoustics, Science and Technology Working Group (FAST.WG. Oostende, April 20-22, 1988)

Parkes, G.E., Hatton, L. (1986). The marine seismic source. D Reidel Publ.

Parkes, G.E., Ziolokowski, A., Hatton, L., Haugland, T. (1984). The signature of an air-gun array: Computation from near-field measurements including interactions - Practical considerations. **Geophysics**, 48(2):105-111

Pearson, W.H., Skalski, J.R., Malme, C.I. (1992). Effects of sounds from a geophysical survey device on behaviour of captive rockfish (*Sebastes spp*.). **Can. J. Fish. Aquat. Sci**. 49(7):1343-1356

Popper, A.N., Fay, R.R. (1993). Sound detection and processing by fish: critical review and major research question. **Brain Behav. Evol** 1993(41):14-38

Popper, A.N., Fay, R.R. (1999). The auditory periphery in fishes. In (Fay, R.R., Popper, A.N. Eds.) Comparative hearing: Fish and amphibians. Springer, Sydney, pp.43-100

Porter, M.B. (1994). The KRAKEN normal mode program. SACLANT Undersea Research Centre, Volume 1

Richardson, W.J., Greene, Jr., C.R., Malme, C.I., Thomson, D.H. (1995). Marine mammals and noise. Academic Press, San Diego

Rogers, P.H., Popper, A.N., Hastings, M.C., Saidel, W.M. (1988). Processing of acoustic signals in the auditory system of bony fish. **J. Acoust. Soc. Am**. 83(1):338-349

Schuijf, A., Buwalda, R.J.A. (1980). Underwater localisation - a major problem in fish acoustics. In (Popper A.N., Fay R.R., eds.) Comparative studies of hearing in vertebrates. Springer-Verlag, New York, pp43-77

Skalski J.R., Pearson W.H., Malme C.I. (1992). Effects of sounds from a geophysical device on catch per unit effort in a hook and line fishery for rockfish (*Sebastes spp*.). **Can. J. Fish. Aquat. Sci**. 49(7):1357-1365

Thompson, P.O., Cummings, W.C., Ha, S.J. (1986). Sounds, source levels, and associated behaviour of humpback whales, Southeast Alaska. **J. Acoust. Soc. Am**. 80(3):735-740

Urick, R.J. (1983). Principles of underwater sound for engineers. (3rd edition) Peninsula Publishing, California

Verbeek, N.H., McGee, T.M., (1995). Characteristics of high resolution marine reflection profiling sources. **J. Applied Geophysics**. 33:251-269

Vincenty, T. (1975). Direct and inverse solutions of geodesics on the ellipsoid with applications of nested equations. **Survey Review**, XXII, 176:88-93

Wardle, C.S., Carter, T.J., Urquhart, G.G., Johnstone, A.D.F., Ziolkowski, A.M., Hamposn, G., Mackie, D. (in press). Effects of seismic air-guns on marine fish. **Continental Shelf Research**

de Vries H.L. (1950). The mechanics of the labyrinth otoliths. **Acta Oto-laryngologica**. 38(3):262-273

van Netten S.M. (1991) Hydrodynamics of the excitation of the cupula in the fish canal lateral line. J. Acoust. Soc. Am. 89(1):310-319